P-176

1 • 9 • 9 • 3

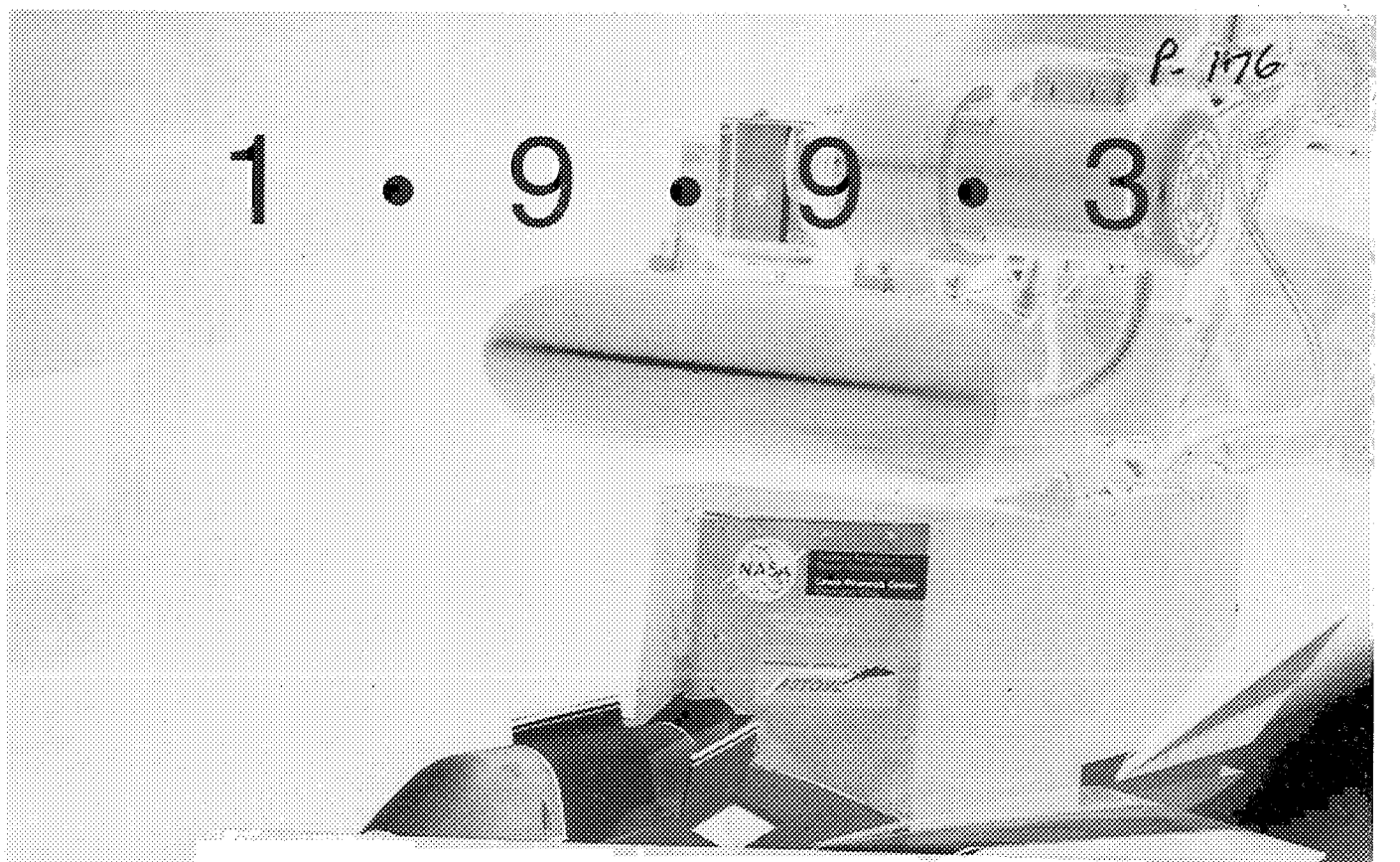

(NASA-TM-106376) RESEARCH AND TECHNOLOGY, 1993 (NASA. Lewis Research Center) 176 p

N94-33046

Unclas

G3/01 0004787

R&T Research & Technology

National Aeronautics and Space Administration

Lewis Research Center
Cleveland, Ohio 44135

Technical Memorandum 106376

About the cover:

A model of a short-takeoff, vertical landing (STOVL) aircraft is being tested in the NASA Lewis 9- by 15-Foot Low-Speed Wind Tunnel. The most viable advanced supersonic STOVL concepts are likely to go into production around the year 2015. To meet this date, critical technology problems must be resolved, such as ingestion of the hot exhaust gases by the engines during vertical landing.

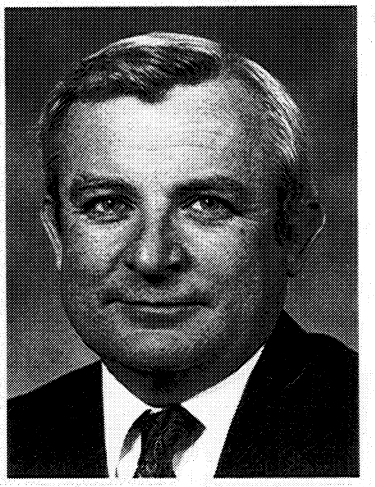

Introduction

NASA Lewis Research Center has seen many changes over the past year. An important thrust that was identified in our Strategic Plan has been pushed to the forefront of all our agendas. Technology transfer activities and opportunities have expanded significantly as NASA attempts to make its resources more easily available to the private sector.

The 1993 Research & Technology report is organized so that a broad cross section of the community can readily use it. A short introductory paragraph begins each article and will prove to be an invaluable reference tool for the layperson. The approximately 200 articles summarize the progress made during the year in various technical areas and portray the technical and administrative support associated with Lewis technology programs. If additional information is desired, the reader is encouraged to contact the authors identified in the articles.

The principal purpose of this report is to give a brief but comprehensive review of the technical accomplishments of the Center during the past year. It is a testimony to the dedication and competence of all the employees, civil servants and contractors, who make up the staff.

The Lewis Research Center is a unique facility, located in an important geographic sector, with a long and distinguished history of performing research and developing technology in support of NASA's mission and the Nation's needs.

L J Ross

Lawrence J. Ross
Director

Inquiries regarding this report can be addressed to the Office of Interagency and Industry Programs, Mail Stop 3–7. The telephone number is (216) 433–2912

PRECEDING PAGE BLANK NOT FILMED

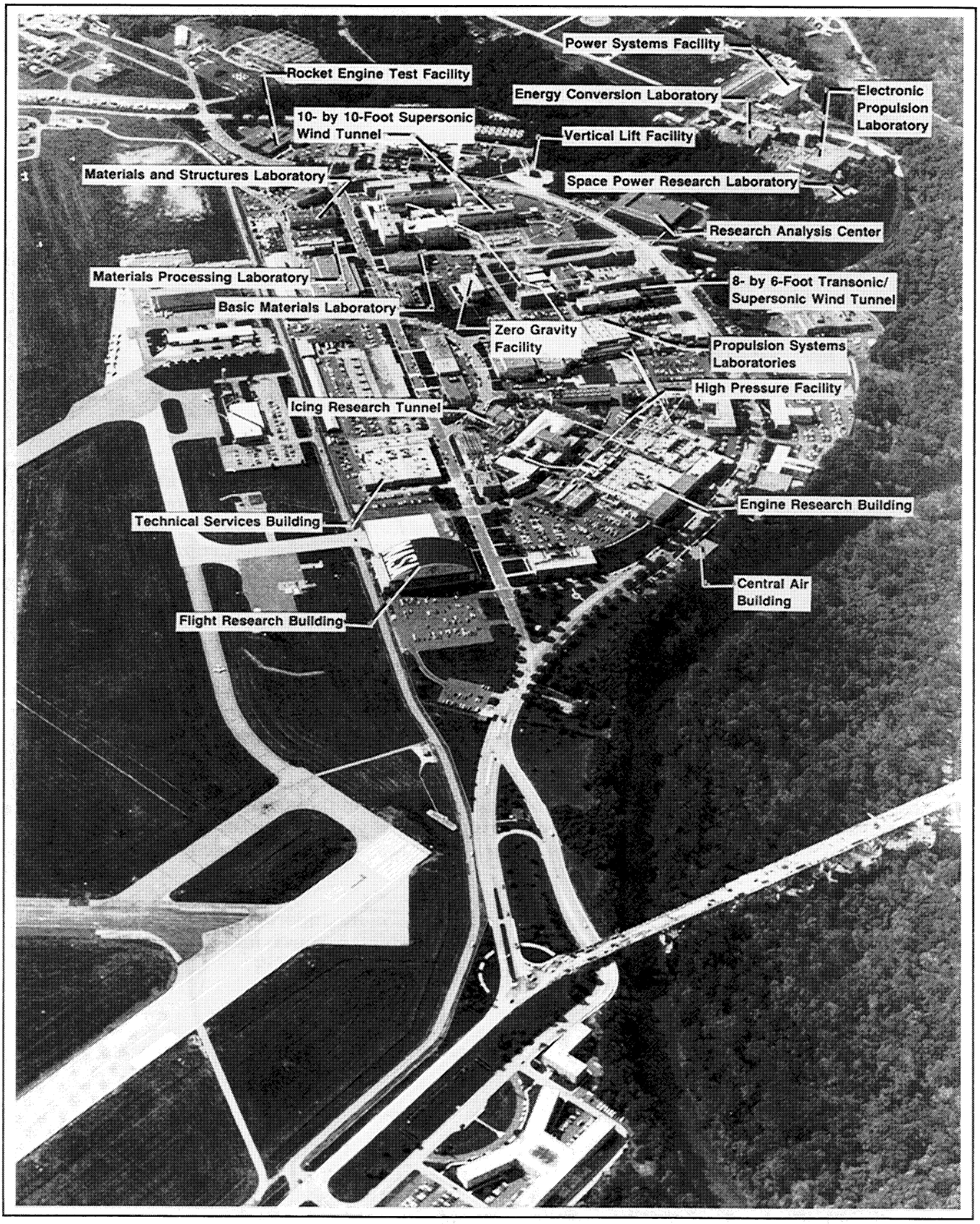

Lewis Research Center, Cleveland, Ohio

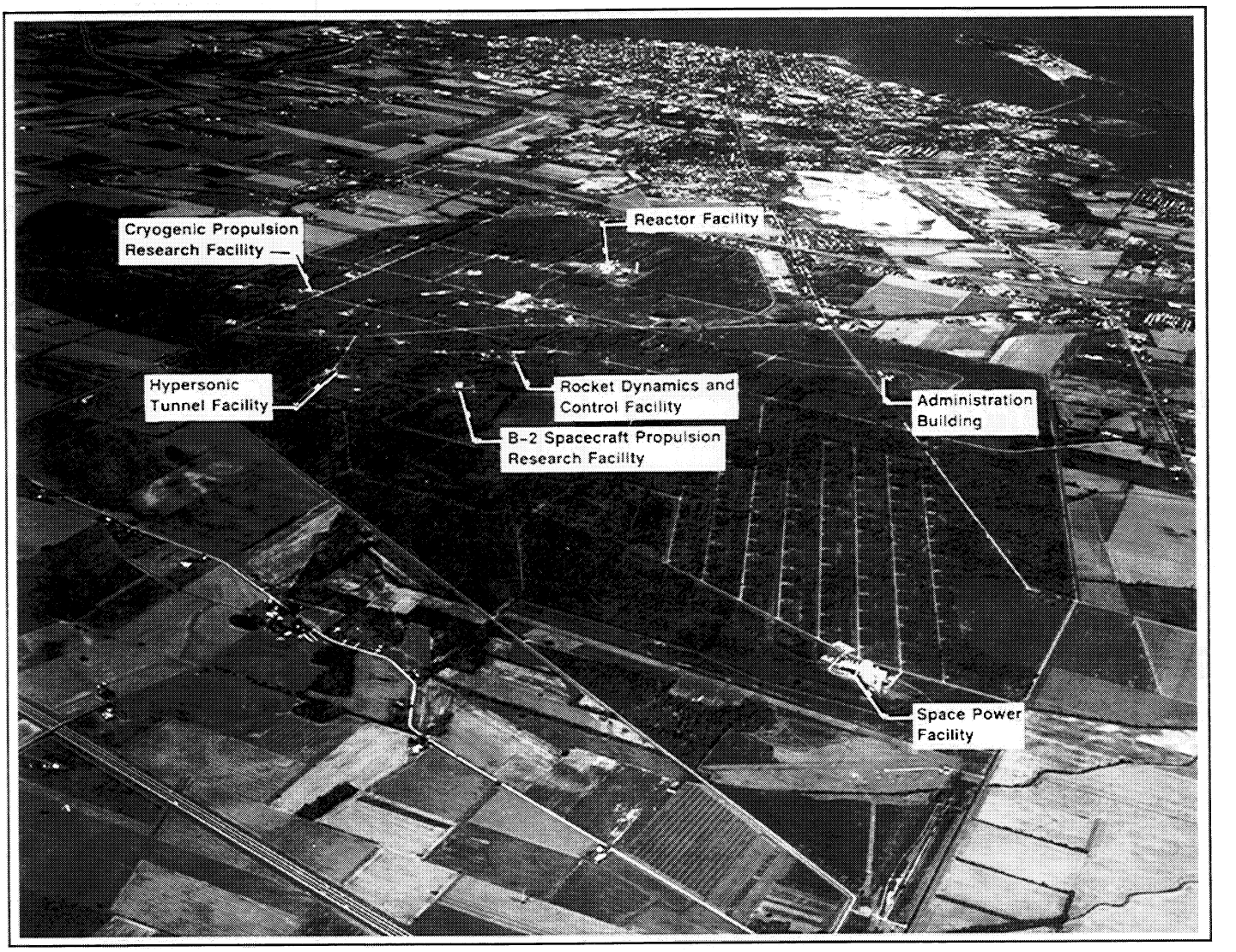

Plum Brook Station, Sandusky, Ohio

NASA Lewis Research Center Senior Management

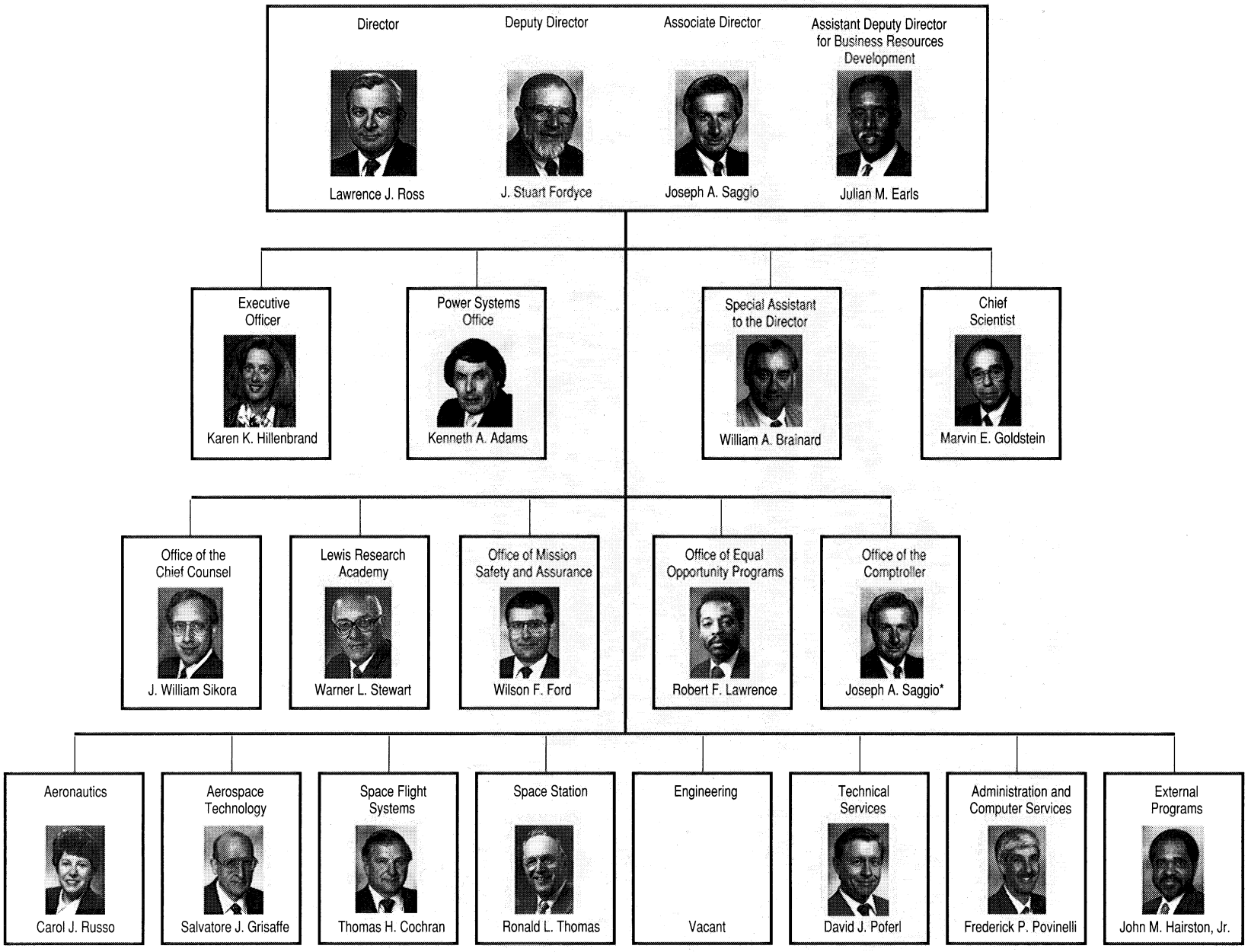

* Acting

CD-48534
August 16, 1993

NASA Lewis Research Center

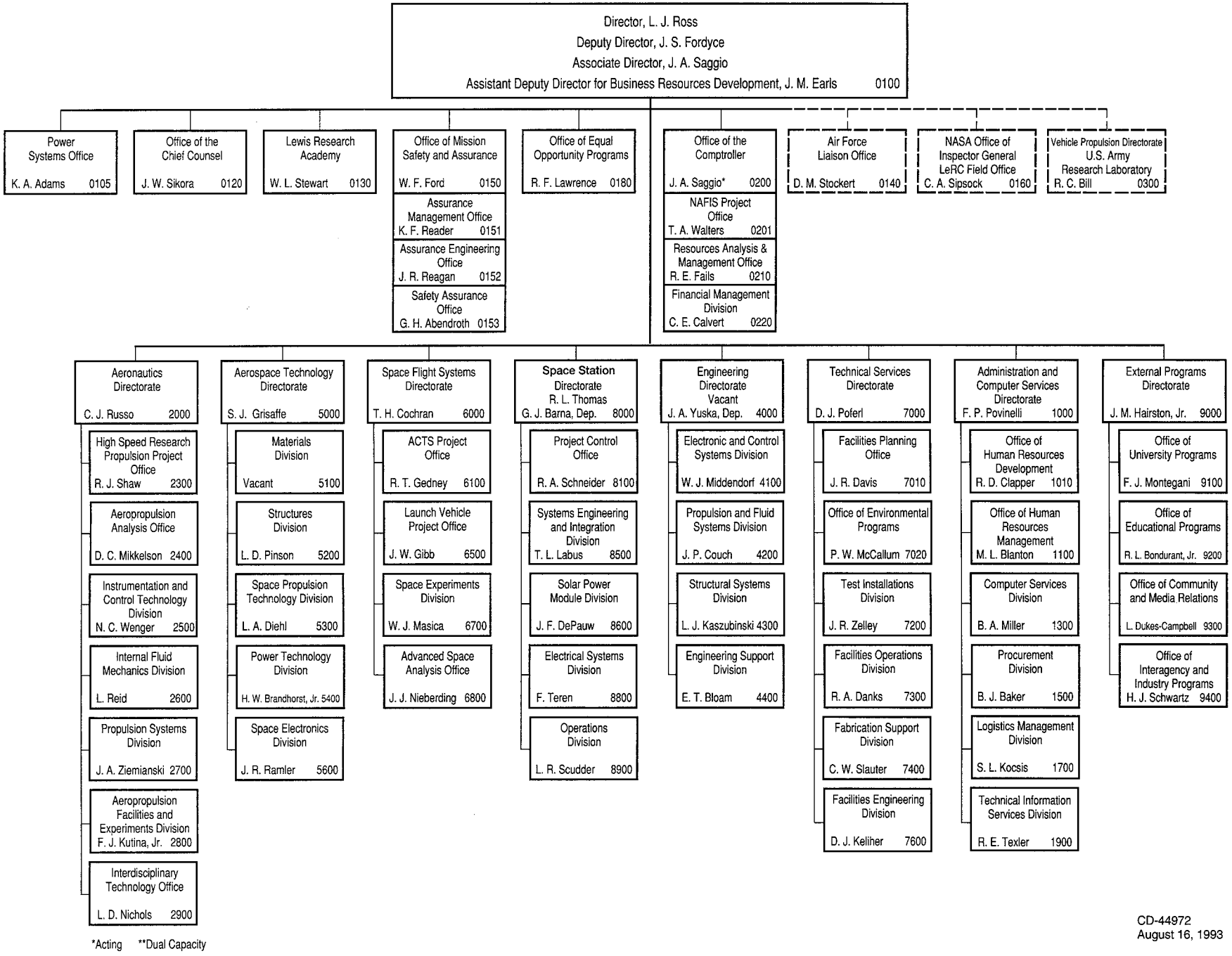

*Acting **Dual Capacity

CD-44972
August 16, 1993

Contents

Aeronautics

Aeropropulsion Analysis 1
Graphical User Interface Eases Aircraft Mission Analysis 1
New Method Accurately Predicts Two-Dimensional Nozzle Supersonic Drag 2

Instrumentation and Control Technology 3
Thin-Film Resistance Strain Gage Developed for High-Temperature Applications ... 3
Optical and PdCr Strain Gages Comparison Tested 4
Wave Rotor Model Validated 5
2000-V Silicon Carbide PN Junction Diodes Improved Through Chemical Vapor Deposition Epitaxy 6
Integrated Flight/Propulsion Controls Design Developed and Evaluated for STOVL Aircraft Concept 7
Drag Probe Utility Extended to Supersonic Flow 8

Internal Fluid Mechanics 9
Interaction of Turbulence With Stagnation-Region Heat Transfer Studied 9
Computation and Experiments Integrated 9
New Compressor Data Base Used as International Computational Test Case 11
NASA Reacting-Flow, Navier-Stokes Code Developed for Combustor Calculations at All Speeds 12
Vortical Flows Studied for Improved Models of Vortex Generators 13
Interactive Design and Educational Tools for Supersonic Flows Completed 13

Propulsion Systems 15
Improved Ceramic Gas Turbine Components Fabricated and Tested 15
Reacting Flow Analyzed for Annular Small Gas Turbine Combustor 16
Helicopter Model Tested in Icing Conditions 17
Advanced Spiral-Bevel Gears Designed for Helicopters 19
Flow Quality of Nozzle Acoustic Test Rig Studied 20
Performance Measured for 2DCD Nozzles With Inflow Swirl 21
Fluid Shield Nozzle Tested at GE 22
2DCD Mixer-Ejector Nozzle Tested at GE 23
STOVL Aircraft Characteristics Evaluated in Low-Speed Wind Tunnel 24
Wave Rotor Research Continues 25
Cooled Radial Turbine Research Completed 27
Aeroacoustic Propulsion Laboratory Self-Noise Level Assessed 28
Fan Noise Predicted for Turbofan Engines 29
Variable-Diameter-Centerbody Inlet Tested in Supersonic Wind Tunnel 30
RNG Turbulence Model Predicts Laminar-Turbulent Flow Transition 32

Aerospace Technology

Materials 33
Advanced High-Temperature Engines Materials Technology Continues Progress 33
Enabling Propulsion Materials Program Supports High-Speed Civil Transport 33
Nickel Aluminum Intermetallics Welded 34

PRECEDING PAGE BLANK NOT FILMED

PAGE viii INTENTIONALLY BLANK

Silicon-Carbide-Fiber-Reinforced, Reaction-Formed SiC Matrix Composites Tested 35
Pioneer II Melt Modulation Fiber Growth System Wins R&D 100 Award 36
Reaction-Formed Silicon Carbide Ceramics Fabricated With Tailorable Microstructure and Properties 37
Microstructures Identified for Optimum Creep Properties of Silicon Carbide Fibers 38
New Gold/Chromium Films Lubricate Ceramics From 25 to 800 °C 39
Effect of Temperature on Fiber/Matrix Bond Strength Determined 40
Hydrogen Annealing Improves Superalloy Oxidation Resistance 41
Lean-Burn, Rich-Burn High-Pressure-Burner-Rig Materials Capability Developed 42
Water Vapor Doubles Oxidation of Silicon-Based Ceramics 43
Interfacial Molybdenum Coating Enhances Mechanical Properties of Al_2O_3/NiAl Composite 44
Amorphous Silicon Nitride Coatings Provide Oxidation Barrier for High-Temperature Polymer Composites 45
1993 Jacquet-Lucas Award Received for Excellence in Metallography 46
Plastic Flow and Fracture Analyzed in B2 NiAl-Base Intermetallic Alloys Containing a Ductile Second Phase 47

Structures 48
Interlaminar Damping Layers Increase Damping in Composite Plates 48
Transpiration-Cooled Seal Concepts Tested for National Aerospace Plane 49
Ultrasonic Imaging Used for Characterizing Advanced Material Microstructure 50
Reliability Evaluated for Laminated CMC Components 52
High-Temperature Dynamic Engine Seal Being Developed 53
Piezoelectric Actuators Control Vibration of Transmission Shaft Line 54
Efficient Forced-Response Analysis System Developed for Compressor and Turbine Blades 55
Turbine Blade Dynamically Analyzed Before and After Ice Impact 57
Behavior of Intermingled-Fiber Hybrid Composite Computationally Simulated 58
Laminates Sized for Uncertainties 58
Tension-Compression Fatigue Testing Performed on SiC/Ti Composite 59
Generalized Method of Cells Models Inelastic Micromechanics 60
Computationally Coupled Deformation-and-Damage Finite Element Approach Developed 61

Space Propulsion Technology 63
Waved Journal Bearing Demonstrates Greater Stability and Load Capacity 63
Fiber-Optic Feedthrough and Sealing Designed, Developed, and Tested 64
Mars Propellant Production and Propulsion Demonstrated 64
Qualitative Diagnostic System Isolates Faulty SSME Components 65
Newer, Smaller Gellants Created for Rocket Fuels 66
Integrated Modular Engine Studies Demonstrate System Modeling and Design Capabilities 67
Brush Seals Demonstrate Reduced Leakage for Cryogenic Applications 69
AETB Fuel Turbopump Completes Critical Design Review 70
High-Activity Hydrogen Conversion Catalyst Developed 71
Russian Thrusters Evaluated for Flight Application 71
High-Performance Arcjets Chosen for Next-Generation Communications Satellites 73
Lightweight 30-cm-Diameter Ion Thruster Developed for Multimission Applications 74

Pulsed Mode Demonstrated for Whistler Wave Plasma Thruster 75
High-Performance Apogee Engines Demonstrated 76
Tank Pressure Control Experiment/Thermal Phenomena Analyzed 78
Viability of Compression Mass Gauging Demonstrated in 1-g Tests Using Fluorocarbons 80
Multilayer Insulation Test Blankets Assembled in New Facility 80
Tests Reveal Centaur-Related Slosh Phenomena 81

Power Technology 82
2-kWe Solar Dynamic Ground Test Demonstration Program Continues 82
Thermal Shield Manufactured for Hubble Space Telescope Solar Array Booms 83
Structurally Healed and Chemically Modified Carbon Materials Make Stronger Composites 85
Solar Simulator Designed for Solar Dynamic Space Power System Testing 86
Heat-Pipe Component Test Power Converter Tested Successfully 86
Advanced Nickel/Hydrogen Cell Passes Test 88
Novel Approach Developed for Extrapolating Short-Time Failure Behavior 89
High-Temperature Power Capacitors Developed 90
Scattered Space Atomic Oxygen Experiment Designed and Built 91

Space Electronics 92
Potential Markets Predicted for Advanced Satellite Communications 92
Telemedicine Spacebridge Project Links United States and Russia 93
Materials and Structures for High-Speed Electronic Devices Characterized Nondestructively 94
Ka-Band MMIC Arrays Being Developed for Future Communications Systems 95
High-Temperature Superconducting Microwave Receiver Built for Space Experiment 96
Ka-Band Earth Terminal Developed for Interference Experiments 97
Ku-Band Earth Terminal Facility Constructed 98
High-Efficiency Ka-Band Traveling Wave Tube Being Developed for Cassini Mission 99
Multichannel Error-Correcting-Code Decoder Implemented 100
Multichannel Demultiplexer/Demodulator Developed for Future Satellite Communications Systems 101
Hi-LITE Prototype Demonstrated for Free-Space Optical Communications 102
Intelligent Assistant Used for Satellite Earth Terminal Operations 103
Monolithic Microwave and Millimeter-Wave Integrated Circuit Packaging Reaches Market 104
High Secondary Electron Emission From Diamond Films Applied to Devices 106

Space Flight Systems

Nuclear Propulsion 107
NEPTool Provides End-to-End System Modeling Capability for Nuclear Electric Propulsion 107

Space Experiments 108
Surface-Tension-Driven Convection Experiment Prepares for Reflight 108
Space Acceleration Measurement System To Fly on Mir 110
Advanced Diagnostic Instrumentation Enhances Combustion Science in Microgravity 111

Experiments Simulate Low-Gravity Flame in Normal Gravity 113
Pool Boiling Experiment Has Successful Flights 113
Solid Surface Combustion Experiment Performs Well 114
Thermal Energy Storage Experiments Readied for Shuttle Launch 115

Advanced Space Analysis 117
Combined Lander and Instrumented Rover Concept Defined 117
Transfer-Orbit Plasma Interaction Experiment Developed 118

Space Station

Systems Engineering and Integration 120
Orbiting Vehicle Shadowing and Power Analysis Computer Programs Integrated 120

Photovoltaic Power Modules 121
Space Station Plasma Contactor Developed 121
Photovoltaic Power Module Neutral Buoyancy Tested 122
FASTMast Fiberglass Flexible Battens Hypervelocity Particle Impact Tested 124
Hypervelocity Impact Fails to Induce Arcing and Kapton Pyrolization in a Plasma Environment 125
Nickel/Hydrogen Battery Cells Selected for Space Station 126
Nickel/Hydrogen Battery Orbital Replacement Unit Tested 128
Battery Charge/Discharge Unit Bilateral Converter Developed 129

Electrical Systems 129
Electric Power System Operations Automated 129

Operations 131
Power Systems Facility Modified for Photovoltaic Power Module Assembly and Testing 131
Solar Array Electrical Simulator Developed 132
Cryosystem Becomes Operational at Space Power Facility 133

Engineering and Computational Support

Electronic and Control Systems 135
Electromagnetic Interference Test Facility Operated Successfully 135
Directional Electrostatic Accretion Process Developed 136

Structural Systems 137
TROPIX Spacecraft Needs Dynamic Analysis 137
Deployable Solar Array Mast for Space Station Strength Tested 138

Computational Support 139
LIBRA Is Software Architecture for an Electronic Library 139
Compact Experimental Data Analysis and Reduction System Developed 140
Lewis Advanced Cluster Environment Installed 141
Telecommuting With ISDN Studied 141
Lewis Advanced Communications Testbed Built 142
NASA Lewis Starts High-Performance Computing K–12 Project 142

Lewis Research Academy

Turbomachinery Flows Modeled 144
Adverse-Pressure-Gradient Boundary Layer Transition Analysis Incorporates Viscous Effects 144
Computational Aeroacoustics Studied 145
Analysis Predicts Refractive Index Effects on Radiation Heat Transfer in Semitransparent Materials 146
New Computational Techniques Predict Energy of Defects 148

Technology Transfer and Utilization

Technology Transfer 149
Carbide Site Competition Epitaxy Disclosed to Three Companies 149
Turbomachinery Design and Analysis Codes Transferred to Smaller Engineering Companies and Consultants 149
Icing Computer Codes Support Industry's Stated Needs 150
Fiber Optic Probe Detects Cataracts 151
Ion Exchange Membrane Purifies Water 152
Tribometer (Pin-on-Disk Wear Testing System) Marketed Commercially 153
CARES Software Boosts Industrial Competitiveness 153
Company Uses Reliability/Cost Analysis Methods Developed at NASA and Saves $1.1 Million 155
Photovoltaic Power System Tested for Use in Antarctica 156
Diamondlike Carbon Coatings Protect Sunglass Lenses 156
SCORE Integrated Circuit Marketed Commercially 157

Technology Utilization 158
EMI Shielding Materials Being Developed 158
Automobile Antennas Characterized and Improved 158
U.S. Competitiveness in Die Casting Industry Improved 159
Microwave Radiation of Bone Tumors Investigated 159
Sensor-Driven Rehabilitation Equipment Used in Hospitals 159
Innovative Technology Transfer Initiatives Begun 160
Space Act Agreement Signed With GLITeC 160

Author Index 161

Aeronautics

Aeropropulsion Analysis

Graphical User Interface Eases Aircraft Mission Analysis

Complex engineering problems, such as aircraft mission analysis, often require a large number of inputs and outputs involving very different disciplines. Understanding and defining all these inputs and outputs can be a difficult task even for experienced engineers. This problem can be simplified with a graphical user interface. The interface allows the user to quickly obtain information about all of the input values, eliminating the need to use documentation that is sometimes hard to find and often out of date. The interface also allows the user to quickly examine the output data, both by editing the output file and by graphing the results. The ease with which this can be performed with the graphical user interface reduces the time required to interpret results and find errors.

XFLOPS is a graphical user interface that has been developed for the NASA Langley mission analysis code FLOPS. The purpose of XFLOPS is to make FLOPS easier to use, both in inputting data and in analyzing results. Data input is made easier through the use of input windows for each of the FLOPS namelists. These windows contain fields to input each individual variable along with information that describes it. Analyzing the results has been made easier through quick display of the output data: First, the output file has been indexed, enabling particular sections to be analyzed quickly by the push of a mouse button. Second, menu picks have been created that allow the user to plot engine and aircraft performance data. Program execution is controlled through a pulldown menu system. Additionally, the user interface has a built-in help system and complete on-line documentation for FLOPS.

XFLOPS was written to work only as a preprocessor and a postprocessor; there are no direct ties between it and FLOPS. When running FLOPS,

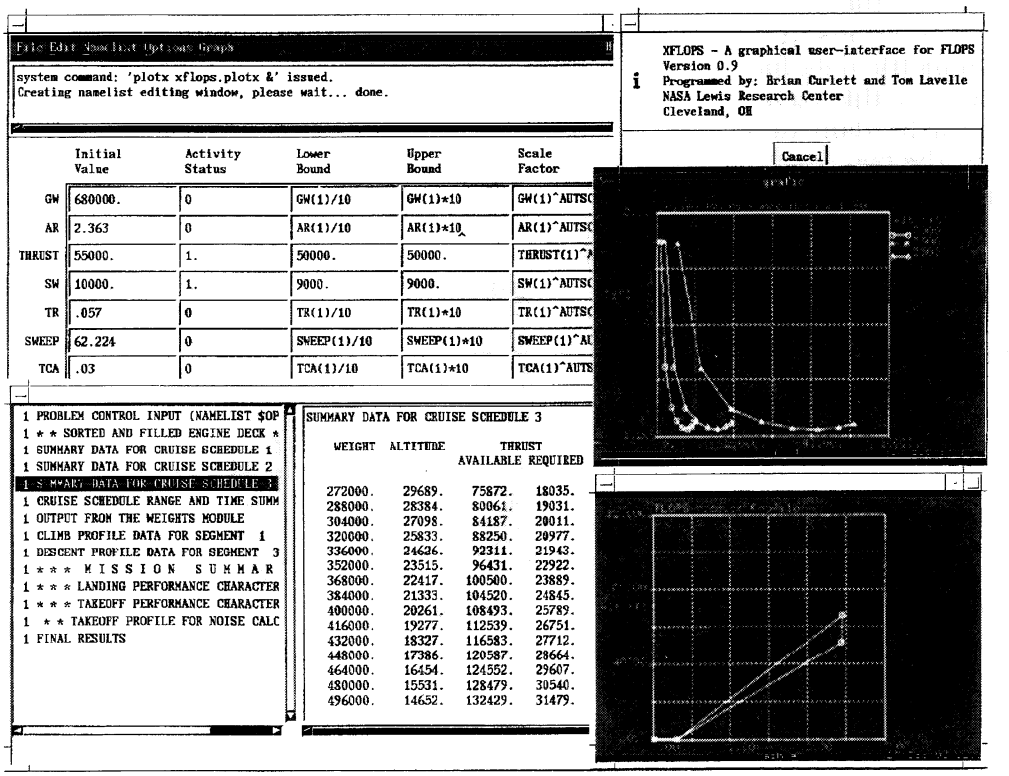

XFLOPS window displaying input and output.

XFLOPS outputs a standard FLOPS input file and executes the batch version of FLOPS. When analyzing results, XFLOPS reads in a standard FLOPS output file. As a result of this structure, XFLOPS can be used with preexisting input and output FLOPS files.

Lewis contact: Thomas M. Lavelle, (216) 977–7042
Headquarters program office: OA

New Method Accurately Predicts Two-Dimensional Nozzle Supersonic Drag

Axisymmetric and two-dimensional nozzles are being studied in the High-Speed Research Program for use on next-generation supersonic transport aircraft. As part of these conceptual and preliminary design studies the external aerodynamic drags of these two nozzle types must be computed to compare the two configurations. The goal of the present study was to identify an accurate method for predicting nozzle drag at supersonic speeds.

Because experimental data are lacking for two-dimensional nozzles, previous nozzle drag studies had attempted to convert these nozzles into equivalent-area axisymmetric configurations in order to utilize the existing axisymmetric data for predicting nozzle drag. The accuracy of this technique is questionable because of the fundamental differences in the flow fields about the two nozzle types. Consequently, an alternative method, the CCWD code, was evaluated. The CCWD code is based on supersonic linear theory and formulated to capture the effects of two-dimensional geometries (ref. 1). The accuracy of axisymmetric and CCWD analyses was evaluated relative to results from three-dimensional Euler solutions. Euler solutions are not yet practical for use directly in conceptual and preliminary design studies.

Euler calculations show that the two-dimensional nozzle drags are consistently larger than the drags predicted by the equivalent-area axisymmetric method. The drag differences ranged from 19 percent at Mach 1.2 to 36 percent at Mach 2.4. The CCWD method predicts wave drag for the two-dimensional nozzles significantly better than the axisymmetric method. The errors relative to the Euler method are less than 1 percent at Mach 1.2 and 12 percent at Mach 2.4 for CCWD as compared with 19 and 36 percent, respectively, for the equivalent-area axisymmetric method. Because of its relative ease of use and its improved accuracy over the equivalent-area method, CCWD is an appropriate choice for calculating two-dimensional nozzle external drag in the High-Speed Research Program.

The effect on required engine net thrust of this more accurate nozzle drag calculation method is significant for mission studies. These calculations assume fully expanded nozzles at both Mach 1.2 and 2.4. The higher drags predicted by the CCWD method are equivalent to 1.2 percent of net thrust at Mach 2.4 and 1.8 percent at Mach 1.2. Mission studies indicate that this adjustment translates into an increase in aircraft takeoff gross weight of approximately 1 percent.

Reference

1. Craidon, C.B.: User's Guide for a Computer Program for Calculating the Zero-Lift Wave Drag of Complex Aircraft Configurations. NASA TM–85670, 1983.

Lewis contact: Joseph M. Holcomb, (216) 977–7040
Headquarters program office: OA

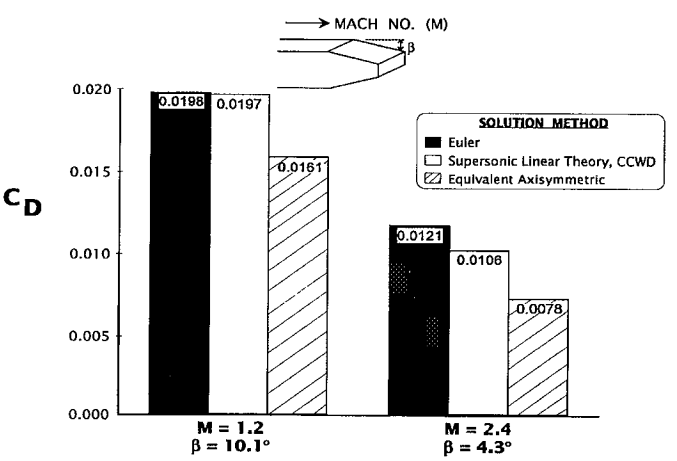

Two-dimensional nozzle external aerodynamic drag.

Instrumentation and Control Technology

Thin-Film Resistance Strain Gage Developed for High-Temperature Applications

In the work to design and develop hypersonic aerospace vehicles and advanced gas turbine engines, there is an urgent need for a strain gage that can provide accurate static strain measurements to validate the design codes. The temperatures on the leading edges of a hypersonic vehicle or an engine turbine blade may exceed 1000 °C (1830 °F). The required accuracy and maximum use temperature exceed the capability of present commercial resistance strain gages.

Work at the NASA Lewis Research Center to develop a high-temperature strain gage has emphasized the palladium–13 wt% chromium (PdCr) alloy. This PdCr alloy was selected by United Technologies Research Center under a NASA contract to be the best candidate material for high-temperature strain gage applications. It is structurally stable at elevated temperatures, and its apparent strain-versus-temperature characteristic is linear, repeatable, and not sensitive to heating and cooling rates. However, it has a higher (but constant) temperature coefficient of resistance and insufficient oxidation resistance. Therefore, efforts were undertaken in-house to develop a temperature compensation technique for minimizing the temperature effect on the gage's resistance change and to develop an enhanced overcoat for protecting the gage systems against oxidation.

A temperature-compensated, coated PdCr-based wire gage thus fabricated has been demonstrated to work reasonably well up to 800 °C (1475 °F). However, the impurities in the PdCr gage wire cause a phase change at approximately 815 °C (1500 °F), limiting the maximum use temperature to approximately 800 °C (1475 °F). A PdCr-based, thin-film gage has been developed for higher temperature applications. The PdCr thin-film gage is fabricated from a PdCr target that has a much higher purity than the wire, eliminating the phase change that occurs in the wire and allowing its use at higher temperature. In addition, the thin-film gage is minimally intrusive to the measurements and is therefore preferred in the harsh testing environment.

The PdCr temperature-compensated, thin-film gage was fabricated on an alumina ceramic bar. The compensator element is a platinum thin film located around the gage grid. The gages were fabricated by sputter-deposition, photolithography, and chemical etching techniques. The lead wires connecting to the measurement instruments are attached to the thin-film gage by parallel gap welding. The strain sensitivity (or gage factor) of this compensated thin-film gage is approximately 1.3 at room temperature and

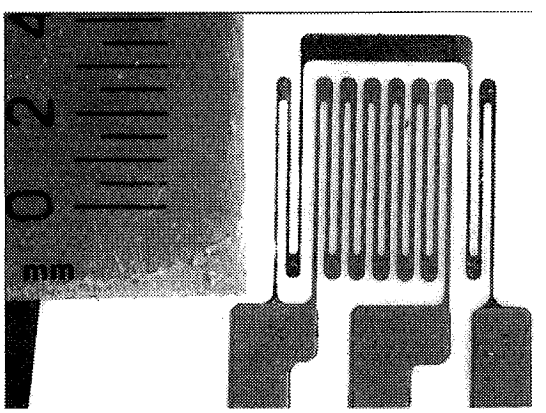

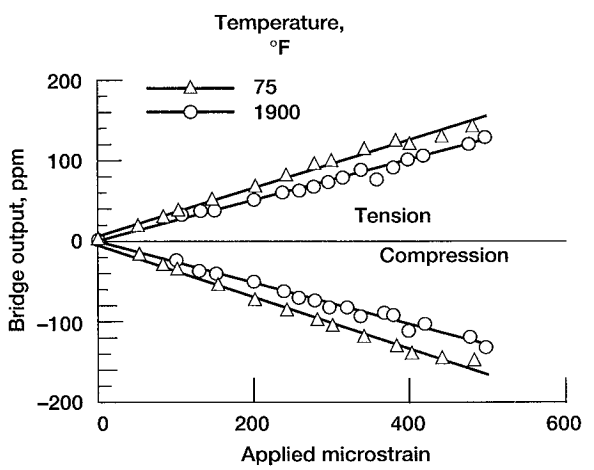

PdCr temperature-compensated, thin-film gage sputter deposited directly on an alumina bar (top) and response to mechanical load (bottom).

decreases only approximately 22 percent from room temperature to 1040 °C (1900 °F). The gage is stable and responds linearly to the mechanical loads even at 1040 °C (1900 °F). The apparent strain of the gage changes by approximately 1500 microstrain with a repeatability of approximately 200 microstrain between thermal cycles to 1040 °C (1900 °F). This is the first thin-film resistance strain gage demonstrated to this very high temperature.

Work is in progress to fabricate a denser, pinhole-free alumina insulating film. This film is needed as a base coat to provide enough resistance to ground for gages on the metallic substrates. Gages thus fabricated will be characterized on various metallic substrate materials for a longer period of time.

Lewis contacts: Dr. Jih-Fen Lei, (216) 433–3922;
Dr. W. Dan Williams, (216) 433–3725
Headquarters program office: OA

Optical and PdCr Strain Gages Comparison Tested

NASA Lewis has been engaged in an ongoing effort to develop both contacting and noncontacting methods of measuring strain at a point. The measurement systems are intended for use on test specimens subject to hostile environments, such as those found in aeronautical and Earth-to-orbit propulsion systems. This parallel effort has focused on strain gages attached to specimens and on laser-based optical systems that require no specimen surface preparation.

The optical system is based on the laser speckle-shift strain measurement technique of Yamaguchi, which utilizes the linear relationship between surface strain and laser speckle shifts in the Fraunhofer diffraction plane. This technique accurately measures surface strains in the presence of rigid-body motions of the specimen. The optical system is very stable and requires no periodic adjustment, once initially aligned. Uniaxial strains have been measured beyond 750 °C, and two principal strains have been measured at 650 °C (refs. 1 and 2).

The PdCr strain gage consists of a fine wire of a palladium–13 wt% chromium alloy and an all-platinum wire acting as a temperature compensator. The alloy wire and the compensator wire form two arms of a Wheatstone bridge. The resistance change with temperature of each arm is designed to be the same, thereby minimizing the effect of temperature on the measurement. The gage is mounted to the substrate by a ceramic flame spray technique. The flame-sprayed gages can be used to approximately 800 °C (ref. 3).

Temperature	Laser	PdCr
	Young's modulus, Mpsi (GPa)	
Room	32.2 (221)	31.1 (214)
600 °C	25.7 (177)	26.2 (181)

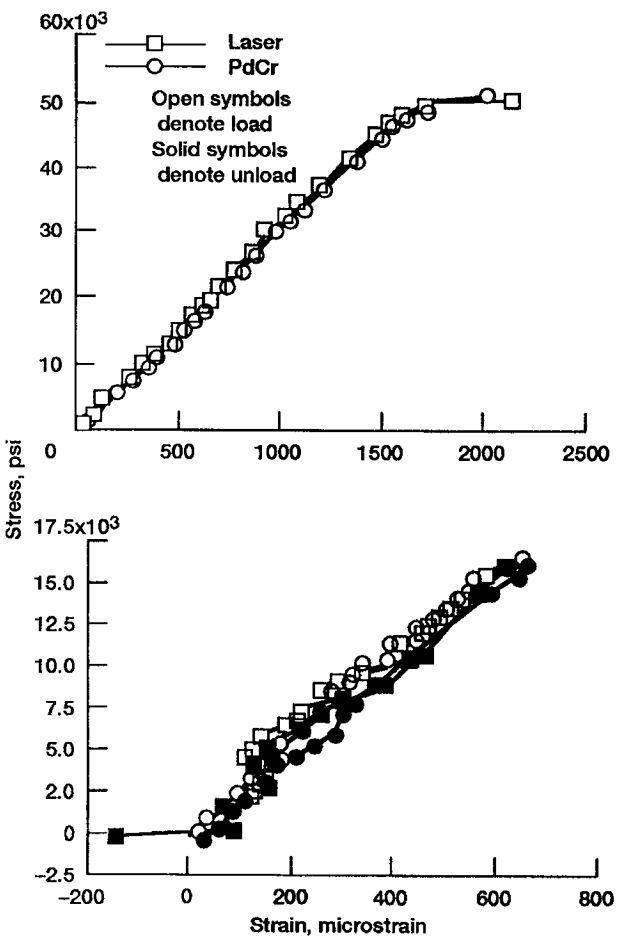

Comparison between laser speckle strain system and PdCr electrical resistance strain gages at room temperature (top) and at 600 °C (bottom).

The strain gage was mounted to a flat specimen of IN600 high-temperature alloy. Tensile tests were conducted at room temperature and at 600 °C. Analysis of the data shows excellent agreement in the value of Young's modulus at room temperature (better than 3 percent) and at 600 °C (better than 2 percent).

References

1. Barranger, J. P.; and Lant, C. T.: Progress in High Temperature Speckle-Shift Strain Measurement System. NASA TM–103255, 1990.

2. Lant, C.T.: Advanced One-Dimensional Optical Strain Measurement System–Phase IV. NASA CR–191184, 1992.

3. Lei, J.-F.: High Temperature Static Strain Measurement With an Electrical Resistance Strain Gage. AIAA Paper 92–5039, 1992.

Lewis contacts: Dr. John P. Barranger, (216) 433–3642; Christian T. Lant, (216) 433–1084; Dr. Jih-Fen Lei, (216) 433–3922

Wave Rotor Model Validated

The wave rotor is being investigated for use as a core gas generator in future multispool gas turbine engines in order to achieve high peak cycle temperatures and pressures. The device uses unsteady waves to transfer energy directly to and from the working fluid through which the waves travel. It consists of a series of constant-area passages that rotate about an axis. Through rotation the ends of the passages are periodically exposed to various circumferentially arranged ports in which the flow is steady, but which initiate unsteady waves within the passages. Because of the unsteady nature of the device, each passage of the wave rotor is periodically exposed to both hot and cold flow over roughly equal time periods. The mean temperature of the rotor material may therefore be expected to remain considerably below the peak cycle temperature. This characteristic, the low rotational speed, and the lack of any "blade loading" stresses give the wave rotor several potential advantages over conventional gas generators.

A model has been developed that follows a single passage of the wave rotor as it is exposed to the various ports at either end. The tube is assumed to have uniform properties at any cross section (i.e., one-dimensional flow), and the gas is assumed to be calorically perfect. The model is capable of assessing losses induced by viscosity, heat transfer to and from the passage walls, the finite opening time of the passage as it enters and exits port regions, and gas leakage between the passage ends and the walls or port manifolds to and from the cavity in the rotor center.
Among other validation tests the model has shown excellent agreement with the results of a simplified wave rotor (a wave divider) experiment being conducted here at NASA Lewis.

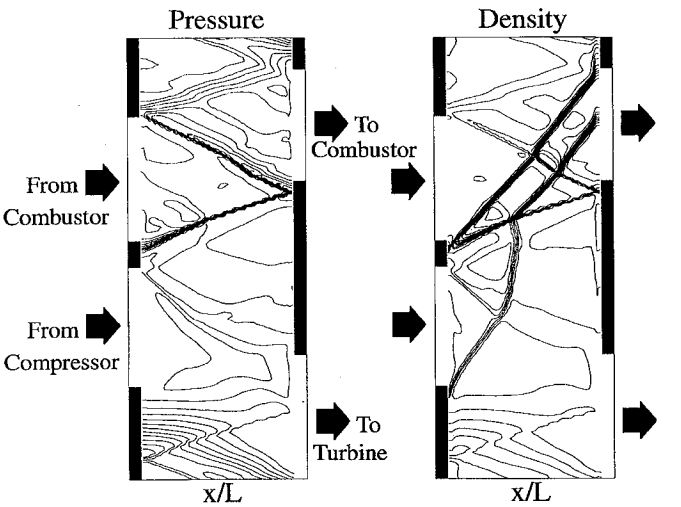

Computed pressure and density contours in a wave rotor passage.

The model has been used to design a four-port wave rotor core for a subsonic engine planned for entry into service in the year 2015. Preliminary results indicate that the wave rotor can readily meet the aero/thermodynamic requirements and maintain a mean passage wall temperature approximately 800 °R below the peak cycle temperature.

Bibliography

Paxson, D.E.: Comparison Between Numerical Modeled and Experimentally Measured Loss Mechanism in Wave Rotor. NASA TM–106279, 1993.

Lewis contact: Daniel E. Paxson, (216) 433–8334
Headquarters program office: OA

2000-V Silicon Carbide PN Junction Diodes Improved Through Chemical Vapor Deposition Epitaxy

The High-Temperature Integrated Electronics and Sensors (HTIES) Program is currently developing a family of silicon carbide (SiC) semiconductor devices for use in high-temperature, high-power, and/or high-radiation conditions where conventional semiconductors (such as silicon and gallium arsenide) cannot operate. In addition to numerous important aerospace-related applications, such as propulsion control, power control, radar and communications, and radiation-hardened circuits, a family of hostile-environment integrated electronics and sensors would find numerous important spinoff applications in the Earth-bound commercial power and automobile industries.

The purity and quality of the semiconductor crystal are critical factors limiting the performance and capabilities of semiconductor devices. The NASA Lewis HTIES group has recently developed a new chemical vapor deposition (CVD) growth process that consistently and reproducibly yields the highest purity single-crystal SiC epilayers reported to date. This growth process, for which a patent application has been submitted, has already been transferred to several U.S. companies active in silicon carbide electronics technology, and the process is already being used to develop prototype SiC devices.

At NASA Lewis the new CVD growth process has been employed in fabricating 6H–SiC PN junction diodes that exhibit record-breaking electrical characteristics. The 2000-V blocking voltage of these diodes at room temperature represents the highest blocking voltage ever reported in an SiC diode, surpassing the largest value previously reported by 600 V.

This advancement is primarily due to the improved purity of the 24-μm-thick n-epilayer (see cross section) that the new CVD growth process makes possible. The controlled incorporation of n- or p-type dopant impurities in concentrations as low as 10^{15} cm^{-3} has been accomplished with the new growth process, representing an order-of-magnitude improvement in controlling SiC doping.

As evidenced by these record-setting diodes the improved-quality SiC offered by the NASA Lewis growth process will greatly enhance the electrical performance of SiC-based devices and circuits.

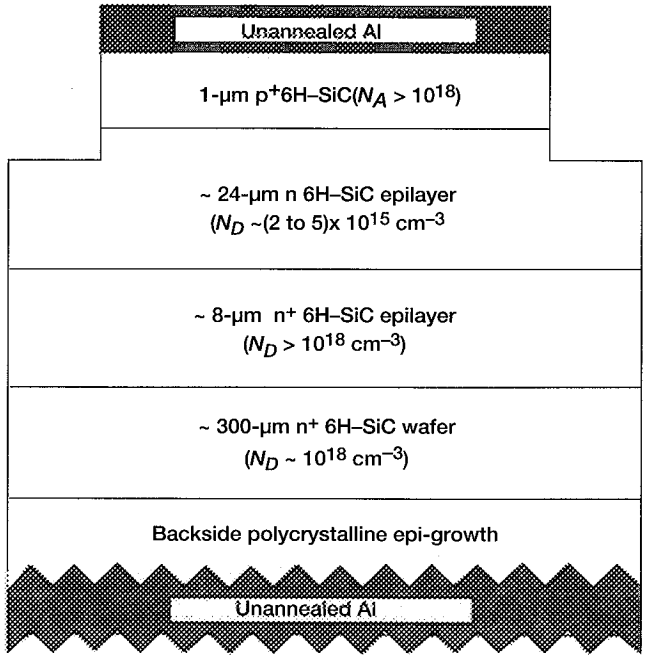

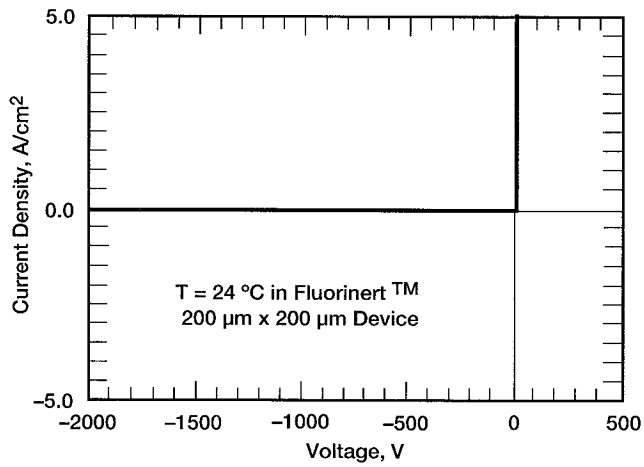

PN diode cross section (top), where N_A is acceptor concentration and N_D is donor concentration, and diode rectifying characteristics (bottom).

Lewis contacts: Dr. Philip G. Neudeck, (216) 433–8902; Dr. David J. Larkin, (216) 433–8718; J. Anthony Powell (216) 433–3652; Dr. Lawrence G. Matus, (216) 433–3650
Headquarters program office: OA

Integrated Flight/Propulsion Controls Design Developed and Evaluated for STOVL Aircraft Concept

A 66-month integrated flight/propulsion controls (IFPC) design study by General Electric Aircraft Engines (GEAE) and Lockheed Fort Worth Company (LFWC) was recently concluded under a joint contract program sponsored by NASA Lewis Research Center and NASA Ames Research Center. The objectives of the program were to develop an IFPC design for an ejector-augmenter, short-takeoff, vertical-landing (STOVL) aircraft configuration and to evaluate the resulting IFPC design in piloted simulations at Ames Vertical Motion Simulator Facility. The aircraft configuration selected for the study was the LFWC E7–D supersonic STOVL airframe with a GEAE F110 powerplant. The multiple control effectors on the aircraft and the significant interaction between the airframe and the propulsion system at low speeds made for a challenging IFPC design problem.

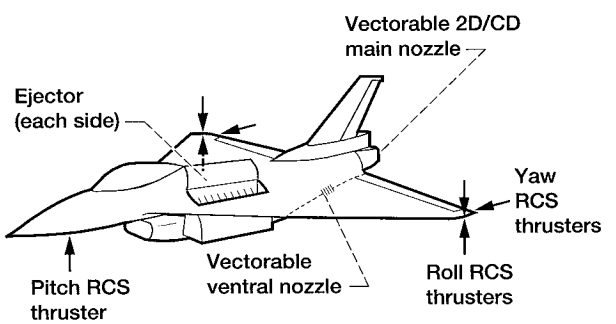

Control effector for E7–D aircraft.

The IFPC design approach used in this program was the decentralized, hierarchical Design Methods for Integrated Control Systems (DMICS) approach. This approach is hierarchical in that a mission-level control design (flight control) that addresses mission requirements is first designed assuming actuator characteristics for the function-level subsystem (propulsion subsystem). Performance specifications for the propulsion subsystem are generated by using the mission-level design, and these are used in designing the propulsion control system. The DMICS procedure is decentralized in that the mission-level and subsystem-level control designs are generated separately.

The IFPC design was developed for subsonic cruise (aerodynamic lift and control), transition (combined aerodynamic and propulsion lift and control), and hover (propulsive lift and control) flight modes. Extensive design iterations were required, with two major unsuccessful attempts at piloted evaluations, before the integrated system performance and stability requirements were met. Fixed-base piloted evaluation at Ames of all operating modes for the final IFPC design was completed in November/December 1992, and piloted evaluation for hover mode was completed on the vertical motion simulator in December 1992. The transition and cruise modes were not tested on the simulator because of an unresolved deficiency in the IFPC design. Evaluations were conducted by pilots from LFWC and NASA Ames and Lewis, and pilot ratings of 2 to 6 on a Cooper-Harper scale (levels I and II flying qualities) were obtained for various precision hover tasks. Pilot/vehicle interface issues had a significant effect on the flying quality ratings. A low-displacement force stick was used in the piloted evaluations to make the cockpit compatible with

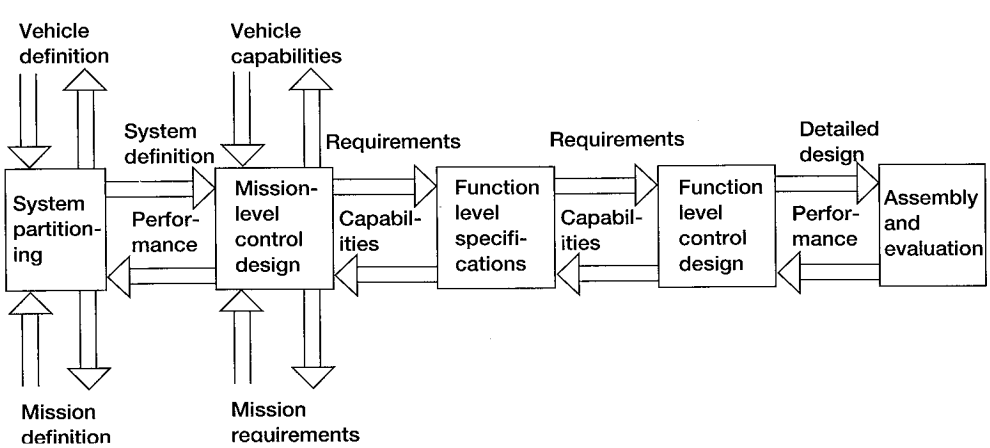

Decentralized, hierarchical DMICS design process.

advanced fighter cockpits. The force stick required the pilots to maintain a steady force in approaching a ship at a constant speed. This resulted in high pilot workload and consequent degradation in pilot ratings.

Although the decentralized, hierarchical DMICS design process is a viable procedure for designing IFPC systems for complex aerospace vehicles such as STOVL aircraft, further development of methodology is warranted to avoid excessive control design iterations. A significant lesson learned from the program was that high-fidelity piloted evaluations should be used as a design tool during the IFPC design development rather than just for evaluating the IFPC design at the end of the design effort.

Lewis contact: Dr. Sanjay Garg, (216) 433–2355
Headquarters program office: OA

Drag Probe Utility Extended to Supersonic Flow

The drag force anemometer, or drag probe, is an instrument originally devised by Krause and Fralick for measuring subsonic flow parameters. It has shown promise in a wide range of applications and is being used now in supersonic flow, where it is difficult to obtain data nonintrusively owing to the presence of shocks.

The drag probe functions by measuring the drag on a flat, cantilevered beam exposed to a flow field. The drag is obtained by measuring the flow-induced strain in the beam with strain gages. The drag force produced by the flow impinging onto this beam can be found from fluid mechanics principles. The relationship between measured strain and the drag force depends on the beam's elastic behavior. A control volume around the drag force imparted on the beam is proportional to $\rho u^2 A/2$. This instrument can thus yield the drag force per unit area or kinetic pressure $\rho u^2/2$ if the constant of proportionality, the drag coefficient C_D, is known.

Inserting this probe into a supersonic flow stream causes a shock to form. To thus apply this probe, which operates in the subsonic flow regime, the flow parameters in the supersonic region ahead of the probe must be related to the subsonic conditions at the probe. The following relation exists

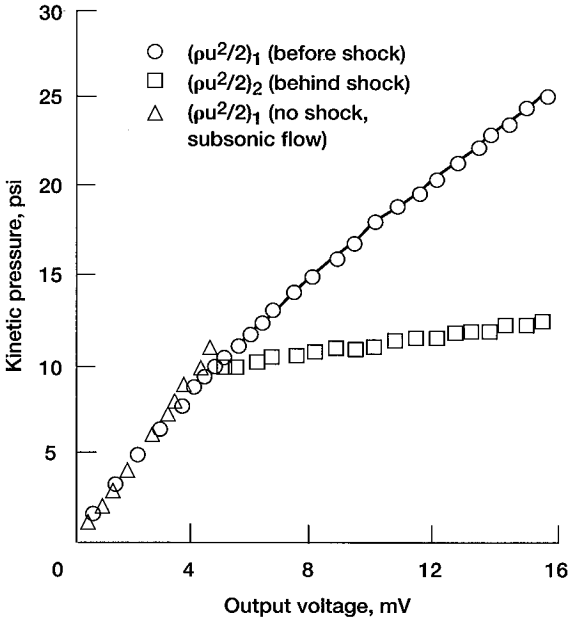

Drag probe calibration curve.

between the supersonic and subsonic kinetic pressures:

$$\left(\frac{\rho u^2}{2}\right)_2 = \frac{\gamma-1}{\gamma+1}\left(\frac{\rho u^2}{2}\right)_1 + \frac{\gamma}{\gamma+1}p_1$$

where

ρ density
u actual velocity
γ specific heat ratio
p pressure

This equation says that measuring $(\rho u^2/2)_2$ behind the shock (subscript 2) with the drag probe and knowing p_1 allows $(\rho u^2/2)_1$ ahead of the shock (subscript 1) to be inferred. This relationship allows a subsonically calibrated drag probe to be said to be supersonically calibrated as well. Other flow quantities can also be directly computed from measured quantities, for instance, the Mach number ahead of the shock

$$M_1 = \sqrt{\frac{(\gamma+1)\dfrac{\rho_2 u_2^2}{\gamma p_1} - 2}{\gamma - 1}}$$

Lewis contacts: Jacques C. Richard, (216) 433–3739; Gustave C. Fralick, (216) 433–3645
Headquarters program office: OA

Internal Fluid Mechanics

Interaction of Turbulence With Stagnation-Region Heat Transfer Studied

Heat transfer to a stagnation region is important in many engineering applications. Nowhere, however, is it more critical than in the gas turbine, where combustor exit temperatures often exceed the melting point of superalloy turbine airfoil materials. In most cases the highest heat transfer rate on a turbine airfoil occurs in the stagnation region, thus making it critical for the design of cooling schemes to obtain an accurate prediction in this region.

The heat transfer in the stagnation region can be calculated for a laminar free stream if the pressure distribution is known. Free-stream turbulence can augment stagnation-region heat transfer above laminar levels; ratios of turbulent-to-laminar heat transfer as high as 1.7 have been measured. In a gas turbine the stream of combustion products approaching an airfoil is not laminar; turbulence intensities of 11 percent have been measured at the exit of a combustor.

Although it has been known for many years that free-stream turbulence can augment stagnation-region heat transfer, results of experiments are inconsistent and attempts to correlate heat transfer augmentation as a function of turbulence intensity and Reynolds number while ignoring the length scale have not been entirely successful. Any resulting correlations usually predict the author's data but not data from other researchers.

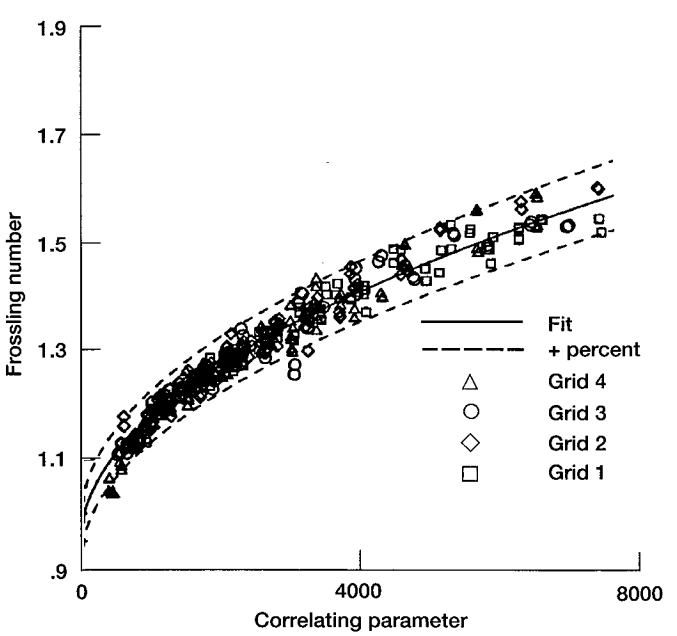

Stagnation-point heat transfer.

For the present study a model with a circular leading edge was fabricated with heat transfer gages in the stagnation region. The model was qualified in a low-turbulence flow by comparing measurements with an exact solution for stagnation-region heat transfer involving a laminar free stream. Several different grids were built to generate nearly isotropic turbulence with different length scales upstream of the heat transfer model.

Data were taken at cylinder Reynolds numbers ranging from 42,000 to 193,000. Turbulence intensities were in the range 1.1 to 15.9 percent, and the ratio of integral length scale to cylinder diameter ranged from 0.05 to 0.30.

Stagnation-point heat transfer that involved the turbulence parameters and Reynolds number compared well with the measured data. It was also discovered that the level of heat transfer augmentation above the laminar was nearly constant in the downstream direction up to the point of separation. Thus, the distribution of turbulent heat transfer downstream of the stagnation point can be predicted by using the laminar solution and the stagnation-point augmentation.

Lewis contact: Dr. G. James Van Fossen, (216) 433–5892
Headquarters program office: OA

Computation and Experiments Integrated

Aerospace component design requires the integration of volumes of information, generated from many sources, into a coherent understanding of component performance. These sources include experimental test facilities and computer models ranging from simple linear models to complex, nonlinear, multidimensional models. Currently, each source has its own specialized user

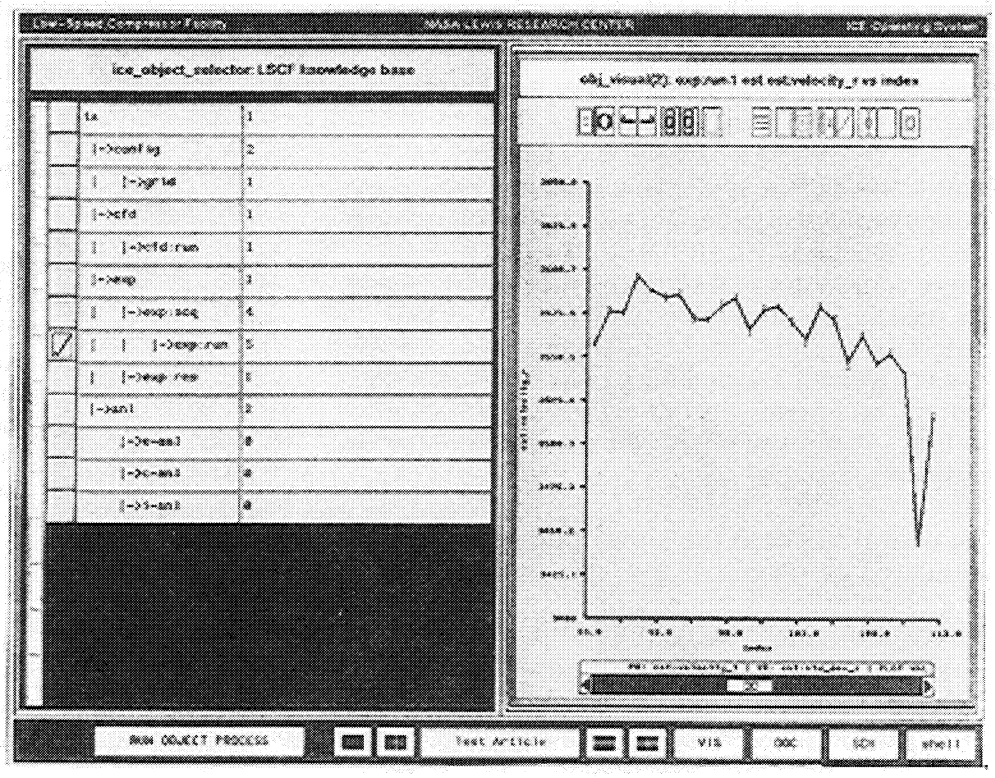

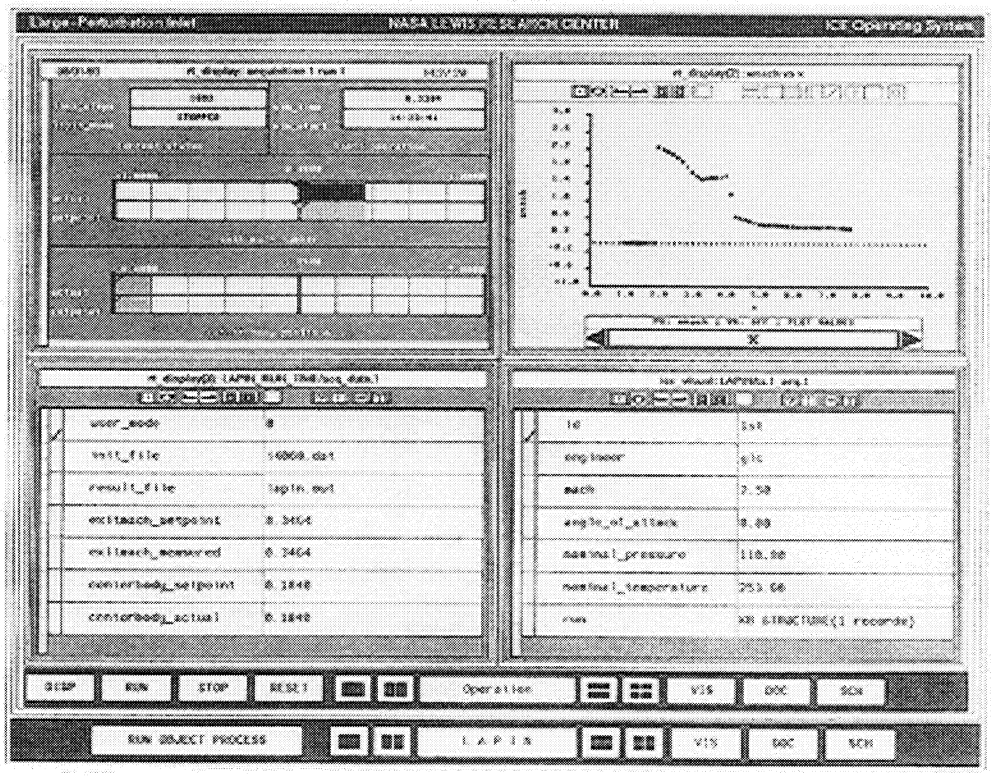

Typical ICE operational display (top) and ICE display from interactive high-speed civil transport inlet simulation (bottom).

interface, fostering operational confusion, and its own initialization and result formats, making it difficult to relate information. Also, tracking difficulties make it impossible to establish the pedigree of information, which must then be discarded. The Integrated Computation and Experiment (ICE) operating system is now available to provide operational and result integration of the design process. ICE currently runs on Silicon Graphics workstations.

ICE is capable of both managing the operation of information-generating processes and maintaining a common knowledge base for their results. It provides a common graphical user interface for process and information management. Included are initialization and control panels, static and dynamic plots (two and three dimensional) and table displays, knowledge-base search facilities, and documentation and editing services. To use ICE, it must be installed for a single purpose, such as the design facility for a class of aerospace components. This class becomes the root class of the knowledge base. It is fanned out into supporting information-generating processes to form the next level of the knowledge-base tree, etc. Each process is further broken down into argument and result classes. Class members can be simple, such as arithmetics or strings, or complex, such as data files, references to other knowledge elements, or other classes. Once designed, the knowledge base is specified as a text file, which in turn provides targeting information to ICE. Interface processes must also be written that serve as drivers between ICE and information-generating processes. ICE provides templates to support driver development.

Currently, ICE is being used to integrate the operation and results of an experimental compressor facility with a complementary three-dimensional fluid dynamics code. ICE provides forms for process initialization; run-time support by sampling real-time laser anemometry data, computing its statistics, and displaying the results; and off-line support for graphical analysis. The class structure of the knowledge-base tree and a typical operational display are shown. The root class is ta (test article), on the next level are config (configuration), cfd (fluid dynamics code), exp (experiment), and anl (analysis). Each of these levels is further broken down. By specifying the desired record number and selecting the class with the button on the left, the contents of the record will be displayed on the right side of the screen. That display shows an experimental velocity data file that is a member of the selected record.

ICE is also being used to provide a run-time interactive user interface to an unsteady simulation of a high-speed civil transport inlet. This application is also shown. In this case the shock position is displayed dynamically by using the Mach-number-versus x plot in the upper right quadrant. It is interactively adjusted by changing the exit Mach number and centerbody position, using the mouse and control panel in the upper left quadrant. The lower left quadrant is a record of dynamic run-time information. The lower right quadrant displays static initialization information from the knowledge base.

Bibliography

Babrauckas, T.L.; and Arpasi, D.J.: Integrated CFD and Experiments Real-Time Data Acquisition Development. ASME Paper 93–GT–97, 1993.

Lewis contact: Dale J. Arpasi, (216) 433–3612
Headquarters program office: OA

New Compressor Data Base Used as International Computational Test Case

In order to provide a forum for assessing the ability of turbomachinery computational fluid dynamics (CFD) computer codes to accurately predict the flow field in modern axial compressors, the American Society of Mechanical Engineers International Gas Turbine Institute (IGTI) Turbomachinery Committee has sponsored a turbomachinery CFD code assessment exercise in which CFD code developers were invited to run their codes for a blind test case.

Data from the NASA Lewis compressor Rotor 37 were selected to serve as the blind test case by the IGTI Turbomachinery Committee. Sufficient details of the geometry and the run conditions to perform a three-dimensional viscous CFD analysis have been distributed to over 40 respondents to the call for papers from around the world. Respondents are to submit their solutions of the blind test case by March 31, 1994, at which time they will be given the experimental data. A special session will be held at the IGTI Gas Turbine Conference in June 1994 at The Hague, Netherlands, where authors will present their results.

Data were acquired at the Rotor 37 design tip speed of 425 m/sec over a range of mass flow rates. Spanwise distributions of outlet pressure, temperature, and flow angle were measured. Laser anemometer measurements were also acquired on several blade-to-blade and cross-channel planes within and downstream of the rotor for the same operating conditions. The laser measurements provide insight into the rotor shock wave structure, tip clearance flow, and downstream wake mixing.

Lewis contact: Kenneth L. Suder, (216) 433–5899
Headquarters program office: OA

NASA Reacting-Flow, Navier-Stokes Code Developed for Combustor Calculations at All Speeds

A critical need for the aerospace industry is a robust, fast, and accurate predictive computational fluid dynamics (CFD) code for the design and analysis of propulsion system combustors. Such codes should properly simulate the fluid mechanics and chemistry of combustion chambers and be capable of rapid turnaround on mainframe computers or workstation networks.

The ALLSPD reacting-flow CFD code has been in development in-house for over two years and represents modern state-of-the-art computation technology packaged to calculate internal chemical reacting flows over a wide Mach number range for complex geometries. The code is designed to provide analysis capability to the designer of advanced propulsion devices, both airbreathing engines and rockets. Currently, ALLSPD is capable of calculating steady and unsteady two-dimensional and axisymmetric flows with combustion and employs a fully implicit coupled numerical approach. A modern k-ε turbulence model is used that has been developed by the Center for Modeling Turbulence and Transition at NASA Lewis. The code simulates liquid fuel sprays with a stochastic spray model. The combustion chemistry is currently a one-step kinetics model, but more complicated chemistry models can be inserted. The code has been run on the Lewis Cray-YMP as well as on IBM RS/6000 model workstations. The code development effort is ongoing with extension to three dimensions now being implemented. More complex and physically realistic models will be incorporated into the code in the future.

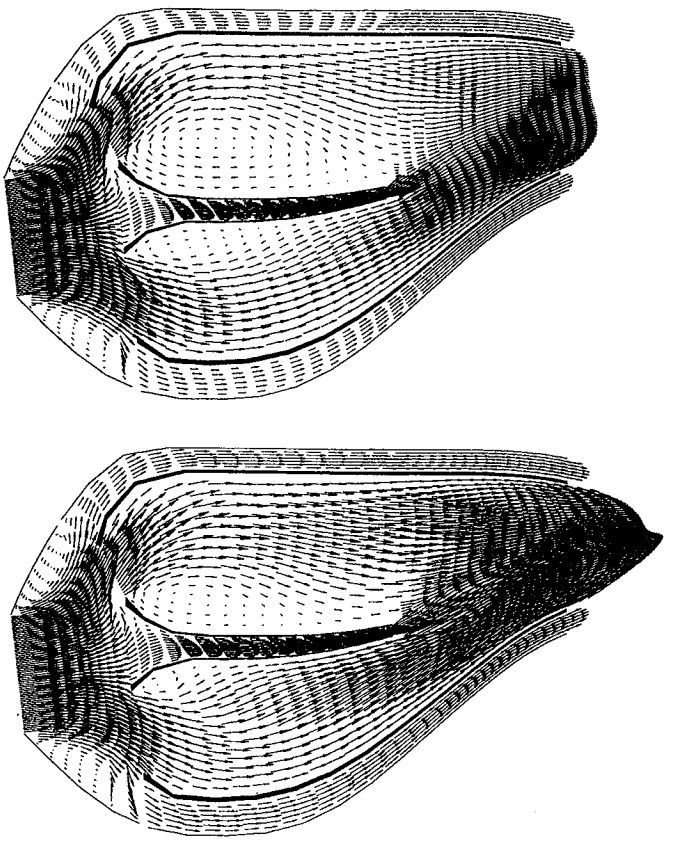

Velocity vectors for noncombustion (top) and spray combustion (bottom) cases for two-dimensional gas turbine combustor flow.

For example, a spray combustor case was calculated for an advanced annular gas turbine combustor. Although the combustor will require a three-dimensional computation, the geometry was simplified in order to utilize the axisymmetric capability of the two-dimensional version of the code. The computed velocity vectors were compared with a converged solution of the cold flow (nonspray/noncombustion) with the same flow conditions. The combustion zones were confined near the inner walls, mainly because swirlers were excluded at the inlet of the combustor domes. Without swirl, fuel-air mixing is relatively poor. The recirculation zones near the inner walls are the only device to hold the flame.

Bibliography

Mularz, E.J.; Bulzan, D.L.; and Chen, Kuo-Huey: Spray Combustion Experiments and Numerical Problems. NASA TM–106069, 1993.

Shuen, J.S.; Chen, K.H.; and Choi, Y.: A Time-Accurate Algorithm for Chemical Non-Equilibrium Viscous Flows at All Speeds. AIAA Paper 92–3639, 1992.

Lewis contact: Dr. Edward J. Mularz, (216) 433–5850
Headquarters program office: OA

Vortical Flows Studied for Improved Models of Vortex Generators

A vortex is a region of fluid flow rotating about a central point. As such, it has unique mixing properties beneficial to many fluids engineering applications. One such application is the control of boundary layer behavior in aircraft engine inlets, diffusers, and other associated internal or "duct" flow components. The root cause of poor performance in such components is excessive flow blockage due to boundary layer flow separation from the duct surface and secondary flow accumulation of boundary layer fluid. If a vortex is produced near the boundary layer through a device known as a vortex generator, the helical motion of the fluid in the vortex will force the high-energy fluid of the main flow into the slower moving fluid of the boundary layer. This mixing action aids in alleviating the aforementioned problems associated with the boundary layer.

Arrays of vortex generators are studied to determine what vortex generator size, spacing, and streamwise location produces optimum flow conditions in a particular duct. This can be done experimentally, as reported in reference 1. However, because of the large number of possible variations in vortex generator array parameters, optimization may be best suited for computational work. The effort required for a computational study hinges on the manner in which the vortex generators are represented in the analysis. A particularly effective approach is to model the shed vortex immediately downstream of the vortex generator, rather than the vortex generator itself. The advantage here lies in the fact that a newly formed vortex may be accurately represented as a streamwise vorticity or crossplane velocity distribution having a simple exponential form. This is the approach taken in the recent work reported in reference 2 where multiple vortex generator array geometries were examined in a diffusing S-duct by using a parabolized Navier-Stokes solver.

In an ongoing research program at NASA Lewis a set of experimental studies are being conducted to acquire the data base necessary for simple analytical modeling of all types of common vortex generators. Recently completed studies on the conventional, or "blade," type of vortex generator (ref. 3) and the low-profile "wishbone" generator (ref. 4) have provided detailed data sets for the modeling of these types of vortex generators over a limited Mach number and Reynolds number range. Future experiments will expand the data sets to cover a larger range of flow conditions, as well as examine other proven vortex generator designs. In conjunction with the experimental effort, computational studies of vortex generator flows are being planned. These studies have the goal of incorporating vortex generator models into three-dimensional Navier-Stokes solvers.

References

1. Reichert, B.A.; and Wendt, B.J.: An Experimental Investigation of S-Duct Flow Control Using Arrays of Low Profile Vortex Generators. NASA TM–106030, 1993.

2. Anderson, B.H.; and Gibb, J.: Applications of Computational Fluid Dynamics to the Study of Vortex Flow Control for the Management of Inlet Distortion. AIAA Paper 92–3177, 1992.

3. Wendt, B.J.; Greber, I.; and Hingst, W.R.: The Structure and Development of Streamwise Vortex Arrays Embedded in a Turbulent Boundary Layer. NASA TM–105211, 1991.

4. Wendt, B.J.; and Hingst, W.R.: Measurements and Modeling of Flow Structure in the Wake of a Low Profile 'Wishbone' Vortex Generator. To be presented at the 32nd AIAA Aerospace Sciences Meeting, Jan. 1994.

Lewis contact: Dr. Bruce J. Wendt, (216) 433–5906
Headquarters program office: OA

Interactive Design and Educational Tools for Supersonic Flows Completed

During the past five years the availability and computing power of desktop workstations and personal computers have mushroomed. Problems that previously required room-sized mainframe computers can now be solved on the desk top. Coupled with this growth in computing power has been the development of interactive graphical user interfaces (GUI's). The user can now more easily communicate with the computer by using a mouse and cursor to "push" buttons on a

cathode-ray-tube screen, and results can be presented to the user in colorful graphics. The new technology has been used in various applications from bank machines to home video games, but it is currently being applied to aerodynamics problems at NASA Lewis.

Two, highly interactive, design or educational tools for studying supersonic flows have been completed. The first package, called VU–INLT, is used to design and analyze the supersonic airflow into an inlet. The inlet must slow the flow down to subsonic speeds to feed a gas turbine engine—but must do so with a minimum of drag and with maximum pressure. Using VU–INLT the designer can manipulate the design of the various components of the inlet and watch the resulting change in geometry and airflow conditions interactively. This process leads to a better, faster, and therefore less expensive design cycle. Because the new package models and displays most of the phenomena present in supersonic inlets, it can also be used by students to learn basic inlet operation and design. The second package, called VU–1135, was derived from VU–INLT but is intended only as an undergraduate educational tool. VU–1135 solves the physics problem of supersonic flow past a ramp by using the equations developed in NACA 1135 (ref. 1). The student can interactively vary the angle of the ramp and the speed of the supersonic flow. The resulting shock waves or expansion fans are computed and graphically presented to the student. Various flow parameters are also presented numerically and with moving "thermometer" charts. The student can produce engineering plots of the variation of the parameters by interacting with the package as with a "desktop wind tunnel." A question-and-answer section leads the student to a better understanding of some of the interesting flow physics one encounters.

These tools are the first attempts at using the new computational technologies for interactive fluid dynamics. Future educational tools could present to the student a variety of physics problems including potential flows and basic airfoil problems. The design tool will be also extended to include more sophisticated analysis techniques. Both packages are available to the public, run

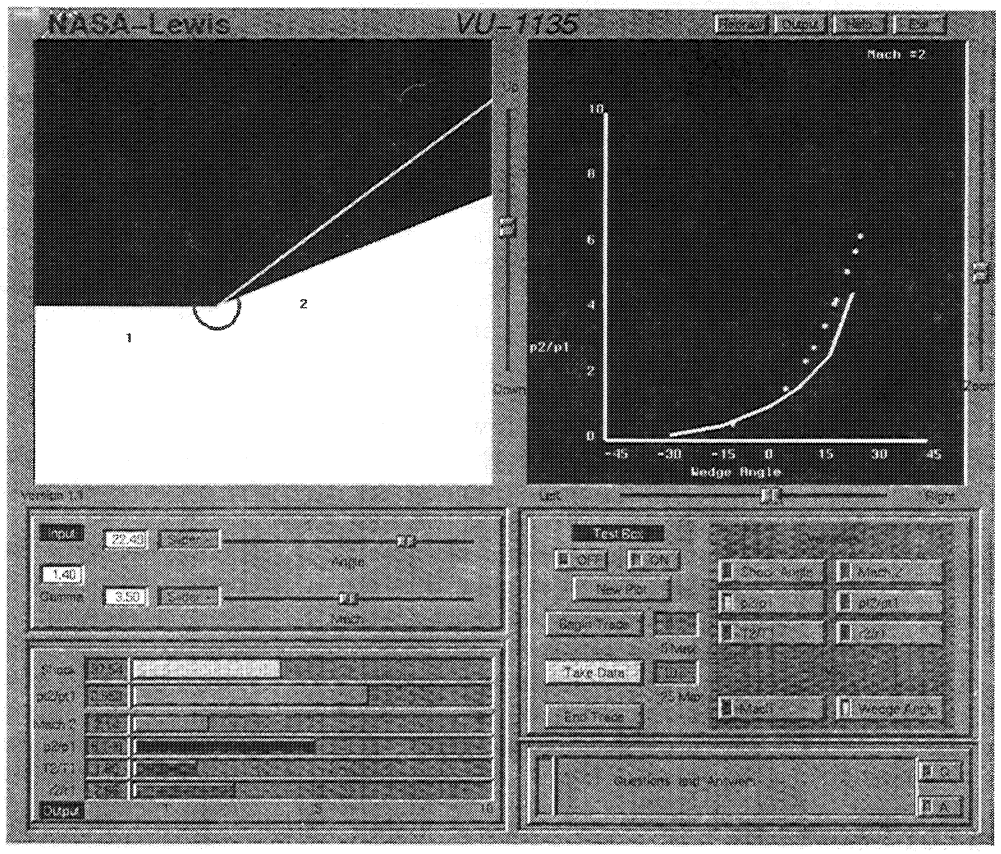

Screen dump from VU–1135.

on either Silicon Graphics or IBM RISC/7000 machines and employ the FORMS library of GUI's (ref. 2). Work is under way to port the packages to 486 PC's and Apple computers by using a different GUI package.

References

1. Equations, Tables and Charts for Compressible Flow. NACA Report 1135, 1953.

2. Overmars, M. H.: FORMS Library, A Graphical User Interface Toolkit for Silicon Graphics Workstations. Version 2.1, Department of Computer Science, Utrecht University, The Netherlands, 1992.

Lewis contact: Thomas J. Benson, (216) 433–5920
(e-mail, benson@ptah.lerc.nasa.gov)
Headquarters program office: OA

Propulsion Systems

Improved Ceramic Gas Turbine Components Fabricated and Tested

In order to exploit the high-temperature performance potential of the gas turbine engine without using strategic materials or exotic hot-section cooling techniques, NASA Lewis is working to develop a ceramic component technology base. As part of the U.S. Department of Energy's Automotive Gas Turbine Program, the Advanced Turbine Technology Applications Project is developing structural ceramic component technology for advanced small gas turbine engines. This research is focused on developing ceramic materials technology for uncooled hot-section components. The work is being conducted under contracts with Allied Signal Engines of the Allied Signal Aerospace Company and Allison Gas Turbine Division of General Motors Corporation. Ceramic component development is under way through subcontracts with U.S. ceramic companies.

Testing of ceramic components in hot rigs at engine operating conditions continued in 1993. U.S.-manufactured ceramic components were successfully tested at gas temperatures to 2500 °F.

Allied Signal Ceramic Components, Ceramics Process Systems, and Norton Advanced Ceramics Company developed second-generation improved silicon nitride and silicon carbide material systems while continuing to work to improve component quality, yield, simplicity, and cost effectiveness. In 1993 the Corning Company fabricated an extruded ceramic regenerator core with over 1000 cells per square inch, representing a more than doubling of the cell density relative to the baseline state of the art. The rectangular cell matrix meets engine performance criteria.

Testing at Allison has progressed from single components to an all-ceramic turbine stage including the turbine rotor and scroll-related static parts. The turbine rotors are silicon nitride, axial flow type with aerodynamic blades. Silicon nitride and silicon carbide scrolls have been tested. A silicon nitride turbine stage was tested for 100 hr over a test cycle that simulated in-vehicle operation from idle to full power including startup and shutdown. Testing included operation to 2500 °F and 100-percent speed.

Preparations are currently under way for a 300-hr cyclic durability test of an all-ceramic turbine stage to complete a major project milestone. The longest test to date logged 267 hr before rig failure. Although the ceramic rotor and scroll were broken, failure was due to overheating of the metal engine housing structure. Completion of the 300-hr test is planned for late 1993.

The Allied Signal 331–200 auxiliary power unit engine is being used to evaluate the long-term durability of ceramic components in an engine environment. The goals are to develop and demonstrate structural ceramic component technology for extended operation in a gas turbine environment. During 1993 the design and fabrication of first-stage ceramic blades and nozzle vanes, as well as the modifications to the metal structures, were completed. Short-term testing of the inserted ceramic blades and nozzle vanes for 100 hr was begun near the end of calendar year 1993.

Bibliography

Smyth, J.R.: Ceramic Gas Turbine Technology Development and Applications. ASME Paper 93–GT–361, 1993.

Lewis contacts: Paul T. Kerwin, (216) 433–3409;
Thomas N. Strom, (216) 433–3408
Headquarters program office: OA

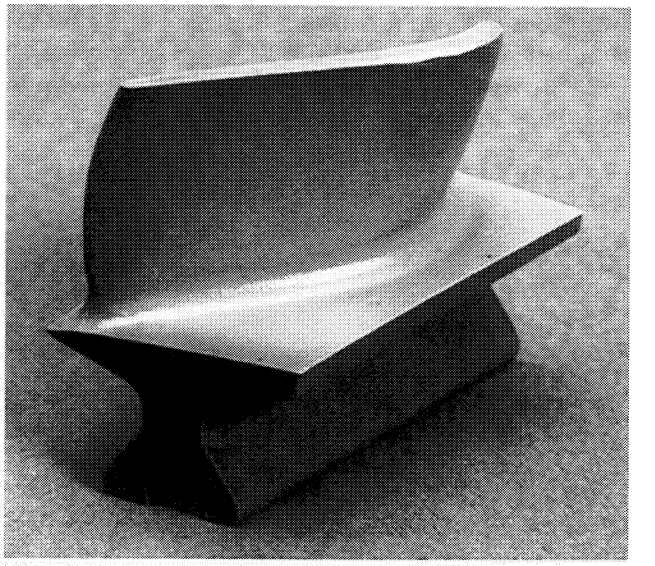

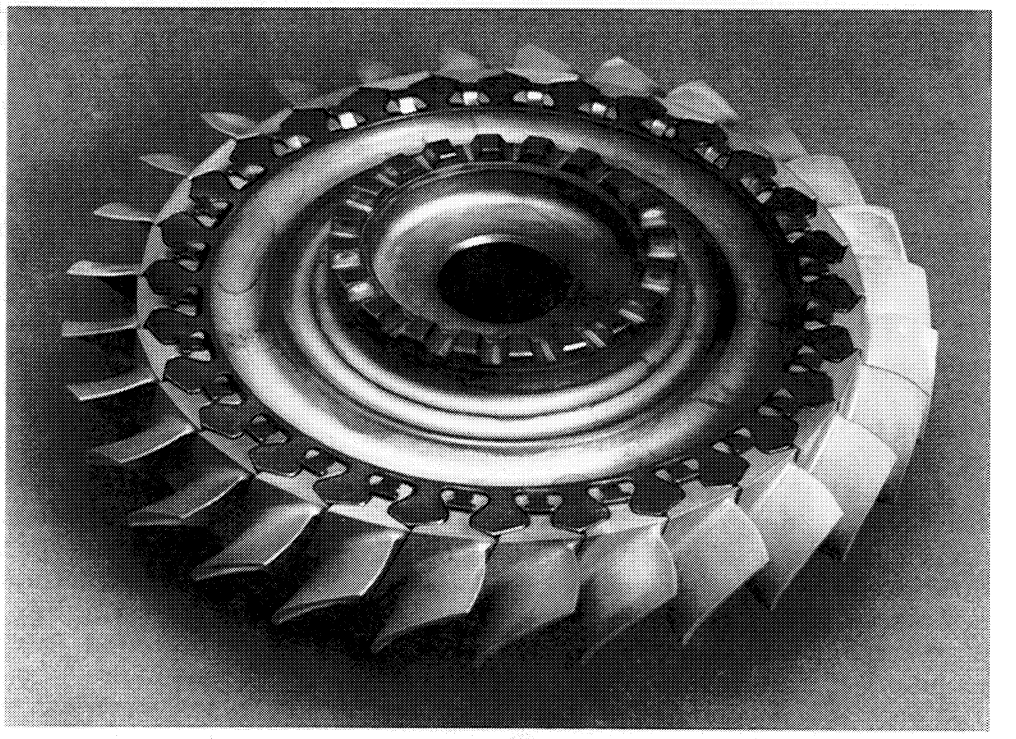

Ceramic silicon nitride blade (top) and blades installed in an auxiliary power unit turbine disk (bottom).

Reacting Flow Analyzed for Annular Small Gas Turbine Combustor

KIVA–II, a reacting-flow computational fluid dynamics flow code for problems involving turbulence and sprays, has been modified to examine a typical annular small gas turbine combustor. The combustor's airblast fuel injectors, cooling baffles, cooling slots, primary and dilution zone jets, and effusion cooling pads are all considered in this analysis. Turbulence is described by the standard k-ε model with wall functions, the combustion-turbulence interaction is considered by using a mixing-controlled combustion mode, and the evaporating fuel spray is treated with a stochastic spray model.

To reduce the time required to complete the analysis on NASA Lewis' Cray-YMP computer, only a 30° sector of the combustor was acutally considered. This sector mesh still contains 58,032 cells. Results of the computation include temperature, pressure, momentum, and species concentrations throughout the flow field.

Work continues on refinements to this analysis. Although not shown in the figures presented here, a reverse-flow duct immediately follows the downstream cooling slots in the actual combustor. A new grid incorporating this feature is currently being created and will be used in future calculations. A PDF combustion-turbulence model is being incorporated into KIVA–II and will also be employed in future analyses, as will a new reduced kinetic mechanism for Jet A combustion that considers both thermal and prompt oxides of nitrogen (NO_x) formation. (The mechanism in the present analysis treats only thermal NO_x formation.)

Bibliography

Cline, M.C.; et al.: Computation of the Flow Field in an Annular Gas Turbine Combustor. AIAA Paper 93–2074, 1993.

Lewis contact: Richard W. Niedzwiecki,
(216) 433–3407
Headquarters program office: OA

Helicopter Model Tested in Icing Conditions

Today, only one helicopter is certified by the Federal Aviation Administration for flight into forecasted icing—the French Super Puma. Aerospatialle spent almost 9 years of flight testing and some $20 million dollars to complete the icing certification process. The U.S. helicopter industry judges these costs to be prohibitive and has encouraged NASA to develop and validate both computer codes and new testing techniques that can be used to substantially reduce the cost and time for certification.

Small annular, reverse-flow gas turbine combustor (left) and 30° sector computational mesh used in present study (right).

NASA, the U.S. Army, and Sikorsky Aircraft recently completed a test program to expand the experimental data base on the performance of helicopter rotors in icing conditions. A 1/6th-scale Sikorsky Black Hawk Helicopter model was tested over a wide range of icing conditions and critical forward-flight conditions in the NASA Lewis Icing Research Tunnel.

This was the second of two test entries funded by NASA and the Army to develop techniques for testing subscale rotors in the Icing Research Tunnel for the purpose of studying rotor performance losses in icing. Sikorsky provided their six-component force balance and data acquisition system for measuring the rotor performance. And NASA provided the rotor blades and developed techniques for constructing molds of the ice buildup on the blades.

This new experimental data base is being used to further refine and validate a computer code that NASA and Sikorsky developed earlier. This code predicts the loss in rotor performance experienced by a helicopter when ice accretes on its rotors during an icing encounter. It is hoped that this code can be used to predict full-scale helicopter performance in icing and that its results can be accepted as an alternative to some of the icing flight testing currently required to certify a helicopter for flight into forecasted icing.

Molds of the ice buildup were used to make castings of simulated ice shapes. These castings will be attached to the leading edges of the rotors of the 1/6th-scale helicopter model, and it will be tested in a conventional (dry air) wind tunnel at the United Technologies Research Center in Connecticut. The dry-air test results for simulated ice shapes will be compared with the Icing Research Tunnel test results. Although leading-edge ice shapes are commonly used as part of the icing certification process for fixed-wing aircraft, this is the first time they have been seriously considered for rotary-wing aircraft.

These pioneering efforts to develop rotor-performance-in-icing codes and to demonstrate the applicability of simulated ice shapes to rotorcraft may ultimately reduce the cost and time to certify civil helicopters for flight into forecasted icing.

Lewis contact: Thomas H. Bond, (216) 433–3414
Headquarters program office: OA

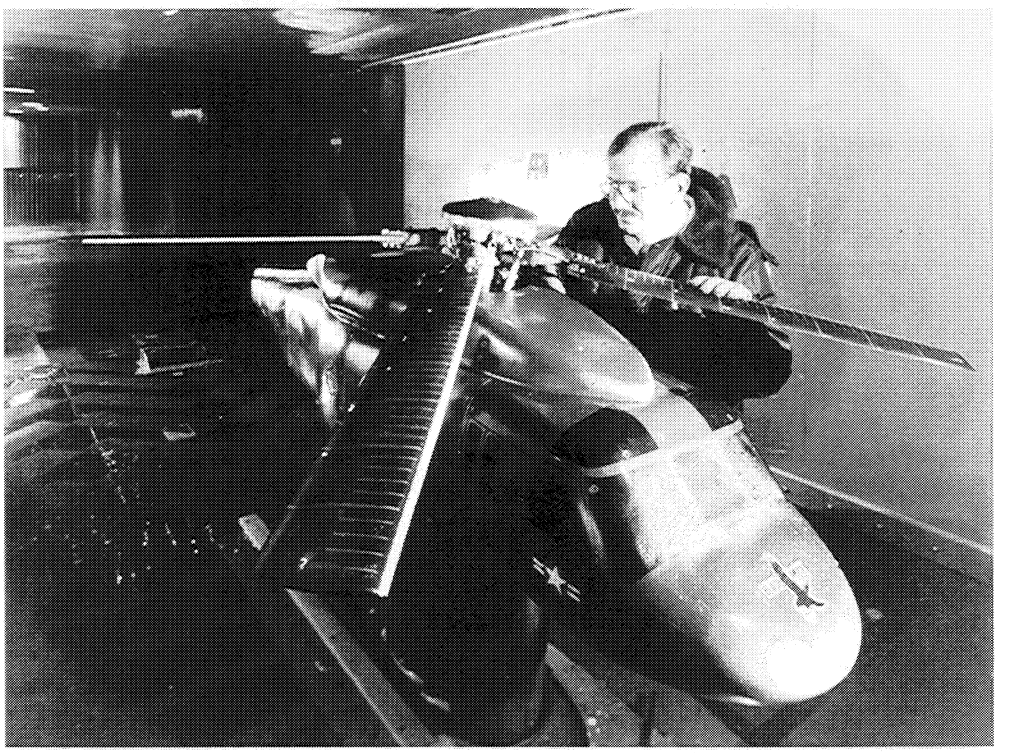

1/6th-Scale Sikorsky Black Hawk helicopter model mounted in NASA Lewis Icing Research Tunnel.

Advanced Spiral-Bevel Gears Designed for Helicopters

Spiral-bevel gears are used extensively in helicopter transmissions to connect high-speed gas turbine engine outputs to rotors. Spiral-bevel gears are a main source of vibration in gearboxes and thus a main source of noise in cabin interiors. In addition, higher strength and lower weight are required to meet the needs of future aircraft. Therefore, analytical and experimental investigations were performed on advanced spiral-bevel gear designs, and significant noise reduction was achieved.

The improvements in spiral-bevel gear design were investigated to support the Army/NASA Advanced Rotorcraft Transmission (ART) Program. The ART Program was an Army-funded, Army/NASA program to develop and demonstrate lightweight, quiet, durable drive systems for next-generation rotorcraft. The NASA Lewis Research Center, the U.S. Army Vehicle Propulsion Directorate, Bell Helicopter Textron (one ART contractor participant), the University of Illinois at Chicago (subcontractor to Bell Helicopter Textron), and the Gleason Works (subcontractor to Bell Helicopter Textron) were involved in a joint project to improve spiral-bevel gears. The project goals were to reduce bevel gear noise and increase strength through changes in gear tooth surface geometry and in tooth fillet and root designs.

Advanced spiral-bevel gears were designed and tested in an OH–58D helicopter transmission using the NASA Lewis 500-hp Helicopter Transmission Test Stand. Three different gear designs were tested. The baseline was the current design of the OH–58D transmission. The second design was a higher strength design that was the same as the baseline but incorporated a full fillet radius to reduce gear tooth bending stress. The third design was a lower noise design that was the same as the higher strength design except that the tooth geometry was modified to reduce transmission error and noise. Noise, vibration, and tooth strain tests were performed.

For the baseline spiral-bevel gear design, dominant tones in the noise and vibration spectra occurred at the spiral-bevel meshing frequencies and harmonics. A significant decrease in the spiral-bevel tones resulted from the lower noise design. At 100-percent torque the noise (sound power) due to the spiral-bevel meshing

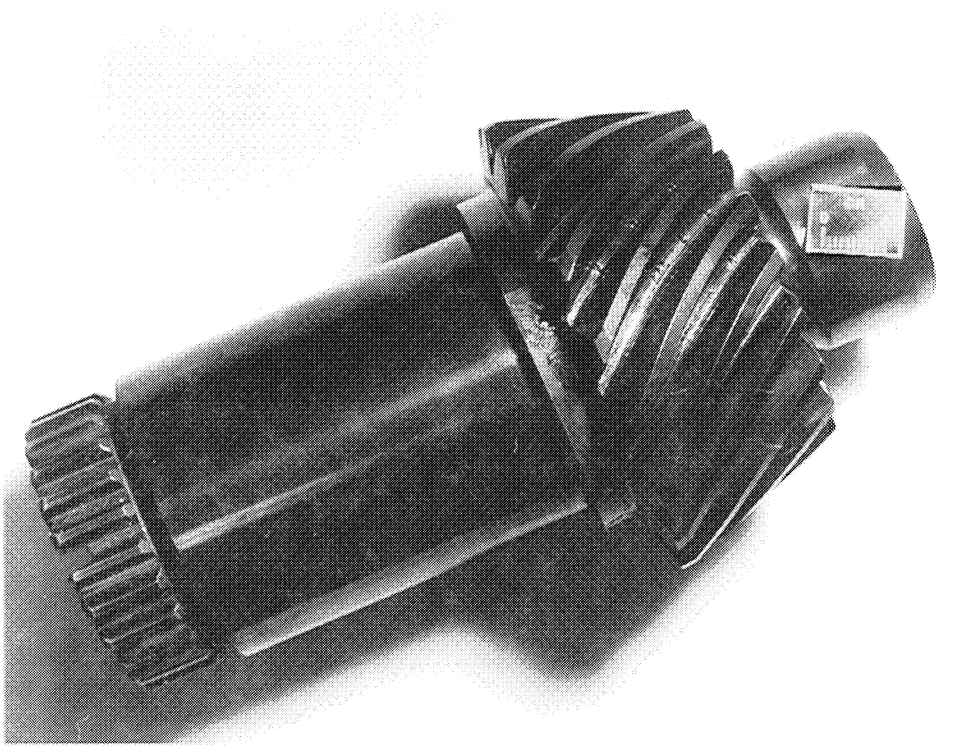

OH–58D spiral-bevel pinion gear.

frequencies of the lower noise design was 12 to 19 dB lower than that of the baseline and higher strength designs. The spiral-bevel gear vibration of the lower noise design was 5 to 10 g's lower than that of the baseline and higher strength designs. The increased fillet radius of the high-strength design had a significant benefit in decreasing tooth bending stress. For tests at 100-percent torque the spiral-bevel pinion maximum tooth bending stress of the high-strength design was on the average 27 percent lower than that of the baseline design.

Bibliography

Bill, R.C.: Advanced Rotorcraft Transmission Program. NASA TM–103276, 1990. (Also AVSCOM TR–90–C–015, 1990.)

Henry, Z.S.: Advanced Rotorcraft Transmission (ART)—Component Test Results. AIAA PAPER 92–3366, 1992.

Lewicki, D.G.; et al.: Low-Noise, High-Strength, Spiral-Bevel Gears for Helicopter Transmissions. NASA TM–106080, 1993. (Also AIAA Paper 93–2149, 1993.)

Lewis contact: David G. Lewicki, (216) 433–3970
Headquarters program office: OA

Flow Quality of Nozzle Acoustic Test Rig Studied

The Nozzle Acoustic Test Rig (NATR) is a newly developed, 53-in.-diameter, free-jet facility with a design Mach number of 0.30. It is located within a 130-ft-diameter, geodesic dome that provides noise transmission loss as well as a hemi-anechoic interior environment necessary for testing advanced exhaust nozzle concepts for the High Speed Research Program (ref. 1). The NATR allows nozzle concepts to be acoustically assessed for far-field (approx. 50 ft) noise characteristics under conditions simulating forward flight. A series of studies has been conducted to determine the flow quality of the free jet and to illustrate the new facility's aerodynamic characteristics.

The velocity profiles and axial turbulence intensity distributions at various locations downstream of the free-jet nozzle exit plane were determined. The studies were performed with a nominal 5-in. conical nozzle installed in the free jet. A large rake instrumented with 14 pitot pressure probes and 2 hot-film anemometers was remotely positioned and surveyed across the exhaust plume. The axial position of the traverse rake was adjusted manually by sliding the rake assembly along floor-mounted rails. The velocity data were acquired with the pitot pressure probes for free-jet Mach numbers of 0.2 and 0.3. The two hot-film anemometers, one positioned on and the other slightly above the free-jet nozzle centerline, were used to measure axial turbulence intensity u'/U. The turbulence intensity data were collected only at a free-jet Mach number of 0.2 owing to the fragility of the hot-film instrumentation.

Neglecting the interference region from the conical nozzle installation, the velocity profiles along the horizontal centerline of the exhaust plume were quite uniform (less than 0.7-percent velocity variation from the mean). Velocity contour data, taken 0.25 free-jet diameters downstream of the exit, indicated the cross-sectional velocity variation to be less than 1.5 percent. Axial turbulence intensity levels u'/U near the free-jet exit plane were found to be approximately 1.8 percent in the core of the free-jet exhaust. Comparable turbulence levels were measured at several other downstream axial stations.

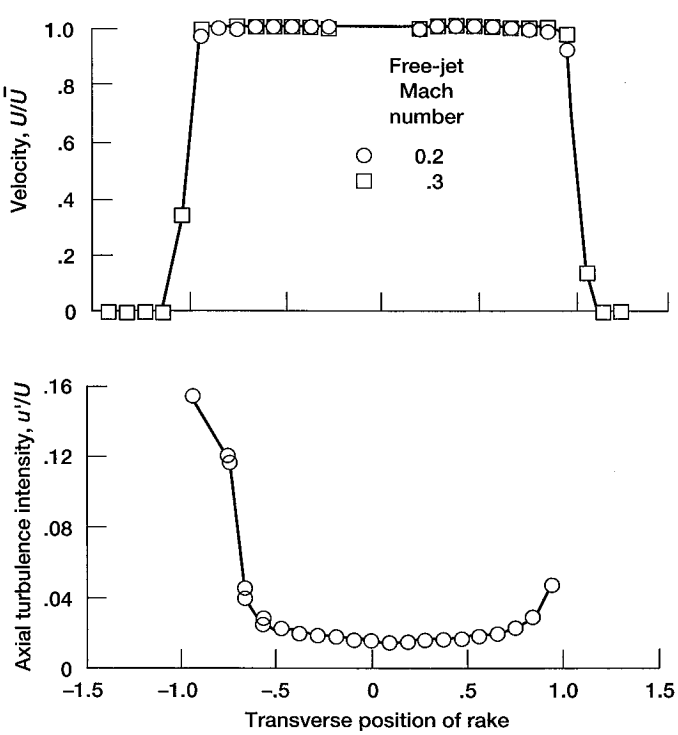

Results of free-jet exhaust plume surveys. Transverse rake located 13.25 in. downstream of exit plane.

In addition to studying the variation of the velocity profiles and turbulence levels, the development of the free-jet plume was investigated. By surveying the free-jet nozzle exhaust at several downstream axial stations, an attempt was made to determine the length of the jet potential core. The complete extent of the potential core was not mapped owing to the limit of the traverse rake rail system in the facility; however, by extrapolating the acquired data the potential core length was estimated to be approximately 5.5 diameters.

In general, the results of the flow quality studies illustrate that the free jet is reasonably symmetric in velocity profiles and turbulence levels. These flow quality measurements indicate that this facility can more than adequately meet the various exhaust nozzle test program requirements. The information gathered from these studies will further be used to determine the types and designs of flow manipulators that can be installed to improve the free-jet flow quality.

Reference

1. Cooper, B.: A Large Hemi-Anechoic Enclosure for Community-Compatible Aeroacoustic Testing of Aircraft Propulsion Systems. NASA TM–106015, 1993.

Lewis contacts: Mary Jo Long-Davis, (216) 433–8708; Raymond S. Castner, (216) 433–5657
Headquarters program office: OA

Performance Measured for 2DCD Nozzles With Inflow Swirl

Modern aircraft need high-performance exhaust nozzles to maximize performance and to minimize takeoff gross weight. Nozzle performance is described by its thrust and discharge coefficients. The thrust coefficient C_T is the ratio of actual to theoretical ideal thrust, and the discharge coefficient C_D is the ratio of actual to theoretical ideal flow rate. Both coefficients are highest when the incoming gas flow is straight and uniform and may decrease when the inflow is swirling. Swirl could be residual swirl from the turbine exit or could be induced by vanes in a swirl afterburner. The swirl afterburner needs no flameholder and burns fuel in a shorter tailpipe length and thus could improve aircraft performance or reduce takeoff gross weight.

NASA Lewis has recently completed a joint program with Pratt & Whitney to measure the performance of a family of two-dimensional, convergent-divergent (2DCD) exhaust nozzles with inflow swirl. Swirl was generated with a calibrated set of vanes mounted upstream of the nozzle inlet station. The tests were done at simulated altitude conditions in the NASA Lewis CE–22 facility, using unheated air, nozzle pressure ratios up to 10, and average inflow swirl angles of 0°, 15°, 25°, and 30°. The results were similar to results obtained in other experiments with round exhaust nozzles. The effect of swirl on thrust was reduced as the nozzle pressure ratio was increased, but the effect on flow rate was set only by the swirl angle. Photographs (not shown) of flow visualization paint streaks on the nozzle walls also were obtained to help in understanding the internal flow patterns.

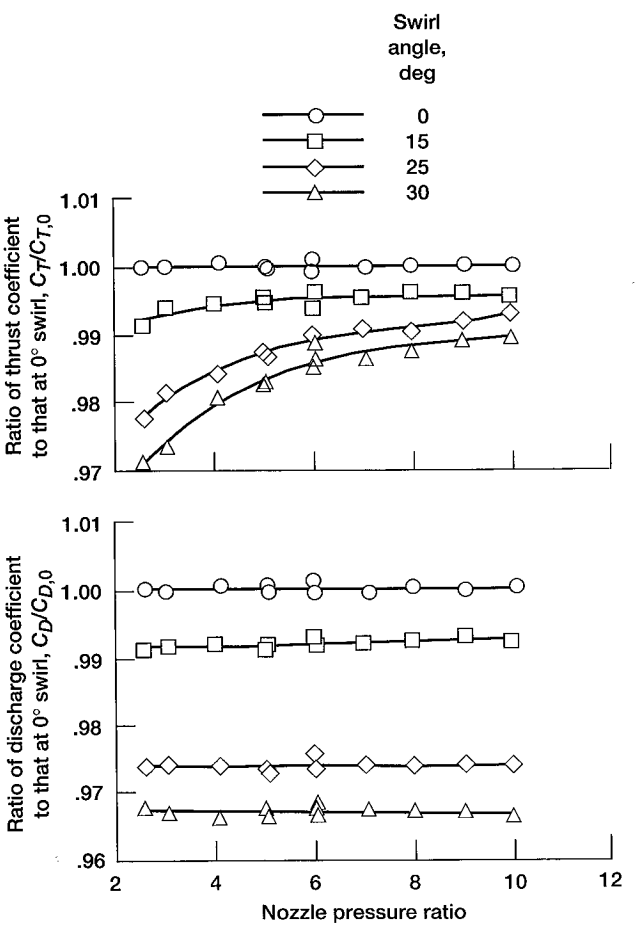

Nozzle performance with swirl inflow.

These data expand the data base by adding a new family of nozzle shapes that could be useful for future high-performance aircraft.

Lewis contacts: Jack G. McArdle, (216) 433–3962; David W. Lam, (216) 433–8875
Headquarters program office: OA

Fluid Shield Nozzle Tested at GE

The high-speed civil transport (HSCT) is a 300-passenger aircraft proposed for the year 2005 that would be capable of cruising supersonically at speeds exceeding twice the speed of sound. For such an aircraft to be economically viable it must cruise efficiently at these high speeds while having no significant effect on the environment over its entire mission. One of the key issues that must be addressed in developing a successful HSCT is the potentially high level of noise generated by the propulsion system at takeoff—in particular by the exhaust nozzles. Historically, noise emanating from aircraft near large airports has always been a problem. Because of increased awareness and sensitivity to this problem, future aircraft will be required by Federal air regulations to meet very stringent, new noise standards.

NASA Lewis and the aerospace industry have been conducting research on noise from aircraft propulsion systems for a number of years. Current work at NASA Lewis, being conducted under the High-Speed Research (HSR) Program, has focused on designing an exhaust nozzle for an HSCT that would meet or exceed anticipated new Federal regulatory guidelines while still maintaining high nozzle efficiency throughout its entire mission.

An exhaust nozzle concept called the fluid shield, designed by the General Electric (GE) Company under a contract with the NASA Lewis, is currently being considered for application to an HSCT. This concept would be used in conjunction with an engine cycle developed by GE called the FLADE (or fan on blade). This engine cycle provides an outer annular flow that surrounds the hot, high-velocity jet exhaust. This additional flow would "shield" the noise generated by the engine jet exhaust from the surrounding community at takeoff.

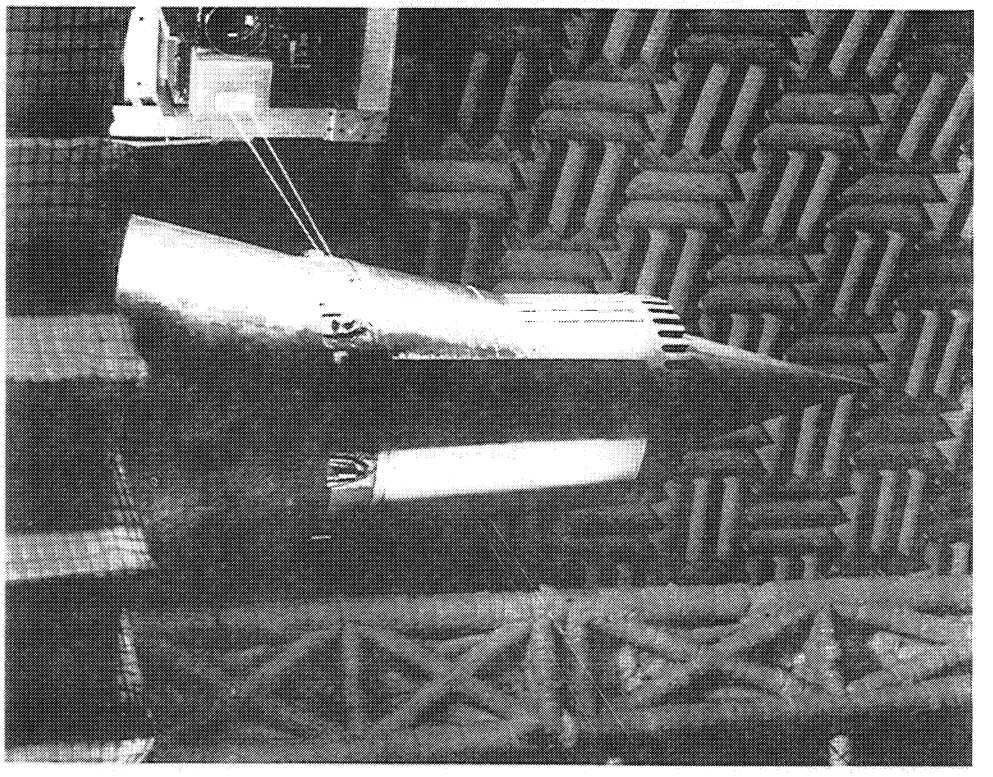

GE fluid shield scale model in Cell 41.

NASA Lewis and GE have conducted acoustic tests of a fluid shield nozzle in GE's acoustic test facility, Cell 41. Several shield parameters, such as shield thickness and angular wrap, were studied. Testing was conducted at conditions representing takeoff with external Mach numbers being approximately 0.32. Cell 41 is a large, anechoic free-jet test facility. It is a cylindrical chamber 13.1 m (43 ft) in diameter and 21.95 m (72 ft) tall. The inner surfaces are lined with anechoic wedges of fiberglass wool to minimize the effect of the chamber's walls on the acoustic data being acquired. The facility is equipped with two systems of microphone arrays to measure the acoustic characteristics of the test nozzles in the far field: a fixed array of microphones and an array on a traversing tower.

Test results indicate that the fluid shield nozzle reduces jet noise a nominal amount but that there is potential for further noise reductions. Second-generation fluid shield nozzles, including rectangular (two-dimensional) and hybrid fluid shield/mixer-ejector nozzles, are being considered for further study in the near future.

Lewis contact: Douglas E. Harrington, (216) 433–3591
Headquarters program office: OA

2DCD Mixer-Ejector Nozzle Tested at GE

In an effort to reduce the exhaust noise of a future high-speed civil transport (see preceding article), NASA Lewis and the aerospace industry are looking at two-dimensional, convergent-divergent (2DCD) nozzles. Over the last several decades a large aeroacoustic data base has been developed for round (i.e., axisymmetric) nozzle concepts. However, few data are available for rectangular (i.e., two-dimensional or convergent-divergent exhaust nozzles.

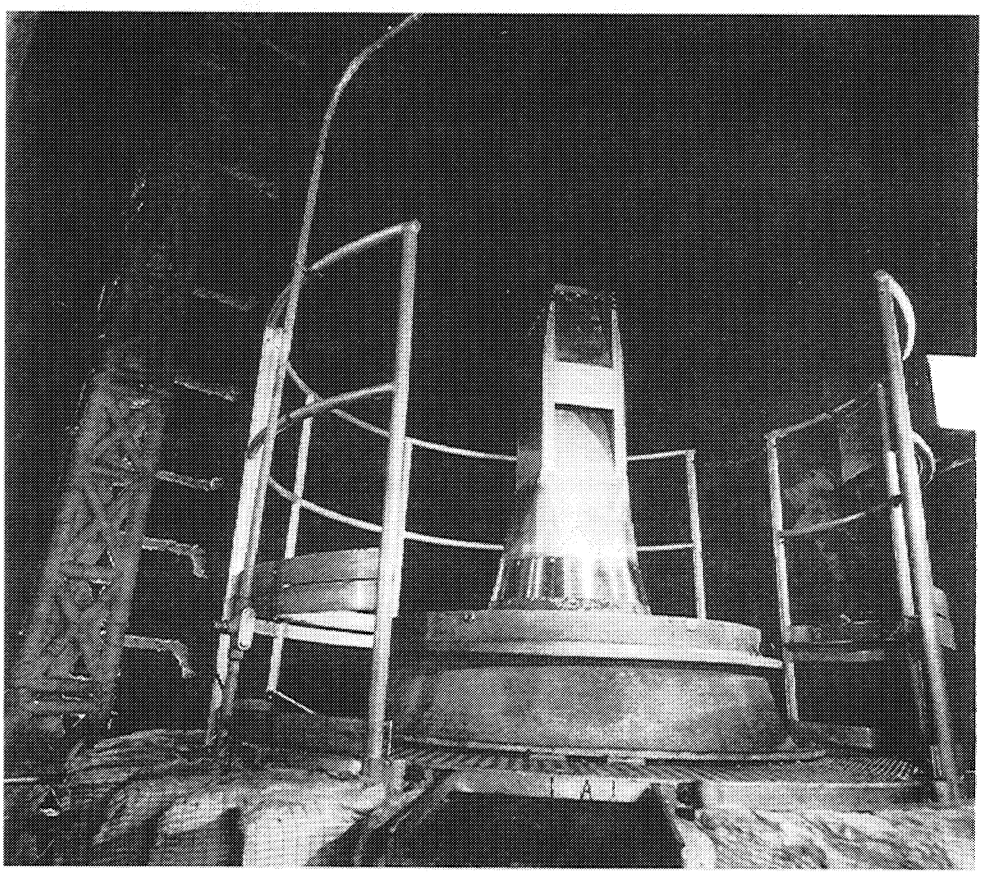

GE 2DCD scale model in Cell 41.

A promising 2DCD nozzle concept currently being considered for application to an HSCT is a rectangular mixer-ejector nozzle designed by the General Electric (GE) Company under a contract with NASA Lewis. This nozzle is designed to entrain moderately high amounts of external (secondary) air at takeoff. This air is then drawn through an array of lobed chutes (the mixer), which is designed to mix the entrained flow with high-velocity (primary) flow jet. This mixing process reduces the total flow velocity at the nozzle exit and results in lower jet noise.

NASA Lewis and GE have conducted acoustic tests of a 2DCD mixer-ejector nozzle in GE's acoustic test facility, Cell 41 (see preceding article for description). Several mixer designs, ejector configurations, and acoustic treatment areas were studied. Testing was conducted at conditions representing takeoff with external Mach numbers being approximately 0.32.

Test results indicate that the 2DCD mixer-ejector nozzle would meet or exceed anticipated new Federal noise regulations for an HSCT when operated at jet velocities of 2400 ft/sec or less. Only a moderate amount of acoustic treatment would be needed on the ejector walls to attain this noise suppression. Thus, the 2DCD nozzle could be a viable nozzle concept when used in a mixed-flow turbofan engine with a low to moderate bypass ratio.

Lewis contact: Douglas E. Harrington, (216) 433–3591
Headquarters program office: OA

STOVL Aircraft Characteristics Evaluated in Low-Speed Wind Tunnel

NASA Lewis and McDonnell Aircraft Company are currently evaluating several concepts that are applicable for the next generation of supersonic short-takeoff, vertical-landing (STOVL) aircraft. The most viable advanced supersonic STOVL concepts are likely to go into production around the year 2015. To meet this operational date, related critical technology problems must be resolved, such as hot gas ingestion and the acoustic environment during vertical landing. During the vertical-landing option, high-energy, high-temperature exhaust gases impinge upon and flow along the ground. In multiple-jet applications the colliding ground flows generate an upwash fountain that impinges on the lower surface of the aircraft. This hot flow migrates forward and can be ingested by the engine. In addition, the hot exhaust gases heat the ground and the aircraft. Jet flow also creates jet-induced interaction that can affect the aircraft's landing behavior.

A model was designed to be configured into several STOVL concepts and nozzle arrangements. The model is supported by a model integrated support system that has four degrees of freedom: pitch + 30°, yaw + 45°, roll + 15°, and height variation up to approximately 2 ft above the ground plane of the NASA Lewis 9- by 15-Foot Low-Speed Wind Tunnel. The ground plane is located under the model and contains pressure and temperature instrumentation. A sliding trapdoor in the ground plane opens to evacuate the hot gases from the nozzles while conditions (nozzle pressure ratio, nozzle temperature, etc.) are being changed. This avoids heating the model and the local environment artificially. The test section sidewalls are vented so that the lateral flow from the nozzle can leave the test section without creating recirculation.

Several data systems make the STOVL testing unique. The data systems include dynamic and steady-state data acquisition of pressures and temperatures; a laser sheet illumination and image enhancement system; acoustic measurements both near field and structural (using a high-temperature fiber optic probe from NASA Langley); high-speed video recording (100 frames per second); nonintrusive measurements; static temperature profiles using the Rayleigh spectral measurements; three-dimensional velocity flow field measurements using laser Doppler velocimeter and Rayleigh techniques; and infrared (from NASA Ames) thermovision to obtain the plume characteristics and the thermal footprint.

A mixed-flow vector thrust STOVL model approximately 4 in. above the ground plane was tested at a headwind of 15 knots. The ground jet (streamwise direction) moved toward the aircraft nose, and some of the flow was ingested into the main inlet. Most of the flow traveled about 4.5 ft

upstream of the main inlet before separating. The spanwise flow did not have a high velocity and dissipated within 3 ft of the model centerline. The test is scheduled for completion by mid-October. The results obtained so far have proven valuable for evaluating STOVL concepts.

Lewis contacts: Albert L. Johns, (216) 433–3972;
George H. Neiner, (216) 433–5661;
Timothy J. Bencic, (216) 433–5690
Headquarters program office: OA

Wave Rotor Research Continues

A wave rotor is a device in which aerodynamic compression and expansion waves play the same role as mechanical compressors and turbines in a conventional jet engine—adding energy to and extracting it from the working fluid. However, the rotor in a wave rotor machine is significantly colder than the air leaving the combustor. In contrast, the turbine in a jet engine is

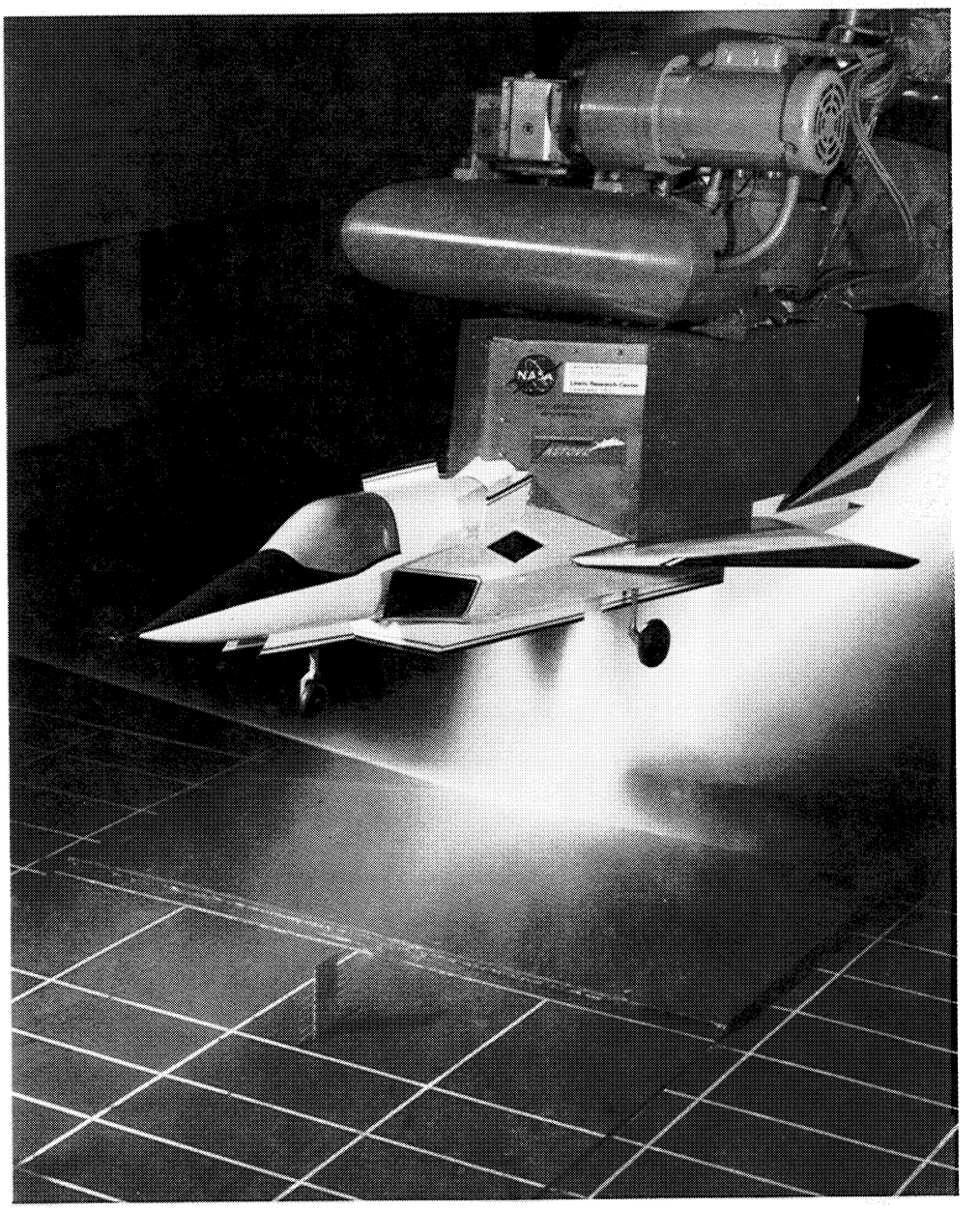

Supersonic STOVL hot gas ingestion model in wind tunnel.

continuously exposed to the gas from the combustor, and its temperature closely approaches that of this gas, limiting jet engine performance. By using a wave rotor as a high-pressure stage for jet engines, this limitation can be raised. NASA Lewis is investigating wave rotors for this application.

Last year it was reported that an experiment had been begun at NASA Lewis to ascertain the sources of losses in a wave rotor. Initial runs (ref. 1) showed that leakage from the space around the rotor into the rotor passages when they are at low pressure constitutes a major loss. The gap between the rotor and the end wall was fixed in the original design of the experiment. To confirm that this leakage is indeed a major loss, and to determine the sensitivity of the loss to the gap size, a set of false, movable end walls was inserted. Runs made with these end walls have shown a dramatic increase in efficiency as the gap was reduced.

A one-dimensional computational fluid dynamics code has been developed at NASA Lewis to predict the performance of a wave rotor of specified geometry over a wide range of operating conditions. The model can account for losses due to leakage, viscosity, finite passage opening time, shock waves, and nonuniform port flows. The model has been very successful in computing the performance, not only of the NASA Lewis experiment, but also previous experiments by J.A.C. Kentfield and by the General Electric Company (ref. 2). A two-dimensional code has been used at NASA Lewis to examine the losses consequent on rapidly opening a rotating passage to a port containing gas at a different pressure (ref. 3). It clearly showed that passage was only partially exposed to the port flow the flow entered as a jet and that vorticity was generated at the interface between the incoming gas and the gas in the passage prior to opening. In addition, a three-dimensional code has been used to look at the effect of rotation on the passage flow (refs. 4 and 5).

References

1. Wilson, J.; and Fronek, D.: Initial Results From the NASA Lewis Wave Rotor Experiment. NASA TM–106148, 1993. (Also AIAA Paper 93–2521.)

2. Paxson, D.E.: A Comparison Between Numerically Modelled and Experimentally Measured Loss Mechanisms in Wave Rotors. NASA TM–106279, 1993. (Also AIAA Paper 93–2522, 1993.)

3. Welch, G.E.: Two-Dimensional Numerical Study of Wave Rotor Flow Dynamics. AIAA Paper 93–2525, 1993.

4. Larosiliere, L.M.: Analysis of Unsteady Wave Rotor Processes in a Rotating Channel. NASA CR–191154, 1993. (Also AIAA Paper 93–2527, 1993.)

5. Larosiliere, L.M.: Three-Dimensional Numerical Simulation of Gradual Passage Opening in a Wave Rotor Passage. NASA CR–191157, 1993. (Also AIAA Paper 93–2526, 1993.)

Lewis contact: Jack Wilson, (216) 977–1204
Headquarters program office: OA

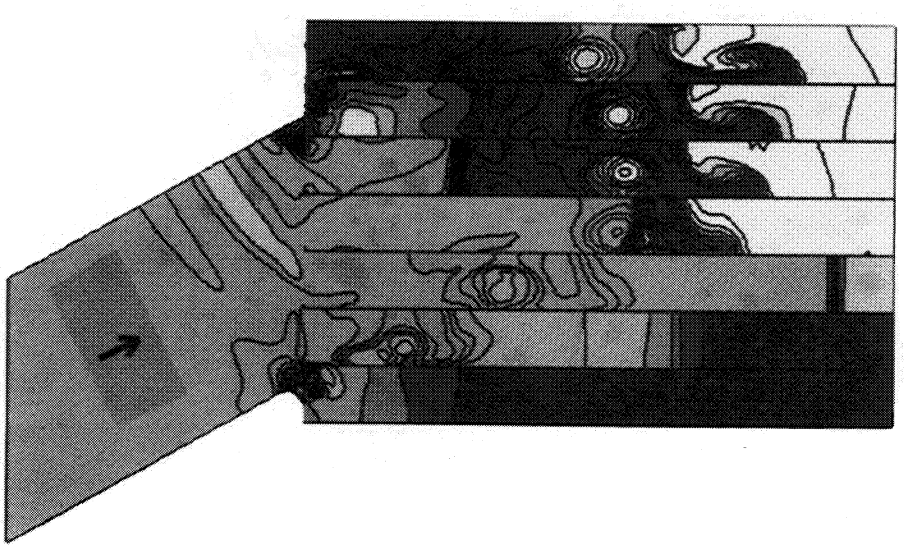

Density contours of flow in wave rotor passages (on right, moving upward) as gas enters from port at left.

Cooled Radial Turbine Research Completed

Currently, high-pressure turbines in small gas turbine engines are cooled axial-inflow machines. Radial-inflow turbines can offer performance and cost benefits at low equivalent mass flow (i.e., small size), but present applications are limited to auxiliary power units and turbochargers, which are uncooled and have a maximum inlet gas temperature of 1900 °F. The turbine inlet temperatures of current and future small propulsion systems range from 2500 to 3000 °F. Rotors made with ceramic matrix composites offer potential for use at these operating conditions, but structural design methods, material properties, and fabrication procedures need further development. The technology for manufacturing viable long-life, uncooled, ceramic radial rotors for human-rated service will likely require a significant time to evolve. In the interim, cooled metallic rotors may increase the performance of high-temperature engines. However, not only is information on radial rotor cooling technology lacking, but also our understanding of the complex aerodynamics and heat transfer occurring both within the cooling passages and over the exterior surface of the blades is far from complete. The recently concluded experimental cooled radial turbine program at NASA Lewis has addressed both issues.

The program pooled the collective efforts of the Army, Allison Gas Turbine Division, United Technologies Research Center (UTRC), Carnegie Mellon University, the Analysis and Design Application Company (adapco), and NASA. It included both experimental and analytical efforts. Building on an earlier Army-sponsored effort and an initial in-house NASA design, Allison completed a modified rotor design and fabricated two rotors: an uncooled solid version and an aerodynamically similar cooled version. NASA Lewis tested both rotors in its Small Engine Component Test Facility and completed computational analyses using several computer analysis codes.

The solid rotor testing provided baseline data for the aerodynamic performance of the rotor design. A quasi-three-dimensional flow analysis code, MTSB (MERIDL/TSONIC/BLAYER), provided computational predictions of the solid rotor performance to compare with the experimental data, including blade surface pressures in a rotating environment. A three-dimensional viscous flow analysis code, RVC3D, provided a more detailed look at the secondary flow effects caused by the tip clearance leakage and the high turning in the turbine stage.

Besides performance data the cooled version of the radial rotor provided internal and external

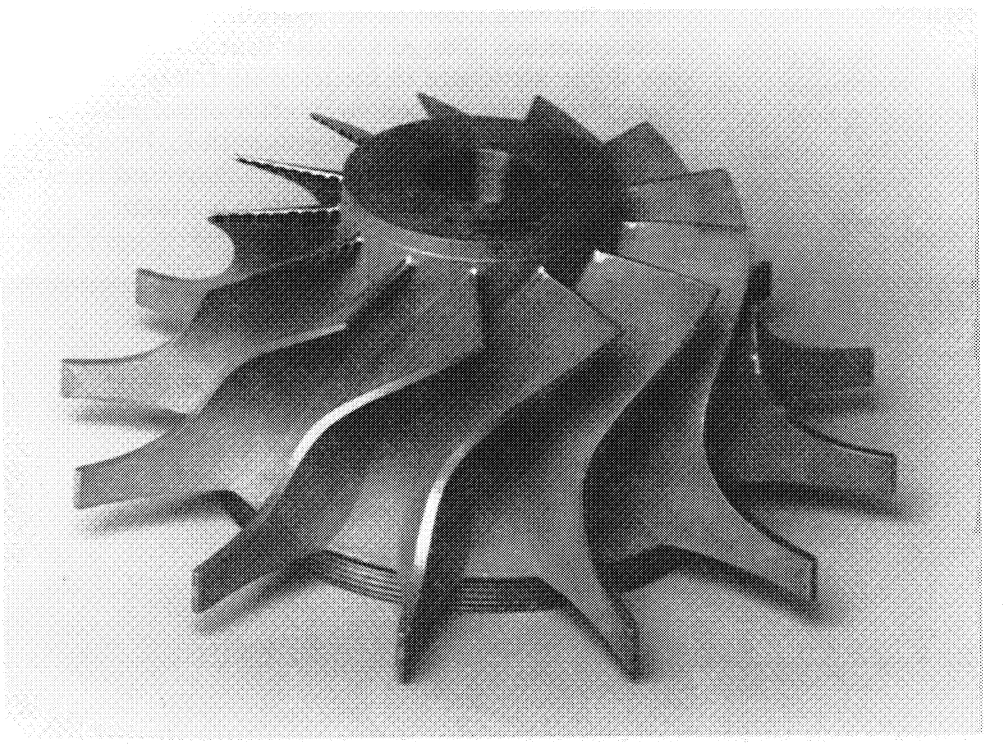

Cooled radial-inflow research rotor.

surface temperatures as well as flow passage coolant temperatures in a rotating environment. Carnegie Mellon supplied a numerical simulation of the flow within the blade coolant passages and has done substantial work on gridding methods for the complicated flow path. Similarly, adapco calculated a solution for the internal flow using its STAR–CD analysis code. Finally, UTRC conducted an experiment using liquid crystal measurement techniques on a rotating model of the coolant passage geometry to provide additional heat transfer information for comparison with the calculated results.

The radial turbine program successfully combined the talents of researchers from the government as well as industrial and academic sectors. The completed research provides a better understanding for the design and manufacture of cooled radial turbines and a data base for validating analysis codes that address the complex aerodynamics and heat transfer occurring both within the coolant flow passages and on the external blade surfaces. Although the testing is complete, the analysis and comparison with the data is ongoing.

Bibliography

Ippolito, J.: Three Dimensional Flow Analysis of the Internal Passage of a Cooled Radial Rotor. Analysis and Design Application Co., Ltd., Report No. 30–02–004, April 1991.

Johnson, B.V.: Heat Transfer Experiments in the Internal Cooling Passages of a Cooled Radial Turbine. UTRC Report 93–270411–1, United Technologies Research Center, East Hartford, CT, 1993.

Larosiliere, L.M.: Navier-Stokes Analysis of Radial Turbine Rotor Performance. NASA CR–191153, 1993.

Stephens, M.; et al.: Grids in the Simulation of Three-Dimensional Flowfields in Turbine-Blade-Coolant Passages. AIAA 93–2557, 1993.

Tirres, L.: A Comparison of the Analytical and Experimental Performance of the Solid Version of a Cooled Radial Turbine. NASA CR–187195, 1991.

Tirres, L.: A Comparison of the Calculated and Experimental Off-Design Performance of a Radial Flow Turbine. NASA CR–189207, 1992.

Tirres, L.; DiCicco, L.D.; and Nowlin, B.C.: Experimental Performance of a Cooled Radial Turbine. NASA TM–106230, 1993.

Lewis contact: Kestutis C. Civinskas, (216) 433–5890
Headquarters program office: OA

Aeroacoustic Propulsion Laboratory Self-Noise Level Assessed

Preliminary tests of Aeroacoustic Propulsion Laboratory (APL) self-noise levels have recently been completed. The 130-ft-diameter, geodesic dome-shaped enclosure provides a research-quality hemi-anechoic interior environment for acoustic testing of aircraft propulsion systems while limiting noise in surrounding residential communities. The APL is the first known geodesic dome structure to incorporate transmission-loss properties as well as interior absorption in a free-standing, community-compatible, hemi-anechoic test facility. Recent background level tests confirmed that the facility's acoustic

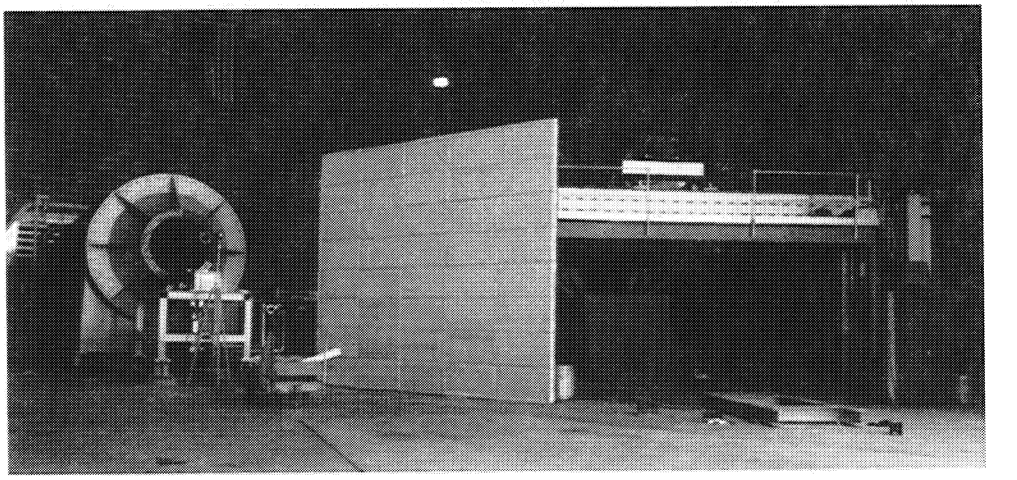

Interior view of hemi-anechoic Aeroacoustic Propulsion Laboratory near completion.

environment is comparable to those of similar facilities in the aeroacoustic propulsion community and will allow researchers to obtain accurate acoustic measurements on low-noise propulsion system components.

The APL houses the Powered Lift Facility (PLF) as well as the Nozzle Acoustic Test Rig (NATR). The latter, a 53-in.-diameter, ejector-powered, free-jet facility with a design Mach number of 0.3, is used to simulate forward flight during the aeroacoustic testing of scale-model aircraft exhaust nozzles and turbomachinery.

A series of checkout tests was conducted to assess and document the self-noise levels of the NATR free jet and to evaluate the installed performance of facility noise reduction measures in preparation for the NATR's first full-capability nozzle test program. In addition, a preliminary assessment was made of the anechoicity to provide a basis for evaluating these self-noise data as well as research data from upcoming test programs.

Background levels measured in the self-noise tests were low enough to allow researchers to obtain noise measurements on low-noise nozzle design concepts. These levels also compared favorably with those of respected jet noise research facilities within the aircraft propulsion industry. Analysis of the anechoicity data indicated that the interior acoustic environment is sufficiently anechoic to ensure the accuracy required for research-quality acoustic measurements.

The acoustic environment in the APL is currently being upgraded. Absorptive fiberglass wedge treatment is being added on the floor surface as well as on all facility surfaces not previously treated. This upgrade to a full anechoic enclosure will allow the APL to accommodate additional acoustic test programs that require a fully anechoic environment and will substantially reduce the time and resources required for acoustic data acquisition and reduction for all test programs. A complete evaluation of the facility's acoustic characteristics will be performed when the modifications now in progress have been completed.

Lewis contact: Beth A. Cooper, (216) 433–3950
Headquarters program office: OA

Fan Noise Predicted for Turbofan Engines

NASA has recently established a noise reduction element in the Advanced Subsonic Technology Program. This program seeks to develop technologies for reducing aircraft noise levels by 10 dB relative to 1992 technology by the year 2000. Specifically, 6 dB will come from reducing engine noise levels. A primary product will be design tools that can be used to evaluate noise from future turbofan engines. In 1991 Pratt & Whitney was contracted to improve a fan noise source code originally developed by Bolt Beranek and Newman Inc. in the early 1980's on a previous NASA contract. The current work has provided an efficient source model that integrates with a finite element radiation code to predict far-field directivity. Although more work is required, this effort provides NASA (and U.S. industry) with an advanced prediction methodology early in the noise reduction program to help guide the low-noise turbofan designs that will be tested over the next decade.

The current prediction methodology is divided into two parts. First, the source code models the interaction between the fan and the exit guide vanes. The rotor wake is prescribed as a vortical gust that interacts with spanwise segments of flat-plate cascades (representing the fan exit guide vanes) to determine the surface unsteady pressure response. Green's function is used to integrate the surface pressures to representative duct modes. Second, the complex pressure amplitudes from the duct modes are used as a boundary condition for a finite element radiation code (developed by Dr. Walter Eversman, University of Missouri–Rolla) to obtain far-field sound level predictions from the inlet. The duct radiation code can model realistic nacelle shapes and accounts for the effects of the mean flow on sound propagation.

The fan noise prediction codes have been applied and compared with model data obtained at NASA Lewis for the Pratt & Whitney advanced ducted propulsor. The model was a 17-in.-diameter fan installed in the 9- by 15-Foot Low-Speed Wind Tunnel to obtain acoustic and aerodynamic data. A unique rotating microphone was used to obtain inlet duct acoustic modes for several operating conditions. Predictions for the sideline sound pressure levels using the rotating microphone data as input to the radiation code were

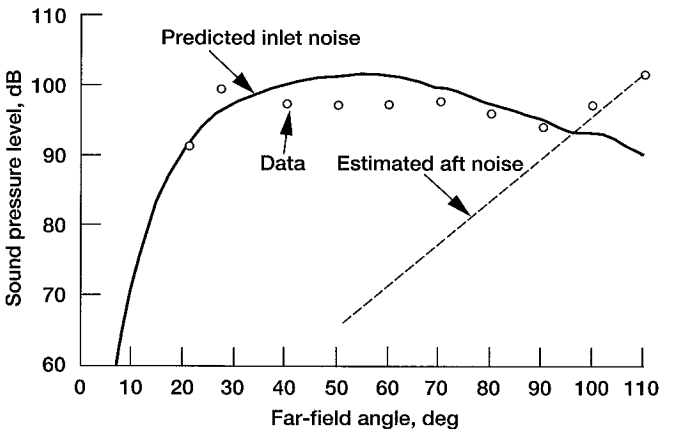

Predicted and measured inlet fan noise directivity from model tests of Pratt & Whitney advanced ducted propulsor.

compared with the measured sideline microphone data. Overall, the peak sound pressure level and the directivity pattern were predicted very well.

Future work will concentrate on developing an aft radiation code that accounts for the shear layer between the bypass flow and the free stream. A liner model will be added to simulate acoustic treatment in the nacelle. The source code will be improved by modeling the acoustic coupling between blade rows and by eventually including three-dimensional unsteady aerodynamics for actual blade geometries.

Lewis contact: Dennis L. Huff, (216) 433–3913
Headquarters program office: OA

Variable-Diameter-Centerbody Inlet Tested in Supersonic Wind Tunnel

Tests of the variable-diameter-centerbody (VDC) inlet were completed in the NASA Lewis 10- by 10-Foot Supersonic Wind Tunnel. This inlet is a candidate concept for the high-speed civil transport (HSCT)—a second-generation supersonic transport. Some elements of its design include high recovery, low bleed, good angle-of-attack tolerance, and excellent engine airflow matching. These features have been demonstrated at Lewis in the past by the testing of fixed hardware models. A significant uncertainty of the VDC concept is the mechanical complexity needed for the variable-geometry feature. The recent set of wind tunnel tests used a new model with the full variable-diameter-centerbody mechanism. The challenge was to duplicate the performance and operability qualities of the fixed hardware model on flight-like hardware that actually incorporated the variable geometry.

Results of the tests are encouraging. Major operability concerns with the concept were investigated during testing. The inlet started without difficulty. Unstart/restart transients and control procedures were investigated. The inlet could be restarted within 1 sec by using either the variable diameter or a more traditional translation of the centerbody mechanism. The comparison of the variable-geometry model performance with the fixed-hardware model performance indicated only a 1/2 percent decrease in recovery with slightly increased centerbody bleed flow. Additionally, a stability bleed bypass scheme was developed that will allow the inlet to tolerate a 10-percent change in airflow without an unstart.

Because inlet selection is tightly coupled to engine cycle and nacelle location on the aircraft, the test data are needed to correctly optimize the HSCT design through careful mission analysis. To develop a better understanding of the flow complexities, the recent tests augmented by computational fluid dynamics support will answer the performance and operability questions of the VDC inlet concept. On-going participation of industry and government researchers throughout the test program will determine the impact of the test results on HSCT inlet selection.

Lewis contract: John D. Saunders, (216) 433–6278
Headquarters program office: OA

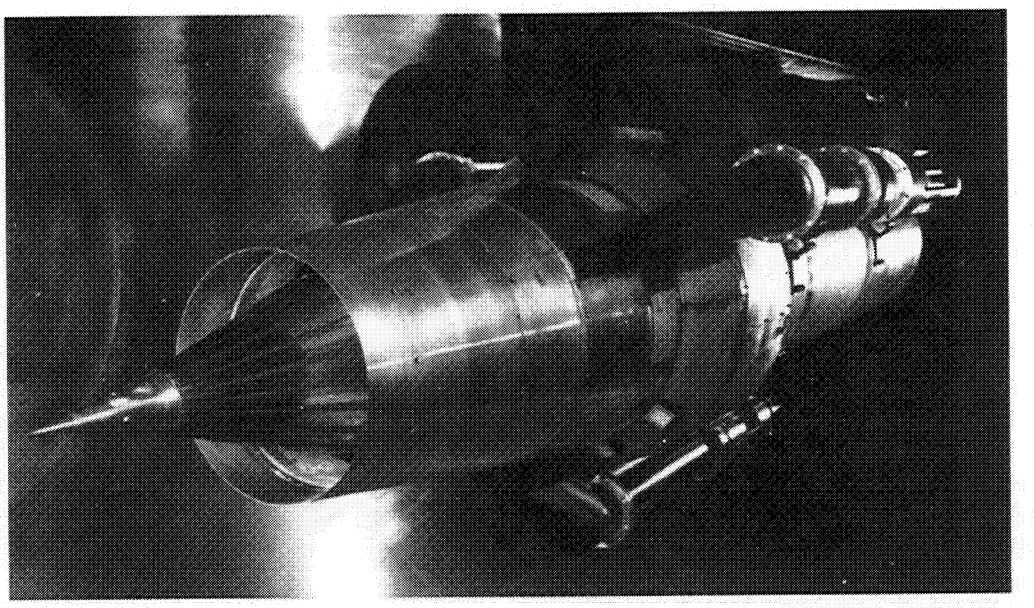

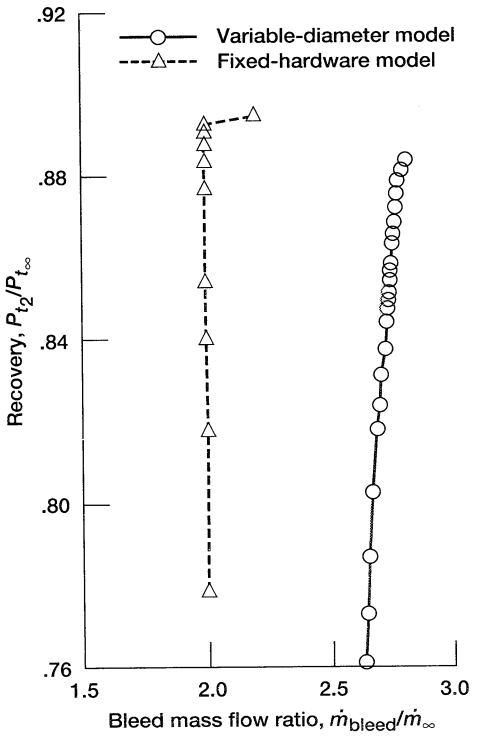

VDC inlet model installed in wind tunnel (top) and performance comparison (bottom).

RNG Turbulence Model Predicts Laminar-Turbulent Flow Transition

With the increasing use of computational fluid dynamics codes as analytical and design tools for subsonic nacelles, a real flow simulation of the laminar and turbulent flow regions becomes more important. For example, the skin friction coefficient and the separation angle of attack associated with a laminar flow are different from those in a turbulent flow. It is wrong to assume that flow is turbulent everywhere. The first step in accomplishing a real flow simulation is to predict the location of transition from laminar flow to turbulent flow correctly.

A renormalization-group-based (RNG) algebraic turbulence model was implemented in PARC2D/AXI and was applied to an NACA 0012 airfoil to test the accuracy of the transition prediction. The preliminary result showed that the method can predict the transition point very well (i.e., $x/c = 0.15$, where x refers to the x coordinate and c is the chord length.). The level of the skin friction coefficient in the turbulence region ($x/c > 0.25$) was slightly higher than the experimental data; however, these results were considered to be fairly good in view of the complexity of the problem.

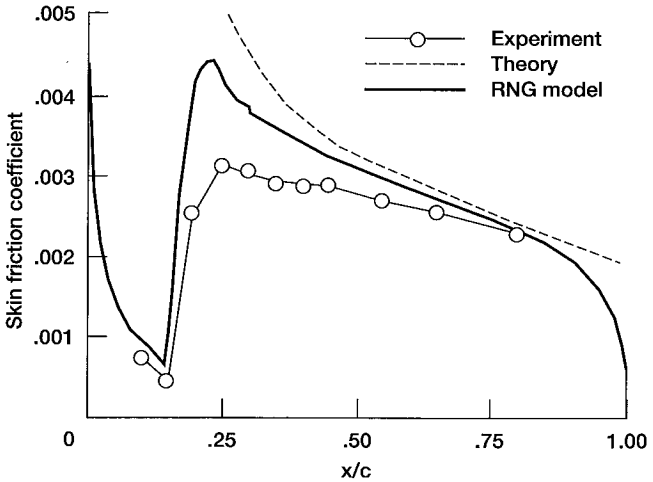

Local skin friction coefficient for NACA 0012 airfoil.

Lewis contact: Dr. Danny P. Hwang, (216) 433–2187
Headquarters program office: OA

Aerospace Technology

Materials

Advanced High-Temperature Engines Materials Technology Continues Progress

The objective of the Advanced High-Temperature Engine Materials Technology (HITEMP) Program is to generate technology for advanced materials and structural analysis that will lead to increased fuel economy, improved reliability, extended life, and reduced operating costs for 21st century civil aviation propulsion systems. The primary focus is on fan and compressor materials (polymer matrix composites), compressor and turbine materials (metal and intermetallic matrix composites), and turbine materials (ceramic matrix composites). These composite materials are being developed by in-house researchers and on grants and contracts.

NASA considers this program to be a focused materials and structures research effort that builds upon our base research programs and supports component development projects, such as NASA's new initiative to develop the technology for advanced subsonic transport engines. HITEMP is closely coordinated with the Advanced Subsonics Technology Program, the Department of Defense/NASA Integrated High-Performance Turbine Engine Technology Program, and the National Aerospace Plane Program. Advanced composite materials from HITEMP may be used in these future applications.

A Lewis-developed process of postcuring polymer matrix composites in a high-pressure nitrogen environment has been transferred to General Electric Company, the U.S. Air Force Materials Laboratory, and Hycomp (an industrial firm). The process greatly improves the properties of polymer matrix composites. An analytical model, the Generalized Method of Cells, has demonstrated the capability to model fiber arrays, fiber shapes, porosity, damaged regions, and interfaces. The arc spray fabrication process has been optimized to make silicon-carbide-fiber-reinforced titanium aluminide composites with excellent quality and mechanical properties. High-strength aluminum oxide fibers have been produced by the melt growth process. A laser speckle strain gage measurement system for determining strain on small-diameter fibers has been developed and is now operational. Coated silicon carbide ceramic vanes have successfully passed burner rig testing in a cooperative project with Williams International. Engine testing will be conducted in the coming year.

The sixth annual review of the HITEMP Program was held October 26 and 27, 1993. Details of research accomplishments are published in a conference report, NASA CP–19117.

Lewis contacts: Dr. Hugh R. Gray, (216) 433–3230; Carol A. Ginty, (216) 433–3335
Headquarters program office: OA

Enabling Propulsion Materials Program Supports High-Speed Civil Transport

The propulsion effort of the NASA High-Speed Research (HSR) Program is addressing the environmental and economic issues of the next U.S. supersonic transport, the high-speed civil transport (HSCT). A low-emissions, low-noise, high-performance propulsion system is required for

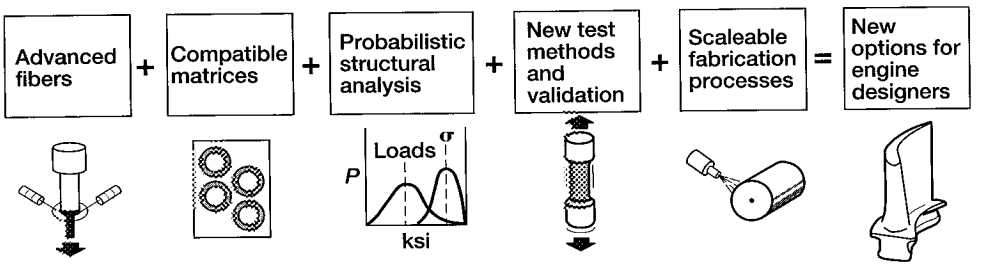

Elements of HITEMP Program.

aircraft entry into service by the year 2005. The objectives of the Enabling Propulsion Materials (EPM) Program are to develop the materials technologies necessary to support the HSR propulsion effort and to maintain U.S. leadership in commercial aircraft propulsion systems. The necessary materials technologies include material and fabrication process development, analytical tools for design and life prediction, and component fabrication and validation through engine testing.

The main focus of the EPM Program is on materials technologies for HSCT propulsion systems that impact the environmental barriers. A high-temperature, long-life combustor liner is required to allow the use of advanced low-emissions combustor concepts. High-temperature, lightweight, durable materials are required for subcomponents in noise-suppressing exhaust nozzles. A secondary focus of the EPM Program that begins next year is on other critical components that impact primarily the economic (performance) barriers. Advanced materials technologies are required for high-temperature fan containment; high-temperature, long-life turbomachinery disks; and a turbine airfoil system that takes advantage of advanced alloys, thermal barrier coatings, and airfoil cooling concepts.

Some key features of the EPM Program are that the two major U.S. aircraft engine manufacturers, GE Aircraft Engines and Pratt & Whitney, have teamed up to conduct the contractual effort. Other U.S. engine companies, material suppliers, and component manufacturers are subcontractors to the GEAE/P&W HSCT team. NASA Lewis is an integral partner of the team, contributing to the contractual effort as well as to in-house alternative research approaches designed to reduce risk and to fill in gaps within the contractual effort. EPM is dedicated to maintaining U.S. leadership in the aircraft industry and accomplishes this by restricting data only to the U.S. HSCT community.

Another key aspect of EPM is the use of integrated product development (IPD) teams. The IPD process implies that all disciplines required to achieve the end product are united into teams that work concurrently. This process is ideally suited for the EPM Program because of the complex teaming arrangements among GEAE, P&W, NASA, and other U.S. industrial companies and because of the challenging technical and schedule milestones. IPD teams have been established for each of the critical components as well as for business management (finance, contracts, procurement, etc.) and product assurance (quality of product, process, etc.).

Technical accomplishments for this year have focused on refining component designs, developing composite materials, and standardizing test methods. Combustor and nozzle liner designs have included detailed attachment schemes that result in stresses below the projected material properties. The strengths of fibers for use in combustor liner ceramic matrix composites (CMC's) have been improved substantially. Intermetallic and metal matrix composite (IMC and MMC) materials and associated fabrication processes for exhaust nozzle applications have been selected following screening characterization tests. Load-frame equipment to test the long-term durability of the composite materials under simulated mission conditions has been procured. Benchmark-testing load frames have also been procured that will provide mechanical property test results on component-shaped specimens. Both long-term durability and benchmark test results are necessary to validate the analytical models under development. CMC/IMC/MMC composite testing methods for tension, creep rupture, tension-tension fatigue, and four-point flexure have been submitted to the ASTM C–28 committee for external distribution.

Lewis contact: Joseph R. Stephens, (216) 433–3195
Headquarters program office: OA

Nickel Aluminum Intermetallics Welded

Nickel aluminum (NiAl) and NiAl–0.1 at.% zirconium (Zr) intermetallics meet many of the requirements for advanced aerospace applications, including oxidation resistance and low density. In order to utilize these materials in structural applications, however, suitable welding processes are required. None are now available. Conventional fusion welding processes, such as electron beam welding and gas tungsten arc welding, are not applicable because of inherently low base metal ductility below about 750 °C. Thus, the development of new welding approaches was necessary to produce sound joints with base metal strength.

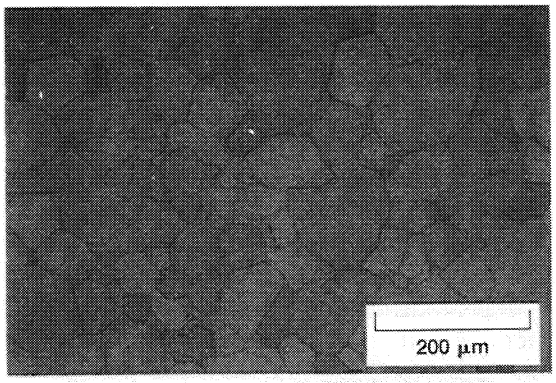

Welded joint in NiAl–0.1 at.% Zr material. (Sealed at 1500 °C and hot isostatically pressed at 1450 °C.)

Over the last couple of years two unique welding methods for intermetallic materials have been developed at NASA Lewis. For both of these methods a glaze of self-generated filler metal is utilized. It is produced when aluminum is evaporated from exposed surfaces heated to 1500 to 1570 °C in vacuum. The self-generated filler metal has a melting point below that of the base metal.

In the first welding method the glaze is produced on the exposed faying surfaces of a set of specimens. The specimens are removed from the vacuum chamber and reassembled in the chamber with the faying surfaces in contact and a small deadweight load on the joint. Welding is accomplished on reheating under vacuum to the melting point of the glaze.

In the second method the faying surfaces are not glazed. The set of specimens is heated to the glazing temperature in vacuum under a deadweight load. Under these conditions the glaze forms only at the periphery and seals the joint. The sealed joint is subsequently diffusion welded by hot isostatic pressing at 1450 °C.

Sound NiAl/NiAl and NiAl–0.1 at.% Zr/NiAl–0.1 at.% Zr weld joints were made by both of these methods. Complete grain growth across the weld interface eliminated visual evidence of the joints. Tensile testing of the weldments showed that welds as strong as the intermetallic materials were produced. Problems involving reproducibility of results remain to be solved. Studies on the effects of the critical variables are in progress. The results to date have shown that two methods are now available to weld nickel aluminum intermetallics.

Bibliography

Moore, T.J.; and Kalinowski, J.M.: Diffusion Brazing NiAl With Self-Generated Filler Metal. High-Temperature Ordered Intermetallic Alloys. V, Materials Research Society Symposium Proceedings, Vol. 288, I. Baker, ed., MRS, Pittsburgh, PA, 1993, pp. 1173–1177.

Moore, T.J.; Kalinowski, J.M.; and Noebe, R.D.: Joining of NiAl and NiAl (0.1 at.% Zr). HITEMP Review 1993: Advanced High-Temperature Engine Materials Technology Program, NASA CP–19117, Vol. 2, 1993, pp. 61–1 to 61–9.

Lewis contacts: Thomas J. Moore, (216) 433–3204; Joseph M. Kalinowski, (216) 433–5524; Ronald D. Noebe, (216) 433–2093
Headquarters program office: OA

Silicon-Carbide-Fiber-Reinforced, Reaction-Formed SiC Matrix Composites Tested

Ceramic matrix composites with high strength and toughness and good thermal conductivity, thermal shock resistance, and oxidation resistance are needed for high-temperature structural applications. These applications are in advanced high-efficiency, high-performance engines for the next generation of aircraft (e.g., the high-speed civil transport) as well as in other power systems. Silicon-carbide-fiber-reinforced, reaction-formed silicon carbide (RFSC) matrix composites show promise of meeting most of the property goals for these applications. These composites meet the criteria of high strength and toughness and have high thermal conductivity and good thermal shock resistance.

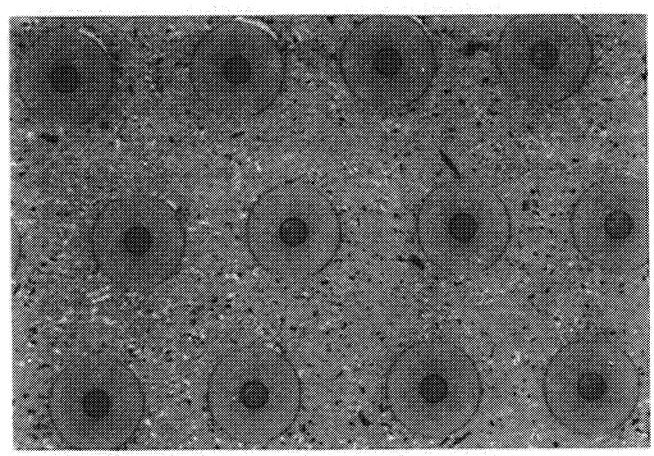

Optical micrograph showing unidirectional SiC (SCS–6)-fiber-reinforced, reaction-formed silicon carbide matrix composite.

Silicon-carbide (SCS–6)-fiber-reinforced silicon carbide composites are being fabricated by NASA's RFSC process. In this process fiber mats are assembled in a mold with a mixture of resin (polymer, pore former, and acid catalyst). The polymer is cured and taken out of the mold for pyrolysis and silicon or silicon alloy infiltration. This processing approach leads to a theoretically dense composite. Matrix microstructure and composition can be tailored for the optimum composite properties.

These composites have been tested in four-point bending at room temperature. The unidirectional composites with ~17 percent by volume of fibers have a first matrix cracking stress above 262 MPa (38 ksi). The interfacial shear strength of this composite is 30 to 60 MPa depending on the processing time, the temperature, and the infiltrant composition. Thermomechanical and thermochemical characterization of these composites under the hostile environments to be encountered in engine applications is under way.

Lewis contacts: Dr. Mrityunjay Singh, (216) 433–8883; Dr. Donald R. Behrendt, (216) 433–5512
Headquarters program office: OA

Pioneer II Melt Modulation Fiber Growth System Wins R&D 100 Award

The key to progress in advanced intermetallic, metallic, and ceramic matrix composites for advanced aerospace and industrial applications centers around the discovery of high-temperature, thermally and chemically compatible fibers. High-temperature applications range from external, actively cooled heat shields to internal engine assemblies. The Pioneer II Melt Modulation fiber growth system provides high-temperature-fiber researchers with the capability to experiment with many unknown materials in growing and evaluating single-crystal fibers for high-temperature composite applications. The flexibility of the process, custom feed rod blending, plus no contamination from crucibles enables the creation and investigation of new materials that would be difficult to produce by traditional techniques.

The Pioneer II Melt Modulation fiber growth system produces single or multiple single-crystal fibers of continuous or discrete length. The fiber is produced from feed rod stock that is introduced to a molten zone. The molten zone is suspended between the feed rod and a single-crystal seed by the forces of surface tension and gravity. The feed rod is a flexible, extruded green body of homogeneous ceramic material. The energy to melt the feed rod is provided by a scanning carbon dioxide laser beam focused onto the molten zone. The Melt Modulation technique used to generate, focus, and control the laser energy gives this system superior capabilities for the production of fibers and has yielded the strongest fibers achieved to date. The rate of fiber growth is governed by microprocessor-controlled motors on the fiber and feed rod pull heads. The Melt Modulation invention provides for one or more fibers to be grown simultaneously and continuously. Growth speeds of over 2 m/hr have been achieved.

The thermal uniformity of the Pioneer II process provides continuous fibers without voids and thus the highest tensile strengths ever achieved. For example, sapphire fibers grown by the commercial edge-defined growth technique have a tensile strength of 3100±500 MPa at room temperature in contrast to 6000±890 MPa for the Melt Modulation fibers tested under the same conditions.

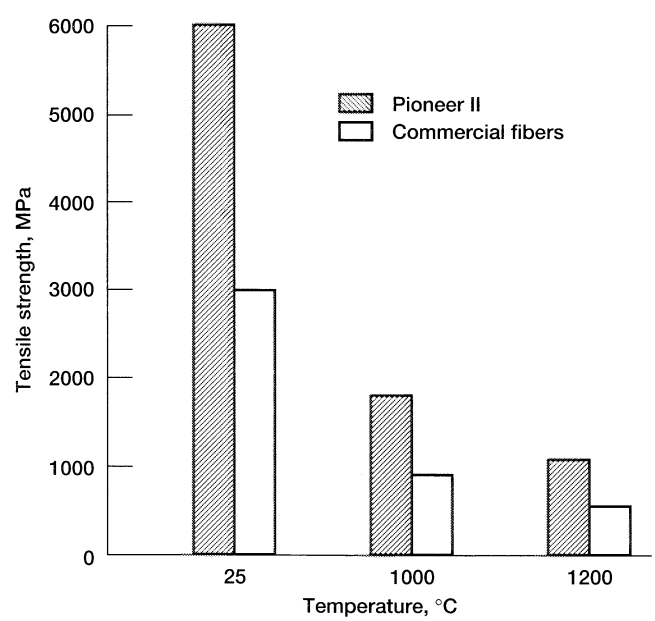

Single-crystal sapphire fibers grown with Pioneer II Melt Modulation compared with commercial sapphire fibers of comparable size.

Bibliography

Gray, H.R.; and Ginty, C.A.: Overview of NASA's Advanced High-Temperature Engine Materials Technology Program, HiTEMP Review 1992, NASA CP–10104, Vol. 1, 1992, pp. 2–1 to 2–25.

Sayir, A.; Farmer, S.C.; and Dickerson, P.O.: Status of Single Crystal and Directionally Solidified Oxide Fibers. HiTEMP Review 1993: Advanced High-Temperature Engine Materials Technology Program, NASA CP–19117, Vol. 3, pp. 83–1 to 83–10.

Lewis contacts: Dr. Ali Sayir, (216) 433–6254; Leonard J. Westfall, (216) 433–5526
Headquarters program office: OA

Reaction-Formed Silicon Carbide Ceramics Fabricated With Tailorable Microstructure and Properties

Silicon-carbide-based ceramics are leading candidate materials for a number of high-temperature applications in aerospace and power generation systems. These ceramics have high strength and modulus and good thermal conductivity and oxidation resistance. Most of the silicon carbide ceramics available today are fabricated by reaction sintering, reaction bonding, hot pressing, and chemical vapor deposition. These techniques are limited by capital equipment, raw materials cost, and processing time and temperature as well as by difficulty in fabricating near-net and complex shapes. All of these factors contribute to the high cost of final components.

The reaction-forming process (RFSC) developed at NASA Lewis overcomes most of these problems. This process produces silicon carbide ceramics at low cost and can fabricate near-net and complex shapes. RFSC has been used to produce dense silicon carbide ceramics with tailorable microstructure and properties. The amount and morphology of second phases (silicon or refractory disilicides) affect the mechanical properties (fracture toughness, flexural strength, and elastic modulus) of these silicon carbide ceramics. For example, the presence of niobium disilicide phase enhances the room-temperature fracture toughness of silicon carbide from 2.5 to 4 MPa $m^{1/2}$ and also reduces the elastic modulus. The room- and high-temperature properties can be tailored to suit design requirements by tailoring the amount and morphology of second phases.

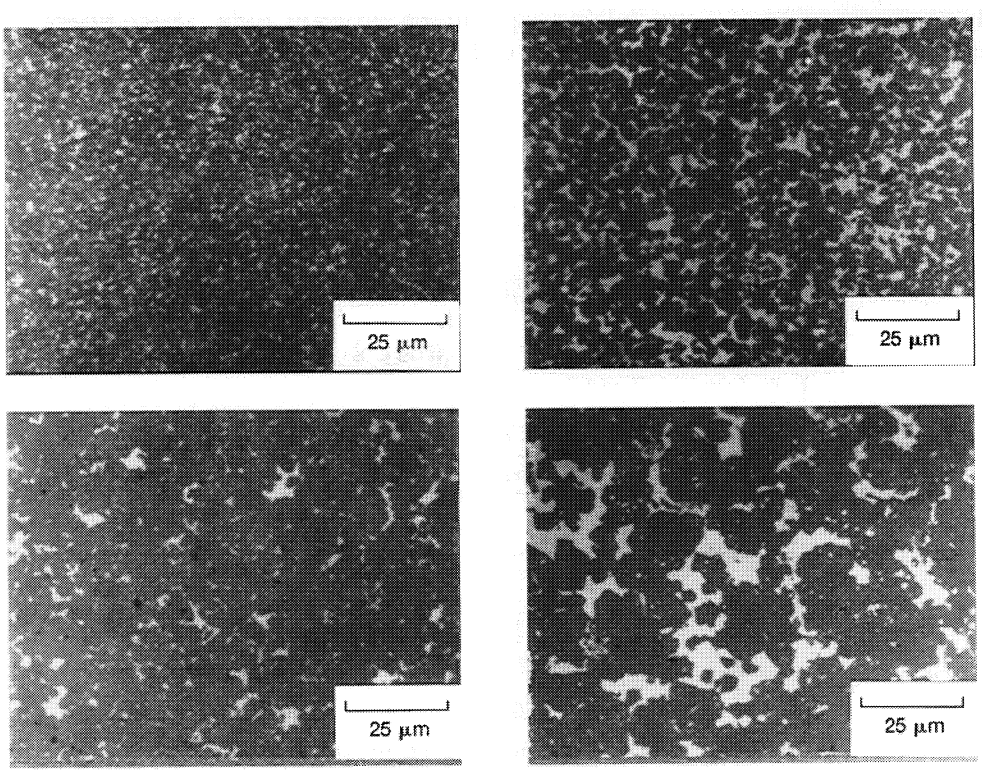

Optical micrographs showing tailorable microstructure of reaction-formed silicon carbide ceramics.

Bibliography

Singh, M.; and Behrendt, D.R.: Studies on the Reactive Melt Infiltration of Silicon and Silicon-Molybdenum Alloys in Porous Carbon. NASA TM–105860, 1992.

Singh, M.; et al.: Mechanical Properties of Reaction-Formed Silicon Carbide Ceramics Containing Silicon and Refractory Disilicide Phases. Ceramic Matrix Composites, American Ceramic Society, Westerville, OH, 1994.

Lewis contacts: Dr. Mrityunjay Singh, (216) 433–8883; Dr. Donald R. Behrendt, (216) 433–5512
Headquarters program office: OA

Microstructures Identified for Optimum Creep Properties of Silicon Carbide Fibers

Creep-resistant ceramic fibers are necessary for high-temperature, long-time ceramic matrix composite (CMC) applications. At present, polycrystalline silicon carbide fibers are the leading candidates for many CMC systems. There are at least four general processing approaches (polymer processing, chemical vapor deposition, chemical conversion, and sintering) for producing developmental polycrystalline silicon carbide fibers. The resulting silicon carbide fibers differ in microstructure and composition owing to processing conditions, impurities, or sintering aids. Consequently, the high-temperature creep properties differ considerably.

Unfortunately, the developmental fibers are difficult to test in pure tensile creep because they are either in short supply, available only in short lengths, or not yet optimized for strength. In order to determine their creep resistance, a bend stress relaxation test (R&T 1990) was used that has been shown to give good correlation of the relative creep resistance of a fiber.

It was found that the creep properties fall into three general categories. The least creep-resistant fibers are mostly polymer-derived fibers (Lox–M Tyranno, Nicalon 201, U. of Florida, and Hi-Nicalon) that have a nanocrystalline silicon carbide–amorphous microstructure with excess carbon and oxygen. The creep resistance, in general, for these fibers is increased as the oxygen content is decreased. The chemically vapor-deposited Textron SCS–6 fiber also falls into this category; however, it is not clear why, since it is an *apparently stoichiometric* polycrystalline silicon carbide.

The moderately creep-resistant fibers have microstructures of stoichiometric silicon carbide grains with excess carbon in grain boundaries or at triple points and/or sintering aids. These fibers were produced by sintering after polymer

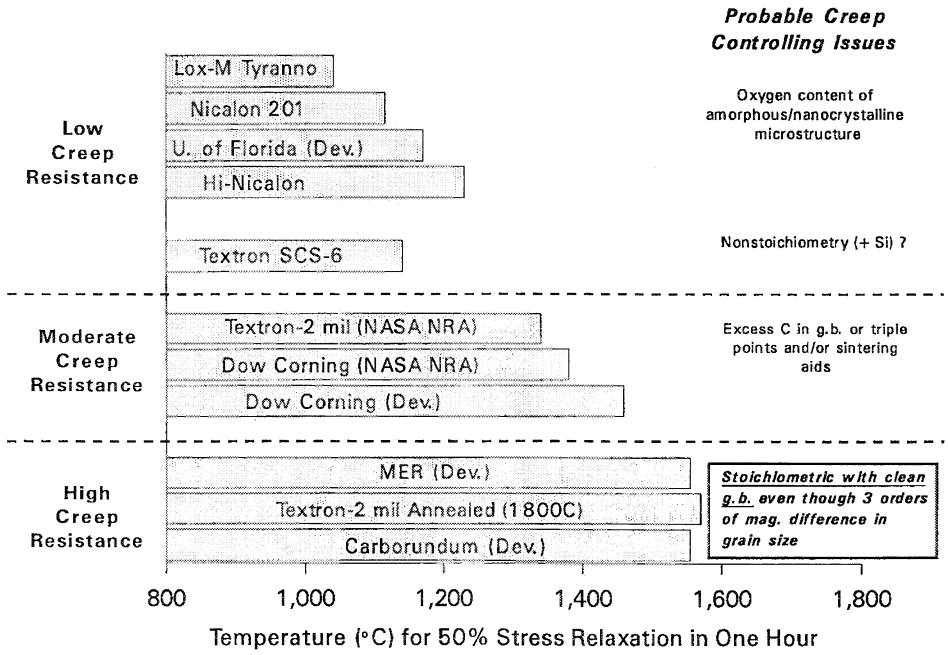

Comparison of relative creep resistance and description of creep-controlling microstructural issues for silicon carbide fibers.

processing (Dow Corning) or by chemical vapor deposition (Textron–2 mil).

The most creep-resistant fibers have microstructures of stoichiometric silicon carbide grains with "clean" grain boundaries. These fibers were produced by sintering (Carborundum), chemical conversion (MER), or chemical vapor deposition followed by high-temperature annealing (Textron–2 mil annealed at 1800 °C). It was also found for these fibers that the creep resistance was approximately the same for differences in grain size of three orders of magnitude. Optimum creep-resistant microstructures depend on stoichiometry and clean grain boundaries and not on grain size. In other words, finer grain fibers may be produced, providing desirable strength properties, without sacrificing creep resistance.

Bibliography

Morscher, G.N.; and DiCarlo, J.A.: A Simple Test for Thermomechanical Evaluation of Ceramic Fibers. J. Am. Ceram. Soc., vol. 75, no. 1, 1992, pp. 136–140.

Morscher, G.N.; and DiCarlo, J.A.: Creep and Stress Relaxation Properties in Relation to Microstructure for SiC Fibers. HITEMP Review 1993: Advanced High-Temperature Engine Materials Technology Program, NASA CP–19117, Vol. 3, 1993, pp. 88–1 to 88–11.

Research & Technology 1990. NASA TM–103759, 1990.

Lewis contact: Gregory N. Morscher, (216) 433–8675
Headquarters program office: OA

New Gold/Chromium Films Lubricate Ceramics From 25 to 800 °C

Ceramics are promising candidates for advanced applications, such as components of turbine engines and aircraft control surfaces, because of their light weight, high-temperature stability, and low thermal conductivity. However, unlubricated ceramics exhibit high friction and wear properties.

Solid lubrication, in the form of thin, soft metallic films, such as gold or silver, appears to be an effective method for lubricating ceramics and has been well documented. Friction is reduced in the sliding contact zone due to the low shear strength of the soft coating coupled with the high load-carrying capability of the hard ceramic substrate. The coatings must, of course, adhere to the substrate during sliding. Unfortunately, relatively inert metals such as silver and gold typically adhere poorly to ceramic substrates. The interfacial bond can be improved by applying the coatings with a high-energy technique, such as ion-beam-assisted deposition. However, metallic films, such as silver, still dewet ceramic substrates at moderate temperatures (about 500 °C).

A more adherent film can be produced by introducing a thin bond layer of a more reactive metal between the inert gold or silver coating and the ceramic substrate. The "binder" or bond metal reacts with the substrate, forming a tenacious interlayer that still presents a metallic surface to the nonreactive solid lubricant. The lubricant film then wets and adheres to the bond metal.

Gold/chromium (Au/Cr) is a coating combination that has shown promise in traditional ceramic applications. As examples, chromium has been used in the electronics industry to bind gold contacts to ceramics and has also been used in the brazing of ceramics. For tribological purposes, gold's low shear strength and excellent thermal and chemical stability make it a potentially good solid lubricant over a wide temperature range. In the Au/Cr system, a thin layer of chromium acts as the interfacial bond between the ceramic substrate and the inert gold solid-lubricant layer.

In recent research sputter-deposited Au/Cr coatings on alumina disks were tested in sliding against bare alumina pins at 25, 500, and

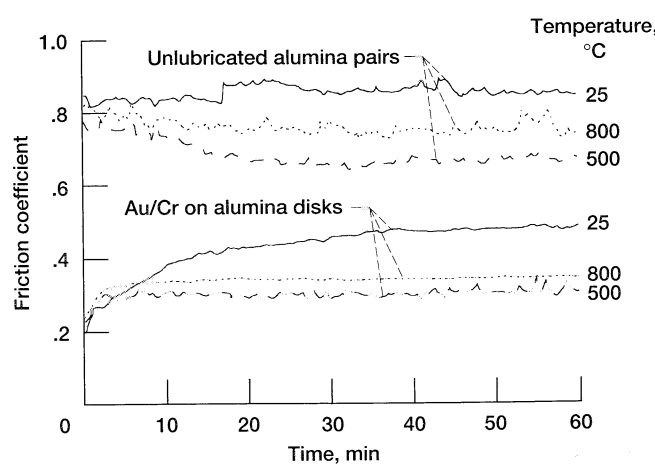

Friction coefficient as function of time for unlubricated and Au/Cr-lubricated alumina specimens.

800 °C. Baseline comparative tests were run at the same temperatures with unlubricated alumina disks sliding against unlubricated alumina pins.

The use of the Au/Cr films reduced friction by about a factor of 2 relative to the unlubricated alumina sliding couple. The coatings prevented wear of the alumina substrate disks and reduced pin wear by one to two orders of magnitude. In addition, wear lives of more than 200,000 sliding passes (9 hr) were observed during sliding at 800 °C. The results suggest that these films show promise for the practical lubrication of many high-temperature sliding components.

Bibliography

Benoy, P.A.; and DellaCorte, C.: Tribological Characteristics of Sputtered Au/Cr Films on Alumina Substrates at Elevated Temperatures. NASA TM–106078, 1993.

Lewis contact: Dr. Christopher DellaCorte, (216) 433–6056
Headquarters program office: OA

Effect of Temperature on Fiber/Matrix Bond Strength Determined

Theory and experiment have shown that the mechanical performance of the fiber-reinforced composite materials being developed for future aeronautics applications depends strongly on the mechanical strength of the interface between the reinforcing fibers and the surrounding matrix. An elevated-temperature fiber pushout apparatus has been developed in-house that measures the strength of the fiber/matrix interface as a function of temperature. This new apparatus provides routine interfacial shear strength measurements to 1100 °C in a nonoxidizing environment. Thus, the composite developer can now select fiber coatings and heat treatments designed to alter fiber/matrix bonding and then measure the actual changes in bonding achieved at temperatures where the composite will be used.

The fiber pushout test measures the force required for an indenter to displace a fiber within a thin slice of composite material. This test has become popular for measuring the interfacial shear strength of the fiber/matrix interface at room temperature. This new apparatus extends this test to elevated temperatures. The specimen is heated by focusing the heating radiation from a quartz halogen lamp outside the test chamber onto the specimen and indenter inside the test chamber. The vacuum environment of the test chamber prevents sample oxidation. An individual fiber being tested is centered underneath the indenter by using a remotely controlled

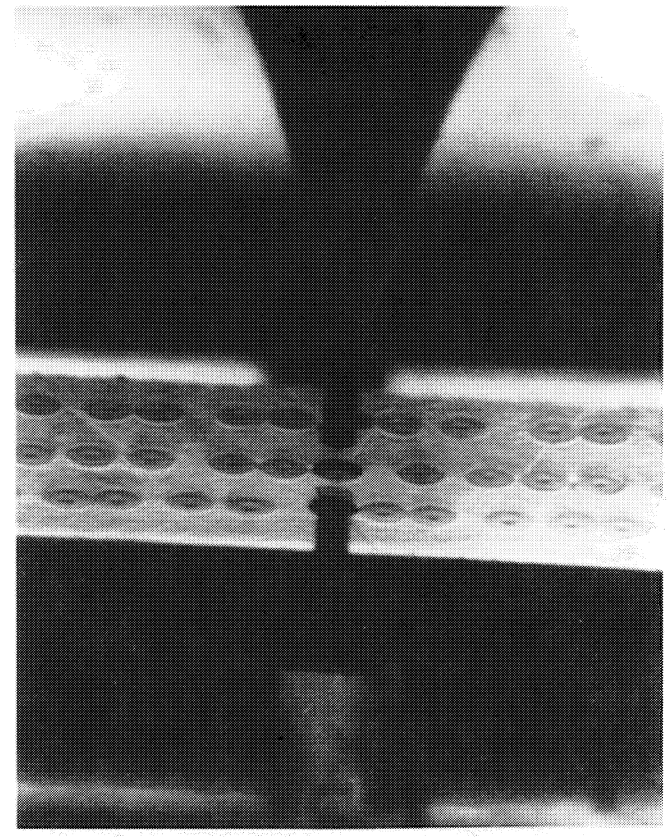

Operator's view of 100-μm-diameter indenter positioned over pushed-out fiber.

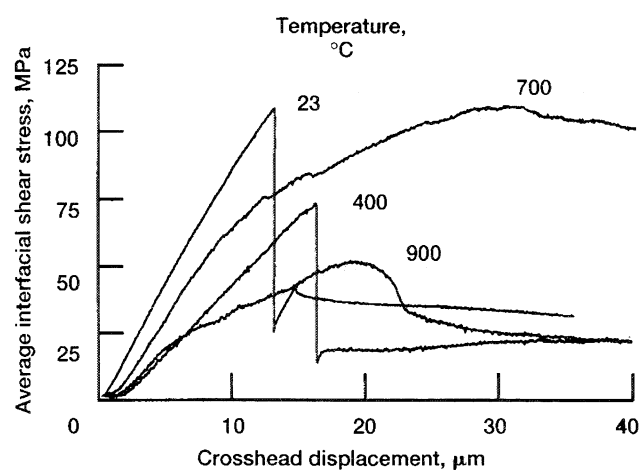

Elevated-temperature fiber pushout curves for sapphire-reinforced NiAl, showing brittle interfacial failure at 23 and 400 °C and ductile interfacial failure at 700 and 900 °C.

translation stage. The indenter is then pushed into the fiber by using a linear motion feedthrough driven by a computer-controlled stepper motor, and the signal is monitored from a load cell to determine the force required to displace the fiber.

The interfacial shear stress was determined as a function of temperature for several silicon-carbide-reinforced, titanium-base matrix composites as well as for a sapphire-reinforced nickel aluminum composite. Differences in fiber debonding and sliding behavior between these composite systems were seen to reflect differences in matrix ductility and wear during fiber sliding. It was shown that not only did the interfacial strength change with temperature, but the mode of fiber debonding changed as well, often from a shear-dominated, brittle failure at lower temperature to a mixed-mode, ductile failure at elevated temperatures. These discoveries have important ramifications for how a composite will perform at various temperatures.

The elevated-temperature fiber pushout apparatus will continue to be used for new composite systems and to evaluate the effect of new fiber coatings and treatments. Its beneficial effect has been evident from the expressed interest of several manufacturers, such as Pratt & Whitney, General Electric, 3M, and Textron Lycoming, in obtaining test results from this instrument.

Bibliography

Eldridge, J.I.: Fiber Push-Out Testing of Intermetallic Matrix Composites at Elevated Temperatures. Intermetallic Matrix Composites II, Materials Research Society Symposium Proceedings, Vol. 273, D.B. Miracle, J.A. Graves, and D.L. Anton, eds., MRS, Pittsburgh, PA, 1992, pp. 325–330.

Lewis contact: Dr. Jeffrey I. Eldridge, (216) 433–6074
Headquarters program office: OA

Hydrogen Annealing Improves Superalloy Oxidation Resistance

The long-term stability of superalloys used as high-temperature turbine blades in jet engines depends in part on the superior oxidation resistance of the metal component. In the past oxidation-resistant coatings were needed to protect nickel-base superalloys in the most demanding applications. These coatings form slow-growing protective and adherent alumina scales. However, coatings decrease the strength of single-crystal superalloys. In recent years single-crystal superalloys have been found to be quite oxidation resistant without a coating, provided that the sulfur impurity level is reduced below one part per million (1 ppm). Hydrogen annealing is a commercially viable technique for producing ultra-clean, low-sulfur components.

Alumina scale adherence (i.e., no spalling at the oxide-metal interface) is required for good cyclic oxidation resistance. This property is usually provided by doping nickel-base alloys with approximately 0.1 percent yttrium or other reactive elements. Critical experiments have shown that the key function of the yttrium is to scavenge parts-per-million levels of sulfur impurities in the alloy and thus prevent segregation to and weakening of the oxide-metal interface. The high-temperature segregation of sulfur on a Pratt & Whitney PWA 1480 single-crystal superalloy surface was indeed found to be large. Levels of 30 at.% resulted from a bulk sulfur content of only 15 ppm. Annealing undoped samples at 1200 to 1300 °C in hydrogen-containing atmospheres chemically purged the sulfur impurity to levels below 0.1 ppm. This resulted in low surface segregation values of 1 at.% as expected from classical surface segregation theory.

Excellent cyclic oxidation resistance then resulted from hydrogen annealing and sulfur removal. A weight loss of only 1 mg/cm^2 resulted from cyclic oxidation at 1100 °C for 1500 1-hr cycles, in contrast to a 20-mg/cm^2 loss after just 400 cycles for unannealed samples. Similarly, General Electric single-crystal René N5 was also effectively purged of sulfur by hydrogen annealing. The annealed sample gained only 2 mg/cm^2 after 1000 cycles at 1150 °C, whereas the unannealed sample lost 24 mg/cm^2 after 500 cycles. These benefits were obtained without yttrium, which attacks mold materials and is difficult to maintain uniformly.

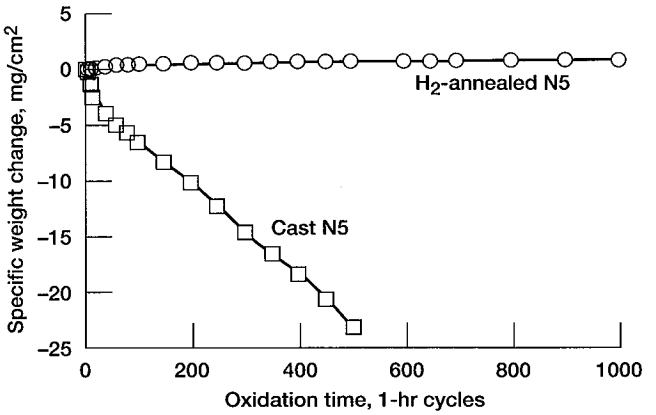

Effect of hydrogen annealing on 2100 °F oxidation: single crystal N5 superalloy as-cast versus 2340 °F, 100-hr hydrogen annealed.

The primary effect has been outside of past NASA programs and is more relevant to engine companies desiring to use uncoated, oxidation-resistant, single-crystal turbine blades. However, a new NASA program, Enabling Propulsion Materials, is now concerned with upgrading the performance of single-crystal turbine blades in the proposed high-speed civil transport engine by using low-sulfur alloys produced by hydrogen annealing.

Bibliography

Jayne, D.T.; and Smialek, J.L.: A Sulfur Segregation Study of PWA 1480, NiCrAl, and NiAl Using XPS With In-Situ Sample Heating. Microscopy of Oxidation, M.J. Bennett and G.W. Lorimer, eds., The Institute of Metals, 1994.

McVay, R.V.; et al.: Oxidation of Low Sulfur Single Crystal Nickel-Base Superalloys. Superalloys, R.A. MacKay, ed., TMS, Warrendale, PA, 1992.

Schaeffer, J.C.; Murphy, W.H.; and Smialek, J.L.: The Effect of Surface Condition and Sulfur on the Environmental Resistance of Airfoils. Submitted to Oxidation of Metals.

Smialek, J.L.: Effect of Sulfur Removal on Al_2O_3 Scale Adhesion. Metall. Trans., A., Vol. 22A, Mar. 1991, pp. 739–752.

Tubbs, B.K.; and Smialek, J.L.: Effect of Sulfur Removal on Scale Adhesion to PWA 1480. Corrosion and Particle Erosion at High Temperatures, V. Srinivasan and K. Vedula, eds., TMS, Warrendale, PA, 1989, pp. 459–486.

Lewis contacts: Dr. James L. Smialek, (216) 433–5500; Douglas T. Jayne, (216) 433–8175

Headquarters program office: OA

Lean-Burn, Rich-Burn High-Pressure-Burner-Rig Materials Capability Developed

The High-Pressure Burner Rig (HPBR) is a unique, in-house facility for conducting environmental durability tests on candidate materials for the High-Speed Research (HSR) Program under way at NASA Lewis. Modified to simulate a high-speed civil transport (HSCT) combustor, the HPBR is a critical test facility to materials development for the combustor designs under study.

The rich-burn, quick-quench, lean-burn (RQL or RBQQ) combustor concept is one potential design being considered for the HSCT vehicle. Developed primarily in response to the requirement to reduce emissions of oxides of nitrogen (NO_x), the RQL combustor will require advanced, lightweight ceramic materials. How these materials behave in the quasi-reducing environment of the rich-burn section of the RQL is of fundamental importance to materials development. As part of NASA's Enabling Propulsion Materials (EPM) Program, a test facility was needed in which sample materials could be subjected to the rich-burn environment (equivalence ratio, temperatures, and flow velocities) projected for the RQL. The HPBR in existence at NASA Lewis was proposed as a facility that could be readily modified to meet program requirements.

Initial experiments demonstrated the feasibility of rich-burn operation. However, subsequent studies concluded that

- The fuel-air mixing was not satisfactory.
- Sufficiently low flow velocities could not be achieved.
- Combustor durability was not satisfactory.
- A water-cooled sample holder would be necessary.
- The byproducts of rich-burn operation were not environmentally acceptable.

Modifying the HPBR to meet EPM requirements mandated extensive redesign and introduction of innovative combustion concepts. Key efforts included implementing a state-of-the-art air blast fuel nozzle, removing environmentally hazardous emissions, and using an inert gas for cooling observation windows, etc. Materials durability

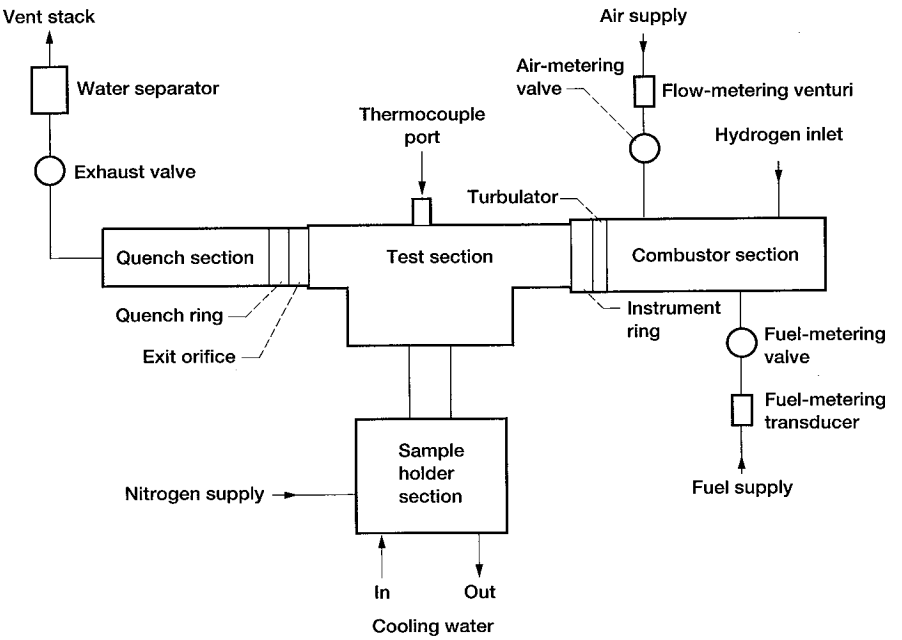

Schematic of HPBR test facility.

problems were another major hurdle in that rig components were expected to have the durability that forms the basis for developing new combustor materials. High-temperature superalloys, along with air and water cooling schemes, were used in designing combustor and sample holder components. Lastly, computer control was added to aid repeatability in facility testing parameters and in providing automated acquisition of key diagnostic test data throughout facility operation. After about a two-year intensive effort the rig has been brought to the point where it meets EPM testing requirements and the materials test program has begun.

As a result the HPBR is operated as a lean- or rich-burn materials test facility. The range of equivalence ratios is 0.3 to 0.9 for lean-burn operation and 1.3 to 2.0 for rich-burn operation. Although the high-temperature region near stoichiometric is avoided to minimize rig component durability problems, gas temperatures above 1550 °C can be obtained for test pressures up to 25 atm. Recently, numerous 50- to 100-hr durability tests have been completed on silicon-based ceramic materials, demonstrating both the reliability and value of the HPBR test facility to the EPM Program.

Lewis contacts: Raymond C. Robinson, (216) 433–5547; Carl A. Stearns, (216) 433–5547
Headquarters program office: OA

Water Vapor Doubles Oxidation of Silicon-Based Ceramics

Silicon-based ceramics and composites are prime candidates for use as components in the hot zones of advanced aircraft engines. Long-term durability of silicon-based materials in the combustion environment is therefore required. Because water vapor is always present as a major combustion product in the engine environment, its effect on the durability of silicon-based ceramics must be understood. Silicon-based ceramics form a protective oxide scale on the surface in combustion environments. Current studies are focused on how water vapor affects the formation of this oxide scale on high-purity silicon carbide (SiC).

Because the combustion environment in advanced aircraft engines is expected to contain about 10-percent water vapor at 10-atm pressure, the durability of SiC in gas mixtures containing 0.1- to 1-atm water vapor is of interest. Initial tests were conducted to determine the SiC oxidation rate in 10-percent water vapor/90-percent oxygen mixtures for 100-hr exposures at temperatures between 1200 and 1400 °C. Parabolic rates were determined from both weight change and oxide (SiO_2) thickness measurements. These oxidation rates were then compared with rates measured in dry oxygen. Oxidation

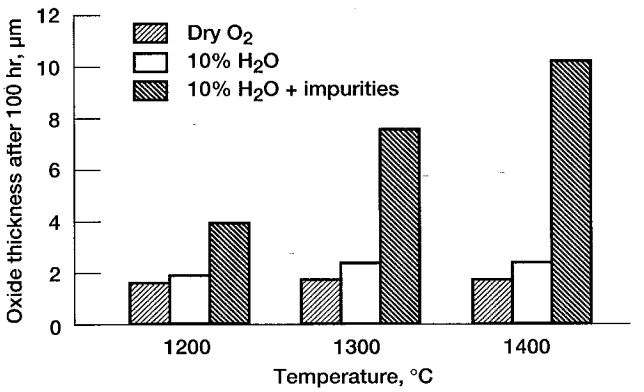

Effect of water vapor and sodium and aluminum impurities on oxide thickness formed on pure SiC at various temperatures.

rates for SiC in 10-percent water vapor were about two times greater than in dry oxygen. However, impurities, such as sodium and aluminum, in the presence of water vapor increased the oxidation rate by a factor of 4 to 30 depending on temperature. The dependence of the oxidation rate on water vapor partial pressure is currently being studied for these same times and temperatures.

Relatively little is known about the performance of silicon-base ceramics over the long term in real combustion environments. An understanding of water vapor effects and impurity effects is essential to applying these new materials.

Bibliography

Opila, Elizabeth J.: The Oxidation Kinetics of Chemically Vapor Deposited Silicon Carbide in Wet Oxygen. To be published in J. Am. Ceram. Soc.

Lewis contact: Dr. Elizabeth J. Opila, (216) 433–8904
Headquarters program office: OA

Interfacial Molybdenum Coating Enhances Mechanical Properties of Al_2O_3/NiAl Composite

Nickel aluminum (NiAl) composites reinforced with continuous fibers of aluminum oxide (Al_2O_3) are of interest as high-temperature structural materials for future aerospace applications. As in any other composite system the fiber/matrix interface has a strong influence on the mechanical properties of an Al_2O_3/NiAl composite. The interface design becomes particularly difficult for an Al_2O_3/NiAl composite because of two factors: the brittleness of NiAl at room temperature, and the mismatch in coefficients of thermal expansion (CTE) between the fiber and the matrix. A weak fiber/matrix bond is required to increase the fracture toughness of the composite at room temperature. In contrast, a strong fiber/matrix bond is required to withstand some of the residual stresses resulting from the fiber/matrix CTE mismatch. One viable interface coating option to accommodate these conflicting bonding requirements is to incorporate a ductile interface layer well bonded to both the fiber and the matrix.

Molybdenum was chosen as the ductile interface layer because of its chemical compatibility with both NiAl and Al_2O_3. An oxide reduction technique was employed to apply molybdenum coatings onto single-crystal Al_2O_3 fibers. The fiber was first coated with a slurry of molybdenum oxide (MoO_3), and the slurry-coated fiber was heat treated in a gaseous-hydrogen-containing atmosphere at high temperature to reduce MoO_3 to Mo. Composites with interfacial molybdenum coating were fabricated by both binderless and powder cloth techniques, and their properties were evaluated.

Fiber pushout tests were conducted to determine the interfacial shear strength. Composites with interfacial molybdenum coating had interfacial shear strengths of 110 to 160 MPa, higher than that for Al_2O_3/NiAl composites with a frictional interface bond. Debonding during pushout always occurred at the Mo/Al_2O_3 interface rather than at the Mo/NiAl interface. The interface failure during fiber pushout was due to ductile fracture of molybdenum adjacent to the interface.

Composites with interfacial molybdenum coating were thermally cycled between room temperature and 1027 °C in an inert atmosphere for as many

as 500 cycles. Debonding at the fiber/coating interface occurred after thermal cycling, the extent of debonding increasing with the number of cycles.

Composite tensile testing at room temperature resulted in limited circumferential debonding at the fiber/matrix interface but no fiber pullout. In contrast, in a frictionally bonded Al_2O_3/NiAl composite (with no interface coating) significant fiber pullout occurs. The fracture surface of the composite after tensile testing at 927 °C revealed extensive circumferential debonding along the fiber/coating interface, suggesting loss of the fiber/coating bond at higher temperatures. This was also reflected in the tensile test data, which indicated load transfer from the matrix to the fiber at room temperature but not at high temperature.

In summary, studies to date have shown that interfacial shear strengths greater than that due to a purely frictional fiber/matrix bond can be achieved with interfacial molybdenum coatings applied by the oxide reduction technique. However, the bond strength between molybdenum and Al_2O_3 needs to be further increased to allow for effective load transfer between the fiber and the matrix at high temperature and to prevent debonding during thermal cycling. Studies are continuing toward achieving this goal. In addition, other ductile metals, such as niobium and platinum, are being investigated as potential interfacial coatings for Al_2O_3/NiAl composites.

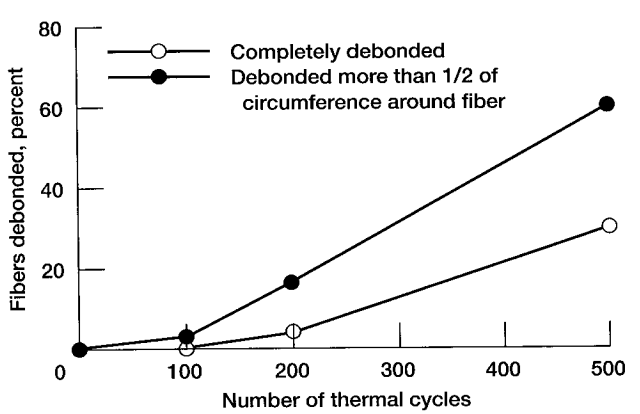

Debonding at Al_2O_3 fiber/Mo coating interface during thermal cycling of Al_2O_3-reinforced NiAl from room temperature to 1027 °C in inert atmosphere.

Bibliography

Misra, A.K.; et al.: Interface Mo Coatings for Al_2O_3/NiAl Composite. HITEMP Review 1993: Advanced High-Temperature Engine Materials Technology Program, NASA CP–19117, Vol. 2, pp. 58–1 to 58–13.

Misra, A.K.; Crandall, K.S.; and Bowman, R.R.: Modification of Interface in Al_2O_3/NiAl Composite. HITEMP Review 1992: Advanced High-Temperature Engine Materials Technology Program, NASA CP–10104, Vol. 2, pp. 39–1 to 39–15.

Lewis contacts: Dr. Ajay K. Misra, (216) 433–5497; Dr. Randy R. Bowman, (216) 433–3205
Headquarters program office: OA

Amorphous Silicon Nitride Coatings Provide Oxidation Barrier for High-Temperature Polymer Composites

The purpose of developing advanced composites for aerospace applications is to attain improved high-temperature performance by using high-strength, low-density materials. One such material is the carbon-fiber-reinforced polymer matrix composite (PMC) made with high-temperature resins. This material possesses a low density (1.65 g/cm^3) and a high strength (1.4 GPa) comparable to titanium. A single factor that limits more widespread incorporation of PMC's in jet engines, however, is the temperature tolerance of the material. The upper usable temperature limit of these PMC's, where the mechanical properties are retained, is determined by the glass transition temperature of the resin (as high as 400 °C). However, the vulnerability of the resin to oxidation limits the maximum use temperature to 316 °C. This use temperature could be extended, and PMC components incorporated into hotter regions of an engine, if a protective oxidation barrier coating could limit the diffusion of oxygen to the substrate and hence retard oxidation.

When selecting a potential coating due consideration must be given to ensuring that the total stress on the coating remains within the yield strength of the coating material. The total stress on the coating is the sum of the imposed thermal stresses (due to a mismatch in the thermal expansion coefficients), an intrinsic stress (due to the deposition conditions and coating composition), and a residual stress (due to thermal

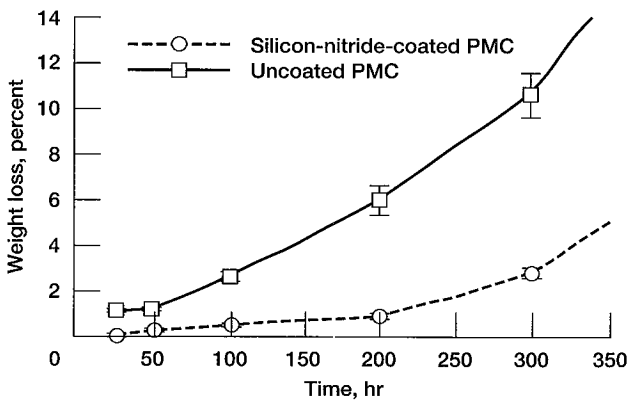

Isothermal aging at 371 °C, in air, of coated and uncoated carbon fiber reinforced PMR–II–50 composites: Error bars reflect 95-percent confidence limits; 10 uncoated and 5 coated PMC's averaged.

instability when aged; i.e., a change in coating microstructure, volume, or composition). Note that the mechanical properties of thin films can differ greatly from those of the bulk material.

In-house experiments use plasma-assisted chemical vapor deposition techniques to deposit amorphous silicon nitride coatings (up to 5 μm thick) on high-temperature PMC's: a PMR–II–50 resin matrix reinforced unidirectionally with T650–35 carbon fibers (65 vol.%). Complete encapsulation of the PMC has been achieved. The as-deposited coatings demonstrate excellent adhesion and conformity to the rough surfaces of PMC's (compression die molded and autoclaved). Thermal cycling (1000 cycles from 25 to 232 °C) had no effect on the integrity and adhesion of the coatings. Long-term isothermal aging of the coated composites in air (500 hr at 371 °C) demonstrated the viability of the coating. Very little weight loss was recorded for the initial 200 hr (an approximately 85-percent reduction in weight loss relative to the uncoated material). The subsequent reduction in oxidation protection was due to the coating failing on the machined sides of the PMC containing the cut-fiber ends. This problem is the subject of on-going research.

Bibliography

Harding, D.R.; Sutter, J.K.; and Papadopoulos, D.S.: Protective Coatings for High Temperature Polymer Matrix Composites. NASA TM–106276, 1993.

Meador, M.A.; Cavano, P.J.; and Malarik, D.C.: High Temperature Polymer Matrix Composites for Extreme Environments. Structural Composites: Design and Processing Technologies, Proceedings of the Sixth Annual ASM/ESD Advanced Composites Conference, ASM International, Materials Park, OH, 1990, pp. 529–539.

Lewis contact: Dr. David R. Harding, (216) 433–6175
Headquarters program office: OA

1993 Jacquet-Lucas Award Received for Excellence in Metallography

A NASA Lewis Materials Division entry, "Qualitative Analysis of Color Metallography," was awarded the 1993 Jacquet-Lucas Award for Excellence in Metallography. The award is presented to the Best of Show recipient in the International Metallographic Contest sponsored jointly by the International Metallographic Society (IMS) and American Society for Metals (ASM) International. The award includes the Jacquet Gold Medal from IMS and the Francis F. Lucas Award for Excellence in Metallography from ASM.

Development of new materials for high-temperature propulsion applications requires state-of-the-art characterization techniques. The complex microstructure of composites consisting of fibers, fiber coatings, matrix, and reaction zones poses unique challenges. Standard methods of showing the structure of a material use an acid solution to attack a highly polished surface. These methods are not always effective on advanced materials because acid attack may show one structure component but no others. A way of showing all differences in chemistry was needed. Interference layering, where a thin film is deposited on the specimen surface, has been found to give color patterns that are unique to a given chemistry. This method has been adapted and refined at NASA Lewis and shared with contractor researchers in the field. The entry details the use of interference layering and color metallography to distinguish various phases in a ceramic composite by color. Each phase is verified by backscattered electron imaging and x-ray dot mapping in an electron microprobe. After the color representing each phase had been verified, interference layering allows more rapid and lower cost observation of phase distributions by optical rather than electron microscopy.

The ceramic composite used in this work is under consideration for use in the Enabling Propulsion Materials Program. Interference layering has also

ORIGINAL PAGE
BLACK AND WHITE PHOTOGRAPH

1993 Jacquet-Lucas Award recipients (left to right): Frank Terepka (NASA), Todd Leonhardt (Sverdrup), Mrityunjay Singh (NRC), and Gayle Soltis (Cortez).

been applied in cases where complex microstructures are encountered. Research on thermal barrier coatings, intermetallic composites, high-temperature superconductors, and iridium/rhenium rocket nozzles have all benefited from the interference layering technique.

Bibliography

Brindley, W.; and Leonhardt, T.: Metallographic Techniques for Evaluation of Thermal Barrier Coatings. Mater. Character., vol. 24, no. 2, Mar. 1990, pp. 93–101.

Lewis contact: Todd A. Leonhardt, (216) 433–3294
Headquarters program office: OA

1992 Materials Division Paper of the Year Plastic Flow and Fracture Analyzed in B2 NiAl-Base Intermetallic Alloys Containing a Ductile Second Phase

The ordered intermetallic compound nickel aluminum (NiAl) has been identified as a potential replacement material for nickel-base superalloys in critical jet engine components such as turbine airfoils. However, the use of NiAl-base alloys in structural applications has been hindered by their lack of tensile ductility and poor fracture toughness at room temperature. The operative flow and fracture mechanisms in monolithic NiAl leading to these unacceptable room-temperature properties have been analyzed in detail during previous work at NASA Lewis—demonstrating the need for a ductile phase toughening approach to alloy design.

This work generated a review of the ductile phase-toughening mechanisms in intermetallic materials in general and in NiAl specifically. Details of specific mechanisms operating in NiAl were determined from model experiments performed on prototypical NiAl-base systems processed at NASA Lewis and examined jointly through a cooperative effort with the University of Michigan. The microstructure of one model alloy was systematically varied by altering the solidification rate—permitting a detailed analysis of second-phase morphology on mechanical properties. In this Ni-30Al alloy, room-temperature ductility could be varied from 4 percent to almost 10 percent tensile elongation depending on the morphology of the ductile phase. In contrast, the single-phase NiAl alloy exhibited negligible room-temperature tensile ductility.

The greatest improvement in ductility was observed in material with a continuous second phase and was attributed to crack-bridging mechanisms. When the ductile second phase was not continuous, both crack deflection and a previously unknown toughening mechanism, known as slip transfer, were observed. Crack bridging and crack deflection work on a macroscopic scale to improve the toughness of a two-phase alloy,

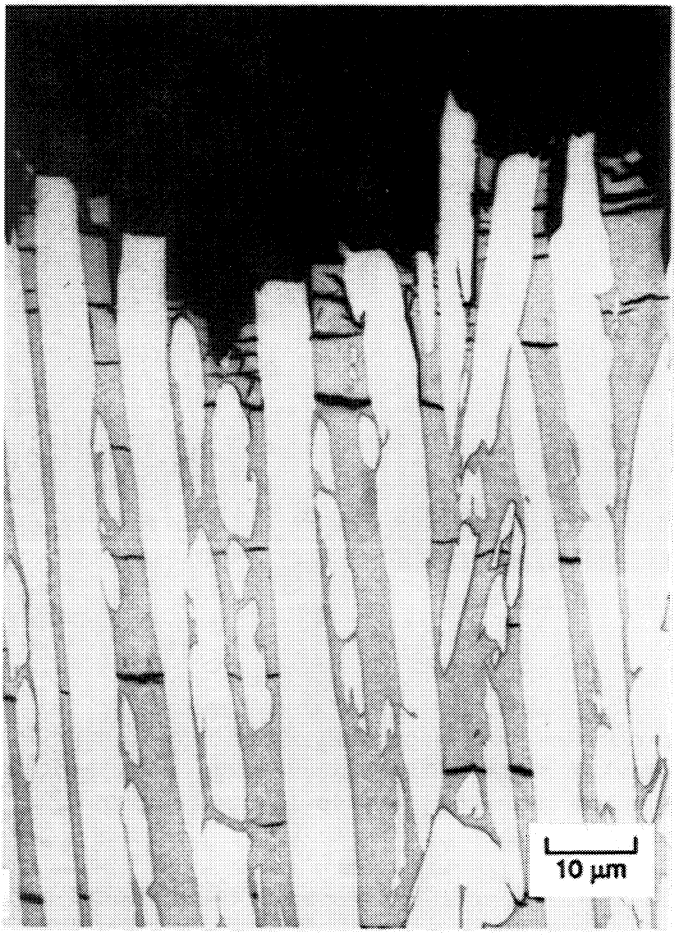

Cross section of an Ni-30Al tensile sample deformed to almost 10 percent strain. Crack bridging occurs by Ni_3Al rods present in the NiAl matrix.

but slip transfer works on a microscopic level by increasing the inherent ductility of the brittle phase through increased dislocation production at the bimaterial interfaces. Second-phase orientation relationships and interface properties necessary to enhance the slip transfer process have been identified and loose guidelines for optimizing two-phase microstructures for improved low-temperature properties have been developed for NiAl-base systems. These guidelines are being incorporated into second-generation alloy development efforts.

Bibliography

Misra, A.; Noebe, R.D.; and Gibala, R.: On the Mechanism of Ductility Enhancement in $\beta+\gamma'$–$Ni_{70}Al_{30}$ and $\beta+(\gamma+\gamma')$–$Ni_{50}Fe_{30}Al_{20}$ in Situ Composites. Intermetallic Matrix Composites II, Materials Research Society Symposium Proceedings, Vol. 273, D.B. Miracle, D.L. Anton, and J.A. Graves, eds., MRS, Pittsburgh, PA, 1992, pp. 205–210.

Misra, A.; Noebe, R.D.; and Gibala, R.: The Role of Interfaces in the Room Temperature Mechanical Behavior of Directionally Solidified $\beta+\gamma'$–$Ni_{70}Al_{30}$ and $\beta+(\gamma+\gamma')$–$Ni_{50}Fe_{30}Al_{20}$ Alloys. High-Temperature Ordered Intermetallic Alloys, Materials Research Society Symposium Proceedings, Vol. 22, I. Baker, ed., MRS, Pittsburgh, PA, 1993, pp. 483–488.

Noebe, R.D.; Misra, A.; and Gibala, R.: Plastic Flow and Fracture of B2 NiAl-Based Intermetallic Alloys Containing a Ductile Second Phase. Iron Steel Inst., Japan Int., vol. 31, 1991, pp. 1172–1185.

Lewis contact: Ronald D. Noebe, (216) 433–2093
Headquarters program office: OA

Structures

Interlaminar Damping Layers Increase Damping in Composite Plates

Composite materials are used extensively because of their high ratios of strength and stiffness to weight. In addition, polymer matrix composites (PMC's), such as graphite/epoxy, have improved damping properties, which can be significant in applications involving noise and vibration, fatigue loading, and impact. Methods have been developed at NASA Lewis to model, predict, and measure the damping properties of layered composite materials.

Recent research in this area has been directed toward investigating the use of viscoelastic damping layers embedded in composite laminates to further improve the damping capacity of composite structures. Finite-element-based mechanics for the damped dynamic analysis of thick composite structures incorporating viscoelastic damping layers have been developed. These methods involve a discrete layer damping theory that allows general laminate layups and the use of viscoelastic properties for the damping layers. Composite laminates incorporating damping layers have been fabricated and tested to quantify the damping improvements and to validate the computational methods.

The composite plates that include the damping layers have shown significant increases in modal damping. For the plates that were tested,

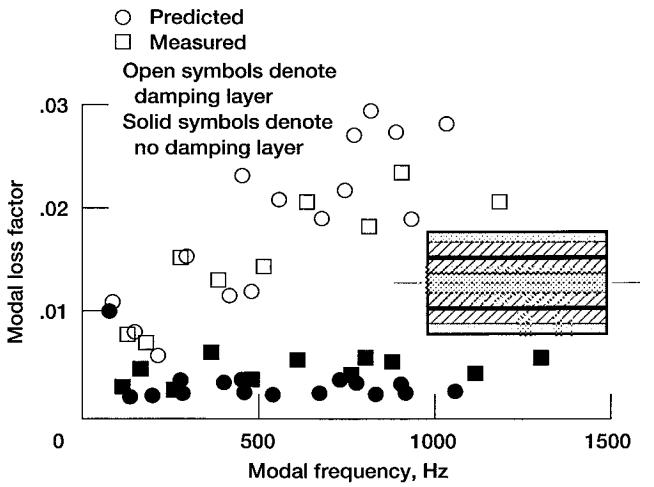

Predicted and measured modal characteristics of a $[45_2/-45_2/i/45_2/-45_2]_s$ T300/934 simply supported plate with ISD110 damping layers.

damping increased by as much as a factor of 5. The very good agreement between predicted and measured results provided credibility to the computational methods. These methods have shown that both the natural frequency and damping of composite structures can be tailored by changing the laminate orientations. Composites with interlaminar damping layers have many applications in engine structures, and methods for tailoring these structures for specified frequencies and damping are now available.

Bibliography

Pereira, J.M.: Dynamic Response of Composite Plates With Interlaminar Damping Layers. Vibro-Acoustic Characterization of Materials and Structures, NCA–Vol. 14, P.K. Raju, ed., ASME, 1992, pp. 51–56.

Saravanos, D.A.; and Chamis, C.C.: Integrated Mechanics for the Passive Damping of Polymer-Matrix Composites and Composite Structures. NASA TM–104346, 1991.

Saravanos, D.A.; and Chamis, C.C.: Damped Dynamic Characteristics of Specialty Composite Materials and Structures. Vibro-Acoustic Characterization of Materials and Structures, NCA–Vol. 14, P.K. Raju, ed., ASME, 1992, pp. 31–38.

Lewis contacts: Dr. Dimitrios A. Saravanos, (216) 433–8466; Dr. J. Michael Pereira, (216) 433–6738; Dr. Christos C. Chamis, (216) 433–3252
Headquarters program office: OA

Transpiration-Cooled Seal Concepts Tested for National Aerospace Plane

Key to the success of the National Aerospace Plane Program is the development of an advanced airbreathing scramjet engine. Conditions inside such an engine approach the physical limitations of most aerospace materials and structures currently used in propulsion systems. Hence, a number of new enabling technologies are required to bring this project to fruition. One of these technologies is the development of engine seals. The seals must not only be able to resist the harsh temperatures and pressures inside the engine, but must also be flexible to accommodate movement and distortion of the engine panels during flight. One promising concept is to make the seals out of porous ceramic rope; cold hydrogen gas would flow through the rope, cooling the seal and containing the engine's hot combustion gases.

In a cooperative effort NASA Lewis and Pratt & Whitney Aircraft entered a joint research program to test the transpiration-cooled seal concept in the hot gas facility in Cell 22 of the Rocket Laboratory. These tests subjected the seals to hot gas flow similar to that expected in the scramjet engine. Instrumentation and infrared image data were recorded for each test and were used to assess the transpiration cooling efficiency of both a woven and a braided seal construction.

These results will influence design decisions currently being made with regard to these high-temperature seals as well as the entire NASP engine itself. The success of this effort has demonstrated the advantages of NASA/industry cooperation and has set the stage for upcoming research programs to advance hypersonic technologies.

Lewis contact: Matthew E. Melis, (216) 433–3322
Headquarters program office: OA

Ultrasonic Imaging Used for Characterizing Advanced Material Microstructure

Traditional nondestructive evaluation imaging methods for characterizing high-performance materials, such as vehicular engine ceramics and composites, include x-radiography, ultrasonics, and thermal scans. In normal application these methods measure the amplitude of transmission of the respective energy used. In general, they provide efficient, quasi-quantitative measures of material homogeneity but may lack the precision necessary for detailed microstructural evaluation of high-performance materials. The use of materials in the harsh operating environments of future engines requires detailed quantitative knowledge of microstructural and compositional variability so that accept-reject criteria can be defined for processes and components. Mechanical testing and direct microstructural examination using discrete and limited sampling procedures cannot adequately measure the extent and nature of material variations.

Therefore, the ultrasonic contact pulse-echo method was used in an automated scanning configuration in an attempt to quantify and map nonuniformity in sintered silicon nitride (Si_3N_4) disks containing distinct regions of high pore fraction formed during sintering. Reflection coefficient, attenuation coefficient, and velocity maps of the Si_3N_4 disks were developed over a wide frequency range (e.g., 30 to 110 MHz) by using spectral analysis of the received ultrasonic waveform. These three types of ultrasonic property map were examined to determine which is most effective in characterizing nonuniformity and what is the nature of the correlation, if any, between the different maps. Spectral analysis was employed to determine if inhomogeneity was a function of frequency and to characterize the elastic (dispersion) behavior for Si_3N_4. Additionally, maps of Poisson's ratio for a disk were constructed from longitudinal and shear-wave velocity images. Thermal wave imaging and Vickers microhardness measurements were used to determine if physical behavior variations correlated with pore fraction variations characterized metallographically and in ultrasonic images. A positive correlation would indicate the usefulness of the ultrasonic measurement as an aid for predicting physical behavior.

Ultrasonic velocity images revealed and quantified the extent of pore fraction variation in the silicon nitride disks. The magnitude and direction of variations in cross-correlation velocity images were very similar to those for pore fraction variations.

Attenuation coefficient images revealed patterns of nonuniformity as the result of scattering at boundaries between regions of high and low pore fraction. The contact scan procedure proved more precise and accurate (i.e., more quantitative) than ultrasonic C-scans by characterizing inhomogeneity in terms of ultrasonic material properties. Spatial patterns of velocity and attenuation coefficient images from a contact scan were nearly identical at frequencies within the 50-percent bandwidth (50 to 80 MHz) but became unfocused at frequency extremes.

Velocity and attenuation coefficient images were nearly identical for machined and polished disks, making the method readily applicable to flat machined materials.

Maps of "apparent" Poisson's ratio constructed from longitudinal and shear-wave velocities quantified Poisson ratio variations across a silicon nitride disk.

Experimental velocity results agreed well with those predicted as a function of pore fraction and frequency. Experimental reflection coefficient results agreed well with those predicted as a function of frequency for couplant thickness of ~0.5 μm but did not show the expected dependence on pore fraction. Experimental attenuation coefficient changes were similar to those predicted due to pore scattering as a function of frequency change for a pore concentration of $10^8/cm^3$.

Thermal wave images of a disk indicated transient thermal behavior variations consistent with observed pore fraction and velocity and attenuation coefficient variations.

Bibliography

Roth, D.J.; et al.: Quantitative Mapping of Pore Fraction Variations in Silicon Nitride Using an Ultrasonic Contact Scan Technique. NASA TP–3377, 1993.

Lewis contact: Dr. Don J. Roth, (216) 433–6017
Headquarters program office: OA

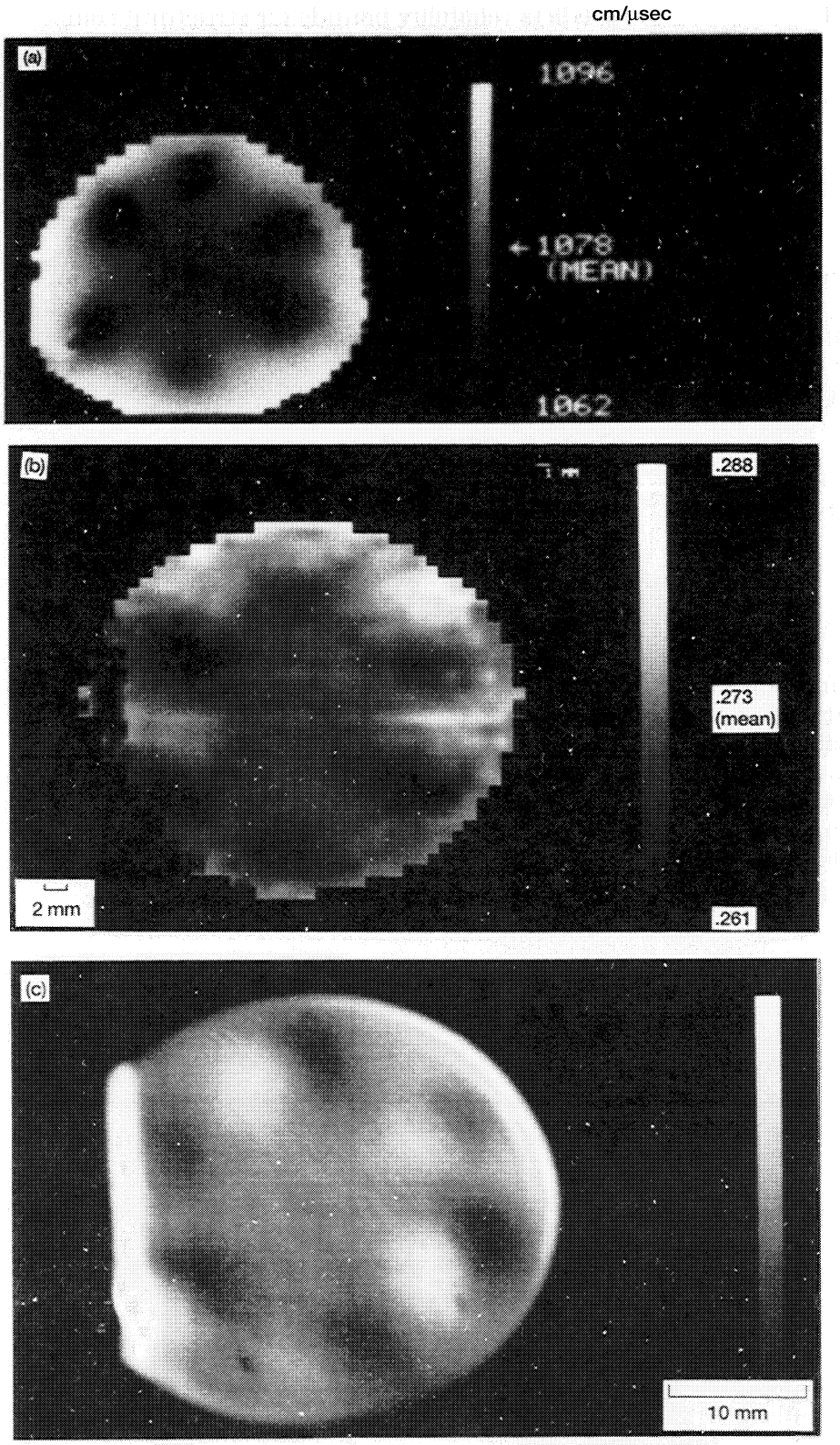

Ultrasonic contact scanning quantifies microstructural and physical property variation within structural materials. (Dark spots indicate high-pore-fraction regions.) (a) Ultrasonic velocity image; (b) ultrasonic Poisson's ratio image; (c) back-echo C scan (reveals but does not quantify).

Reliability Evaluated for Laminated CMC Components

Structural components fabricated from laminated ceramic matrix composite (CMC) materials are being considered for a broad range of aerospace and industrial applications, specifically those involving high-temperature environments. These engineered CMC material systems exhibit desirable properties, such as strength retention at high temperatures, chemical inertness, and low density, but their general variability in strength (especially in directions transverse to the fiber reinforcement) requires a rethinking of design concepts. Traditional factor-of-safety design procedures rooted in deterministic engineering mechanics and commonly used for the metal alloys must be abandoned in favor of probabilistic design methods.

In order to establish this new design philosophy, the integrated design program C/CARES (for composite ceramics analysis and reliability of structures) has been developed with funding from the Advanced High-Temperature Engine Materials Technology Program (HITEMP). This ongoing project of developing probabilistic design methods is being supported by personnel at NASA Lewis working under a cooperative agreement with Cleveland State University. The goal is to provide design engineers with a computer program that predicts reliability bounds for structural components fabricated from laminated CMC material systems. Component stress fields obtained from finite element analyses are fundamental in the prediction of component reliability. The C/CARES program has been interfaced with several commercial finite element codes, including ANSYS, ABAQUS, MSC/NASTRAN, and MARC. In general, the program utilizes a formatted neutral data base that readily allows coupling C/CARES to any general-purpose finite element program that supports laminated composite analysis.

To date, C/CARES has been released to several American companies for beta testing. In particular, C/CARES has been used to aid in the design of a laminated CMC heat exchanger for industrial furnace applications. Future versions of the program will include the ability to account for the time-dependent reliability of CMC components.

Bibliography

Duffy, S.F.; Palko, J.L.; and Gyekenyesi, J.P.: Structural Reliability Analysis of Laminated CMC Components. NASA TM–103685, 1991.

Starlinger, A.; et al.: Reliability Analysis of Laminated CMC Applying Shell Subelement Techniques. AIAA Paper 92–2348, 1992.

Lewis contact: Joseph L. Palko, (216) 433–5587
Headquarters program office: OA

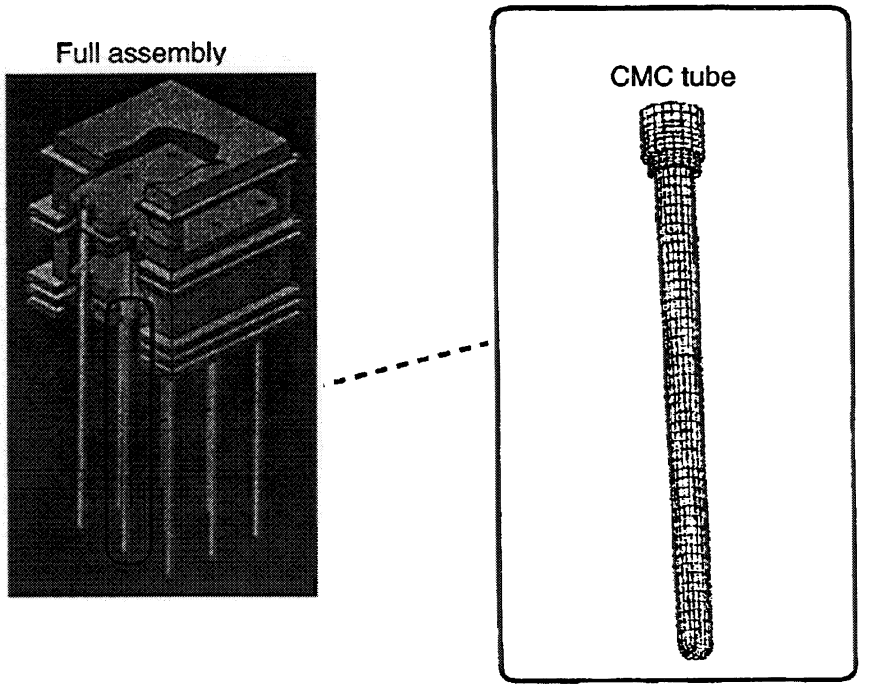

Advanced heat exchanger.

High-Temperature Dynamic Engine Seal Being Developed

Combined-cycle ramjet/scramjet engines being designed for advanced hypersonic vehicles, including the National Aerospace Plane (NASP), require innovative high-temperature dynamic seals to seal the sliding interfaces of the articulating engine panels. New seals are required that will operate hot (1200 to 2000 °F), will seal pressures ranging from 0 to 100 psi, will remain flexible to accommodate significant sidewall distortions, and will resist abrasion over the engine's operational life. NASA Lewis is developing advanced seal concepts and sealing technology to meet these demanding seal challenges.

The current study reviews the recent high-temperature durability screening assessments of the braided ceramic rope seal concept, which is braided of emerging high-temperature materials. The current work presents durability data for the fundamental seal building blocks (a range of candidate ceramic fiber tows) and for braided rope seal subelements that were scrubbed under engine simulated sliding, temperature, and preload conditions.

Alternative fiber durability tests were run to assess the relative sliding durability of a range of candidate ceramic materials under both air and hydrogen environments. Tests were run at room temperature, 930 °F, and 1650 °F. These tests demonstrated the deleterious effects on the high-temperature sliding durability of Nextel 312 and 440 caused by heat treating the fibers at 1750 °F for 12 hr. This heat treating, or material conditioning, is recommended by the manufacturer to improve fiber resistance to steam environments. Unfortunately, this preexposure temperature falls well within the intended seal operating temperature. The tow durability tests also revealed the encouraging result that a new fiber, Nextel 550 (Al_2O_3-SiO_2), was not degraded by this temperature preexposure. A second sequence of tow durability tests with the same fibers were run in hydrogen at the same three temperatures. These tests showed that the oxide ceramic fibers exhibited somewhat better sliding durability in hydrogen than in air at temperature.

The relative sliding durability of a range of seal subelement architecture and material combinations was assessed in a joint program between NASA, Pratt & Whitney, and Drexel University. The high-temperature durability of five different braided rope seals was assessed. Only the hybrid braided rope seals, which have a metal sheath braided over a dense uniaxial ceramic core, survived the full 2000-cycle duty cycle. Although the all-ceramic seals exhibited lower leakage rates than the hybrid seals, the all-ceramic seal sheaths were severely damaged after only 14 to 42 percent of the duty cycle. The hybrid seals also exhibited lower friction at temperature, a key for smooth engine panel articulation.

On the basis of the results obtained, the hybrid architecture will be further optimized to exploit its excellent durability and low friction while reducing leakage flow rates. These seal development and optimization studies will be performed in a new high-temperature dynamic seal test rig under development at NASA Lewis. This fixture

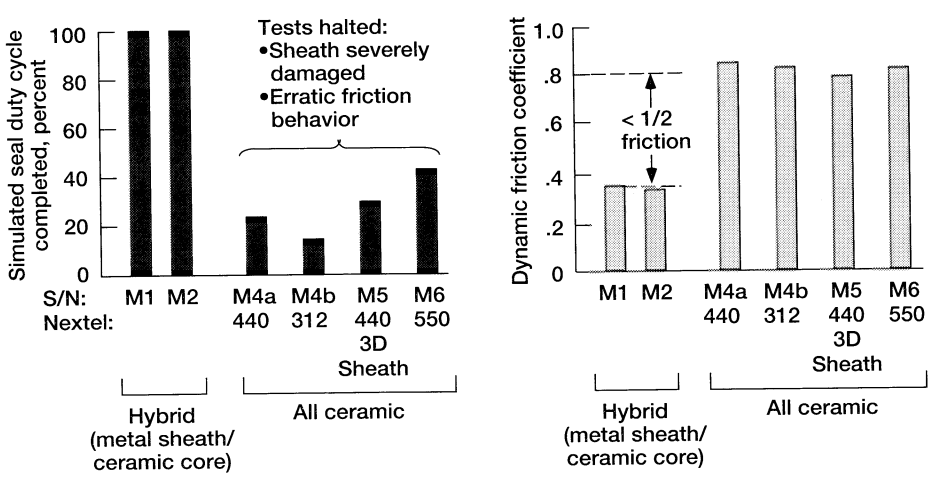

Comparison of solid seal dynamic performance at 1300 °F.

will be used to assess the change in seal leakage versus wear cycles at engine simulated temperatures to 1500 °F, pressures to 100 psi, and sliding velocities to ±1 in./sec.

Lewis contact: Dr. Bruce M. Steinetz, (216) 433–3302
Headquarters program office: OA

Piezoelectric Actuators Control Vibration of Transmission Shaft Line

T700 series engines are used in the U.S. Army's utility and attack helicopter fleet. Piezoelectric actuators were installed as part of an active vibration control system on a T701 gas turbine engine test stand. The test stand consists of the engine, a coupling shaft, a spindle flexibly mounted on ball bearings, a second coupling shaft, a torquemeter, a gearbox, and finally a dynamometer. Piezoelectric actuators apply a control force at the aft end bearing of the spindle

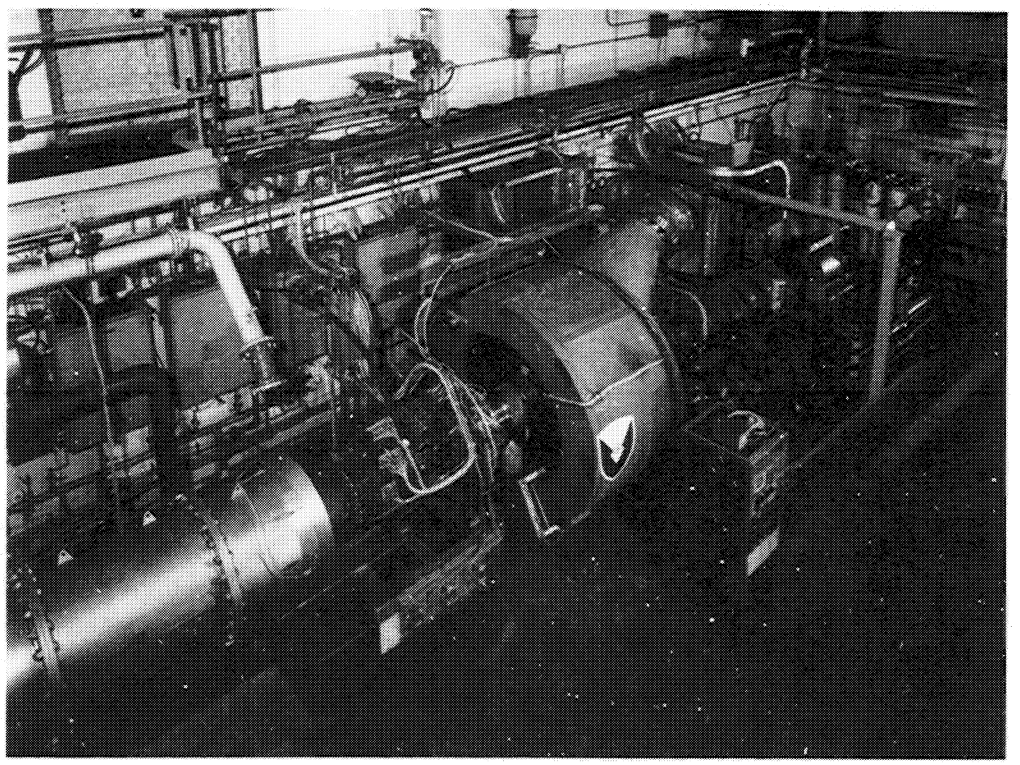

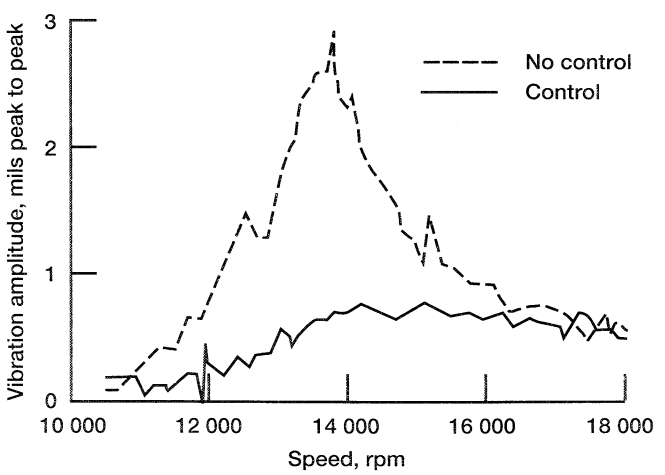

T700 engine test stand at NASA Lewis (top); vibration response with and without control for sensor y′ (bottom). Slow roll subtracted.

shaft. Opposing actuators are aligned in orthogonal axes. Displacement sensors provide feedback signals and are oriented along a second set of orthogonal axes. The signals must be transformed into the coordinate system of the actuators to provide truly collocated feedback.

Vibrations were measured at five planes along the shaft line. An analog proportional/derivative control circuit used a differentiator that had a built-in rolloff to inhibit high-frequency noise. The actuator power amplifiers showed a flat frequency response above 10,000 Hz. The transfer function of the free-tip piezoelectric actuator remained flat to approximately 2000 Hz. Vibrations of the T701 shaft line were suppressed over the entire operating speed range. Test results show that the speed-scheduled distribution of active stiffnesses and dampings is most effective in suppressing vibration.

In addition to the proportional/derivative analog feedback, test results were obtained by using digital signal-processing active control.

Lewis contact: Albert F. Kascak, (216) 433–6024
Headquarters program office: OA

Efficient Forced-Response Analysis System Developed for Compressor and Turbine Blades

Vibration of turbomachinery blading is a major cause of fatigue in many rocket and aircraft engines. Fatigue of turbomachinery blades has often been responsible for increased engine development costs, operational restrictions, and elevated maintenance costs. Controlling the forced vibratory response of turbomachinery blades is crucial for reliable operation of both rocket and aircraft engines. In rocket engines (e.g., the fuel and oxygen turbopump turbine blades of the space shuttle main engine), forced-response problems have contributed to delays and increased costs.

The reliability of engine designs is generally ensured with expensive and time-consuming engine testing. As a supplement or alternative to engine testing, blade designers could employ advanced numerical tools to predict the associated response quantities. If such computational methods are to be successful, their predictions must accurately model the complex interaction between multidisciplinary effects. In addition, the numerical tools must be efficient enough to be used in a design environment. In this spirit a computer program called FREPS (for forced response prediction system) is being developed under the Earth-to-Orbit Propulsion Technology Program to predict the vibratory response of turbomachinery blades.

The unsteady excitations on the blade row can be broadly classified according to their origins as aerodynamic, mechanical, and thermal excitations. Generally, aerodynamic excitations of interest consist of viscous wakes from upstream blade rows or the inlet flow distortion effects. Other sources of aerodynamic excitation to the blade row are upstream and downstream potential disturbances, compressor surge, rotating stall, and turbulence. Sources of mechanical excitation include blade tip–casing contact, cooling jets, shaft and gear meshing, and foreign object damage. FREPS has the unique capabilities to efficiently predict blade response to aerodynamic and mechanical excitations.

Although the Campbell diagram technique for forced-response design has proven very successful over the past few decades, the push for higher stage loading and lighter engine weight raises many more forced-response problems. That no quantitative information can be obtained from the Campbell diagram is a significant barrier for life prediction. The drawbacks of the Campbell diagram approach are reflected in long development cycles, expensive testing procedures, and turbomachines that do not provide the desired life. Therefore, the broad objective of the FREPS program is to create a system that will enable a designer to quantitatively predict the turbomachinery response due to the many inherent sources of excitation. Turbomachinery designers could then improve the fatigue characteristics of the blades in a systematic manner. Efficiency of the computational procedure has been a key consideration in the development. Blade structural dynamic and steady and unsteady aerodynamic analyses are efficiently integrated to calculate the forced vibration response amplitudes in turbomachinery blades to a variety of excitations.

The specific objectives of the FREPS system are to determine the aeroelastic stability of the turbomachinery rotor at given incident flow conditions and the maximum principal stresses in turbomachinery blading for given mechanical excitation forces and incident gust excitations.

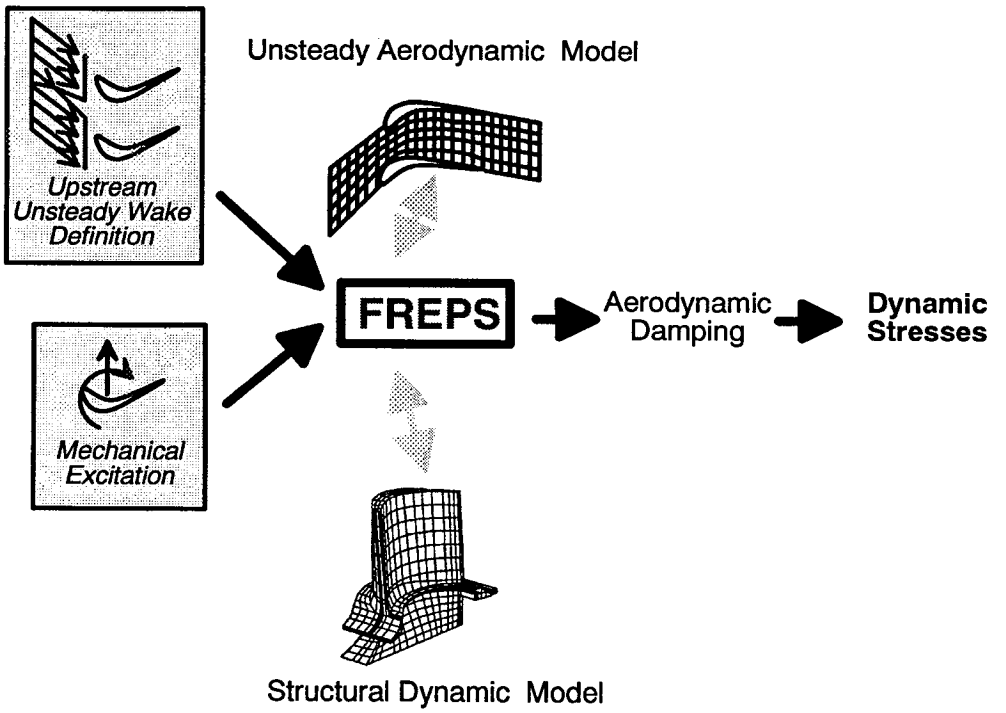

Forced-response prediction system.

The rotor's aeroelastic stability is determined by considering the equilibrium of elastic, inertial, and damping forces of structural as well as aerodynamic origin. An eigenvalue problem is formulated and the resultant damping is calculated. If the resultant damping is negative, the rotor is aeroelastically unstable. If the resultant damping is positive, the forced-response problem may be solved to calculate the maximum principal stresses due to mechanical or aerodynamic excitations. The mechanical excitation forces and the incident gust amplitudes (along with phase relationships) must be specified by the user. The actual excitation forces on the blade due to wake excitations are calculated within the code. The structural model is a three-dimensional, finite element model. The unsteady aerodynamic model is two-dimensional and linearized and accounts for the effects of thickness, camber, incidence, and gust distortion through the blade passage. The three-dimensional structural model and the two-dimensional aerodynamic model are integrated by using user-defined aerodynamic strips.

A complex eigenvalue problem is solved for the flutter analysis option, for all interblade phase angles specified in the input. All excitation forces are ignored at this stage. When the forced-response option is selected, both the motion-dependent and the motion-independent aerodynamic forces as well as any user-specified external excitation forces are taken into account. The response is calculated in terms of generalized coordinates after calculating all the required matrices and vectors. The generalized coordinate response is then transformed to a response in physical displacements. The stress response is obtained by similarly transforming the generalized coordinate response to a physical stress response by using the normalized modal stress vectors provided by finite element analysis.

The FREPS system is written in FORTRAN 77 and is operational on the Cray-YMP system at NASA Lewis. The aerodynamic damping or flutter portion of the FREPS code has been partially validated by comparing it with test data and other codes. The forced-response portion of the code is now being validated.

Lewis contacts: Dr. Durbha V. Murthy, (216) 433–6714; George L. Stefko, (216) 433–3920
Headquarters program office: OA

Turbine Blade Dynamically Analyzed Before and After Ice Impact

At high altitude when an aircraft travels through clouds of supercooled water droplets or regions of rain, water particles attached to the engine inlet edges undergo a phase change and become ice. With time the ice accretes on the inlet, sheds due to the structural vibration of the aircraft, and impacts the fan blade. The ice impact velocity relative to the blade is very large and hence can cause severe local deformations. These deformations may significantly alter the blade geometry and its dynamic characteristics, degrading engine performance and even leading to catastrophic blade and engine failure. Hence, it is necessary to study the dynamic characteristics of the blade under pre- and post-ice-impact conditions.

Recent efforts at NASA Lewis have led to the development of the computer code BLASIM (for blades assessment for ice impact). BLASIM can assess the damage caused by ice impact locally and at the blade root. It can be used to perform static, dynamic, fatigue, and flutter analyses of turbine blades. This code has been enhanced to simulate identical sequential ice impact on the same blade with geometry update of the blade after each impact. The change in the dynamic characteristics of the blade due to the first ice impact as well as the effect of ice impact location, ice size, and ice velocity are subjects for the present investigation.

The first three mode shapes were determined before and after the ice impact. The natural frequencies showed significant changes due to the first ice impact. Of these the frequency that corresponds to twisting appeared to be affected most. Also, the variation in the dynamic characteristics due to ice impact became less significant as the impact location moved toward the blade tip. For a given blade and ice impact location there exist an ice radius and velocity that correspond to maximum change in the blade natural frequencies.

Bibliography

Abumeri, G.H.; et al.: Dynamic Analysis of a Pre-and-Post Ice Impacted Blade. NASA TM–105829, 1992.

Reddy, E.S.; and Abumeri, G.H.: BLade Assessment for Ice Impact (BLASIM). User's Manual. NASA CR–191075, 1994.

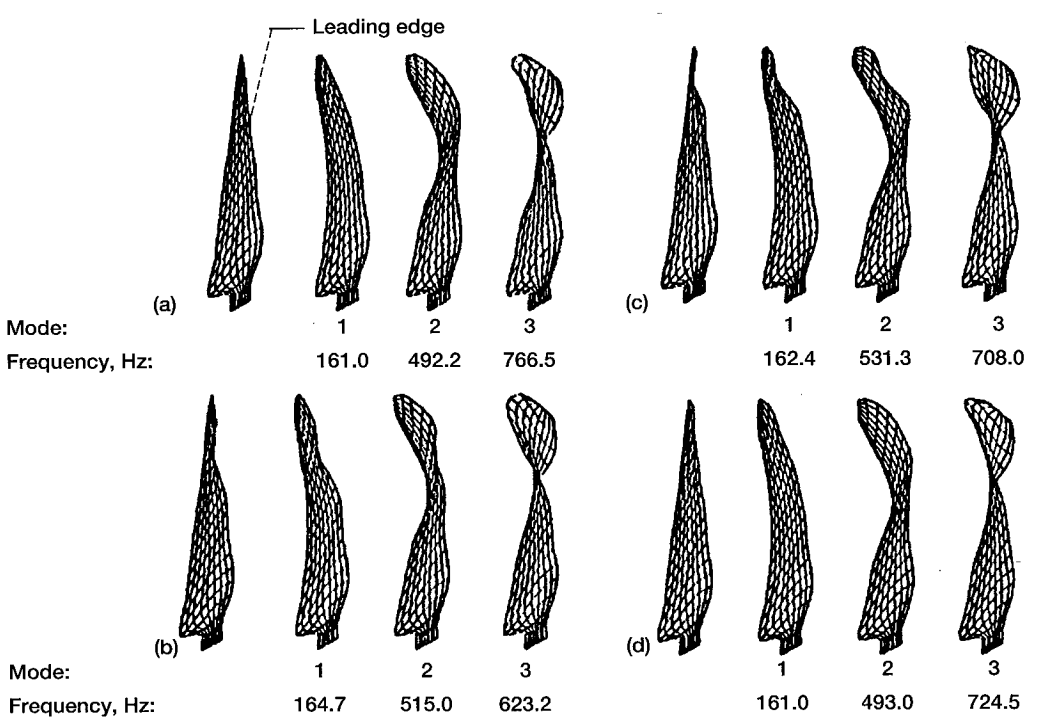

Effect of ice impact location on blade and its mode shapes (a) before ice impact; (b) after ice impact at 69 percent of span; (c) after ice impact at 80 percent of span; (d) after ice impact at 89 percent of span. Engine speed, 400 rpm; ice velocity, 129 knots; ice radius, 0.8 in.

Reddy, E.S.; et al.: Analysis of Aircraft Engine Blade Subject to Ice Impact. NASA TM–105336, 1991.

Lewis contact: Dr. Christos C. Chamis, (216) 433–3252
Headquarters program office: OA

Behavior of Intermingled-Fiber Hybrid Composite Computationally Simulated

The incorporation of two or more fibers within a single matrix is known as hybridization, and the resulting material is called a hybrid composite. Hybrid composites can be classified either as intraply hybrids, having more than one type of fiber within a ply, or as interply hybrids, where only one type of fiber is placed in a single ply and then the different plies are dispersed through the laminate.

In recent years, high-modulus fibers, such as boron and graphite, have been widely used in many aerospace applications because of their exceptionally high ratios of stiffness to weight. However, the impact properties of these composites have been found to be generally low. An effective method of improving the impact properties of graphite-fiber-reinforced composites is to add a small percentage of a low-modulus, high-strength fiber. Glass fibers are generally used for this purpose. In addition, the incorporation of glass fibers can also reduce the overall cost, as many times cost is a limiting factor for using graphite fibers.

The objective of this work is to evaluate a commingled- or intermingled-fiber hybrid composite consisting of 54 percent high-modulus graphite (P–75) fiber in an epoxy (R–930) matrix with varying percentages of S-glass fibers used as hybridizing fibers. The composite properties and response are evaluated by using both three-dimensional finite element analyses and a micromechanics-based computer code called ICAN (for integrated composite analyzer). The mechanical properties and response evaluated by both methods are generally in good agreement.

Collectively, the results demonstrate that both the finite element analysis and the composite micromechanics equations can be used with confidence to obtain the properties of hybrid composites needed for analysis and design of hybrid composite structures. However, caution should be exercised in interpreting finite element results to ensure that the computational simulation model geometry simulates the conditions assumed in the micromechanics equations.

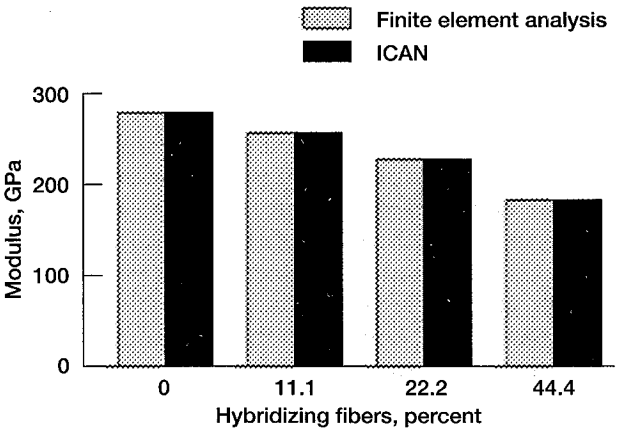

Comparison of ICAN and finite element analysis.

Bibliography

Mital, S.K.; and Chamis, C.C.: Computational Simulation of Intermingled-Fiber Hybrid Composite Behavior. NASA TM–105666, 1992.

Murthy, P.L.N.; Ginty, C.A.; and Sanfeliz, J.G.: Second Generation Integrated Composite Analyzer (ICAN) Computer Code, NASA TP–3290, 1993.

Lewis contact: Dr. Christos C. Chamis, (216) 433–3252
Headquarters program office: OA

Laminates Sized for Uncertainties

Design of composite structures is complicated because a number of variables are involved both at the material and structure levels. Since different materials are combined at microscopic scale to form the composite, predicting the properties of the composite at macroscopic level is complicated. Also, controlling the fabrication process of composite structures is difficult. Therefore, several parameters involved in making composite structures have variations associated with them.

Traditionally, composite structures are designed by estimating the lower bound on the material strength and the upper bound on the loads. However, the properties of constituents, fabrication process variables, loads, and environment have

uncertainties associated with them. Also, composite material behavior and strength depend on the magnitude of the applied load. Therefore, the material properties and the strength with respect to the stress levels in the composite material need to be considered in the design. Quantifying such effects and their variations is a difficult process. The conventional approach yields a design with different safety factors related to different failure modes and hence a nonuniform reliability with respect to these failure modes.

In order to develop a robust design methodology, it is imperative to consider the actual variation in the constituent properties, fabrication process, loads, environment, and material behavior in a rational way. The probabilistic approach provides a logical procedure to arrive at a reliability-based design and risk quantification.

During the last decade NASA Lewis has been actively engaged in developing a methodology that accounts for uncertainties in design and analysis variables in order to perform probabilistic assessments of structures. Recently, such a methodology for composite structures has been developed and implemented into the IPACS (for integrated probabilistic assessment of composite structures) computer code. IPACS performs the probabilistic micromechanics and composite structural analysis.

A multilevel probabilistic analysis of a composite radome structure was performed (ref. 1) to size the laminates so as to yield the maximum structural reliability. Uncertainties associated with properties of the constituents, fabrication parameters of a composite material, the structural parameters, and the loads were considered in the analysis. IPACS was modified to include the multifactor interaction equation (MFIE) model to simulate material degradation. Also, a probabilistic parametric study of the laminate size parameters, such as ply thickness, fiber volume ratio, void volume ratio, and fiber orientation, was performed to study their effects on material strength and structural reliability. A probability-based laminate design methodology for a desired level of reliability was outlined, and the effectiveness of the methodology was demonstrated by probabilistically designing a radome structure of an airframe.

The significance of probabilistic sensitivity factors to design reliability is discussed in reference 1, as

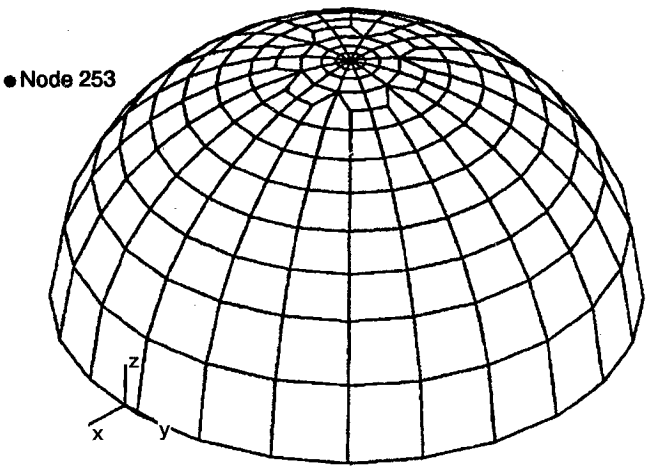

Radome structure of finite element model.

are those of laminate configurations and uncertainties in constituent properties, fabrication variables, and loads. The methodology generates a wealth of results that provide quantifiable information on which to assess different designs with respect to their structural reliability. For the composite radome investigated laminate configurations exist that increased the reliability from three failures in 1000 to zero failures in 1 million, and the sensitivity of loads decreased with increasing structural reliability.

Reference

1. Shah, A.R.; Liaw, D.G.; and Chamis, C.C.: Probabilistic Sizing of Laminates With Uncertainties. NASA TM–106145, 1992.

Lewis contact: Dr. Christos C. Chamis, (216) 433–3252
Headquarters program office: OA

Tension-Compression Fatigue Testing Performed on SiC/Ti Composite

Titanium (Ti) matrix composites are being considered for advanced, high-temperature aerospace applications requiring high strength and light weight. An understanding of the fatigue behavior of these materials is necessary to develop accurate life prediction models. Most knowledge about fatigue of silicon carbide (SiC)-fiber-reinforced titanium matrix composites is based on data generated under tension-tension, load-controlled conditions. (The available material is typically less than 2.5 mm thick and therefore unable to withstand compressive loads without buckling.)

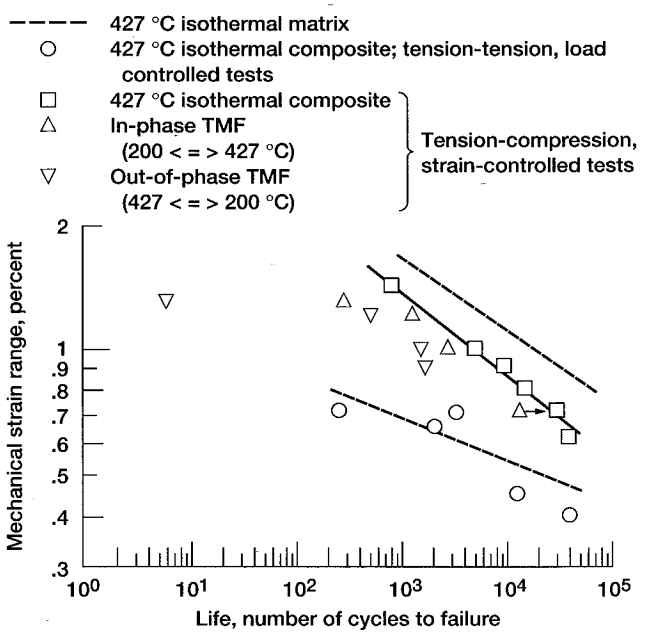

Fatigue life as a function of mechanical strain range for $[\pm 30]_{8s}$ composite and unreinforced matrix. Arrow indicates test stopped prior to failure.

Although such thin composites will be used in airframes, engine components will likely be thicker. Additionally, the severe thermal gradients of actual service cycles will impose tension-compression (i.e., fully reversed) loading in these structures.

It is necessary to understand the behavior of metal matrix composites (MMC's) under strain-controlled, tension-compression conditions to accurately predict structural behavior. To this end, a series of isothermal fatigue tests were conducted on a 32-ply, thick MMC, and the fatigue behavior in strain-controlled, fully reversed tests and tension-tension, load-controlled tests was compared. Fully reversed, strain-controlled thermomechanical fatigue (TMF) tests were also performed.

Tests on $[\pm 30]_{8s}$ SiC/Ti-15-3 showed that for isothermal fatigue the fully reversed, strain-controlled specimens had orders of magnitude longer lives than those specimens tested under the typical load-controlled, tension-tension conditions. Damage in the fully reversed specimens was in the form of a few long matrix cracks, typical of subcritical fatigue crack growth. The tension-tension specimens showed more severe damage, such as broken fibers and many short matrix cracks, both of which are typical of an overload situation—a manifestation of the strain ratchetting that occurs during load-controlled, tension-tension conditions. The fully reversed, TMF lives of the composite were nearly identical to those from the isothermal fatigue tests. This is surprising because other studies have shown that under tension-tension, load-controlled conditions TMF lives of MMC's are drastically shorter than isothermal fatigue lives. Additionally, both isothermal and TMF tests under fully reversed, strain-controlled conditions produced lives nearly equivalent to those of the unreinforced matrix. These results suggest that only life data generated under the appropriate loading conditions should be used when predicting the life of an MMC structure.

Bibliography

Lerch, B.A.; and Halford, G.R.: Fully-Reversed Fatigue of a Ti-MMC. Presented at the 17th Annual Conference on Composites, Materials, and Structures (Restricted Sessions), Cocoa Beach, FL, 1993.

Lerch, B.A.; Verrilli, M.J.; and Halford, G.R.: Fully-Reversed Fatigue of a Ti-MMC. Presented at the ASC 8th Technical Conference on Composite Materials, Cleveland, OH, 1993.

Lewis contacts: Bradley A. Lerch, (216) 433–5522;
Michael J. Verrilli, (216) 433–3337;
Dr. Gary R. Halford, (216) 433–3265
Headquarters program office: OA

Generalized Method of Cells Models Inelastic Micromechanics

The use of metal matrix composites (MMC's) may provide benefits in the design of advanced engines because they can allow higher operating speeds and longer durability in addition to decreased weight. To fully realize the benefits offered by MMC's, however, computationally efficient design and life prediction methods must be developed. These analysis tools will necessarily require the incorporation of physically based, viscoplastic deformation and life models in order to accurately describe the complex thermomechanical load histories typical in the aerospace structures of interest. Consequently, to assist not only the structural analyst but also the material scientist in developing and utilizing these material systems, a computationally efficient micromechanics approach capable of handling the required unified viscoplastic constituent constitutive models was developed.

The original method of cells is such a micromechanical model and has been shown to accurately predict the overall macrobehavior of various types of composites given the required constituent properties (ref. 1). In particular, the method yields explicit effective constitutive equations for the macro-inelastic behavior of MMC's that can be directly used in a global structural analysis code. Although the original method has been shown to be an accurate and efficient tool for analyzing the inelastic response of MMC's over a wide temperature range, it suffers from several drawbacks. The two primary ones are that only regular arrays with, at most, two different fiber spacings can be analyzed and that the use of a repeating unit cell with only four subcells precludes the possibility of including an interfacial region between the fiber and the matrix phase as well as considering more complex fiber shapes.

These restrictions have recently been removed in the generalized formulation of the method of cells, or GMC (refs. 2 and 3), wherein the repeating unit cell has been subdivided into an arbitrary number of subcells for the modeling of multiphase periodic composites. This generalization extends the modeling capability of the method of cells to include the following:

- Modeling of variable fiber shapes
- Analysis of different fiber arrays
- Modeling of porosities and damage
- Modeling of interfacial regions and their degradation around inclusions

In addition to representing doubly periodic composites (i.e., unidirectional continuous reinforced materials), GMC also can represent triply periodic arrays of multiphased composites (i.e., discontinuous reinforced composites).

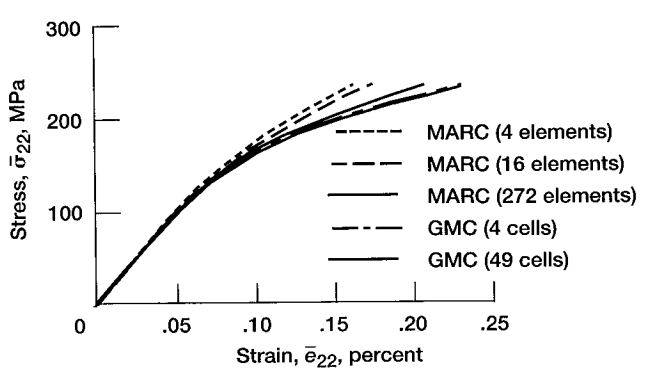

Comparison of GMC and MARC codes.

Consequently, GMC satisfies the need for a sufficiently general micromechanics approach that allows for the inclusion of physically based viscoplastic constitutive models which can be easily incorporated into a structural finite element analysis code. In addition the generalization is particularly advantageous when analyzing the complex thermomechanical viscoplastic response produced during the fabrication of advanced multiphased metal matrix composite systems.

References

1. Aboudi, J.: Mechanics of Composite Materials: A Unified Micromechanical Approach, Elsevier, Amsterdam, 1991.

2. Paley, M.; and Aboudi, J.: Micromechanical Analysis of Composites by the Generalized Cells Model. Mech. Mater., vol. 14, 1992, pp. 127–139.

3. Aboudi, J.; and Pindera, M.J.: Micromechanics of Metal Matrix Composites Using the Generalized Method of Cells Model (GMC), User's Guide. NASA CR–190756, 1992.

Lewis contact: Dr. Steven M. Arnold, (216) 433–3334
Headquarters program office: OA

Computationally Coupled Deformation-and-Damage Finite Element Approach Developed

In advanced engine designs it is desirable to use materials that allow higher operating speeds and longer durability in addition to decreased weight. Using metal matrix composites (MMC's) may provide these potential benefits. However, to fully realize the benefits offered by MMC's, computationally efficient design and life prediction methods must be developed. In this regard, a life prediction algorithm was developed that is fully coupled with the finite element method. The evolution of material damage is coupled with the incremental finite element analysis by using the concept of effective stress. Therefore, as the finite element analysis progresses, stress redistribution occurs while the damage propagates through the structure during subsequent load cycles.

The fatigue damage calculations are accomplished by employing a recently developed transversely isotropic continuum damage mechanics (CDM) model (ref. 1). The multiaxial, isothermal

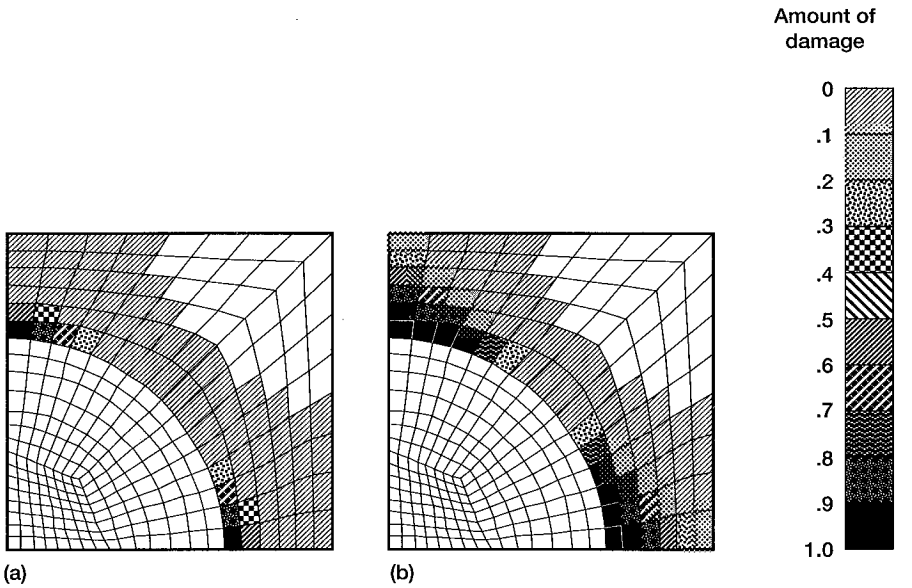

Damage propagation in unit cell. (a) Life consumed ≈ 0.5; (b) life consumed = 1.

fatigue model is phenomenological and stress based and assumes a single scalar internal damage variable. The model's evolution is anisotropic and is associated with the initiation and propagation of transgranular defects. The development of this fatigue damage evolutionary law (model) is founded on the definition of an initially transversely isotropic fatigue limit surface, a static fracture surface, and a normalized stress amplitude function. The anisotropy of the model is defined through physically meaningful invariants reflecting the local stress and material orientation.

The fatigue damage algorithm has been applied on the micro- and macroscale for two composite structures. The first application was on the *micro*scale, in which a fiber/matrix unit cell representing a square-pack, 35-percent-fiber-volume-ratio silicon carbide/titanium (SiC/Ti-15-3) composite was analyzed. The fatigue damage model, taken in its isotropic form, was characterized for the Ti-15-3 matrix constituent. An SCS–6 fiber was represented by an experimentally motivated model of ultimate tensile strength (UTS) degradation as a function of time and temperature. In addition, the UTS fiber failure criterion was consistent with the stress-based fatigue damage model used for the matrix. The CDM model correlated well with experimental data. The second application was on the *macro*scale, in which an SiC/Ti-15-3 MMC ring consisting of a composite core with matrix cladding was analyzed. For the life prediction analysis both the composite core and the matrix cladding used perfect plasticity models. The transversely isotropic form of the fatigue damage model was applied to the composite core, and the isotropic form was used for the matrix cladding (ref. 2). These applications serve to demonstrate the applicability of the fatigue damage model and the associated algorithm to both macro (structural) and micromechanical analyses.

References

1. Arnold, S.M.; and Kruch, S.: Differential Continuum Damage Mechanics Models for Creep and Fatigue of Unidirectional Metal Matrix Composites. NASA TM–105213, 1991.

2. Arnold, S.M.; and Wilt, T.E.: A Deformation and Life Prediction of Circumferentially Reinforced SiC/Ti-15-3 Ring. Presented at the 10th Biennial Conference on Reliability, Stress Analysis and Failure Prevention, Albuquerque, NM, Sept. 19–22, 1993.

Lewis contact: Dr. Steven M. Arnold, (216) 433–3334
Headquarters program office: OA

Space Propulsion Technology

Waved Journal Bearing Demonstrates Greater Stability and Load Capacity

Rolling-element bearings, particularly ball bearings, have been the bearings of choice for nearly all rocket turbopump applications. These bearings are inherently stable, but they are limited in speed and are prone to wear out relatively quickly. Journal, or hydrodynamic, bearings are not limited in speed and generally exhibit little or no wear, but they are inherently unstable. Journal bearings can, however, be made stable by changing the smooth geometry to incorporate recesses, holes, steps, lobes, or other such modifications so as to interfere with the portion of the bearing hydrodynamics that causes the instability. The drawback to these variations of the journal design, to date, has been that all of them have resulted in a significant loss in load capacity. A numerical model of the new waved journal bearing design developed at NASA Lewis has shown it to be stable in operation while significantly increasing load capacity above that of a conventional journal bearing. Therefore, the advantages of this bearing include a high-load, high-speed capability along with a high degree of stability and the potential for little or no wear.

The unique characteristic of the waved journal bearing that gives it improved capabilities over conventional journal bearings is the low-amplitude waves of its inner diameter. The clearance is typically on the order of one ten-thousandth of the journal, or shaft, radius. The wave amplitude is nominally one-half the clearance. These small-amplitude waves allow the waved journal bearing to maintain a thin, load-bearing film between the journal and the bearing, thereby generating a high load capacity. However, the waves are large enough to interfere with the fluid film dynamics so that bearing instabilities are avoided.

Initial experimental results from an ongoing, in-house waved journal bearing test program at NASA Lewis agree well with results from the numerical model and show that the bearing does operate in a stable manner over a wide range of speeds and loads.

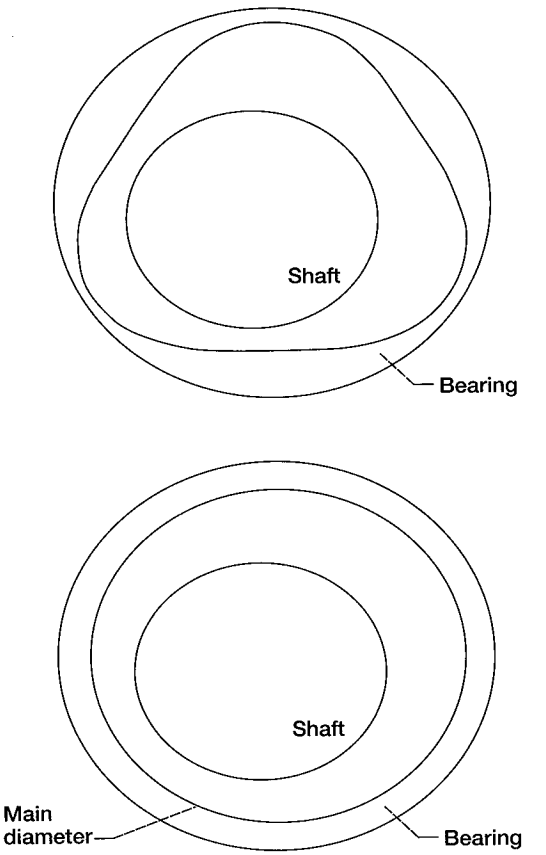

Waved journal bearing concept (wave height and clearance greatly exaggerated). Waved journal bearing (top); conventional journal bearing (bottom).

The combination of high load capacity and high stability opens a whole new realm of potential applications for hydrodynamic bearings. The most notable of these is rocket engine turbopumps, where cryogenic fluids present significant problems for bearing design.

Bibliography

Dimofte, F.: Waved Journal Slider Bearing. Patent Proposal, NASA Case No. LEW–15, 267–1.

Dimofte, F.; and Liebler, K.: Free-Piston Stirling Converter Dynamic Gas Bearing. Proceedings of the 27th IECE Conference, IEEE, New York, 1992, pp. 5.387–5.392.

Lewis contacts: Dr. Florin Dimofte, (216) 977–7468; Harold E. Addy, (216) 977–7467
Lewis Director's Discretionary Fund

Fiber-Optic Feedthrough and Sealing Designed, Developed, and Tested

In the interest of improving fiber-optic technology toward application on liquid rocket engines, a contract has been let to improve the hermetic sealing for fiber-optic links to engine controllers. This work is part of a research effort at NASA Lewis to provide safer and more reliable instrumentation systems for ground- and space-based rocket engines through the use of fiber optics. Under a Small Business Innovative Research (SBIR) contract, LiteCom, Inc., has been developing and testing a hermetically sealed fiber-optic feedthrough that will withstand the environmental requirements of the space shuttle main engines (SSME) as well those of space-based vehicles (such as long exposure to space radiation).

This SBIR work began in 1991 and is scheduled to be completed by May 1994. The innovative sealing material developed by LiteCom fills a technological gap in sealing and bonding at cryogenic applications. Our studies have revealed that conventional materials are not available that meet the environmental specifications of the SSME instrumentation system. To meet this need, the LiteCom phase II contract was awarded to build and test several prototype feedthroughs according to SSME specifications, with additional testing for operability in a radiation environment.

During the first phase of the contract the feasibility of applying LiteCom's sealing materials to our unique application was established. The state of the art in optical fibers and feedthrough materials suitable for typical rocket environments was established, and various optical fibers were selected and tested for their ability to form a seal with the LiteCom material in the specified environment. Helium leak rate testing was performed for the different fibers sealed with both zircon silicate and polycrystalline material, showing that leak rates of less than 10^{-8} and 10^{-9} cm^3/sec, respectively, could be obtained. Feedthrough devices were then assembled and limited testing was performed on the prototype feedthroughs.

The development phase is currently under way, during which LiteCom will develop, test, evaluate, and deliver a fiber-optic feedthrough and sealing device that is hermetically sealed and can be used on a rocket engine controller interface. The feedthrough assemblies, which include a backshell and feedthrough with appropriate sealing materials and optical fibers, are currently being subjected to cryogenic temperatures at or below –320 °F, high temperatures at or above 392 °F, vibration testing from 20 to 2000 Hz and shock testing at 40 g's, helium leak rate testing at a pressure differential indicative of a space environment, and testing for hardness to radiation levels representative of long-duration exposure to space. Preliminary results have shown a leak rate of below 10^{-11} cm^3/sec and an insertion loss of less than 0.01 dB for the chosen design when tested in an ambient environment.

Lewis contact: Amy L. Jankovsky, (216) 977–7498
Headquarters program office: OACT

Mars Propellant Production and Propulsion Demonstrated

The exploration of Mars, both by humans and robots, will require large masses lifted from the Earth's surface. Large launch masses translate into high mission costs, which may prohibit or reduce the pace of exploration. By making propellants on Mars instead of transporting the return propellants, the launch masses and costs can be greatly reduced.

NASA Lewis has been investigating how the in-situ propellant combination of oxygen and carbon monoxide can benefit Mars exploration missions. A study was conducted comparing the use of oxygen and carbon monoxide in-situ propellants versus terrestrial propellants for a Mars sample return mission. A Mars sample return mission study performed by the Jet Propulsion Laboratory using chloropentafluoride and hydrazine as propellants was used as the baseline mission. Using oxygen and carbon monoxide in place of the baseline propellants for the return portion of the mission was found to decrease the Earth launch payload mass by 13.6 percent. This translated into an increased Earth launch payload mass margin of 32 percent in contrast to the 14-percent mass margin of the baseline mission (assuming an Atlas IIAS launch vehicle). The increased mass margin was found to allow the oxygen and carbon monoxide mission to return a larger sample mass, carry an additional rover for redundancy, and potentially use a smaller launch vehicle, the Atlas IIA.

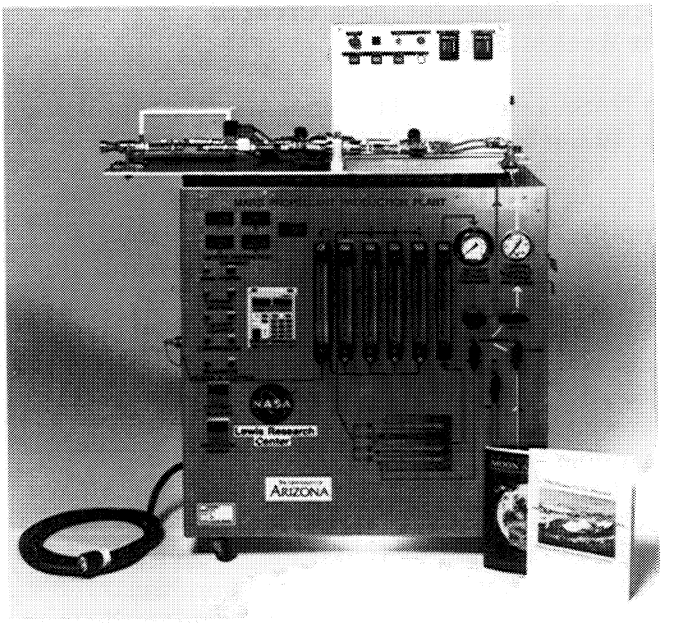

Mars in-situ propellant production and propulsion demonstration unit.

To investigate and demonstrate how an in-situ propellant production and propulsion system would work during an actual mission, NASA Lewis has teamed up with the University of Arizona. The production plant uses yttria-stabilized zirconia electrolyte tubes for the thermochemical decomposition of the carbon dioxide and subsequent removal of the oxygen. A cuprous chloride adsorbent material then selectively adsorbs the carbon monoxide out of the mixed gas exhaust stream to separate it from the undissociated carbon dioxide.

Both the oxygen and carbon monoxide are collected and stored at pressure in two small propellant tanks. After an hour of propellant production, a small rocket engine (0.1 lbf) is fired by using a pressure-fed system. The entire production plant and engine system is portable and can be easily transported by car or airplane. The plant is approximately 30 in. wide by 30 in. high and 12 in. deep. The engine system can be disconnected from the production plant by using two quick-disconnect fittings—just like an actual spacecraft would be disconnected from the production plant on the Martian surface before returning home. The robustness of the demonstration unit as well as its relatively simple operation will be used to convince mission planners that the benefits identified by the mission analyses can be achieved in the near future and with a high degree of confidence.

Bibliography

Wadel, M.F.: Benefits of In Situ Propellant Utilization for a Mars Sample Return Mission. AIAA Paper 93–2244, 1993. (Also NASA TM–106243, 1993.)

Lewis contact: Diane L. Linne, (216) 977–7512
Headquarters program office: OACT

Qualitative Diagnostic System Isolates Faulty SSME Components

NASA Lewis researchers have been developing a qualitative diagnostic system (QDS) for rocket engine condition monitoring. QDS combines qualitative simulation with model-based reasoning techniques for fault detection and isolation. Qualitative simulations are symbolic representations of first-principle relations between system parameters. These simulations require less design information about the actual system than numerical models and therefore can be applied to new rocket engine systems and systems containing limited sensor information. Combining qualitative simulation with model-based reasoning techniques offers a more complete description of possible system behaviors in a given situation than do current heuristic techniques.

The QDS comprises a data-processing algorithm, a qualitative model, a qualitative model solver, and model-based reasoning tools. Numerical data from the rocket engine are converted into symbolic information and passed to the model solver. The solver then applies a series of filtering techniques to the qualitative model to determine if a consistent solution exists for the input information. If no solution is found, model-based reasoning tools suspend sections of the qualitative model to isolate the engine subsystem where the anomalous behavior is occurring. The current version of the QDS is capable of solving steady-state constraints and contains an automated constraint suspension routine.

A qualitative model solver has been developed in Prolog, a logic programming language with inherent properties of instantiation, recursion, and backtracking. A qualitative simulation has been demonstrated on a subsystem of the interpropellant seal package (ISP) from the space shuttle main engine's (SSME) high-pressure oxidizer turbopump. The response of the system to individual seal clearance changes showed that the

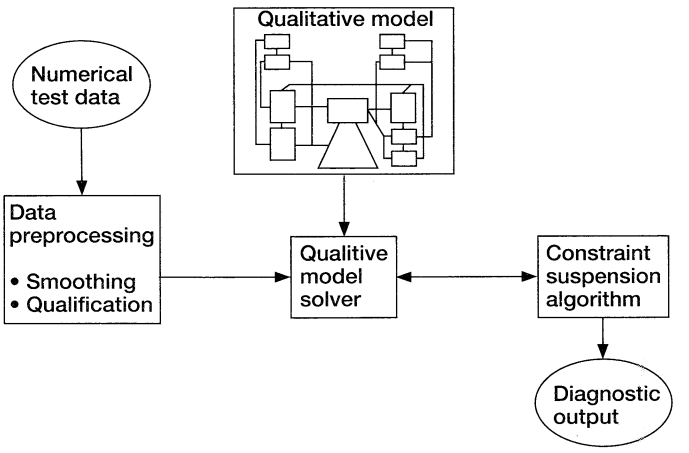

QDS information flow.

ISP simulation was capable of determining all seal clearance combinations compatible with a given input set. The output from this demonstration compared favorably with results from a numerical simulation of the ISP.

A qualitative model of the SSME's liquid-oxygen-side subsystems has been developed, and actual test data have been qualified and passed through the simulation. The QDS fault isolation capabilities were demonstrated on four fault cases: three cases generated from simulated data and one case generated from actual fault data. In each test case the QDS identified the actual faulty component as one of the possible components that could have contained the fault. This SSME liquid-oxygen-side model can be extended to include fuel-side components, the main combustion chamber, and the fuel cooling circuit, thereby providing an entire engine simulation.

Bibliography

Binder, M.; et al.: Rocket Engine Diagnostics Using Qualitative Modeling Techniques. AIAA Paper 92–3164, 1992. (Also NASA TM–105714, 1992.)

Maul, W.; et al.: Qualitative Model-Based Diagnostics for Rocket Systems. AIAA Paper 93–1779, 1993. (Also NASA TM–106234, 1993.)

Lewis contact: William A. Maul, (216) 977–7496
Headquarters program office: OACT

Newer, Smaller Gellants Created for Rocket Fuels

At NASA Lewis and TRW Inc., methods for using metal particles in gelled liquid fuels have been developed (refs. 1 to 3). Gelled fuels are used to increase the rocket's level of safety, its specific impulse, and/or its density by increasing the thickness or viscosity of the liquid fuel and allowing tiny metal particles to be suspended in it. TRW Inc., with NASA Lewis, has created special microscopic particles called nanoparticulates (refs. 4 and 5). They have a very high surface area per weight of material (1000 m^2/g) and can "grab" and hold onto a large amount of matter and gel the liquid (refs. 6 and 7). This innovation allows fuels to be gelled with much less material, increasing the rocket's performance over past formulations. In contrast, gellants from the 1960's and 1970's required 20 to 40 percent of the fuel's weight to be a gellant, significantly reducing their performance.

The new gellant is a compound including boron, methyl groups, silicon, and ethane and when formed is a long-chain polymer. Special chambers are used to form the polymer and a "freeze-drying" cycle finally creates the fluffy particles of gellant. The more historical low-temperature gelling materials were typically frozen hydrocarbons, such as ethane or methane.

After making the gellant, TRW Inc. constructed a rheometer to measure the properties of cryogenic gelled fuels. The primary rheometer measurements will be of the viscosity and the shear stress of metal-laden gelled liquids. These fuels are made at extremely low temperatures, as low as 20 K (–423 °F). Different amounts of metal were added to hydrogen, ethane, propane, or hexane, and up to 70 percent aluminum was added during the tests.

The properties of metallized gelled ethane and propane with and without added aluminum were measured and some of the results are shown here. Without gelling, the viscosities for ethane and propane are 0.192 and 0.220 centipoise (cP), respectively. The data for each fuel show that its viscosity is controlled by its flow rate (or shear rate) in the rheometer. This shear rate simulates the fuel flow in the tubing from its propellant storage tank to a rocket engine. As the shear rate goes up, the viscosity approaches that for the ungelled fuel. As a comparative example, the

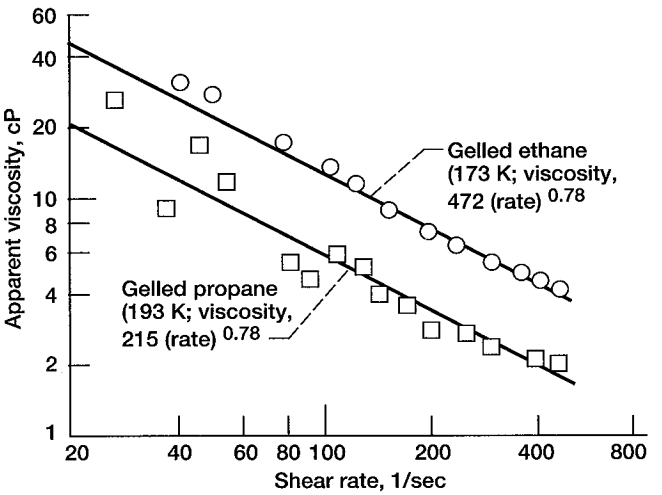

Gelled fuels with flow-varying viscosity (BTMSE gellant at 7.5 kg/m^3).

viscosity of liquid water at 293 K (68 °F) is near 1 cP. Thus, when they are flowing in a rocket feed system, the viscosity of these gelled cryogens is slightly higher than that of water.

Although ethane and propane are not typical fuels for NASA vehicles, they were attractive candidates for low-cost testing of the gellant materials with cryogenic fuels. Experiments with gelled hydrogen-aluminum fuel will be completed soon.

References

1. Palaszewski, B.; et al.: Launch Vehicle Performance Using Metallized Propellants. AIAA Paper 91–2050, 1991. (Also NASA TM–104456, 1991.)

2. Palaszewski, B.; et al.: Design Issues for Propulsion Systems Using Metallized Propellants. AIAA Paper 91–3484, 1991. (Also NASA TM–105190, 1991.)

3. Palaszewski, B.: Upper Stage Using Liquid Propulsion and Metallized Propellants. NASA TP–3191, 1992.

4. Fricke, J., ed.: Aerogels: Proceedings of the First International Symposium. Springer Proceedings in Physics, Vol. 6, Springer, New York, 1986.

5. Teichner, S.: Aerogels, A Source of Adsorbents, Insulators, Catalysts and Ceramics. Rev. Phys. Appl., Coll., Tom. 24, Suppl. no. 4, Apr. 1989, pp. C4–1 to C4–6.

6. Kistler, S.: Coherent Expended Aerogels and Jellies. Nature, vol. 127, 1931, p. 741.

7. Kistler, S.: Coherent Expended Aerogels. J. Phys. Chem., vol. 34, 1932, pp. 52–64.

Lewis contact: Bryan A. Palaszewski, (216) 977–7493
Headquarters program office: OACT

Integrated Modular Engine Studies Demonstrate System Modeling and Design Capabilities

Integrated modular engine (IME) designs are currently being considered for various space propulsion applications. Integrated modular engines differ from conventional systems in the arrangement of the components. In conventional, discrete rocket engine systems each engine is a stand-alone unit. If more than one engine is required, these discrete engines operate separately and are not interconnected. Therefore, if a single engine component fails to operate, the entire engine must be shut down. In the IME, however, components are interconnected by the use of common manifolds. In this system a component, such as a turbopump or a thrust chamber, could be shut down independently without the loss of good, operating components. Therefore, the IME offers the potential advantages of increased reliability and fault tolerance relative to conventional designs. It was the purpose of this effort to investigate the IME concept and to evaluate the advantages of the system. Several studies were performed in-house at NASA Lewis to examine the IME (refs. 1 to 3).

A design effort was initially performed to determine methods of physically assembling the IME. The design effort showed the feasibility of constructing an expander cycle configuration for the IME. The design had half the number of turbopumps as a conventional system. However, the IME requires approximately twice the number of valves as a discrete engine system due to the isolation required for fault tolerance. This larger number of valves as well as the manifold connections create the potential for more leakage points with the IME. Therefore, the operability and reliability concerns of leakage must be considered in the IME.

A study was also performed to evaluate the reliability of IME concepts. Several analysis techniques were used, and from the results the IME was found to be less reliable than the discrete system. The key reliability drivers in the IME are the manifolds, and the IME requires low manifold failure rates for the concept to show benefit over discrete systems.

Finally, a steady-state computer model was developed to determine the operating conditions of the IME system under various failure scenarios. From

the results of this analysis the IME was shown to be less tolerant to individual component failure than previously thought. In some cases when one component, such as a liquid oxygen turbopump, was shut down, the system would not be able to achieve the required thrust level. Therefore, the system model was found to be a critical tool for understanding the operation of the IME.

The studies on the IME at NASA Lewis have expanded the understanding of modular engine concepts. Results from these system studies provide a solid basis for future design of multiple rocket engine systems.

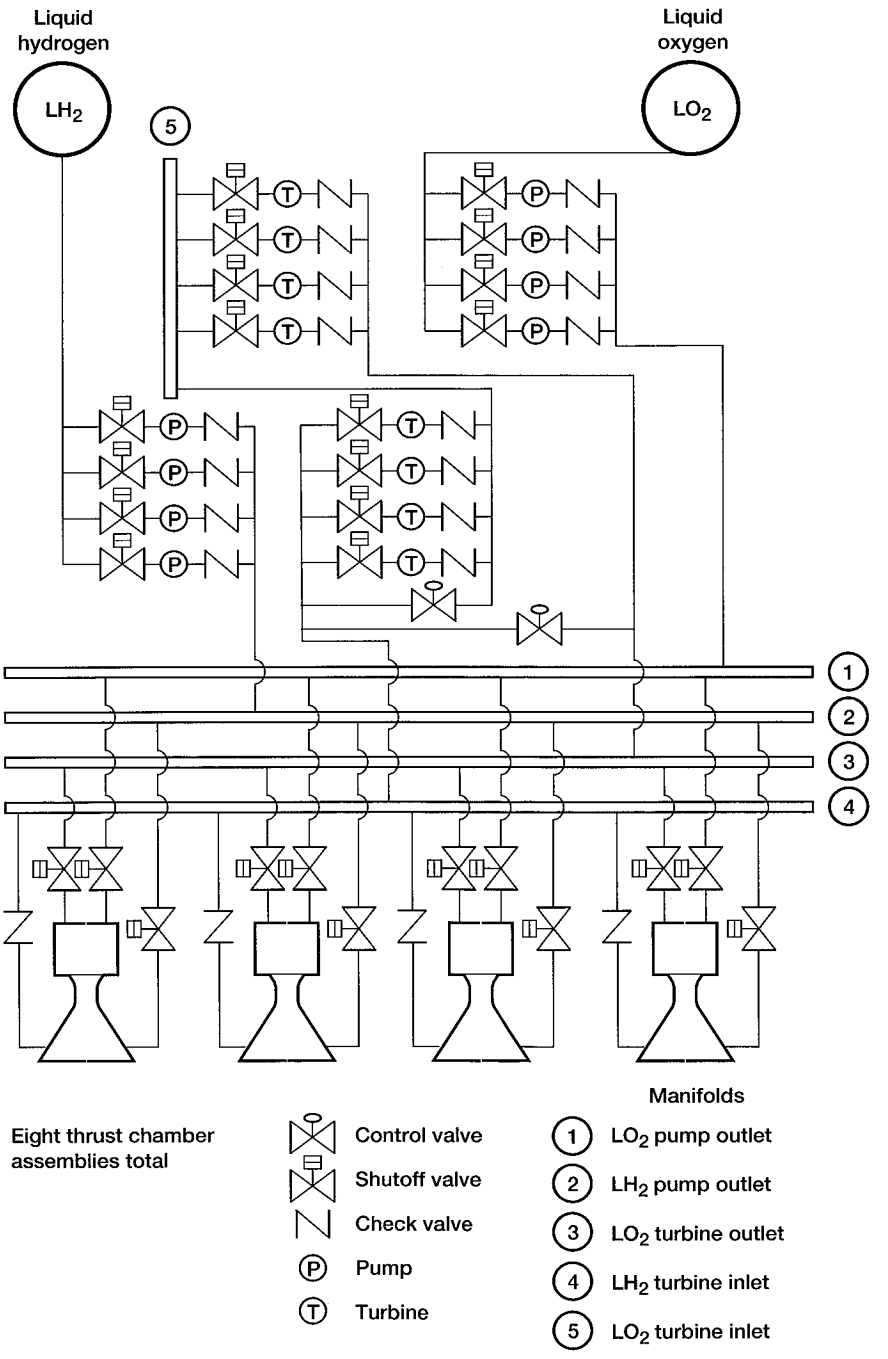

IME schematic diagram, expander cycle configuration.

References

1. Frankenfield, B.; and Carek, J.: Fluid System Design Studies of Integrated Modular Engines. AIAA Paper 93–1887, 1993.

2. Hardy, T.L.; and Rapp, D.C.: Reliability Studies of Integrated Modular Engine System Designs. AIAA Paper 93–1886, 1993.

3. Binder, M.P.; and Felder, J.L.: Predicted Performance of an Integrated Modular Engine System. AIAA Paper 93–1888, 1993.

Lewis contact: Terry L. Hardy, (216) 977–7517
Headquarters program office: OACT

Brush Seals Demonstrate Reduced Leakage for Cryogenic Applications

Engineers at NASA Lewis are testing brush seals in cryogenic fluids to determine their applicability to cryogenic turbopumps for rocket engine systems. Labyrinth seals in many aircraft gas turbine engines are being replaced by brush seals because brush seals are compliant, reliable, and cost competitive. They have been shown to leak less and to enhance rotor stability. Hence, brush seals may be a good candidate in cryogenic turbopumps, where long-life, low-leakage, reliable seals are essential.

A brush seal is simply a ring of wire bristles sandwiched between a front and back washer. The bristles usually have a 5- to 10-mil interference fit with the shaft and are installed at a 30° to 60° angle to the radius so that the bristles can bend as cantilever beams during shaft perturbations. The back washer is on the low-pressure side of the seal and has an inside diameter just slightly larger than the bristle bore diameter. It supports the bristles, preventing them from blowing downstream, and acts as a fixed clearance seal should the bristles fail.

In a cryogenic turbopump brush seals may be used to seal either liquid hydrogen or liquid oxygen at locations near the pump or the bearings, or they may be used to seal hot gaseous hydrogen, warm gaseous oxygen, or helium at locations near the turbine or purge seals. In this environment large temperature gradients, oxygen compatibility, and hydrogen embrittlement are concerns. Also, the shaft speeds attained in cryogenic turbopumps for rocket engine systems are high, to 200,000 rpm for a liquid hydrogen turbopump. Because brush seals are contact seals, their wear rates under these conditions are important.

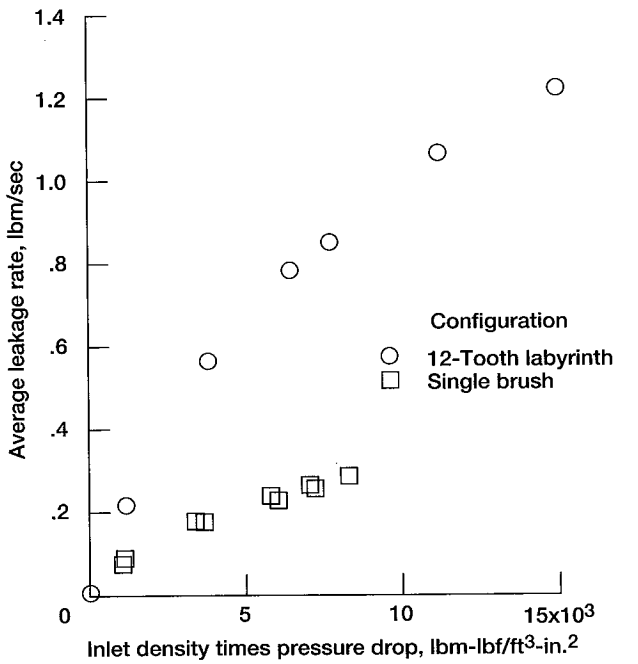

Comparison of leakage performance in liquid nitrogen of a 12-tooth labyrinth seal of 0.00513-in. radial clearance and a single brush seal of 0.004375-in. radial interference at 35,000 rpm.

Two-in.-bore-diameter brush seals with a 5-mil interference with the shaft have been tested in liquid nitrogen at shaft speeds to 35,000 rpm and in liquid hydrogen to 65,000 rpm. The leakage flow rate through a single brush seal in liquid nitrogen measured two to three times less than the leakage flow rate measured for a 12-tooth labyrinth seal with a 0.00513-in. radial clearance. Staging effects were studied, and it was found that two brush seals far apart leaked less than two brushes tightly packed. A blowout test at zero shaft speed demonstrated that the bristles did not blow out downstream at pressure drops to 550 psid across the seal. The maximum groove depth in the Inconel 718 rotor after 4½ hr of accumulated shaft rotation time in liquid nitrogen was 1 mil. The Haynes 25 bristles wore approximately 1 to 3 mils. In liquid hydrogen the bristles wore approximately 5 mils, and the bristle material actually transferred to the rotor. There was no rotor wear. Additional testing will be done to determine the wear mechanism and good material combinations and to further quantify staging

effects on leakage performance. The data will also be used to calibrate and update an analytical computer code developed at NASA Lewis that models brush seal performance.

Lewis contact: Margaret P. Proctor, (216) 977–7526
Headquarters program office: OACT

AETB Fuel Turbopump Completes Critical Design Review

A critical design review of the Advanced Expander Testbed (AETB) fuel turbopump was held on June 22, 1993, at NASA Lewis. The stretchout of the AETB Program caused by limited fiscal year funding dictated that the AETB final design effort be done in a serial fashion rather than in the normal parallel fashion. The critical design review for the AETB oxidizer turbopump was held in September 1992.

The AETB fuel turbopump is a high-pressure, high-speed, three-stage, centrifugal, liquid hydrogen pump. The fuel turbopump consists of a primary and a secondary pump mounted back to back and counterrotating. The primary pump includes an inducer, a first-stage impeller, and a high-efficiency, single-stage, high-reaction turbine on a common shaft. The secondary pump includes the second-stage impeller, the third-stage impeller, and a single-stage turbine on a second common shaft. The two single-stage turbines are driven by the hot (1000 °R) hydrogen thrust chamber coolant flow.

The AETB is a 20,000-lb-thrust rocket engine operating at 1200-psia chamber pressure. In order to provide margin and flexibility as a testbed engine, the AETB is being designed for 25,000-lb thrust and 1500-psia chamber pressure. The basic operating cycle of the AETB is as a split expander (i.e., all the fuel flows through the primary pump and only that portion of the fuel flow required for thrust chamber cooling flows through the secondary pump). The AETB can also be run as a full expander, in which the total fuel flow is pumped through both the primary and secondary pumps.

Operating characteristics of the AETB fuel pump at the design point (25,000-lb thrust/1500-psia chamber pressure) as a split expander are

- Primary pump: speed, 97,200 rpm; discharge pressure, 1820 psia
- Secondary pump: speed, 98,000 rpm; third-stage discharge pressure, 4500 psia

A key design feature of the AETB is continuous, stable throttling from 100- to 5-percent thrust. Because the AETB design point is 125 percent thrust, the AETB fuel turbopump inducer, impellers, and turbines are designed for stable operation from 125- to 5-percent thrust. The primary and secondary pumps both operate at subcritical speeds over the entire throttle range.

The remaining AETB components and subsystems requiring final design are the thrust chamber and nozzle, the control system plus valves, and the total engine system. These final design efforts will be completed for an AETB system critical design review in January 1994.

Lewis contact: William K. Tabata, (216) 977–7534
Headquarters program office: OACT

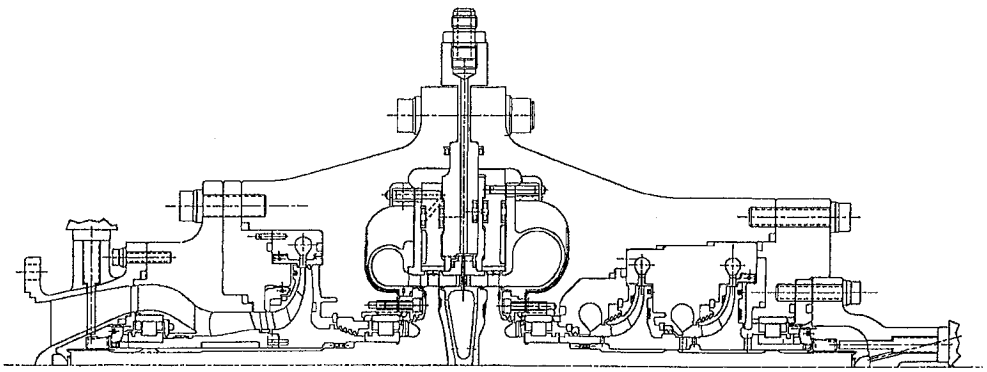

Cross section of fuel turbopump.

High-Activity Hydrogen Conversion Catalyst Developed

The parahydrogen-to-orthohydrogen conversion is being developed to enhance the cooling capability of the hydrogen-fueled propulsion system. The parahydrogen-to-orthohydrogen conversion offers a potential increase in hydrogen cooling capacity of 35 percent in the cryogenic temperature region (100 to 250 °R). Although the conversion occurs in nature, it is too slow to be of any benefit in a hydrogen-fueled/cooled propulsion system and a catalyst is needed. The commercially available catalysts are not active enough to sufficiently speed up the conversion for the aerospace application. Therefore, a contract with Allied Signal Research and Technology (prime contractor) and Accel Catalysis Inc. (subcontractor) was issued to develop a high-activity parahydrogen-to-orthohydrogen conversion catalyst for use in hydrogen-fueled/cooled propulsion systems.

The contractors began by trying to understand how and why the existing catalysts work and then tried to develop an improved catalyst. Beta, the term used to describe the activity of a catalyst, is defined as the ratio of the mass of catalyst to the mass flow rate of hydrogen needed to promote conversion to a defined percentage of the equilibrium composition at a particular operating temperature. For this program the focus is on the β value at 70-percent conversion to equilibrium composition at 140 °R. In the laboratory the catalyst to promote the orthohydrogen-to-parahydrogen conversion was improved by almost an order of magnitude. For the commercially available catalysts β is 20 lb of catalyst per pound mass per second of hydrogen flow. The catalyst activity was improved to 5 lb of catalyst per pound mass per second of hydrogen flow.

The contractors have produced ruthenium alumina catalysts with beta values consistently in the 4 to 6 range. The catalysts are granular. A highly porous alumina support, approximately the size of a grain of sand, is impregnated with a form of ruthenium that is active in promoting the parahydrogen-to-orthohydrogen conversion. The catalyst is then activated by passing a gas over it at an elevated temperature for a specified period of time. The activation procedure is unique to each particular catalyst and needs to be developed in conjunction with formulating the catalyst. The activation procedure is as important as the catalyst's chemical makeup in promoting the parahydrogen-to-orthohydrogen conversion. The contractors measure the catalyst conversion activity by using a small-scale (1- to 2-g catalyst sample) facility. Because the propulsion systems that will utilize the catalyst will use 10 to 100 lb, a set of scaling issues have been identified that need to be addressed in order to take the catalyst from the contractor's small-scale facility to a larger system. An in-house parahydrogen-to-orthohydrogen conversion test facility at NASA Lewis has been used to identify and study these scaling issues.

The contract is a part of the program at NASA Lewis to develop the parahydrogen-to-orthohydrogen conversion for use in hydrogen-fueled/cooled propulsion systems. The catalyst is the major component of that development. The contract has been completed and a final report on the work will be completed by November 1993.

Lewis contact: Gary S. Williamson, (216) 977–7520
Headquarters program office: OA

Russian Thrusters Evaluated for Flight Application

Russian low-thrust propulsion systems have now become available. These systems have generated significant interest in the international community, and several efforts to commercialize this technology are in progress. The most advanced of these systems is the Russian stationary plasma thruster (SPT) manufactured by Fakel Enterprises. A 1.35-kW version of this thruster has been proposed for several classes of space missions including stationkeeping, orbit insertion, repositioning, and maneuvering. NASA Lewis is currently working with the Ballistic Missile Defense Organization (BMDO) to evaluate this and other Russian devices for practical applications.

The SPT is also known as a Hall accelerator and its design is relatively straightforward. The device has an annular discharge chamber containing a toroidal anode. The anode has flow passages through which most of the propellant (xenon) is introduced. The cathode is external to the device, and magnet coils are used to create a radial magnetic field in the discharge chamber. In operation, electrons emitted by the cathode are retarded by the magnetic field, and ions formed by electron-

atom collisions in the chamber are accelerated by the axial electric field.

Although performance levels measured with the SPT are high, major issues related to thruster lifetime and spacecraft integration require evaluation before operational application on U.S. spacecraft. The Lewis program is focused on the latter, and a large-scale effort to assess plume contamination, electromagnetic interference, optical signature, and plume impacts on communications signals is in progress in the Lewis spacecraft integration testbed. A breadboard power-processing unit to operate the thruster was developed at Lewis (ref. 1). In addition to integration testing, performance was measured at very low facility background pressure levels (ref. 2).

To evaluate radiated electromagnetic interference (EMI) characteristics, direct measurements were taken in the Lewis testbed using a set of antennas (measurement range, 14.5 kHz to 40 GHz) mounted in an arc behind the thruster. Experiments were also performed to directly assess the effects of the ambient plasma on the EMI measurements. Signals above analyzer background noise levels were observed at frequencies to approximately 6 GHz. The levels measured in typical communications bands were below generic specifications typically applied across the industry but may be of concern in specific applications. To assess plume contamination, a set of optical-quality quartz plates in several types of holders were placed in an arc 2 m from the thruster and exposed to the thruster plume for 50 hr (ref. 3). On the basis of these test results, an extended test is planned under a cooperative program with an industrial partner. To assess plume effects on communications, electrostatic probes were used (ref. 4) to quantify the plasma characteristics of the plume, and emission spectroscopy was used (ref. 5) to provide a plume signature requested by a flight program office.

The Russian SPT has been examined in detail, and further testing to evaluate integration impacts is planned. Also planned are tests of a flight-qualification propulsion unit (with a 0.6-kW-class SPT) for a potential Air Force flight experiment and tests of a 1.5-kW-class Hall device, known as the anode layer thruster, which has recently been obtained from another Russian source through the BMDO Program.

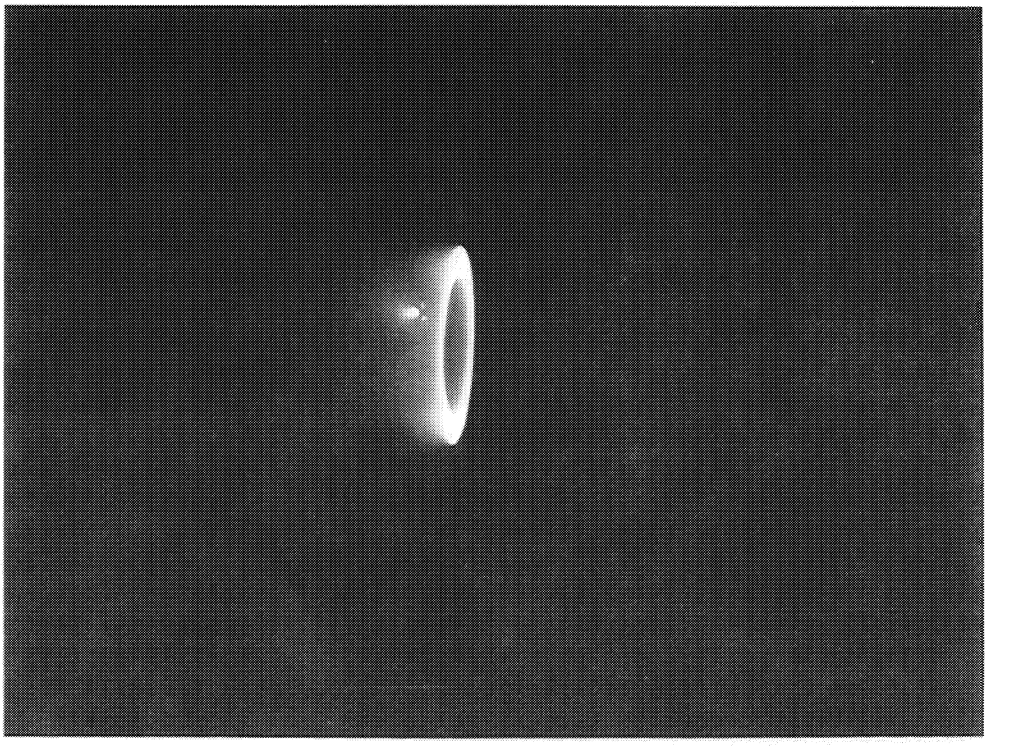

Russian stationary plasma thruster operating at NASA Lewis.

References

1. Hamley, J.A.; Hill, G.M.; and Sankovic, J.M.: Power Electronics Development for the SPT–100 Thruster. Report IEPC–93–044, 1993.

2. Sankovic, J.M.; Hamley, J.A.; and Haag, T.W.: Performance Evaluation of the Russian SPT–100 Thruster at NASA LeRC. Report IEPC–93–094, 1993.

3. Pencil, E.J.: Far-Field Plume Sputtering Characterization of the SPT–100. Report IEPC–93–098, 1993.

4. Myers, R.M.; and Manzella, D.H.: Stationary Plasma Thruster Plume Characteristics. Report IEPC–93–096, 1993.

5. Manzella, D.H.: Stationary Plasma Thruster Plume Emission. Report IEPC–93–097, 1993.

Lewis contact: Dr. Frank M. Curran, (216) 977–7422
Headquarters program office: OACT

High-Performance Arcjets Chosen for Next-Generation Communications Satellites

First-generation arcjets have now been accepted for use on four geosynchronous satellite series. In operation the arcjet system (thruster, power processor, and gas generator) uses energy from the spacecraft batteries to increase the enthalpy of the propellant before it is exhausted at high velocities through a converging/diverging nozzle. Use of an arc discharge heating process is the unique feature of the device. Although the arc reaches temperatures in the range of 17,000 °C, the engine design ensures that critical internal surfaces are protected by a cool gas boundary layer. Materials limits inherent to conventional thrusters are thus avoided, and the first-generation devices will increase fuel economy for north-south stationkeeping by a factor of more than 1.5 over state-of-the-art chemical and resistojet systems. Following these acceptances, an industry requirement for higher performance arcjets was identified. In fact, arcjet technology capable of a mission-average performance level of 600 sec was recently baselined for application on a new (next generation) satellite series. The NASA Lewis effort to develop a high-performance, 2-kW-class arcjet is currently in progress to ensure that this technology is available.

The high-performance arcjet program is being conducted through in-house efforts and a contract with the Olin Rocket Research Center, the manufacturer of commercial arcjet systems. Early program efforts indicated that the increased specific power levels (power per mass flow rate of propellant) required to obtain higher mission-average specific impulse levels lead to higher anode and nozzle temperatures. These elevated temperatures were found, in turn, to cause unacceptable throat deformation in the state-of-the-art anode material (pure tungsten). After an extensive search a high-strength, high-temperature material was identified. This tungsten-base alloy containing rhenium and hafnium carbide was first developed at NASA Lewis. Initial tests of an anode made from this material indicate that its properties will meet program goals (ref. 1). A life test

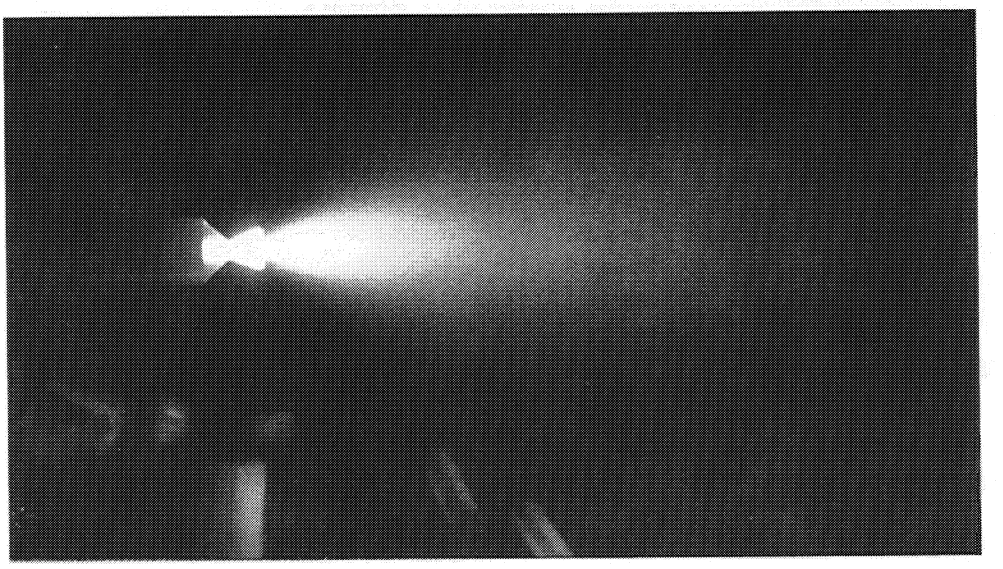

High-performance arcjet.

under conditions anticipated on orbit will be performed in fiscal 1994.

The long-term, high-performance arcjet program goal is to ensure U.S. competitiveness in the low-thrust area, and the program will continue to explore the practical limits of the device. For this, several new, high-temperature materials from Russia were recently obtained and a process to strengthen the alloy now under test was identified. These materials will be evaluated for use in the arcjet over the coming year.

Reference

1. Lichon, P.; and Sankovic, J.M.: Development and Demonstration of a 600 Second Mission Average Arcjet. Report IEPC–93–087, 1993.

Lewis contact: John M. Sankovic, (216) 977–7429
Headquarters program office: OACT

Lightweight 30-cm-Diameter Ion Thruster Developed for Multimission Applications

A 30-cm-diameter xenon ion thruster is under development at NASA Lewis to provide an ion propulsion option for missions of national interest. The thruster is being proposed for use on the U.S. Air Force/TRW space surveillance, track, and autonomous repositioning (SSTAR) platform to validate ion propulsion. Under this program NASA Lewis would supply an ion propulsion subsystem that would be flown as a secondary payload, using SSTAR as the carrier. The SSTAR spacecraft is designed to test key technologies associated with the development of electric orbit transfer vehicles and includes 10 kW of solar array power and an ammonia arcjet propulsion system. The ion propulsion subsystem would consist of the NASA 30-cm-diameter ion thruster, a power processor, a xenon feed system, and a diagnostics instrumentation package. The preliminary mission plan calls for operating the subsystem at a nominal 2.5-kW power level to demonstrate repositioning and orbit transfer and to evaluate its performance and interactions with other spacecraft engineering subsystems.

The 30-cm-diameter ion thruster under development at NASA Lewis incorporates innovations in design, materials, and fabrication techniques relative to conventional ion thrusters. Goals of the development effort include a thruster mass of 7 kg and an operating power envelope of 0.5 to 5.0 kW. The present thruster hardware under test

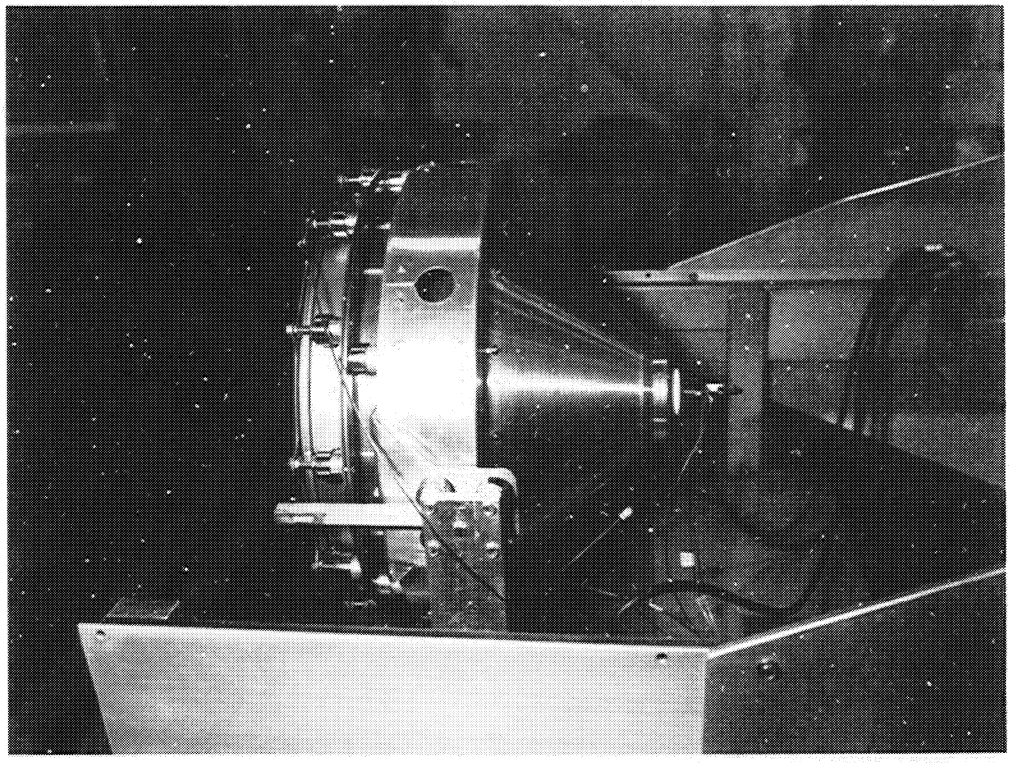

NASA 30-cm ion thruster on test stand.

is at a functional model level of maturity. Specific development efforts include thruster design optimizations, component life testing and validation, vibration testing, and performance characterizations. Under this test program the ion thruster will be brought to engineering model development status.

Performance data for the thruster were obtained over a 0.7- to 4.9-kW power envelope to verify the performance of the aluminum, partial-conic discharge chamber design and to evaluate its stability, to quantify overall thruster performance, and to evaluate power throttling at fixed-mass-flow-rate conditions. The thruster performance stability, as measured by the specific impulse and efficiency sensitivities to variations in cathode flow rate, compared favorably with that of other thrusters. Overall thruster efficiencies varied from a peak of 0.72 at 4030-sec specific impulse and 4.9-kW input power down to 0.45 at 2290-sec specific impulse and 0.7-kW input power. The demonstrated power throttling range at fixed propellant flow rates was approximately 1.7:1 at 1.1-A beam current and dropped to approximately 1.35:1 at 3.0-A beam current.

For the NASA Lewis 30-cm-diameter thruster the erosion of the molybdenum accelerator grid due to charge-exchange processes is believed to be the dominant life-limiting wear mechanism. However, in-space lifetimes greater than 10,000 hr are anticipated for all thruster performance conditions.

The SSTAR mission plan calls for approximately 2.4 kW of power available to the 30-cm thruster. At this input power level, typical thruster performance is 95-mN thrust at 3250-sec specific impulse and an overall thruster efficiency of 0.63. At these conditions the thruster xenon consumption rate is 2.97 mg/sec, or approximately 10.7 kg per thousand hours of operation. At −150 V accelerator grid voltage a molybdenum mass efflux rate from the thruster of 2.9 g per thousand hours of operation is anticipated in space, with a somewhat higher mass efflux rate expected during ground testing. This in-space mass efflux rate is believed to be consistent with an accelerator grid lifetime of greater than 24,000 hr.

Additional on-going activities to bring the thruster to engineering model development status include vibration testing, component life testing, and generation of a computer-assisted drawing package. As these activities are completed, efforts will be started to evaluate thruster interfaces, to verify thruster lifetimes, and to integrate the thruster with a power processor.

Bibliography

Patterson, M.J.; Haag, T.W.; and Hovan, S.A.: Performance of the NASA 30 cm Ion Thruster. IEPC–93–108, 1993.

Patterson, M.J.; Haag, T.W.; and Williams, G.J.: Derated Ion Thruster Development Status. AIAA Paper 93–2225, 1993.

Lewis contacts: Michael J. Patterson, (216) 977–8481; James S. Sovey, (216) 977–7454
Headquarters program office: OACT

Pulsed Mode Demonstrated for Whistler Wave Plasma Thruster

An experiment is being conducted at Tank 7 of the Electric Propulsion Research Building to evaluate an advanced electric propulsion concept known as the whistler wave plasma thruster. The concept potentially offers very high thrust per unit of propellant used, competitive with that of ion and magnetoplasmadynamic thrusters, and accelerates plasmas of densities comparable to or greater than those in other types of plasma thrusters. The preferred propellant is deuterium (heavy hydrogen), but the thruster will operate with a wide range of propellant gases.

The whistler wave propulsion concept relies on highly efficient heating of electrons in the propellent gas by the absorption of energy from a whistler, or surface, electromagnetic wave generated from helical antennas surrounding the plasma column. The heating takes place where the wave frequency, 915 MHz in the current experiment, is resonant with the electron cyclotron frequency in an externally applied, solenoidal magnetic field. (The cyclotron frequency refers to the rate at which an electron spins about a magnetic field line.) The heated electrons ionize the propellant gas, forming a high-density plasma column in the thruster. The magnetic and electric fields present force the electrons to migrate in the exhaust direction, dragging and accelerating the plasma ions to supersonic speeds (by ambipolar diffusion). The expelled ions produce the device's thrust.

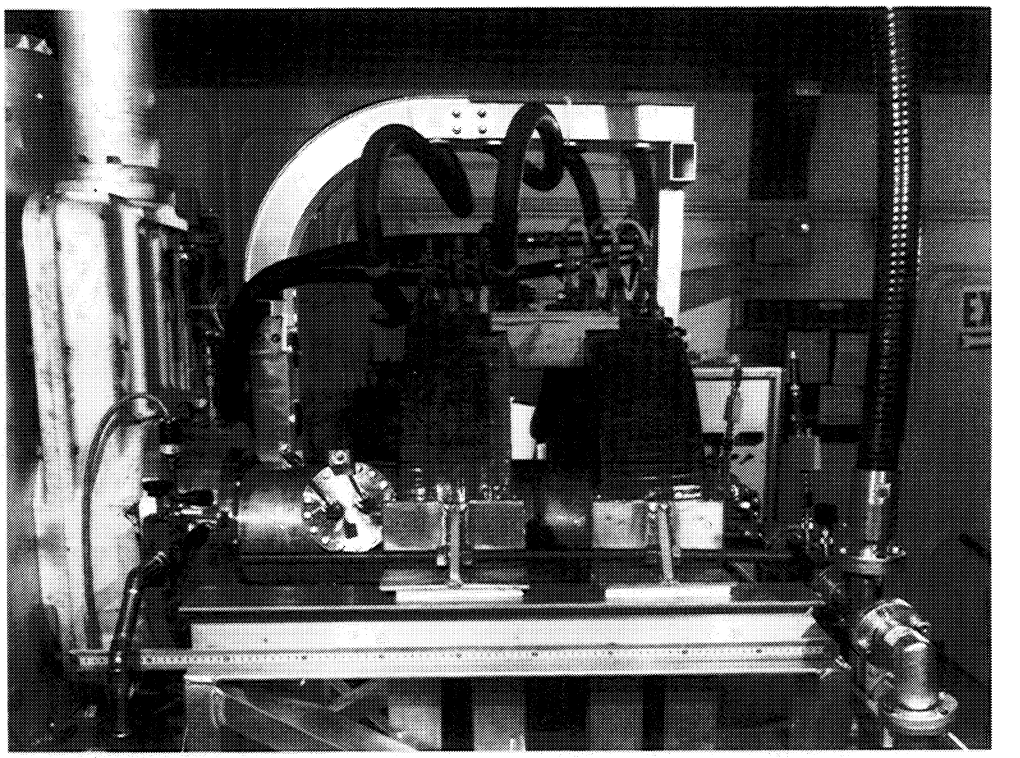

Whistler wave plasma thruster apparatus.

This experiment is a collaboration, under a cooperative research agreement, with Lawrence-Livermore National Laboratory scientists. In the experimental setup the device is attached by a gate valve to the vacuum tank. The propellant gas is introduced into the chamber through a gas plenum and valves attached to the gate valve. The interleaved helix antennas extend inside the chamber to within a few inches of the gas feed plenum, and the plasma column forms inside of them. The antennas are powered from a microwave generator. The magnet coils produce a magnetic field "hill," with the coil current adjusted to place the electron cyclotron resonance heating plane just to the right of the gas feed plenum.

Preliminary testing has recently been conducted in a pulsed mode, successfully generating plasma pulses with densities approaching 10^{12} ions/cm^3 and electron temperatures of 7.5 eV. The pulsed-mode operation is for convenience in these initial tests. A flight thruster employing the concept would be operated in a continuous-wave mode. Further testing to evaluate the feasibility of the concept for propulsion purposes is planned with this apparatus. The whistler wave plasma thruster is a candidate advanced propulsion system for future NASA space missions requiring moderate- to high-power thrusters with extremely high propulsion efficiency relative to the propellant consumed.

Lewis contact: John L. Power, (216) 433–8687
Headquarters program office: OACT

High-Performance Apogee Engines Demonstrated

High-performance apogee engines have been demonstrated by two manufacturers. Aerojet, under contract, has demonstrated 321 sec of performance and 6.2 hr of operation on the AJ10–221 with nitrogen tetroxide and monomethylhydrazine propellants. TRW, through the Space Act Agreement, has demonstrated 328 sec of performance with nitrogen tetroxide and hydrazine on their advanced DM–LAE. These high-performance rockets will be used in satellite onboard propulsion systems for orbit maneuvering. In particular, engines of this type are used to circularize the orbits of satellites placed in geosynchronous transfer orbits by staged launch vehicles. These rockets can also be used for other maneuvers, such as orbit raising and lowering and orbital plane change. High-performance

apogee engines enhance satellite performance by increasing satellite life, number of mission functions, and performance of components with optical and radiative heat transfer surfaces.

High performance results from the use of very high-temperature combustion chambers, made possible by the technical breakthrough of pairing the refractory metal rhenium with an oxidation-resistant coating of iridium in chamber fabrication. Rhenium was selected for its high melting point (3400 K), excellent strength at high temperature, and freedom from the ductile-to-brittle transition common in other refractory metals. Iridium was chosen as the oxidation-resistant coating for rhenium because of its relatively high

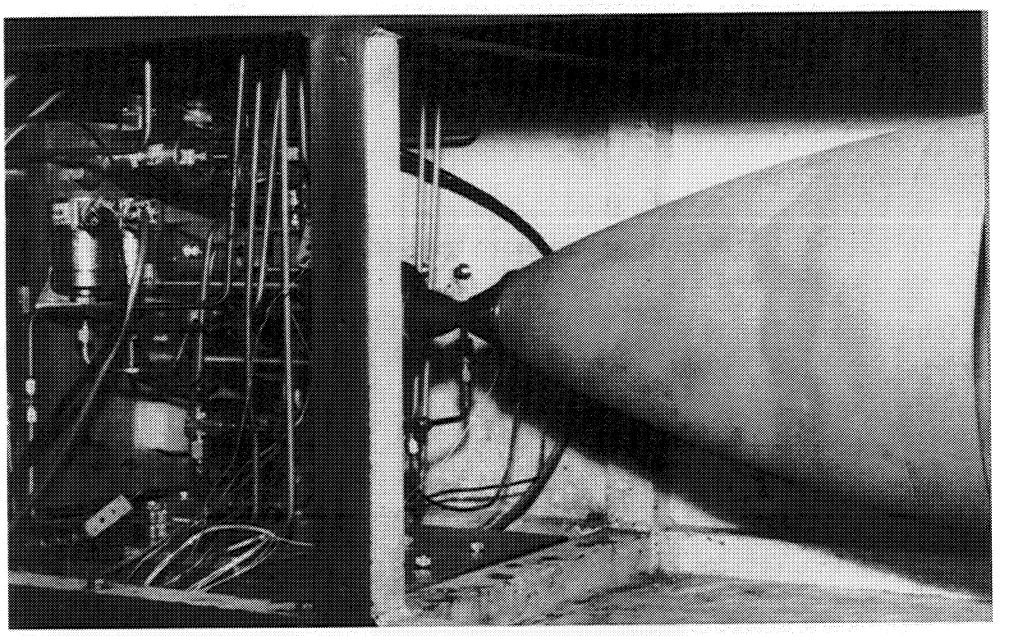

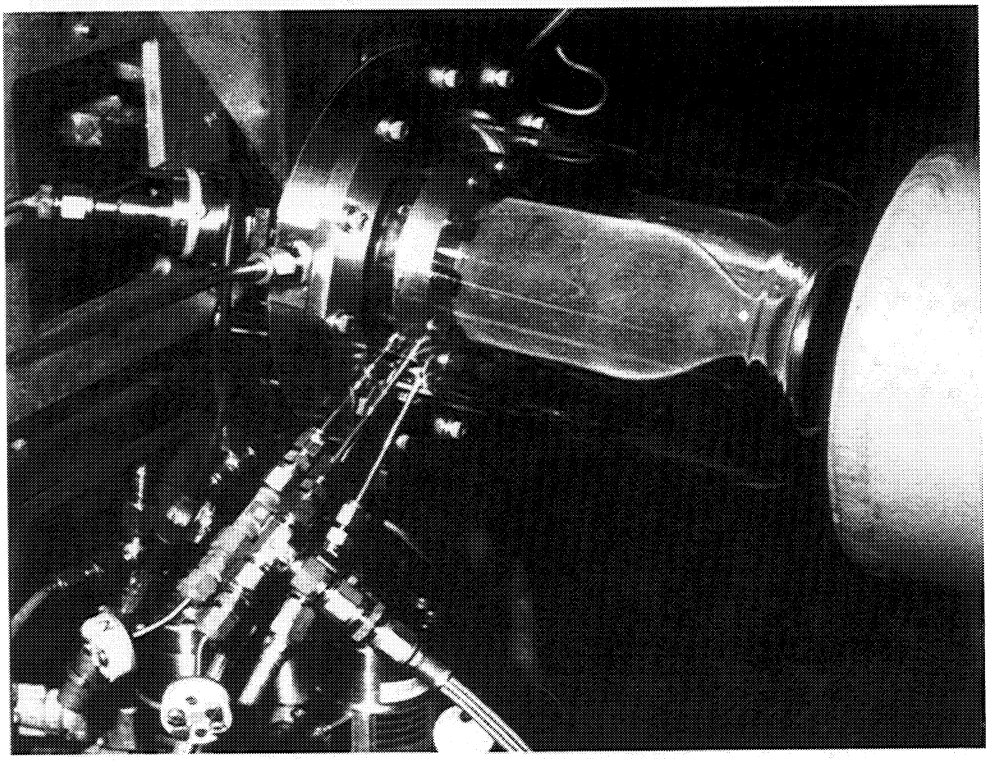

Aerojet AJ10–221 apogee engine in test (top); TRW DM–LAE apogee engine in test (bottom).

melting temperature (2720 K), excellent oxidation resistance (three orders of magnitude better than rhenium's), a coefficient of thermal expansion close to that of rhenium, adherence to rhenium, and ductility. Together, these materials enable the rocket chambers to operate at 2500 K, an operating temperature 800 degrees higher than those previously achieved in rockets of this general type. The ability to operate at higher temperatures enhances rocket performance by permitting rocket designs without fuel film cooling and its associated performance losses. These designs also decrease rocket plume contamination of satellite surfaces by unburned fuel in rocket boundary layers, which can be deposited on and impede performance of optical and radiative heat transfer satellite surfaces.

Bibliography

Schoenman, L.: 4000 °F Materials for Low Thrust Rocket Engines. AIAA Paper 93–2406, 1993.

Schoenman, L.; Rosenberg, S.D.; and Jassowski, D.M.: Test Experiences, 490 N High Performance (321-Sec I_{sp}) Engine. AIAA Paper 92–3800, 1992.

Lewis contact: Dr. Steven J. Schneider, (216) 977–7484
Headquarters program office: OACT

Tank Pressure Control Experiment/Thermal Phenomena Analyzed

An important issue in microgravity fluid management is controlling pressure in on-orbit storage tanks for cryogenic propellants and life support fluids, particularly liquid hydrogen, oxygen, and nitrogen. The purpose of the Tank Pressure Control Experiment/Thermal Phenomena (TPCE/TP) is to provide some of the data required to develop the technology for pressure control of subcritical cryogenic tankage. TPCE/TP is a reflight of the highly successful Tank Pressure Control Experiment (TPCE), which flew onboard STS–43 in August 1991.

TPCE, which used Freon 113 as a test fluid in a 0.5-ft^3 tank, was designed to provide data on jet-induced mixing for controlling tank pressure in low gravity. It met all of its objectives and significantly increased the knowledge base in fluid mixing (refs. 1 and 2). In addition, it gave some limited insight to the thermal phenomena involved in the stratification and self-pressurization of subcritical fluids and the boiling phenomena (ref. 3) occurring during the heating process in a low-gravity environment. TPCE also gave some surprising results relative to the dependence of pressure rise rate on ullage location and heat source location. Pressure spikes, on the order of 30 percent of the nominal tank pressure, were encountered under certain heating conditions. These spikes represent a potentially hazardous condition for the long-term storage of cryogenic fluids for future NASA missions. The purpose of the reflight, TPCE/TP, was to focus on these thermal phenomena. The space shuttle *Columbia* (STS–52), launched on October 22, 1992, carried the TPCE/TP experiment onboard.

The software for the flight computer was modified to provide more tests where the pressure spikes

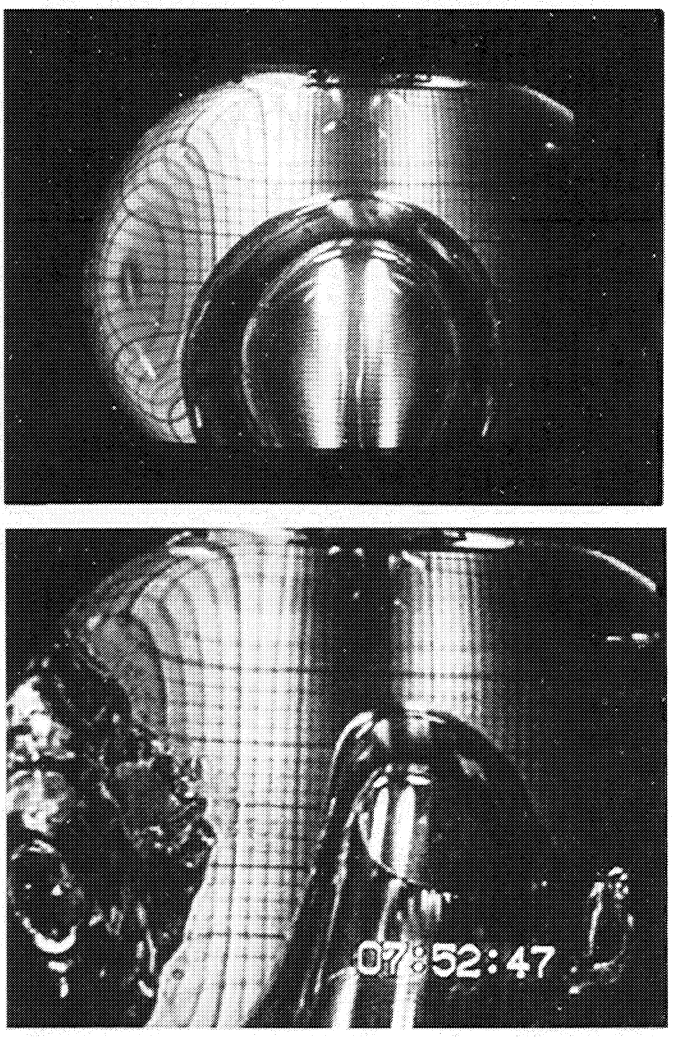

Liquid-vapor configurations: (top) prior to explosive boiling (wall superheat, 17.9 °C; tank pressure, ~50 kPa); (bottom) approximately 2 sec after explosive boiling caused a 20-kPa pressure spike.

were likely to occur and to provide extended video coverage during the heating process. Additional data on fluid mixing at very low flow rates were also acquired to supplement the data provided by the previous TPCE flight. A total of 21 tests over a 16-hr period were performed. Heating time, heater power, and jet flow rate were varied during the experiment. Temperature, pressure, flow rate, heater power, and acceleration data were taken along with 4 hr of video.

The video and digital data show that all test objectives were met. Besides showing the thermal processes occurring when a subcritical liquid is heated in low gravity, the video graphically illustrates the fluid dynamics associated with jet mixing at low flow rates. The pool boiling process at extremely low heat fluxes was also recorded from the inception of boiling to steady-state nucleate boiling at the heater surface. The unique features of the experimental results are the sustainability of high liquid superheat for long periods and the occurrence of explosive boiling at low heat fluxes (0.2 to 1.2 kW/m^2; ref. 4). For a heat flux of 1.0 kW/m^2 a wall superheat of 17.9 °C was attained in 10 min of heating. This superheat was followed by an explosive boiling accompanied by a pressure spike and a violent bulk liquid motion. This microgravity phenomenon demonstrated by the TPCE/TP data is of direct relevance to the design of space-based cryogenic fluid systems.

References

1. Bentz, M.D.; Meserole, J.S.; and Knoll, R.H.: Jet Mixing in Low Gravity: Results of the Tank Pressure Control Space Experiment. AIAA Paper 92–3060, 1992.

2. Bentz, M.D.: Tank Pressure Control in Low Gravity by Jet Mixing. NASA CR–191012, 1993.

3. Hasan, M.M.; et al.: Nucleate Pool Boiling in the Long Duration Low Gravity Environment of the Space Shuttle. AIAA Paper 93–0465, 1993.

4. Hasan, M.M.; et al.: Explosive Boiling at Very Low Heat Fluxes: A Microgravity Phenomenon. Presented at the ASME 1993 Winter Annual Meeting, New Orleans, LA, Nov. 28–Dec. 3, 1993.

Lewis contact: Dr. Mohammad M. Hasan, (216) 977–7494
Headquarters program office: OACT

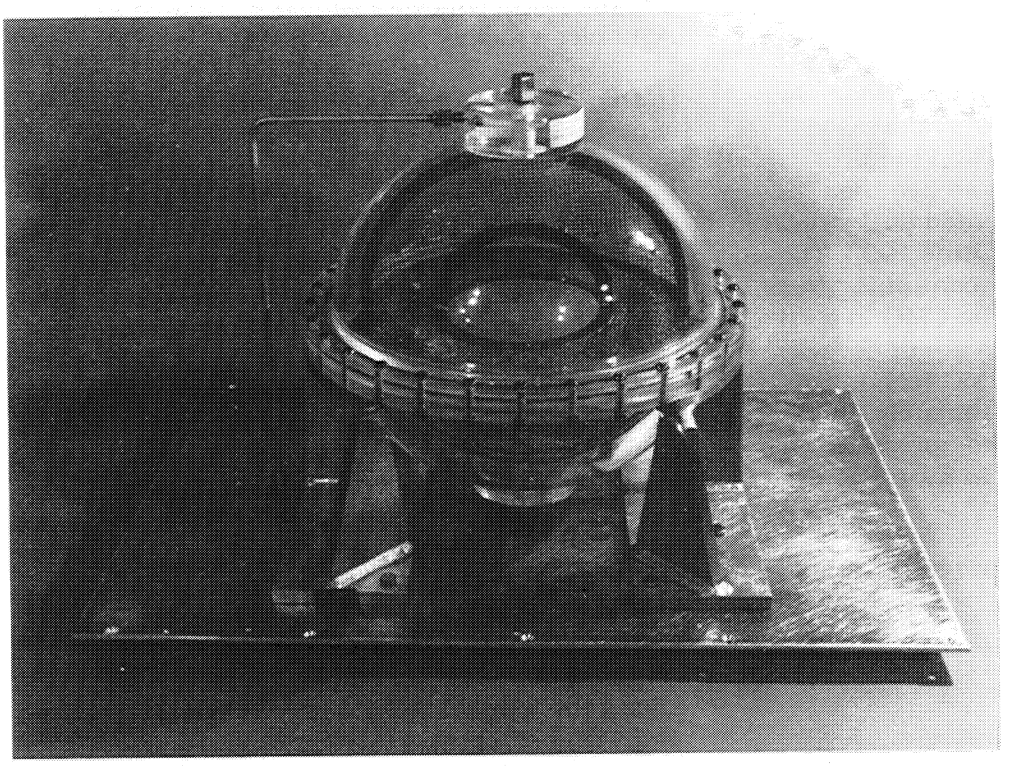

CMG test hardware.

Viability of Compression Mass Gauging Demonstrated in 1-g Tests Using Fluorocarbons

The ability to accurately measure quantities of cryogenic fluids in a low-gravity environment is a critical requirement for future space exploration missions. In low gravity the position of the liquid in the container may be markedly different than it is on Earth. Instead of settling in the bottom of the container the fluid may become a mixture of gas bubbles interspersed within the liquid, which may be located randomly throughout the container. Consequently, the familiar gauging methods used on Earth are not generally applicable in space. The need to develop a gauging system that will work in low gravity is evident. The compression mass gauge (CMG) testing effort currently being led by NASA Lewis is addressing this technology problem. The CMG concept is based on the principle that the pressure of a gas changes when its volume changes. In operation the tank volume is changed slightly by an oscillating bellows and the corresponding change in tank pressure is measured.

The test program includes initial testing in a 1-g environment using a cryogenic stimulant, either a fluorocarbon or a hydrofluorocarbon. This testing was required to prove the viability of the CMG concept. NASA Lewis has concluded tests on a small-scale tank using HCFC–123. Additional tests using Freon 11 have been conducted by Southwest Research Institute under a Space Act Agreement with NASA. These tests addressed issues of accuracy, instrumentation requirements, displacer volume, and fluid heating. The results of these tests were presented at the AIAA Joint Propulsion Conference in June 1993. These tests also provided the basis for continuing tests. One-g tests are planned using the CMG in a cryogenic tank, and low-gravity tests are under way to determine the suitability of CMG technology for low-gravity mass gauging. Ultimately, these data could be used to design a compression mass gauge that could be used in future space systems.

Lewis contact: John M. Jurns, (216) 977–7416
Headquarters program office: OACT

Multilayer Insulation Test Blankets Assembled in New Facility

The feasibility of future space missions depends strongly on the ability to store large quantities of cryogenic fluids in various space environments for long periods of time. This storage capability requires a lightweight, high-performance thermal protection system. Experimental data indicate that some type of a multilayer insulation (MLI) system, consisting of alternate layers of radiation shields and low-conducting spacers, holds the greatest promise of meeting the performance requirement.

NASA Lewis is implementing a ground-based test program to characterize the performance of thick (25 to 300 layers) MLI systems. These systems will consist of a number (2 to 12) of 0.5-in.-thick blankets. Each blanket will contain 25 layers of double-aluminized Mylar (aluminizing on both sides of the Mylar) separated by two layers of Dacron net. The insulation concepts will be evaluated in a vacuum environment by using a cylindrical, liquid-hydrogen-filled calorimeter. Specific areas of interest will be the thermal and venting characteristics of a large number of insulation layers using various seam concepts and the thermal performance of various concepts for insulating around penetrations. The various blanket and seam concepts will be fabricated in a semi-clean facility at NASA Lewis.

In this temperature- and humidity-controlled, semi-clean facility, one roll of aluminized Mylar and two rolls of Dacron net are installed horizontally on a stand located at one end of a smooth, flat, level table. Each roll is suspended on a shaft supported by ball bearings for minimum drag when rotating. As the material comes off the rolls, it is pulled across the table, passing through a pair of rollers at each end of the table, the Mylar and Dacron net are then attached to a horizontally supported drum that simulates the test calorimeter. The table serves as a means of aligning the material. The drum, which rotates slowly, draws the material from the rolls. When 25 layers have been wrapped, a metal fixture is fastened to the drum, compressing the material to the drum. The material is then cut by using a knife blade installed in a sabre saw and guided in a track centered in the fixture. This creates the seam that allows the blanket to be removed from the drum and wrapped around the test tank. By using a simple hand-held tool commercial nylon fasteners

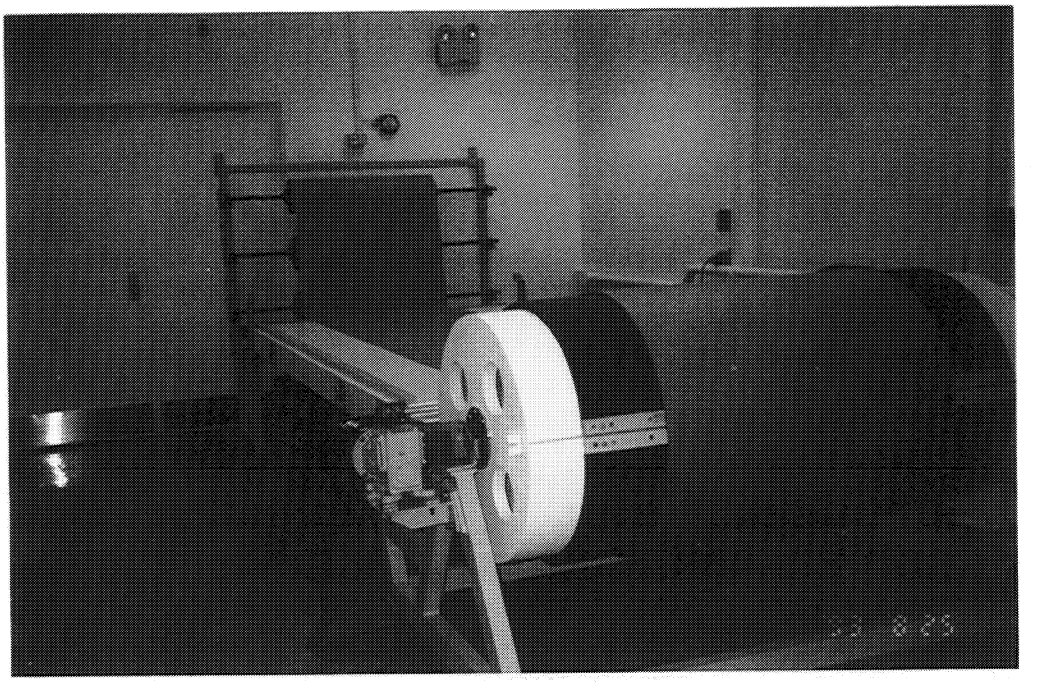

Semi-clean facility for fabricating multilayer insulation blankets.

are inserted through the blanket to tie it together as a unit. Similar fasteners with open hooks are inserted at one end of the blanket as a means of suspending it on the test calorimeter.

As the number of blankets increases around the tank, each succeeding blanket must be made to fit around a correspondingly larger diameter to ensure proper fit-up. To provide this feature, a series of 0.5-in.-thick foam spacers are attached to the drum, as required, to simulate the blankets immediately beneath the one being fabricated. Each spacer covers one half of the circumference of the drum. Both ends of each spacer are glued to full-length, narrow wooden slats, which attach to the drum or to the previous spacer's slats. This system is designed to allow the blade that cuts the blankets to fit between the wooden slats. Once fabricated, the blanket is then removed from the drum and either hung on a vertical fixture that simulates the calorimeter, with the smallest blanket next to the fixture, or laid in a cradle where the largest blanket is laid down first.

Lewis contact: Robert J. Stochl, (216) 977–7522
Headquarters program office: OACT

Tests Reveal Centaur-Related Slosh Phenomena

Sloshing of liquid hydrogen in a propellant tank can result in significant condensation and cooling of the ullage gas. This effect impacts the amount of pressurization gas required to increase and/or maintain pressure in the propellant tank for liquid expulsion. Greater pressurant demands translate into larger mass requirements for the pressurization system of a launch vehicle. A joint program is under way to investigate such sloshing conditions in the Centaur hydrogen tank during specific flight maneuvers.

The experimentation phase of the program has recently been completed at NASA Lewis' K-site facility at Plum Brook Station using a 5-ft-diameter tank. The joint effort is part of a Space Act Agreement between NASA Lewis and General Dynamics Space Systems Division to examine the effects of selected slosh conditions on pressure response and pressurant requirements in a liquid hydrogen tank. Gaseous helium dissipators used on the Centaur vehicle to inject helium for pressurization were installed in the K-site test tank. One dissipator was mounted at the top of the tank, and the other was located near the tank midline. The aluminum tank is extensively instrumented with temperature sensors and is mounted inside a 20-ft-diameter vacuum

chamber. A video camera records the internal tank conditions through a viewing port. Slosh is produced by a shaker mechanism capable of 6 in. of total displacement at 1 Hz for this test series. Test parameters were carefully selected to simulate conditions that exist in the Centaur liquid hydrogen tank.

Detailed interpretation of the data is under way and will be followed by analytical simulation of the tests conducted. Preliminary observations indicate that single-wave slosh scenarios under the conditions tested do not dramatically affect helium pressurant requirements. Furthermore, even with the dissipator fully submerged in liquid hydrogen, rapid pressurization of the tank was possible. However, for continuous high-amplitude waves near resonance, rapid pressure collapse was observed. Many additional results of these testing and analytical programs are expected to aid in future Centaur missions as well as in those of other cryogenic launch vehicles.

Lewis contact: Matthew E. Moran, (216) 977–7525
Headquarters program office: OACT

Power Technology

2-kWe Solar Dynamic Ground Test Demonstration Program Continues

The 2-kWe Solar Dynamic Ground Test Demonstration Program provides an opportunity to demonstrate a solar dynamic power system that is of sufficient scale and fidelity to ensure confidence in the availability of the technology. Applications include space stations, communications and Earth-observing satellites, and electric propulsion.

An aerospace industry/government team is working together to design, fabricate, build, and test a solar dynamic space power system that includes energy storage in an environment simulating a representative low Earth orbit in a test facility (Tank 6) at NASA Lewis. The Tank 6 vacuum facility includes a solar simulator to supply the equivalent of "one Sun," a liquid-nitrogen-cooled wall to simulate the space environment, and an electric load simulator capable of dissipating electric power. To minimize cost, the program is using existing hardware wherever possible (the turboalternatorcompressor and recuperator from the Brayton Isotope Power System Program of the mid-1970's and the gas cooler from a U.S. Air Force program).

The solar dynamic ground test demonstration system is a complete system that includes the following major subsystems and components: a solar concentrator, a solar receiver with thermal energy storage, a power conversion subsystem, a waste heat subsystem, the appropriate controls and power conditioning, and the necessary auxiliaries required to make up the complete system. The solar dynamic system with energy storage is estimated to produce about 2 kW of electric power at a Sun-to-electric-system efficiency of over 15 percent.

The concentrator is designed to receive the solar energy from the NASA simulator and deliver

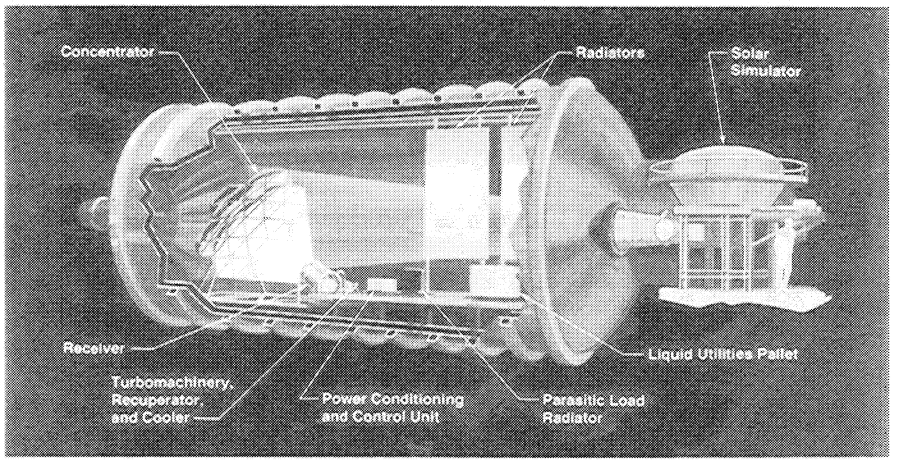

Solar dynamic ground test demonstration system in Tank 6.

12.5 kW of energy into the receiver aperture. The concentrator, made up of seven hexagonal panels, has an effective diameter of 4.57 m. The solar receiver is used to convert the solar energy into heat, transfer part of this heat to the power conversion subsystem, and store the heat for use during an eclipse period. The closed Brayton cycle is the major component of the power system. It changes heat into electricity. The unused heat is removed by using two identical radiator panels with liquid coolant. The power conditioning and control subsystem maintains constant electric power.

The aerospace industry team is working very closely with the NASA team to successfully test this power system in 1995. At the start of the program both teams agreed to work together in close cooperation to complete this project on or ahead of schedule and at or below negotiated cost with a system that satisfies government requirements. To reduce program costs to the government, this program has made use of preexisting hardware from the Space Station *Freedom* Program and from a U.S. Air Force program. The industry team is headed up by Allied Signal, which is responsible for the closed Brayton cycle engine and control system. The sister division of Allied Signal in Los Angeles, California, is responsible for the solar receiver. Loral Vought Systems is responsible for the radiator, Harris Corporation for the concentrator, and Rockwell International for system integration and testing. The NASA Lewis team is responsible for the overall technical management of the project and ensuring that the facility is ready and available for testing. This includes ensuring that the solar simulator will provide the "one Sun" intensity required for the solar dynamic test.

Lewis contact: Richard K. Shaltens, (216) 433–6138
Headquarters program office: OACT

Thermal Shield Manufactured for Hubble Space Telescope Solar Array Booms

The Hubble Space Telescope has experienced "jittering" or shaking as the spacecraft orbits into and out of daylight due to a temperature gradient across the bi-stem booms that support its solar arrays. This jitter sometimes caused the telescope to lose its lock on an object and also blurred images. During Hubble's first shuttle servicing mission the solar arrays were replaced with new ones that have thermal shields on their bi-stem booms to minimize this temperature gradient and thus the jitter problem. NASA Goddard Space Flight Center, responsible for the first servicing mission, requested NASA Lewis to use its in-house facilities to evaluate a candidate thermal shield material, with and without protective coatings, for durability to vacuum ultraviolet radiation and atomic oxygen. These hazards are present in Hubble's operating environment and are potentially detrimental to many materials.

A second-surface mirror material, aluminized fluorinated-ethylene-propylene (FEP) Teflon (Al/FEP), was chosen as the candidate thermal shield material because of its ability to reflect a large portion of the incident solar radiation and to reject or emit excess heat. The materials tested included uncoated Al/FEP provided by Sheldahl Corporation, Al/FEP coated with silicon oxide, and Al/FEP coated with a multilayered oxide system developed by Optical Coatings Laboratory Inc. (OCLI). The silicon oxide coating provides a barrier to atomic oxygen, which is known to erode Teflon (ref. 1), and the OCLI coating provides protection from both atomic oxygen and ultraviolet radiation, which has been shown to embrittle the surface of Teflon (ref. 2). Prior to testing, the extent to which the uncoated material would be damaged by 5 years of exposure to atomic oxygen and ultraviolet radiation in Hubble's orbital environment was unknown, and therefore protective coatings were evaluated in addition to the uncoated material.

After initial electron beam exposure and thermal cycle testing at NASA Goddard, samples of these materials were exposed to vacuum ultraviolet radiation and atomic oxygen and were analyzed by using microscopy at NASA Lewis. Both the OCLI and Sheldahl coatings were found to spall and flake off the aluminized Teflon. Further collaborative work between Lewis and Goddard provided evidence that the oxide coating delamination occurred during thermal cycling. This problem was attributed to lack of adhesion of the silicon oxide coating to the Teflon and the thickness (7000 to 14,000 Å) of the OCLI coating, whose coefficient of thermal expansion is different from that of Teflon. Loose coating flakes would be detrimental to Hubble's optical components. The uncoated material showed good performance, indicating only slight degradation at a near-end-of-life equivalent exposure to atomic oxygen and

ORIGINAL PAGE
BLACK AND WHITE PHOTOGRAPH

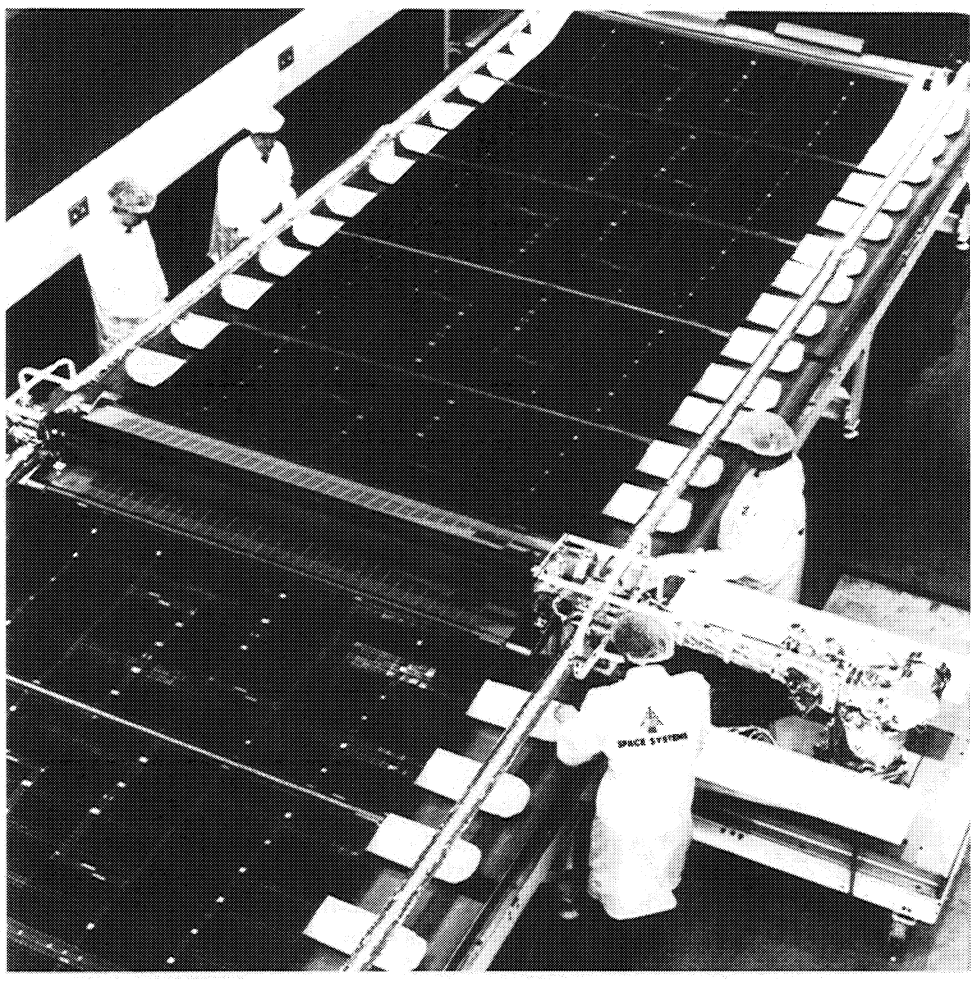

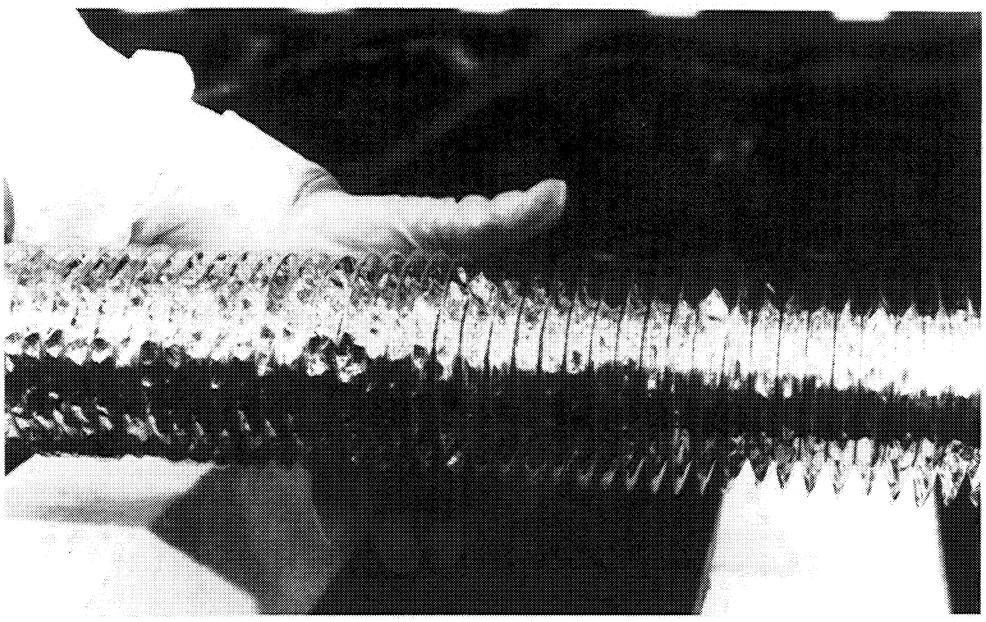

Under contract to the European Space Agency, British Aerospace Space Systems Limited has manufactured a replacement pair of double roll-out solar arrays for the Hubble Space Telescope fitted with the bi-stem boom thermal shielding.

C-2.

vacuum ultraviolet radiation. As a result of this research, uncoated Al/FEP thermal shields were used on the bi-stems on Hubble's replacement solar array assemblies, which were deployed during STS–61, the first servicing mission.

References

1. Banks, B.A.; et al.: Atomic Oxygen Interactions With FEP Teflon and Silicones on LDEF. LDEF: 69 Months in Space. First Post-Retrieval Symposium, Pt. 2, NASA CP–3134–Pt–2, A.S. Levine, ed., 1991, pp. 801–815.

2. Brinza, D.E.; et al.: Vacuum Ultraviolet (VUV) Radiation-Induced Degradation of Fluorinated Ethylene Propylene (FEP) Teflon Aboard the Long Duration Exposure Facility (LDEF). LDEF: 69 months in Space. First Post-Retrieval Symposium, Pt. 2, NASA CP–3134–Pt–2, A.S. Levine, ed., 1991, pp. 817–829.

Lewis contacts: Joyce A. Dever, (216) 433–6294; Kim K. de Groh, (216) 433–2297
Headquarters program office: OACT

Structurally Healed and Chemically Modified Carbon Materials Make Stronger Composites

Defluorination of graphite fluoride into carbon materials at 250 to 450 °C in chemically reactive environments is a new and possibly inexpensive process for producing new carbon-based materials quickly. For example, $CF_{0.68}$ fibers, made from Amoco P–100 carbon fibers, were defluorinated in 370 °C $BrH_2C\text{-}CH{=}CH\text{-}CH_2Br$ vapor and subsequently graphitized at 2700 °C in argon. This process produced carbon fibers with an unusually high modulus and a graphite layer structure that can be healed and crosslinked. Conversely, a sulfur-doped, visibly soft carbon fiber, $CS_{0.1}$, was produced by defluorinating $CF_{0.9}$ fibers, made from Amoco P–25 carbon fibers, in 390 °C sulfur vapor and then heating to 660 °C in nitrogen. Furthermore, defluorination of the $CF_{0.68}$ fibers in bromine produced fragile, structurally damaged carbon fibers. Heating these fragile carbon fibers to 1100 °C in nitrogen resulted in 20-percent mass loss and further structural damage, but heating them to 150 °C in $CHBr_3$ and then to 1100 °C in nitrogen resulted in the healing of the defects and therefore stronger carbon products.

The defluorination product of graphite fluoride, tentatively called activated graphite, has the composition and molecular structure of graphite, but is chemically more reactive. It is a scavenger of manganese, and it can be intercalated with magnesium. Also, it can pick up a large quantity of an alloy made from copper and AISI 304 stainless

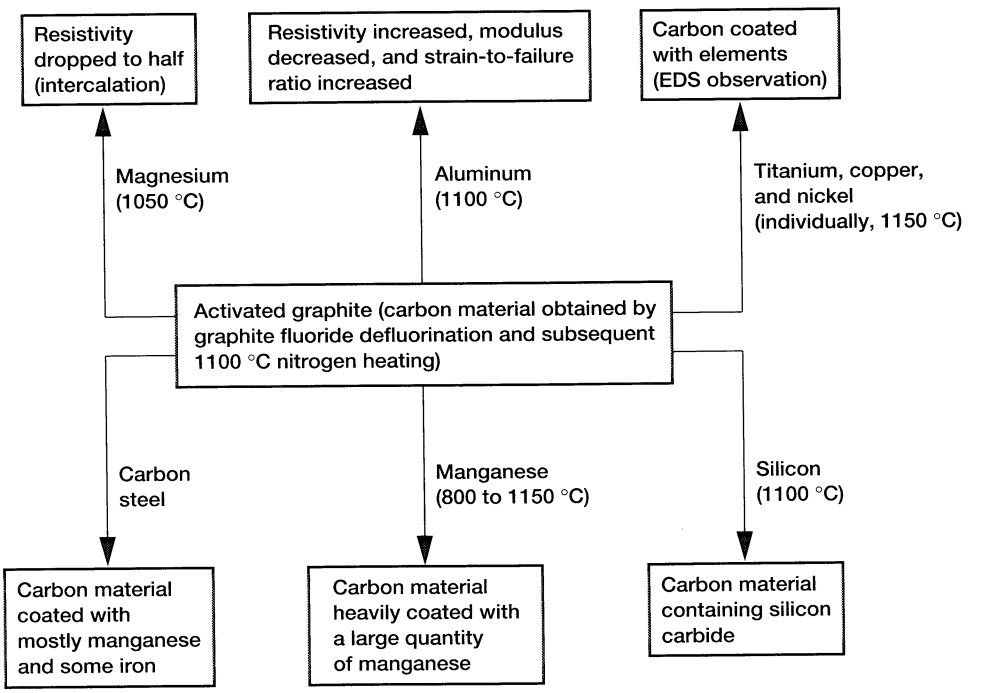

Chemical reactivities of "activated graphite."

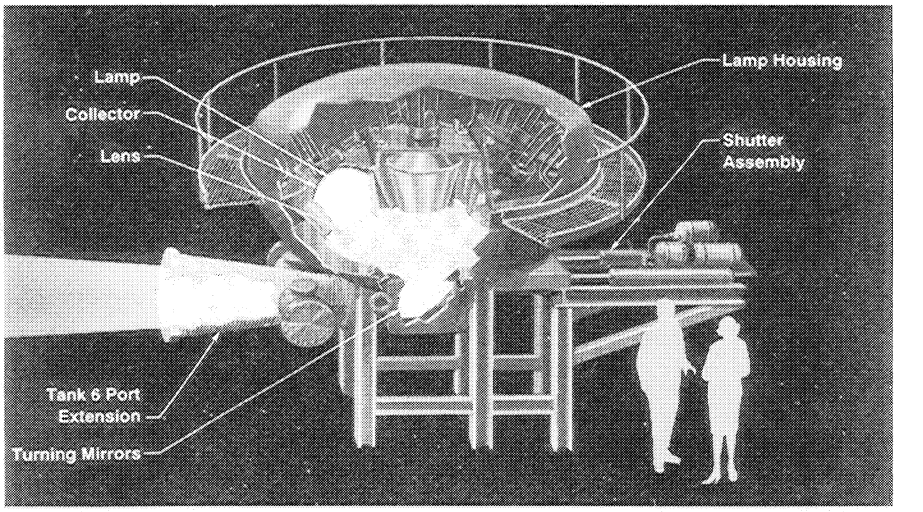

Solar simulator.

steel and easily forms a composite with this alloy at 1-atm pressure. Finally, its surface can pick up some metals and semiconductors at 1100 °C. Therefore, it can form a stronger metal or ceramic matrix composite than the pristine carbon fibers can. Also, it may be used to carry a large quantity of metal for certain engineering applications, such as catalyst or battery fabrication.

Lewis contact: Dr. Ching-cheh Hung, (216) 433–2302
Headquarters program office: OACT

Solar Simulator Designed for Solar Dynamic Space Power System Testing

Planned ground testing of a solar dynamic space power system required duplication of the high vacuum, low sink temperature, and intense solar flux that are present in space. The high vacuum will be provided by a large vacuum tank at NASA Lewis; the low sink temperature will be provided by nitrogen-cooled cold walls; and the intense solar flux will be provided by the solar simulator described here.

Several solar simulators had been previously built and used for vacuum tank testing of various space systems. These simulators produced beams with high intensity and excellent uniformity of intensity. However, the apparent solar subtense angle (i.e., the angular size of the apparent Sun as viewed from the experiment) of these solar simulators is too large to enable testing of solar dynamic systems. The design of the existing solar simulators could have been modified to provide the required subtense angle, but the simulator would have been large and expensive. Instead, a new design was developed to satisfy the requirements of the solar dynamic testing by using a smaller, less expensive solar simulator.

This new design eliminates the collimating mirror used in conventional simulators to transform the diverging beam into a parallel beam, has a redesigned lamp module that includes a lens to increase efficiency, and uses a segmented reflective surface to combine the beams from the individual lamp modules at the pseudo-Sun.

Developing a new solar simulator design for testing the solar dynamic system instead of modifying current designs cut the cost in half, increased the efficiency by 50 percent, reducing operating costs by one-third, and reduced the volume occupied by the solar simulator by a factor of 10.

Lewis contact: Richard K. Shaltens, (216) 433–6138
Headquarters program office: OACT

Heat-Pipe Component Test Power Converter Tested Successfully

A major milestone of the Stirling space power converter development program was recently achieved with the successful testing of the heat-pipe component test power converter (CTPC). While operating at the design temperature ratio

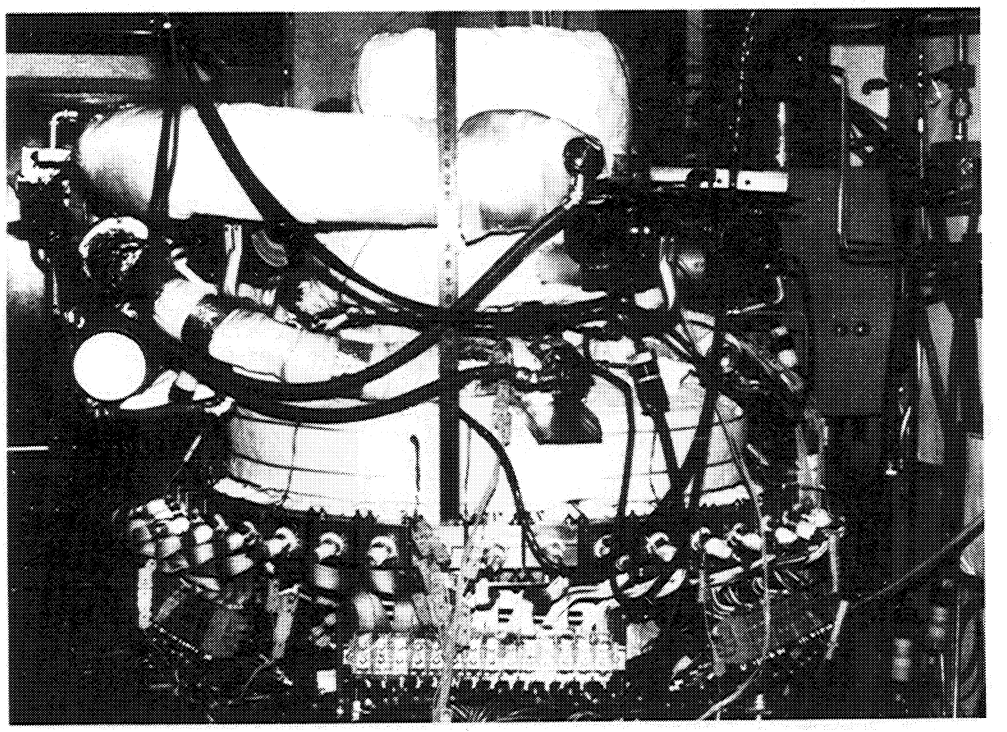

Heat-pipe component test power converter.

of 2, the converter exceeded its design goals. It produced more than 12 kW of electric power at 70 Hz and operated at an efficiency of nearly 22 percent. The CTPC is being developed by Mechanical Technology Inc. (MTI) of Latham, New York. The purpose of this technological development effort, which began in 1988, is to develop a high-efficiency, low-specific-weight, 12.5-kWe power converter capable of a 60,000-hr life for space applications. Because of the inherent high efficiency of the Stirling power converter relative to other power converters, it is the best choice for space applications.

To optimize the size and mass of the radiator that rejects heat from the cold side of the power converter to the space environment, the cold-side temperature should range between 425 and 550 K. Depending on the material of the hot side of the converter, the Stirling heater head, the heater head may operate between 850 and 1050 K. With an increase of the temperature ratio, which is the ratio of hot-side to cold-side temperature, the Stirling converter can generate more power at a higher efficiency. The CTPC heater head is made of Inconel 718 and, from known material properties of this alloy, can achieve a lifetime of 60,000 hr if the heater head is operated at about 915 K. The same lifetime, at a higher power output and efficiency, can be achieved at a heater head temperature of 1050 K if Udimet 720 is substituted for Inconel 718. For other applications where heat can be rejected at a lower temperature (e.g., a marine application), the power converter can be operated at a higher temperature ratio with a subsequent increase in power output and efficiency. For example, at a temperature ratio of 3, with slight modification, the CTPC is capable of producing 24 kW of electric power at 35-percent efficiency. This near doubling of power output and 50-percent increase in efficiency demonstrates the potential of this technology for diverse applications.

Successful testing of the CTPC was made possible by major accomplishments that required technological breakthroughs in several areas, including bearings, alternator, heater head, and heat pipe. A simple, passive, and efficient internally supplied hydrostatic gas bearing system was developed that relies on the piston gas springs to supply gas to bearing supply and drain plenums located within the pistons. Insulation materials were incorporated into the alternator that allow its operation above 525 K. A robust, lightweight, high-performance, sodium-vapor-to-helium, heat-pipe heat exchanger was fabricated to provide

efficient heat transport into the Stirling heater head.

The heat-pipe CTPC is now ready for endurance testing and integration into a power-generating system for a specific application.

Lewis contact: James E. Dudenhoefer, (216) 433–6140
Headquarters program office: OACT

Advanced Nickel/Hydrogen Cell Passes Test

Innovative design that achieves extended low-Earth-orbit (LEO) cycle life also has down-to-Earth benefits. Martin Marietta (formerly GE Astro-Space) is evaluating advanced nickel-hydrogen cell technology for the Earth Observing System (EOS). EOS will enhance our understanding of the global environment, enabling early prediction of volcanos and earthquakes and saving lives. It will also monitor the effects of industrial and automobile pollution on ozone depletion and global warming. The advanced battery can also be used for environmentally friendly electric vehicles, which create zero environmental pollution.

The primary function of the advanced, rechargeable, individual-pressure-vessel (IPV) nickel/hydrogen (Ni/H_2) cell is to provide electric energy storage for long-term (>5 years, >30,000 cycles), low-Earth-orbit spacecraft missions. An advanced Ni/H_2 cell has been designed to meet this goal. It includes 26 percent rather than 31 percent potassium hydroxide electrolyte; a patented catalyzed wall wick; serrated-edge separators to facilitate gas and electrolyte management; and a floating stack to accommodate nickel electrode expansion, which results from charge/discharge cycling.

NASA Lewis had a contract with Eagle Picher to fabricate six 125-Ahr cells based on this design. Three of the test cells contained all the features of the advanced design; and three control cells did not contain a catalyst on the wall wick. All six cells are being evaluated in a LEO-cycle-life test (60-percent depth of discharge, 10 °C) at the Naval Weapons Support Center under a NASA Lewis contract. The catalyzed wall wick cells have been subjected to more than 24,500 charge/discharge cycles with continuing successful operation of all cells. In contrast, all three of the noncatalyzed wall wick cells failed at 9588, 13,900, and 20,575 cycles, respectively. These results conclusively demonstrate the importance of a catalyzed wall wick for achieving stable voltage performance and long cycle life.

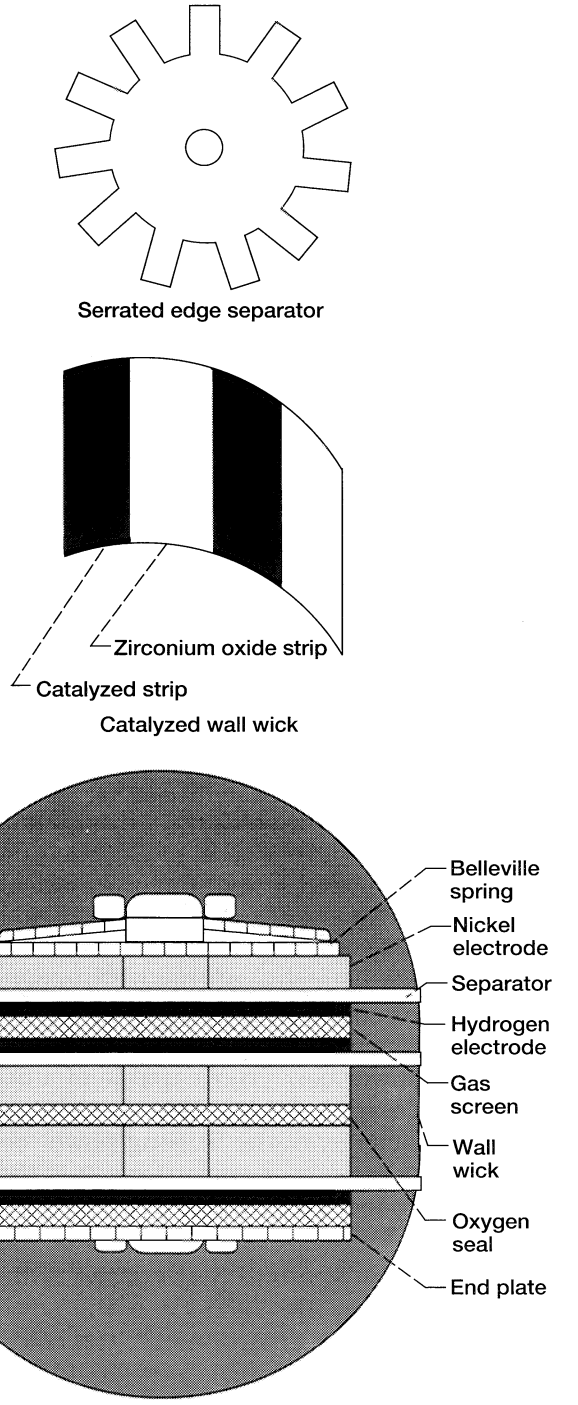

NASA advanced-design IPV nickel/hydrogen cell catalyzed wall wick.

In this advanced design the oxygen generated at the end of charge is recombined chemically with hydrogen on the catalyzed wall wick, where the heat of recombination is much easier to remove. The cell average temperature at the end of charge is thus reduced by about 5 deg C relative to state-of-the-art cells, which recombine the oxygen on the catalyzed electrode surface in the stack. This lower operating temperature and reduced internal temperature gradients also enhance electrolyte management by reducing water vapor transfer. Damage to the hydrogen electrodes due to concentrated oxygen recombination is also eliminated by using the catalyzed wall wick. Oxygen management was further improved by using the serrated-edge separators to facilitate the flow of oxygen and hydrogen within the cell. Accommodation of nickel electrode expansion due to cycling was improved by using an expandable stack, which allows for a 30-percent increase in electrode thickness.

Lewis contacts: James E. Smithrick, (216) 433–6140; James E. Dudenhoefer, (216) 433–6140
Headquarters program office: OACT

Novel Approach Developed for Extrapolating Short-Time Failure Behavior

By using the minimum-commitment method (MCM) for multiheat analyses developed over the past several years at NASA Lewis and Case Western Reserve University, a procedure has been developed whereby a relatively small amount of creep-rupture data, limited in many cases to 8 to 12 data points in the 1000-hr range, can be used to obtain accurate estimates of creep-rupture properties to 100,000 hr. This procedure has been made possible by a recently developed, extensive data base from material tested in the United States, Britain, and especially Japan with actual test times in the 100,000-hr range. The procedure can be most useful for new applications, such as the Stirling engine or nuclear propulsion, where the special materials requirements dictate new compositions that previously have not been tested to long times but wherein long-time service is a necessity.

Studies of multiheats at NASA Lewis over the last two decades have revealed a remarkable result: If a large amount of data is available on various

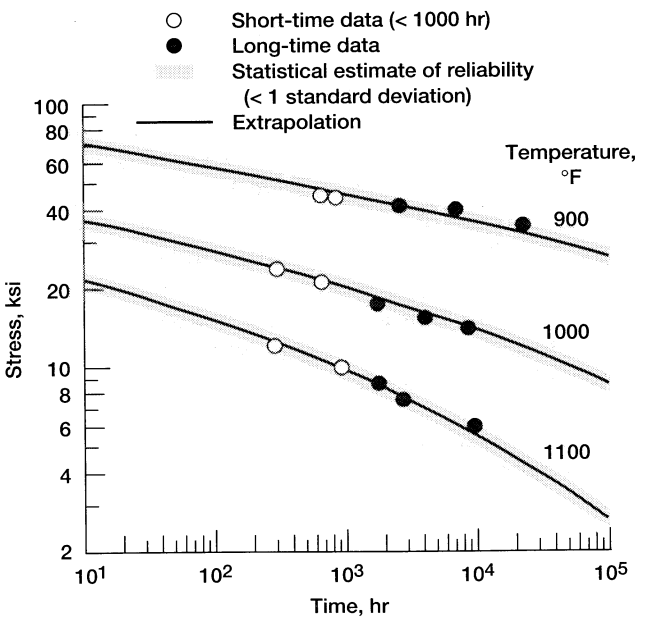

Example of extrapolation using novel approach—for aluminum 7075.

individual heats, it becomes possible to extrapolate data on a new heat of this multiheat, even if the new data are very limited and available for only a short time range. Over these decades we have collected extensive data for at least 38 multiheat systems, using mainly the extensive data base generated at the National Research Institute for Metals in Japan. The concept has been developed that it might be possible to extend this result to a single heat of a new material, totally unrelated to the multiheats already analyzed.

Many possible criteria for placing the new heat within the universe of characterized multiheats were investigated. Strength levels, activation energies, melting points, etc., were studied but were unacceptable. The best criterion was found to be a plot of stress-rupture using values from the 38 multiheats to determine which multiheat yields the best straight line according to statistical analyses. An isothermal stress-rupture line for this heat thus can be constructed and extrapolated to any reasonable time level desired. Because the baseline multiheats are characterized to rupture times of 100,000 hr, the short-time data for the single heat can usually be extrapolated to 100,000 hr with some confidence.

We have analyzed the data of numerous single heats according to this approach. Data within the

1000-hr rupture range are adequate if there are eight or more data points spread over a wide stress range. Remarkably, the best matching multiheat may bear no metallurgical relationship to the specific material being studied. For example, a plot for aluminum alloy 7075 was derived by matching with a steel. It is only necessary that the basic pattern of behavior be matched, and data in the 1000-hr rupture range appear adequate to establish the basic pattern. For many single heats short-time data can be extrapolated to much longer times, and the extrapolations compare well with existing long-time data.

Lewis contact: James E. Dudenhoefer, (216) 433–6140
Headquarters program office: OACT

High-Temperature Power Capacitors Developed

A combined research effort, utilizing contracts and in-house testing facilities at NASA Lewis, has led to the development of power capacitors capable of continuous operation at 200 °C. Because there is no air or water in space, heat can only be eliminated by radiation, an inefficient process. By operating the spacecraft radiator and power electronics at a higher temperature, the radiator becomes more efficient allowing its size to be reduced, thus decreasing the spacecraft's weight and reducing launch costs. These power capacitors could also be used in the control electronics for turbine and automotive engines. The operating temperatures of these engines constrain designers to locate the electronics in relatively cool areas or compartments away from the engine. The resulting use of wiring harnesses adds weight to the vehicle, requires additional space, decreases reliability, and adds to fuel costs. Additionally, the successful and efficient drilling of wells for geothermal energy extraction necessitates the use of electronic sensors that can withstand prolonged exposure to the high temperatures encountered in down-hole drilling operations. These sensors collect information about the nature of the underlying rock and soil formations that provides clues about the presence of oil or gas.

State-of-the-art power capacitors are limited to maximum operating temperatures of 105 °C with some devices functioning at temperatures to 150 °C. Some signal-level capacitors are capable of withstanding temperatures to 200 °C, but these devices only operate at low currents and voltages—typically only a few milliamperes at voltages less than 125 V—and are unsuitable for use in power applications. The major barriers to operating capacitors continuously at 200 °C and high power levels are the dielectric material and the thermal and electrical packaging design. The dielectric material must withstand temperatures above 200 °C from internal heating while under electrical bias; it must also have low dielectric loss to reduce internal heating and exhibit high electrical breakdown strength. The package must efficiently dissipate internally generated heat, provide low loss, and have low-inductance lead structures capable of conducting the high currents associated with power capacitors.

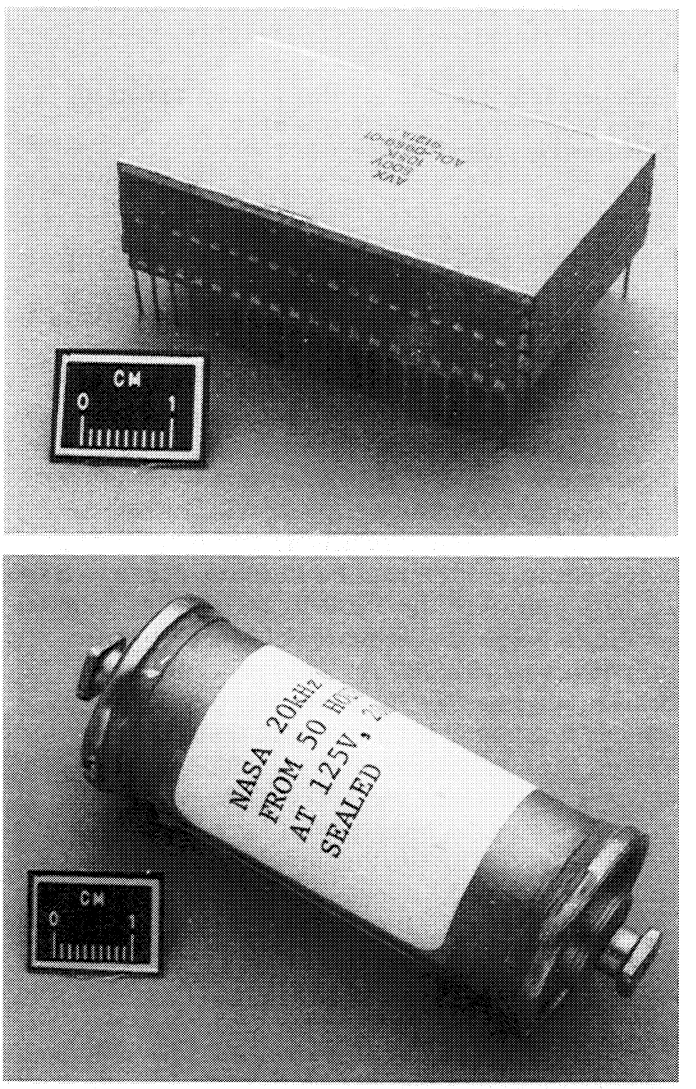

AVX multilayer ceramic capacitor (top) and Westinghouse/3M film capacitor (bottom).

NASA Lewis researchers are now performing extensive multistress tests on a multilayer ceramic capacitor developed by AVX Corporation and on a foil-film capacitor, using a proprietary 3M Company polymer film, developed by Westinghouse Research and Development Center. The 1-μF AVX ceramic capacitor can withstand 500 V dc and operates at 250 V ac, 20 kHz, and 30 A. The Westinghouse film capacitor has a rating of 0.8 μF and operates at 125 V ac, 20 kHz, and 8 A. The capacitors are now being characterized for capacitance stability, dielectric loss, and dc leakage as a function of temperature, frequency, and electrical bias. They will then be subjected to multistress life testing at temperature and full electrical bias. Finally, the capacitors will be integrated with inductors and a transformer, also developed during this program to operate at 200 °C, into a 20-kHz inverter circuit and tested as a single function unit at high power and temperatures to 200 °C.

Bibliography

Hammoud, A.N.; et al.: Electrical Characterization of Glass, Teflon, and Tantalum Capacitors at High Temperatures. Presented at 26th IEEE Conference on Electrical Insulation and Dielectric Phenomena, Knoxville, TN, Oct. 20–24, 1991.

Hammoud, A.N.; Baumann, E.D.; and Overton, E.: Electrical Properties of Teflon and Ceramic Capacitors at High Temperatures. Presented at IEEE Electrical Insulation Symposium, Baltimore, MD, June 7–10, 1992.

Overton, E.; Hammoud, A.N.; Baumann, E.D.; and Myers, I.T.: Thermal Aging Effects on the Electrical Properties of Film and Ceramic Capacitors. Presented at Electrical/Electronics Insulation Conference, Chicago, IL, Oct. 4–7, 1993.

Lewis contact: James E. Dudenhoefer, (216) 433–6140
Headquarters program office: OACT

Scattered Space Atomic Oxygen Experiment Designed and Built

Atomic oxygen is the predominant species in low Earth orbit (LEO), where spacecraft such as the space station will orbit. Atomic oxygen is formed when ultraviolet radiation photodissociates molecular oxygen. As spacecraft orbit the Earth, exterior materials impact LEO atomic oxygen and oxidation can occur. Many sensitive spacecraft materials, such as organic materials and several metals, react with atomic oxygen and degrade or erode. To help better understand the complex

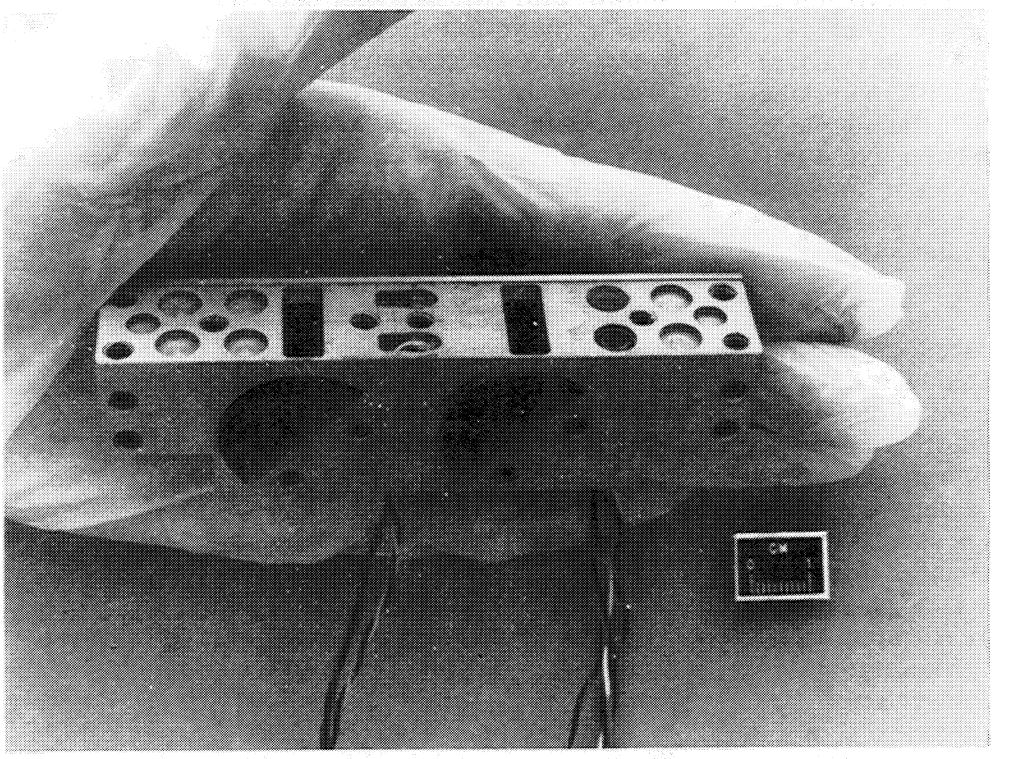

Inside view of SSAOE showing passive and active scatterometers, two photodiodes, and eight passive samples.

interactions of atomic oxygen with materials, NASA Lewis has designed and built an inexpensive active experiment. This experiment, called the Scattered Space Atomic Oxygen Experiment (SSAOE), will be exposed to LEO atomic oxygen on STS–60.

Metal oxide coatings, such as silicon dioxide, have been found to protect oxidation-susceptible materials such as Kapton polyimide, which is used for space station's photovoltaic array blanket material. Atomic oxygen degradation can still occur at defect sites, such as pinholes and scratches, in the protective coating. The resulting undercutting threatens the integrity of the protected material.

A Monte Carlo model has been written that predicts atomic oxygen undercutting of oxidizable materials at these defect sites. One reason undercutting occurs with direct ram impact is that most impacted atomic oxygen thermally accommodates and scatters with a near cosine distribution (~86-percent scattering for Kapton). The erosion yield of oxidizable materials depends on the energy of incident atomic oxygen. Ram atomic oxygen impacts surfaces with an average energy of 4.5 eV. Scattered, thermalized atomic oxygen has an energy of approximately 0.1 eV. We know, from previous spaceflight experiments, the direct ram erosion yield of several materials (such as Kapton), but we do not know the erosion yield of thermally accommodated oxygen with materials. To understand, model, and predict the atomic oxygen durability of protected polymers that fail by undercutting mechanisms, we must know the erosion yield of thermally accommodated atomic oxygen in addition to the ram erosion yield of susceptible materials.

The SSAOE is designed to compare the in-situ erosion of fused silica slides coated with opaque diamond-like carbon (DLC) exposed to direct ram atomic oxygen with the erosion of others exposed to thermally accommodated scattered atomic oxygen. Opaque DLC becomes transparent when reacted with atomic oxygen and is sensitive to extremely low fluences. Light-detecting devices (photodiodes) located behind the DLC-coated fused silica samples will measure the amount of both sunlight and artificial light transmitted through the exposed samples. The scattered atomic oxygen experiment is set inside a semicylindrical scatterometer. A fused silica slide tilted at a 45° angle will scatter the incident atomic oxygen. A passive scatterometer (of the same dimensions as the active one) will be used to determine the degree of specular scattering and allow the scattered fluence at the photodiode position to be accurately predicted. To maximize this experiment, eight small passive samples have been incorporated into the top, ram-facing surface of the SSAOE.

The scheduled launch date is January 1994. Data from this experiment will help to better predict the atomic oxygen durability of spacecraft materials.

Lewis contacts: Kim K. de Groh, (216) 433–2297; Bruce A. Banks, (216) 433–2308
Headquarters program office: OACT

Space Electronics

Potential Markets Predicted for Advanced Satellite Communications

An extensive study recently completed by Booz Allen & Hamilton (ref. 1) identifies trends in the volume and type of traffic offered to the U.S. domestic communications infrastructure. These trends were extrapolated through the year 2011. Traffic in three general categories was addressed: voice, data, and video. Voice services including message telephone service, private lines, private networks, and 800 and 900 services were analyzed. Specific data services examined were facsimile, electronic mail and terminal operations, imaging, on-line information services, electronic funds transfer, electronic data interchange, and research networks. Video capacity demand was projected for network, cable, and educational broadcasting; video on demand (viewer-choice television); and business television (conferencing and one-way intracorporate communications).

To describe how telecommunications service providers are adapting to the identified trends, the study assessed the status, plans, and capacity of the domestic communications infrastructure. Cable, satellite, and radio components of the infrastructure were examined separately. Existing and future applications for three types of cable (fiber optics, coaxial cable, and twisted pair) were identified. Existing and future applications were

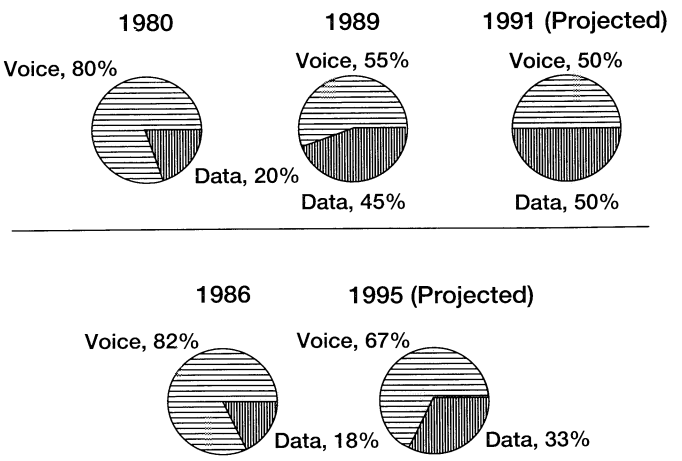

Data traffic percentage growth for private corporate networks (top) and for public long-haul networks (bottom).

also identified for geosynchronous and low-Earth-orbit satellites. Satellite systems accessed by means of very-small-aperture terminals (VSAT's) were examined separately. The radio component of the domestic infrastructure covers two types of microwave technologies: frequencies used for short-haul applications and frequencies used for long-haul applications.

The study also assessed the following major applications making use of the infrastructure: (1) broadband services, including the broadband Integrated Services Digital Network, switched multimegabit data service, and frame relay; (2) mobile services, including voice, location, and paging; (3) VSAT, including mesh VSAT; and (4) direct broadcast satellite for audio and video.

Specific applications and market segments appropriate to the features and capabilities of communications satellites were identified in the study. The volume and dollar value of these market segments were estimated. The study also examined the potential of each satellite-based application to capture business from alternative technologies.

Reference

1. Adamson, S.; et al.: Potential Markets for Advanced Satellite Communications. NASA CR–191145, 1993.

Lewis contact: James E. Hollansworth, (216) 433–3458
Headquarters program office: OACT

Telemedicine Spacebridge Project Links United States and Russia

An emerging application of telecommunications technology is telemedicine. Telemedicine is the use of telecommunications to aid in the medical process through such applications as consultation, telediagnosis, teleradiology, and telepathology. The telemedicine spacebridge uses satellites and terrestrial telephone links to connect Moscow, Russia, with several U.S. medical centers. The Telemedicine Spacebridge Project provides a two-way video link between medical specialists at participating medical institutions in the United States and their counterparts in the Russian republic. The operational spacebridge link addresses such topics as disaster medicine, routine patient consultation, medical evaluation, exchange of patient information and relevant literature, and space medicine issues. The relative success that NASA has enjoyed with its telemedicine experiences in the past would suggest that this current effort could revolutionize the way medical services are delivered around the world. Furthermore, the life sciences experiences gained by the United States and Russia through the telemedicine spacebridge effort will enhance the capabilities and knowledge for manned space missions for all future spacefaring nations.

The heart of the spacebridge link is the gateway facility now in place at NASA Lewis in Cleveland, Ohio. Two main components of this facility are the domestic Ku-band Earth terminal and the Russian Space Data Relay Network (SDRN) Earth terminal. The domestic Ku-band Earth terminal has a 5-m antenna and a 280-W transmitter and can communicate with any satellite in the visible geostationary orbital arc. The spacebridge currently is using the GTE GStar II satellite for U.S. distribution of the spacebridge signals. The SDRN Earth terminal has a 2-m antenna and a 50-W transmitter, which are used to communicate with the Russian West Space Data Relay Network (WSDRN) geostationary satellite located at 16° west longitude. The WSDRN satellite, also known as "Loutch," is analogous to NASA's TDRSS satellite system in that its main purpose is to communicate with the *Mir* space station and act as a data relay for any other orbiting spacecraft. There are two other spacecraft in the SDRN constellation spaced around the geostationary orbit.

The signals are transmitted from NASA at 15.155 GHz and received at 13.528 GHz, which

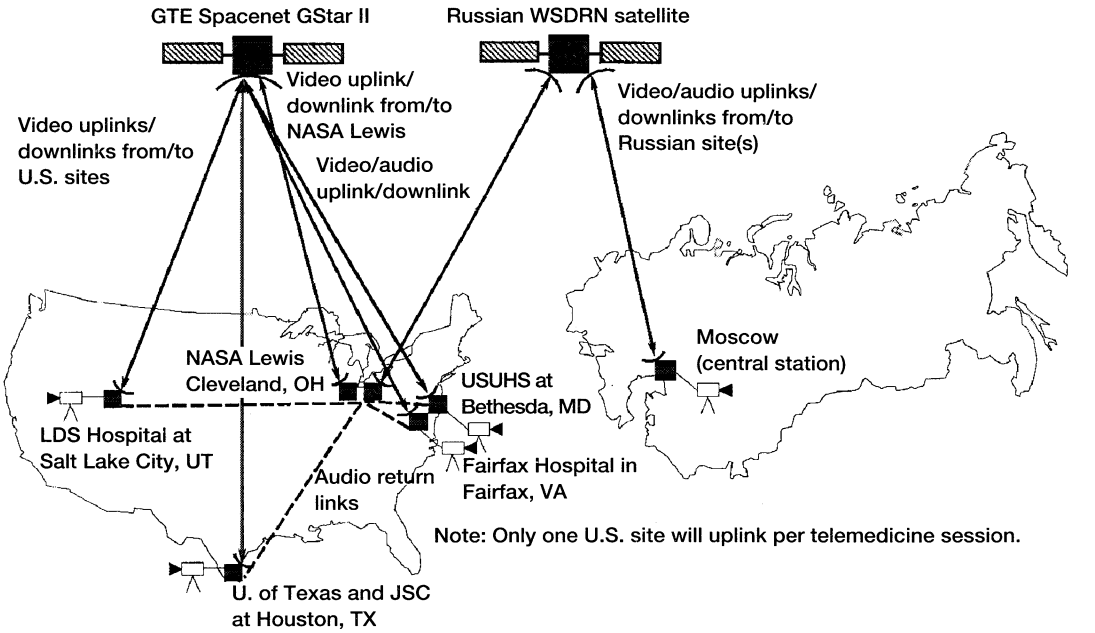

Telemedicine spacebridge system overview.

are in restricted portions of the Ku band. NASA has received special permission to transmit and receive in these bands for the telemedicine demonstration project. The signals are received from Moscow and transmitted to Moscow as full-bandwidth analog video by using the phase-alternating line video standard used throughout much of Europe. The domestic distribution uses the National Television Standards Committee video standard used in the United States, with conversions from one standard to the other taking place at the gateway facility in Cleveland. The video signals transmitted and received in the United States are scrambled by using a MacroVision scrambling system to ensure patient privacy. One U.S. site uplinks per session, with the others participating by voice only.

Lewis contacts: John E. Zuzek, (216) 433–3469; Michael A. Cauley, (216) 433–3483
Headquarters program office: OLMSA

Materials and Structures for High-Speed Electronic Devices Characterized Nondestructively

In the past decade new types of devices have been developed for high-speed electronics, both for digital and analog applications. These devices are based on III–V compound semiconductor heterostructures. This progress was made possible by the development of a new crystal growth technique called molecular beam epitaxy (MBE). The first generation of these devices was based on gallium arsenide (GaAs) and was developed in the 1980's. The second generation is being developed at the present time and is based on indium phosphide (InP). In both cases monolithic integration of many devices is possible to achieve a complex integrated circuit (e.g., a receiver or a transmitter). Large-scale applications of GaAs-based circuits are now being undertaken by both the telecommunications industry and the military.

A typical device structure contains two or three types of materials, grown by MBE, as thin layers over a GaAs or InP substrate. Some of these materials are pseudobinaries (e.g., $Al_xGa_{1-x}As$, $In_xGa_{1-x}As$, and $In_xAl_{1-x}As$). An adequate materials and structures characterization technique is required to estimate, nondestructively, the thickness of all layers, the composition parameters x of the pseudobinaries (if any), and the lateral homogeneity of the structure on the wafer. This characterization step is needed both for the MBE

chamber calibration and for screening wafer quality before the expensive device-processing step. NASA Lewis decided to develop the optical technique of ellipsometry for this new application. This is presently the best of all nondestructive techniques for characterizing the structure of these materials.

In the first stage of this work, performed in collaboration with a NASA Lewis grantee (University of Nebraska), GaAs-based heterostructures were characterized. In the second stage, performed solely at NASA Lewis, MBE-grown, InP-based heterostructures were characterized. This recent work included two steps: first, measuring the optical calibration function of $In_{0.52}Al_{0.48}As$; second, using this calibration to characterize several heterostructures used in practical devices. Thicknesses of four layers, with the thickest one being about 550 Å, were estimated simultaneously. The accuracy of the estimates is of the order of 10 Å for the thicker layers and as low as 1 Å for 50-Å-thick layers. Problems in the MBE chamber calibration and in the material quality were identified. For example, deterioration of the $In_{0.52}Al_{0.48}As$ layer due to possible oxidation was detected. In parallel, lateral homogeneity measurements were performed on several heterostructures grown on 3-in.-diameter GaAs wafers. These heterostructures had layers as thick as 900 Å. In this case an accuracy of 5 Å or better was achieved for all thicknesses, and the composition parameter x, which had a value of 0.3, was estimated to within 0.005 (i.e., better than 2 percent of its value).

Another aspect of ellipsometry applications for high-speed electronic devices is now being developed in industry, especially by a new company that is a spinoff from a NASA Lewis grant to the University of Nebraska. In this application ellipsometry and in-situ, real-time measurements are used to monitor and control electronic material processing. In this context, processing includes material growth, dry etching, and temperature measurement.

Bibliography

Alterovitz, S.A.; et al.: Ellipsometric Characterization of $In_{0.52}Al_{0.48}As$ and of Modulation Doped Field Effect Transistor Structures on InP Substrates. Appl. Phys. Lett., vol. 62, no. 12, 1993, pp. 1411–1413.

Lewis contact: Dr. Samuel A. Alterovitz, (216) 433–3517
Headquarters program office: OACT

Ka-Band MMIC Arrays Being Developed for Future Communications Systems

Ka-band monolithic microwave integrated circuit (MMIC) arrays have long been considered as having high potential for increased communications systems capability in terms of scan performance, data rate, and connectivity at reduced size, weight, and power consumption. The ability of the array to generate multiple shaped beams that can be dynamically reconfigured while in operation will also enhance service flexibility. NASA Lewis is committed to the development of Ka-band MMIC arrays to provide the enhanced service flexibility and capacity required by future communications systems.

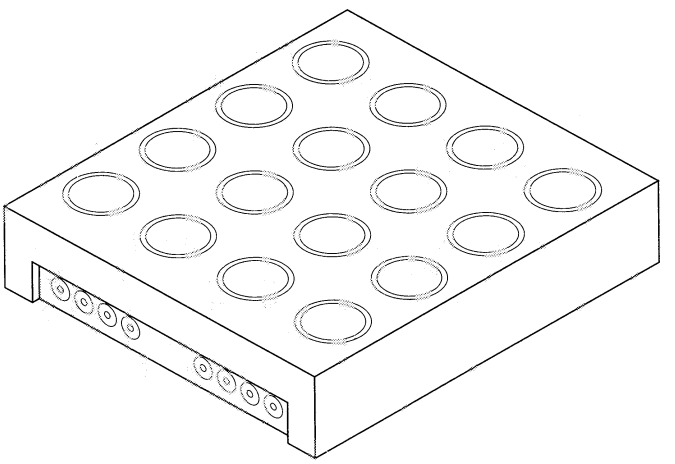

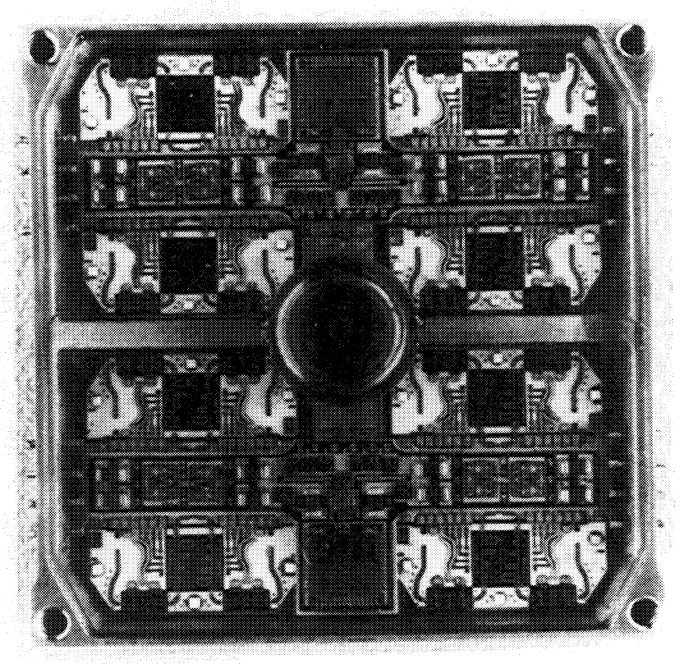

4×4 MMIC subarray module. Schematic (top); photograph showing inside of module (bottom).

The 16-element, 4×4, 30-GHz MMIC subarray presently being developed under Texas Instruments contract NAS3–25718 is the most ambitious MMIC array development yet attempted. The proof-of-concept array features a high-density, thin-profile "tile" configuration (1.3 by 1.3 by 0.3 in.) integrating thirty-two 30-GHz MMIC chips. The radiating elements are cavity-backed, aperture-coupled, linearly polarized circular microstrip patches. Active beam steering and distributed power amplification are provided by a 4-bit phase shifter and a constant-gain amplifier at each radiating element. The 1:16 beam former uses a 16-way planar microstrip power divider with a perpendicular coaxial interface. Two multilayer, thin-film boards with custom application-specific integrated circuit chips provide direct-current and logic distribution with only eight bias and control inputs each. The subarray design is modular, enabling the assembly of several subarray modules into a larger array. The modules, each weighing 27 g, will be hermetically sealed.

One complete subarray has been assembled and tested. Results demonstrate excellent scanning performance and very good operational stability. The subarray has a scan loss of –2.7 dB at ±30° and an effective radiated power of over 60 W at boresight. Two such subarrays will be mounted side by side to form a 32-element 4×8 array for the ACTS Aero-X Experiment.

Lewis contact: Dr. Richard Q. Lee, (216) 433–3489
Headquarters program office: OACT

High-Temperature Superconducting Microwave Receiver Built for Space Experiment

In collaboration with NASA's Jet Propulsion Laboratory, NASA Lewis is fabricating a superconducting, low-noise microwave receiver as a candidate for inclusion on the Naval Research Laboratory's (NRL) High Temperature Superconducting Space Experiment (HTSSE–II). The overall objective of the NRL program is to demonstrate the viability and survivability of high-temperature superconducting devices and subsystems in space. The proposed receiver is such a system, incorporating a superconducting preselect filter, a semiconductor low-noise amplifier, a semiconductor downconverter, and a superconductor-stabilized local oscillator. The low-noise amplifier and downconverter, although not superconducting, are designed for optimum operation at a temperature

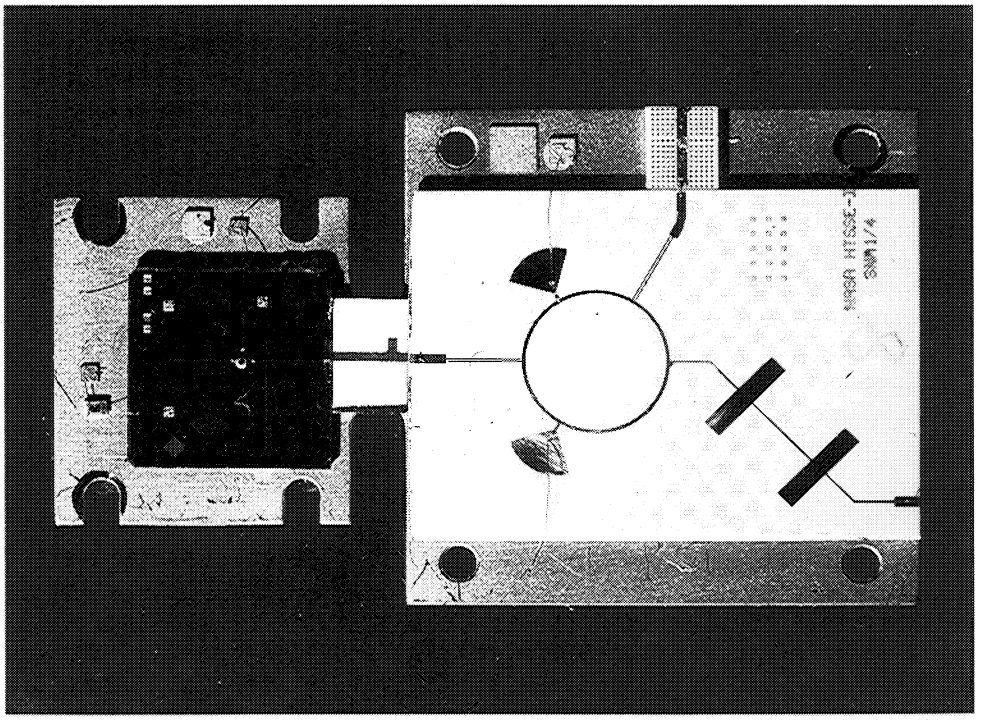

Quality model mixer and local oscillator for superconducting microwave receiver.

of 77 K. NASA Lewis has designed, fabricated, and tested the mixer and the local oscillator. JPL has designed the preselect filter and the low-noise amplifier, as well as carrying out the integration and packaging.

The high-temperature superconducting subsystem that has been designed and fabricated operates at an input radiofrequency of 7.2 GHz, utilizes a local oscillator frequency of 8.4 GHz, and produces an output signal at 1.2 GHz. These frequencies are representative of systems employed in the deep-space communications network.

The benefits of using a superconducting receiver of the type being developed here are fourfold:

- Cryogenic operation dramatically reduces the noise figure of most of the devices associated with the receiver. The resulting improved signal-to-noise ratio permits significant (60 percent) reductions in the radiated power required at the transmitting end of a communications link.

- Cryogenic operation enhances mixer performance so that local oscillator drive levels may be drastically reduced, thereby minimizing total power consumption.

- Using superconducting materials permits the design of much smaller planar preselect filters with dimensions on the order of 0.5 by 1.0 cm without incurring losses that would degrade the noise performance of the system.

- Using high-temperature superconducting materials in the design of the local oscillator circuit allows frequency stability far superior to that otherwise achievable in the desirably compact planar implementation.

Greater frequency stability means less phase noise, which translates directly into reduced data transmission errors.

In the past year a prototype version of the receiver was built and delivered to NRL for evaluation there. Following the acceptance of the prototype, a quality model has been developed that will meet JPL's standards for space qualification of a class-D experiment. The quality model, presently being assembled and packaged at JPL, is scheduled for delivery to NRL in January 1994. The quality model mixer and local oscillator were fabricated at NASA Lewis. Fabrication of flight hardware has begun and is scheduled for delivery to NRL in May 1994. Launch of the HTSSE–II satellite is anticipated for September 1995.

Lewis contact: Dr. Kul B. Bhasin, (216) 433–3676
Headquarters program office: OACT

Ka-Band Earth Terminal Developed for Interference Experiments

NASA Lewis has developed a Ka-band Earth terminal for use in space communications interference experimentation (INTEX) with NASA's Advanced Communications Technology Satellite (ACTS). The INTEX Earth terminal, located at NASA Lewis, is fully compatible with the ACTS wideband matrix switch mode of operation. It is also compatible with the ACTS link evaluation terminal in terms of radiofrequency and digital formats. The terminal will be used for a number of ACTS experiments at Lewis and is also available for use by organizations outside of NASA. In conjunction with the link evaluation terminal the INTEX terminal provides a useful testbed for space communications technologies using ACTS.

The INTEX terminal operates over a bandwidth of approximately 800 MHz, centered at 29.5 GHz on the uplink and 19.8 GHz on the downlink. The transmitting amplifier provides 60 W of uplink power. The receiver subsystem has a noise figure of 6 dB on the downlink. The end-to-end link margin for a 220-Mbps, minimum-shift-keyed modulated signal is 9.2 dB, without accounting for rain attenuation.

The INTEX terminal uses a digital Earth terminal subsystem based upon a serial minimum-shift-keyed modem operating at dual rates of 220 or 110 Mbps. The Earth terminal digital subsystem provides a bursted data format allowing throughput rates ranging from 200 to 1.25 Mbps. The experiment control and monitor computer provides all control and data collection for the INTEX terminal, including transmitted and received power levels, bit-error-rate measurement, and downlink noise insertion.

Digital data streams containing audio, video, data, and other types of information can be

transmitted and received through the INTEX terminal by meeting the Earth terminal interface requirements. The terminal can accommodate experiments using other modulation and coding formats provided that their equipment meets a 2.8- to 3.9-GHz intermediate-frequency interface.

Lewis contact: Robert J. Kerczewski, (216) 433–3434
Headquarters program office: OACT

Ku-Band Earth Terminal Facility Constructed

New baseband satellite communications technology developed at NASA Lewis can now be tested over existing commercial Ku-band satellites by using a recently constructed Ku-band Earth terminal located here at Lewis. This facility is fully compatible with all U.S. domestic Ku-band satellites. The current configuration includes two receivers with a 300-W transmitter connected to a 5-m autotracking antenna. The station is capable of fully saturating any domestic Ku-band transponder.

The transmitted signal from Lewis can be received by ordinary low-cost, television receive-only satellite antennas equipped for Ku-band reception. These "dishes" are commonly found in the backyards of homes and at most larger business locations. The Earth terminal uses the same satellites that commonly carry cable television and live news feeds.

The Earth terminal can be used to demonstrate and prove new satellite communications technologies and to assist in transferring Lewis-

Lewis Ku-band Earth terminal facility.

developed technology to the commercial sector. For example, with minor modifications the Lewis station can be used for live satellite demonstrations of new satellite modulation techniques. The facility can be used in place of a satellite transponder simulator testbed to fully demonstrate and prove, over an actual satellite link, new developments in hardware. Collaborative experiments between Lewis and our customers may be accommodated over a live satellite link. Example uses may include networking experiments; high-low data rate modem development; video compression tests; and time-, frequency-, and code-division multiple access experiments.
In the near term the Earth terminal will be used on a part-time basis to support the U.S./Russian Telemedicine Spacebridge Project.

The Earth terminal is also connected to the laboratory-wide fiber optic system, permitting audio and video to be transmitted to a commercial Ku-band satellite from almost anywhere on the laboratory. Example uses would include the live transmission of symposia hosted by Lewis and U.S. distribution of NASA video programming.

Lewis contact: Michael A. Cauley, (216) 433–3483
Headquarters program office: OACT

High-Efficiency Ka-Band Traveling Wave Tube Being Developed for Cassini Mission

Several programs in place at NASA Lewis are focused on improving the efficiency of microwave traveling-wave-tube amplifiers (TWTA's) for space communications and other applications. A TWTA includes either a traveling wave tube (TWT) and its power supply or an electronic power conditioner. A low-power, high-efficiency TWTA operating in the Ka frequency band (32 GHz) is being developed in a cooperative and contractual arrangement between NASA Lewis and the Electron Dynamics Division of Hughes Aircraft Company for application to the Cassini mission. The Jet Propulsion Laboratory (JPL) is responsible for that mission, planned for launch to the environment of Saturn in 1997.

To meet JPL's requirements for Cassini, the TWTA must produce 10 W of radiofrequency power although the direct-current input power from the spacecraft is limited to approximately 30 W. Achieving that performance goal, more than doubling the efficiency of available Ka-band TWTA's at this power level, will permit the transmission to Earth of all the data produced in the mission. To accomplish the required efficiency increase, several Lewis-developed technologies, including computer-aided advanced designs of the helix and the multistage depressed collector (MDC) along with suppression of secondary electron emission from the MDC electrode, were incorporated into the TWT design. More specifically, the helix for the TWT's radiofrequency-interaction output section was designed at NASA Lewis to include an advanced dynamic velocity taper. This "tapering" is a continuous, nonlinear reduction in helix pitch with output section length. It slows the circuit wave and enhances synchronization between the circuit wave and the electron beam. The MDC design, also performed at Lewis, predicted spent-beam electron trajectories to identify effective electrode geometries and spacings. It uniquely includes the effects of the secondary electron emission characteristics of the electrode surfaces. Further, the MDC employs oxygen-free, high-conductivity copper electrodes that are treated at NASA Lewis for secondary electron emission suppression by means of an in-house-developed ion-bombardment process.

A TWT fabricated in this program is to be used directly as the flight tube for Cassini. The electronic power conditioner (EPC) is to serve as the immediate predecessor to the flight power supply. In coordination with JPL, the TWT and EPC flight packaging requirements and environmental

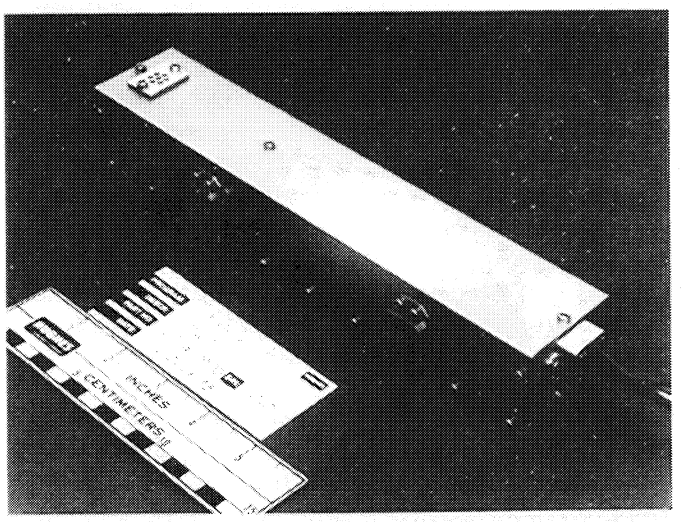

Engineering-model Ka-band TWT in flight configuration.

testing procedures have been specified and are being implemented. An engineering-model TWT meeting JPL's requirements has been fabricated and successfully operated for over 4500 hr in performance testing. The tube has been packaged in flight configuration. Following further evaluation it will be integrated with the engineering-model EPC developed in the program, and the resulting TWTA will be subjected to full environmental testing, including thermal-vacuum, vibration, and pyroshock studies.

A candidate flight-model TWT also meeting the Cassini mission requirements has been fabricated and is presently being evaluated. That tube produces 10.47 W of radiofrequency output power at saturation with 40.62-dB gain. To ensure program success, at least two more flight candidate TWT's are planned to be fabricated in the program. The current schedule requires the engineering-model TWT and EPC to be fully qualification tested and delivered to JPL in March 1994.

Reference

1. Curren, A.; et al.: A Low-Power, High-Efficiency Ka-Band TWTA. AIAA Paper 92–1822, 1992.

Lewis contact: Arthur N. Curren, (216) 433–3519
Headquarters program office: OACT

Multichannel Error-Correcting-Code Decoder Implemented

NASA Lewis has an ongoing program in modulation and coding and onboard processing and switching. Since 1990 we have been investigating various meshed very-small-aperture terminal (VSAT) architectures that utilize onboard-processing technology. Multichannel demultiplexers, time-shared multirate demodulators, and high-speed codecs have been developed under contract in support of the mesh VSAT architectures. A key element of this regenerative satellite architecture that has been neglected to date is the development of a time-shared decoder.

NASA Lewis is proceeding with a project to incorporate a time-shared decoder into the mesh VSAT onboard-processing architecture. The primary goal is to demonstrate a time-shared decoder for a regenerative satellite using asynchronous frequency-division multiple access uplink channels, thereby identifying hardware and power requirements and fault-tolerance issues that must be addressed in an operational system. A secondary goal is to integrate and test, in a system environment, two NASA-sponsored proof-of-concept hardware deliverables: the Harris high-speed Bose-Chaudhuri-Hocquenghem codec and the TRW multichannel demultiplexer/demodulator. A beneficial byproduct of this project is the development of flexible, multichannel, uplink signal-generation equipment.

The system consists of a bit-error-rate test set, uplink signal-generation equipment, a multichannel demultiplexer/demodulator including radiofrequency link simulation equipment, and the time-shared decoder.

The bit-error-rate, off-the-shelf test set can generate pseudorandom data at approximately 64 kbps. The uplink signal-generation equipment consists of a multichannel error-correcting-code encoder card, four digital modulator cards, a digital combiner and upconverter unit, and clock and mixing signal-generation cards. The

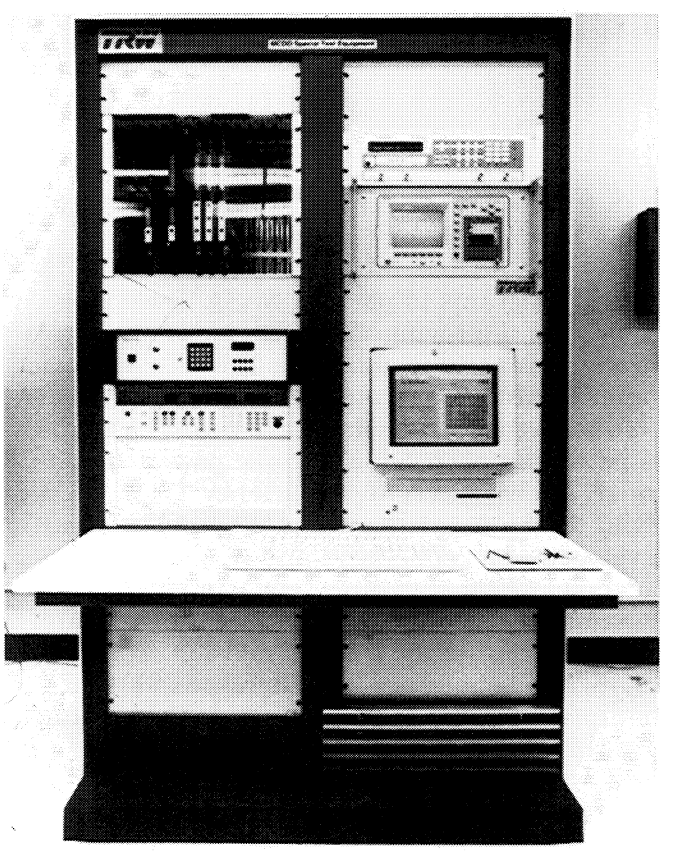

Time-shared decoder and system testbed.

multichannel demultiplexer/demodulator and the radiofrequency link simulation equipment were developed under a contract with TRW. The latter provides the calibrated noise generation. The former channels and demodulates either 2.084 Mbps or 64 kbps spectrally shaped offset-quadrature-phase-shift-keyed signals.

The time-shared decoder, which was implemented by using commercial parts, consists of a unique-word detector card, an encoder block-builder card, a multichannel error-correcting-code decoder card, and a data-switch interface card. The unique-word detector card identifies the beginning of data packets for each of 32 channels and notifies the encoder block-builder card (BLK) when a block has been identified and in which channel that block resides. The BLK builds up each block for 32 separate channels and notifies the multichannel error-correcting-code decoder card (MED) when a full block of data is available for decoding and in which channel it resides. The MED decodes individual blocks in a time-shared manner, stores the decoded blocks and channel identifiers, and notifies the data-switch interface card (DSI) of available channels. The DSI synchronizes the blocks so that all have headers and passes these on to the switch. For bit-error-rate testing the DSI outputs a selected channel's data and clock to the BER test set. A time-shared decoder capable of decoding 32 simultaneous asynchronous frequency-division multiple access channels could be implemented with a custom application-specific integrated circuit, two small dual-port random-access memories, and a codec chip residing in a multichip module.

Testing will be performed to verify operation of the multichannel error-correcting-code decoder card and to characterize the information channels through the multichannel demultiplexer/demodulator at various signal-to-noise levels with and without adjacent channel interference.

Lewis contact: William D. Ivancic, (216) 433–3494
Headquarters program office: OACT

Multichannel Demultiplexer/Demodulator Developed for Future Satellite Communications Systems

NASA Lewis has an ongoing program in advanced satellite communications architectures, onboard processing, and technology development. Studies have indicated that meshed very-small-aperture terminal (VSAT) satellite communications networks utilizing frequency-division multiple access uplinks and time-division multiplexed downlinks are required to meet future communications needs. A critical satellite technology in such a network is a multichannel demultiplexer/demodulator (MCDD).

TRW Electronic Systems Group has completed contract NAS3–25866 to develop a proof-of-concept MCDD model using advanced digital technologies. This model demonstrates the capability of demultiplexing and demodulating multiple low- to medium-data-rate frequency-division multiple access uplinks with potential for expansion to hundreds or thousands of narrowband uplinks. The TRW approach uses baseband sampling followed by successive wideband and narrowband channelizers. Each channelizer feeds into a multirate, time-shared demodulator. A full-scale MCDD would consist of an eight-bit, analog-to-digital converter sampling at 92.16 MHz, four wideband channelizers capable of demultiplexing eight wideband channels, 32 narrowband channelizers capable of demultiplexing one wideband signal into 32 narrowband channels, and 32 multirate demodulators. The proof-of-concept model consists of an eight-bit, analog-to-digital converter sampling at 23.04 MHz, one wideband channelizer, 16 narrowband channelizers, and three multirate demodulators.

The demultiplexing is done with polyphase filtering techniques. This channelizer is implemented as a time-domain fast Fourier transform in a wideband/narrowband cascade. The algorithm processes the data in the time domain by windowing and presumming followed by a single fast Fourier transform to heterodyne the signal. This technique optimizes the use of hardware to realize a parallel bank of filters. The window/presumming function has been implemented in an application-specific integrated circuit as this function is repeated throughout the design.

A group of multirate, time-shared demodulators follow the channelizer and can demodulate either one 2.048-Mbps channel or thirty-two 64-kbps channels. The modulation format is filtered offset-quadrature-phase-shift keying such that a 64-kbps channel resides in a 45-kHz bandwidth and a 2.048-MHz channel resides in a 1.44-MHz bandwidth. The implementation loss at a ratio

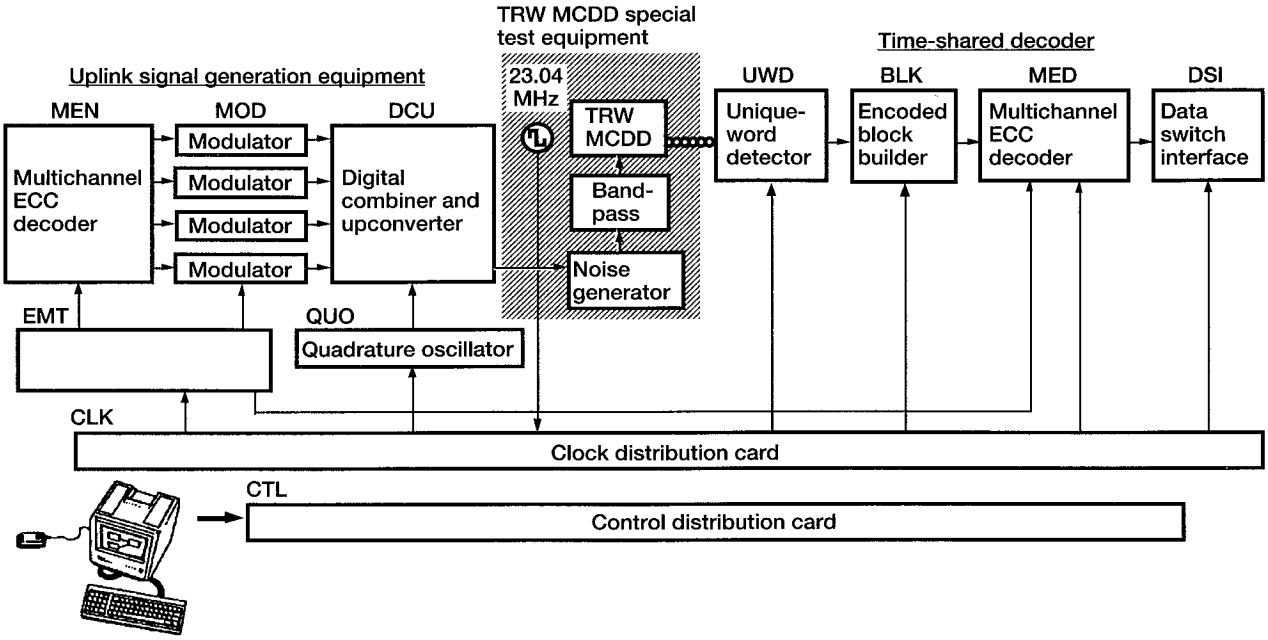

Digitally implemented MCDD and special test equipment.

of energy per bit to noise power of 10^{-7} is 0.3 dB for the 2.048-Mbps processed channels and 0.75 dB for the 64-kbps channels.

There are a number of advantages to the digitally implemented MCDD:

- Only one MCDD is required for both the wideband and narrowband channels.
- The modulation format can be changed simply by changing the lookup tables in the derotation circuitry of the demodulator.
- The demodulator can handle asynchronous users because each channel maintains its own symbol, carrier, and phase offsets.
- There is a potential to condense the design down to a few chips by using custom very-large-scale integration design and multichip module packaging.

Future work includes improving the packaging and addressing the many fault-tolerance issues within both the demultiplexing and demodulation functions.

Lewis contact: William D. Ivancic, (216) 433–3494
Headquarters program office: OACT

Hi-LITE Prototype Demonstrated for Free-Space Optical Communications

High-Speed Laser Integrated Terminal Electronics (Hi-LITE) is the communications electronics portion of a free-space optical communications program. Laser communications offer data capacity and efficiency improvements over existing radio-frequency communications. The Hi-LITE Project has successfully demonstrated prototype hardware and its high-data-rate capabilities, which may be used to link future constellations of satellites in low Earth orbits with relay satellites in geostationary orbits and with deep-space planetary probes. The Hi-LITE system consists of a modulator/demodulator (modem), video and test data equipment, satellite simulation equipment, and the control and monitoring computer. Signals between the modulator and the demodulator are transmitted optically by a laser link.

This prototype modem was constructed at NASA Lewis with discrete high-speed components mounted on 22 special circuit boards housed in three chassis. This prototype design has been collapsed down to one digital application-specific integrated circuit design, one analog hybrid circuit board design, and technology to incorporate the attributes required for flight-qualifiable size, mass, and power consumption.

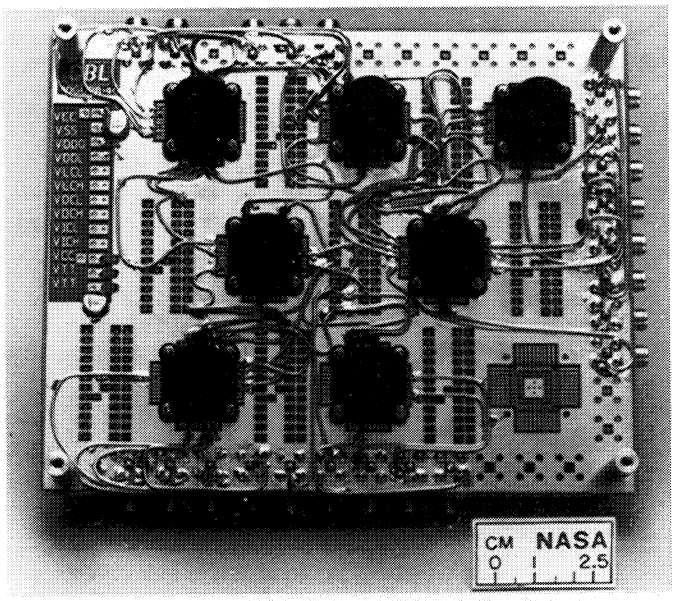

Typical Hi-LITE circuit board.

The modem is capable of transmitting and receiving data at 650 Mbps. Transmitting 650 Mbps is equivalent to transmitting 8.9 volumes of the Encyclopedia Britannica every second. At these data rates digital logic design takes on aspects of radiofrequency circuit design, where interconnection of signals is subject to transmission line considerations. Special circuit boards were used for the gallium arsenide (GaAs) digital integrated circuits, chip resistors, chip capacitors, and semirigid coaxial cables in much of the Hi-LITE subsystem fabrication. This careful attention to circuit design has proven successful, as shown in the modem's 1-dB-from-optimal, bit-error-rate performance.

The modem has three different modes of operation: single 650-Mbps data, dual 325-Mbps data, and interleaved 325-Mbps data. The dual 325-Mbps mode allows both video and test data to be sent simultaneously; interleaving the two 325-Mbps channels allows quantitative testing of video data. Regardless of the mode or data source, the Hi-LITE modem needs no special data patterns or unique words in the data stream to synchronize the demodulator, as is commonly required with other systems.

The laser, the optical detector, and other associated optical equipment were provided by Goddard Space Flight Center. Turned off and on by the modulated digital data stream, the high-power, high-bandwidth laser sends infrared light pulses through the air to the detector, an avalanche photodiode (APD). The APD converts the optical pulse back to an electrical signal for the demodulator. Degradations in an actual space-based laser link due to the much longer distances are simulated with optical attenuators placed between the laser and the APD. Other degradations are provided with the satellite simulation equipment.

All of the satellite simulation equipment, as well as the modem and laser link, are controlled and monitored by a computer. This allows for a user-friendly interface, automated testing, and performance data collection.

Lewis contact: James M. Budinger, (216) 433–3496
Headquarters program office: OACT

Intelligent Assistant Used for Satellite Earth Terminal Operations

NASA Lewis has incorporated artificial intelligence (AI) technology into an advanced Earth terminal to simplify the maintenance, use, training, and documentation of Earth terminal hardware and software systems. The AI techniques are currently being used as an experimenter interface to the link evaluation terminal (LET) and have been named "space communications artificial intelligence for the link evaluation terminal" (or SCAILET).

The advanced high-burst-rate (HBR) LET Earth terminal can transmit 220 Mbps of data at 30-GHz uplink frequency and 20-GHz downlink frequency. The HBR–LET terminal has seven major subsystems. A minicomputer controls and monitors these subsystems through IEEE–488 and RS–232 protocol interfaces. Test procedures, defined by design and test engineers, configure the HBR–LET for proper operation and data acquisition. However, the procedures are difficult to use and maintain and require a steep learning curve, discouraging experimenters from using the full capabilities of the HBR–LET system.

The primary component of SCAILET is an intelligent assistant module. The intelligent assistant replaces the cryptic programming procedures with a high-level, English-based command language. Expert system technology is used to check

for possible constraint violations in all stages of experiment design. The intelligent assistant's graphical interface was developed by using the ToolBook windows application development environment. An expert system shell (KAPPA PC) monitors all activity in the background and communicates with ToolBook through a dynamic data exchange protocol. In addition, the intelligent assistant is linked to the minicomputer by a custom communications link through the RS–232 protocol. SCAILET displays experimental results in easy-to-understand dynamic graphics.

As a part of the SCAILET Project a multimedia reference manual was developed to provide an on-line documentation resource for the experimenter. By applying multimedia, experimenters can find information quickly, without being overwhelmed by the nonuniform and vast amount of the HBR–LET design documentation.

Finally, AI software has been developed to provide fast and accurate satellite commands for configuring the HBR communications channels aboard the Advanced Communications Technology (ACTS) satellite. Previously, commands were generated by hand, requiring data lookup and command construction involving long tedious number conversions between decimal, binary, and hexadecimal. With the command generation software all the necessary data can be selected and automatically assembled into commands at the click of a few buttons. The software uses object-oriented programming style to intelligently analyze user input and to verify that requested configurations do not violate HBR programming constraints. Generated commands are stored in well-commented American Standard Code for Information Interchange (ASCII) files until they are transmitted to the digital control unit onboard ACTS. The software can also read and analyze previously generated command files.

For demonstration purposes a floppy diskette has been developed that describes many SCAILET functions in a "tour" type of format. This tour is designed primarily to familiarize potential experimenters with the general capabilities of SCAILET. A copy of the diskette can be obtained by anyone interested.

Lewis contact: Edward J. Petrik, (216) 433–3493
Headquarters program office: OACT

Monolithic Microwave and Millimeter-Wave Integrated Circuit Packaging Reaches Market

High-frequency integrated circuits will play a critical role in the advanced communications systems of the future. To ensure that these small, fragile circuits move successfully from the laboratory environment to real-world systems, NASA Lewis has been developing advanced packaging technology through a technically aggressive research-and-development program. The program focuses on monolithic microwave and millimeter-wave integrated circuits (MMIC's) operating in the 18- to 44-GHz frequency range—the key elements in electronically steered antennas. The packages are designed to withstand the challenging space environment of a communications satellite but are also directly applicable to a wide range of airborne and terrestrial systems.

An MMIC package was developed under contract by Hughes Aircraft Company. In addition to providing mechanical protection for the MMIC device, the package offers full hermeticity, heat removal from the device, and low electrical losses (<1.5 dB) through 44 GHz. The 0.28- by 0.28- by 0.05-in. package is constructed of high-purity ceramic with a metal lid and base. Radio-frequency signals enter and exit the package through impedance-matched hermetic seals at opposite ends of the package. Ten bias and control lines are provided along the sides of the package. Its flexibility allows the package to be refitted for a different MMIC by modifying only one of its four layers.

The single-chip package has moved rapidly from a research component to a marketable product. Estimates place the cost of a typical package at less than $20 for small quantities, with substantial savings under mass production.

A second packaging effort is examining the feasibility of multielement or multicircuit packages as they would be applied to advanced phased-array antenna systems. This approach permits several MMIC's to be placed in close proximity to one another in a single package to achieve the tight spacing required between the radiating elements of an antenna. Each MMIC is installed in an individual compartment to eliminate crosstalk between chips and to suppress electrical moding. An application-specific integrated circuit (ASIC) is included in the package to demultiplex a single serial data stream and thereby reduce the

MMIC package.

number of interconnect lines sent from a system controller. The ASIC and the radiofrequency MMIC's are joined through multilayer interconnects located below the radiofrequency ground plane. This technique has permitted greatly increased packaging density to be achieved.

The ongoing program will examine the performance of both single- and multichip packages when operated in relevant space and aircraft environments. Additionally, emerging technologies such as fiber optics, multilayer high-density interconnects, and self-correcting system-level integrated circuits are being developed for integration into antenna packaging. Space qualification testing of this and related packages is being funded by the Headquarters Office of Safety and Mission Assurance.

Lewis contact: Kurt A. Shalkhauser, (216) 433–3452
Headquarters program office: OACT

High Secondary Electron Emission From Diamond Films Applied to Devices

NASA Lewis recently reported secondary electron emission yields σ as high as 27 from diamond thin films grown by chemical vapor deposition and deposited onto molybdenum. (σ is the number of secondary electrons produced by each primary electron.) Hydrogen termination of the diamond surface is responsible for this high number. (High-yield materials used in electronic devices usually have a secondary yield of not more than 3.) We are currently pursuing device applications utilizing this high secondary electron emission property of diamond. The possible applications include electron multiplier tubes, channeltrons, channelplates (night vision devices), secondary emission cathodes, crossed-field amplifiers, gated-emission amplifiers, and magnetrons.

We have constructed a prototype electron multiplier for operation in ultrahigh vacuum with eight diamond/molybdenum dynodes. The multiplier operates in a constant partial pressure of hydrogen to maintain the high secondary electron yield. Initial measurements indicate possible gains significantly higher than those of existing electron multipliers.

We are concurrently investigating other substrate materials, such as palladium, that naturally store hydrogen. The hydrogen can be delivered to the diamond surface from the bulk of the substrate upon heating. Our initial measurements while heating the sample show constant yields as high as 25 during continuous electron exposure, with maximum yields of 45.

It is difficult to underestimate the importance of a material with such a high secondary electron yield, particularly a material like a diamond film, which is relatively easy to manufacture and which has outstanding physical properties. Although the use of large, cleaved, single-crystal diamond surfaces is hardly viable for many applications, the technology is now available for growing epitaxial oriented films of diamond on suitable substrates. Various chemical vapor deposition methods for synthesizing polycrystalline diamond have been developed successfully over the past 13 years. The ability to produce a diamond film with such high secondary electron emission yield may turn a new page in improving a variety of devices.

Lewis contact: Dr. Isay L. Krainsky, (216) 433–3509
Headquarters program office: OACT

Space Flight Systems

Nuclear Propulsion

NEPTool Provides End-to-End System Modeling Capability for Nuclear Electric Propulsion

The ongoing study at NASA Lewis of advanced propulsion systems, such as nuclear electric propulsion, for potential human exploration and robotic space science missions requires preeminence in design, modeling, and analysis of these systems. NASA Lewis has therefore begun an effort to develop an end-to-end system modeling and analysis capability, or analysis tool, for nuclear electric propulsion (NEP). A test case model has been developed that utilizes a separately available Unix-workstation-based modeling environment called General Purpose Simulator (GPS) authored and maintained by the Department of Energy's Argonne National Laboratory (ref. 1). This preliminary, system-level model will help potential users investigate the feature of the analysis tool.

GPS is a system simulation architecture and control code for steady-state or transient system representation. It has object-oriented control language with numerous procedures for optimizations, equation solving, system constraints, and parametric analysis. GPS is written in C language and is designed for modern workstation environments. GPS is enhanced by GPSTool, a graphical user interface tool providing "point and click" creation and control of simulations, including component selection for insertion, deletion, or rearrangement, parameter changes, and "drag and drop" loading of input files.

The technical starting point for developing the desired analysis tool was a number of separate stand-alone FORTRAN codes that model the major subsystems inherent to an NEP system. Subsystem models had been previously developed by the Oak Ridge National Laboratory for the reactor (ref. 2); by the Rocketdyne Division of Rockwell International for power conversion, heat rejection, and power management and distribution (refs. 3 to 6); and by Sverdrup Technology for the thrusters (ref. 7). At least two inherently different technology options were modeled for each subsystem.

The desired product for the near term is a tool that will provide for quick, detailed prototyping of an NEP system comprising a pin type of reactor, Brayton power conversion, pumped-loop heat rejection, and ion electric propulsion. Such a model would allow for performance (mass or radiator area) to be analyzed against such primary system parameters as bus electric power, reactor-payload separation distance, and thruster specific impulse, as well as against such secondary system parameters as Brayton heat engine pressure ratio, compressor inlet temperature, and transmission voltage and frequency. The tool would be able to optimize (minimize) that mass (or radiator area) versus these parameters. Such a tool should reduce the analysis time required to create parametric performance curves from as much as 1/2 hr (of analyst's time) per data point to mere seconds (the time it takes for a Unix workstation to respond to the touch of a single keystroke); see reference 8.

The current test case model is a somewhat simplified representation of an NEP system. It is made up of NASA Lewis' ion engine electric propulsion model (ref. 7) and a thermionic reactor model previously created by Argonne National Laboratory. The ion engine model will perform design calculations to yield total number of thrusters, thrust per unit engine, and total thruster subsystem mass versus input electric power and desired output specific impulse. The thermionic model provides just the user-desired input electric power.

References

1. Geyer, H.K.: GPS—A Postscript-like Language for System Simulation. Report AL-TR-90-085, Aerojet Strategic Propulsion Co., Sacramento, CA, Jan. 1991.

2. Difilippo, F.C.: Scoping Calculations of Power Sources for Nuclear Electric Propulsion. NASA CR-191133, 1994.

3. Johnson, G.A.: Potassium-Rankine Power Conversion for Nuclear Electric Propulsion. NASA CR-191134, 1994.

4. Ashe, T.; and Otting, W.: Brayton Power Conversion System Parametric Design Modeling for Nuclear Electric Propulsion. NASA CR-191135, 1994.

5. Moriarty, M.P.: Heat Pipe Cooled Heat Rejection Subsystem Modeling for Nuclear Electric Propulsion Systems. NASA CR-191132, 1994.

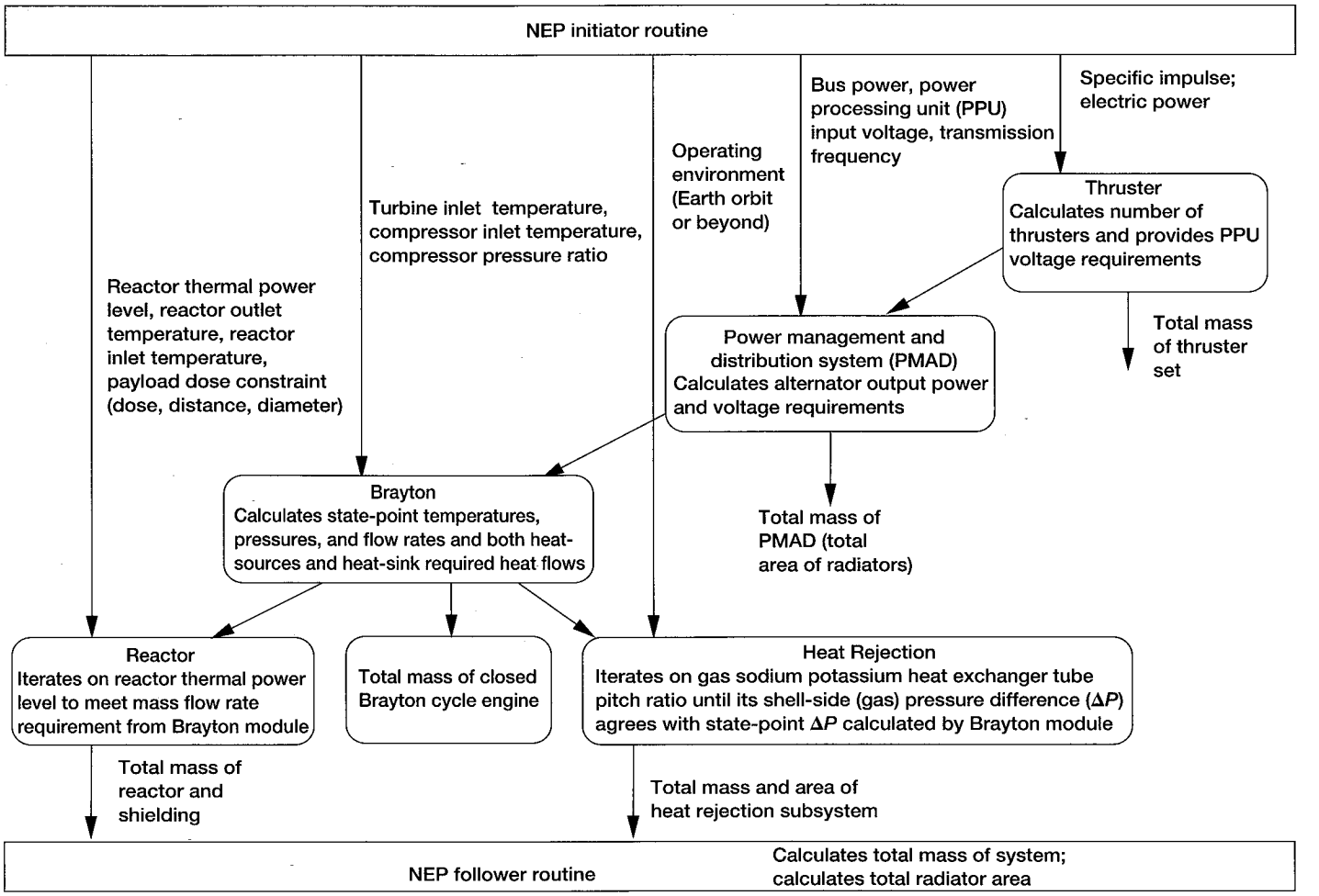

NEPTool data flow for ion engine system model.

6. Metcalf, K.J.: Power Conditioning System Modeling for Nuclear Electric Propulsion. NASA CR–191136, 1994.

7. Gilland, J.H.: Megawatt Electric Propulsion Thruster Modeling. NASA CR–191137, 1994.

8. Doherty, M.P.: Utilization of Recently Developed Codes for High Power Brayton and Rankine Cycle Power Systems. NASA CP–10122, 1993.

Lewis contacts: Michael P. Doherty, (216) 433–6641; Jeffrey A. George, (216) 977–7108
Headquarters program office: OACT

Space Experiments

Surface-Tension-Driven Convection Experiment Prepares for Reflight

Surface tension causes liquid to form a spherical shape if the liquid is contained in extremely small areas, such as capillary tubes, or is no longer subjected to gravity forces, such as in free-fall. Variation in surface tension can cause convection to occur within a liquid. Colder liquid, with higher surface tension, will pull warmer liquid, with lower surface tension, which in turn will pull bulk liquid up to the surface. These thermocapillary flows were studied in the Surface-Tension-Driven Convection Experiment (STDCE), which was planned by the principal investigators from Case Western Reserve University (CWRU), Simon Ostrach and Yasuhiro Kamotani.

The STDCE flight hardware was designed and built at NASA Lewis for integration into a Spacelab rack on the USML–1 mission, which flew on STS–50 in June 1992. A cylindrical test cell, 10 cm in diameter and 5 cm deep, was filled on-orbit with 10-cSt silicone oil, creating either a flat or curved free surface. The surface was centrally heated either internally with a cartridge or externally with a laser. The flows were measured by particle image velocimetry using a laser light sheet and a video camera to record light scattered from particles dispersed in the oil. Oil surface temperatures were measured with an infrared scanning imager.

Over 12.5 hr of video and digital data were obtained from the 38 tests conducted during USML–1. Steady-state data were analyzed and showed good agreement with the CWRU thermocapillary model's computer calculations. Their theory predicted that, even though the critical Marangoni number was exceeded, no oscillations would occur because the test cell was too large and the silicone oil too viscous. The STDCE results were presented in Huntsville, Alabama, in September 1993.

A second experiment, STDCE–2, received approval in December 1992 and will be conducted on the USML–2 mission in September 1995. This reflight required design changes to accommodate smaller test cells (diameters of 1.2, 2.0, and 3.0 cm) and 2-cSt silicone oil located in six interchangeable test modules. A significant event during 1993 was the successful critical design review held in September. The STDCE design team with "their ingenuity, competence, and experience has led to the brilliant design of a complex experimental apparatus and diagnostics and control systems," according to the assessment of Simon Ostrach.

New optics developed for STDCE–2 include

- The free-surface deformation measurement system, a single-channel Ronchi method for determining surface slopes from 5 to 30 μm/mm
- The three-dimensional flow visualization system
- An infrared telescope for the infrared imager

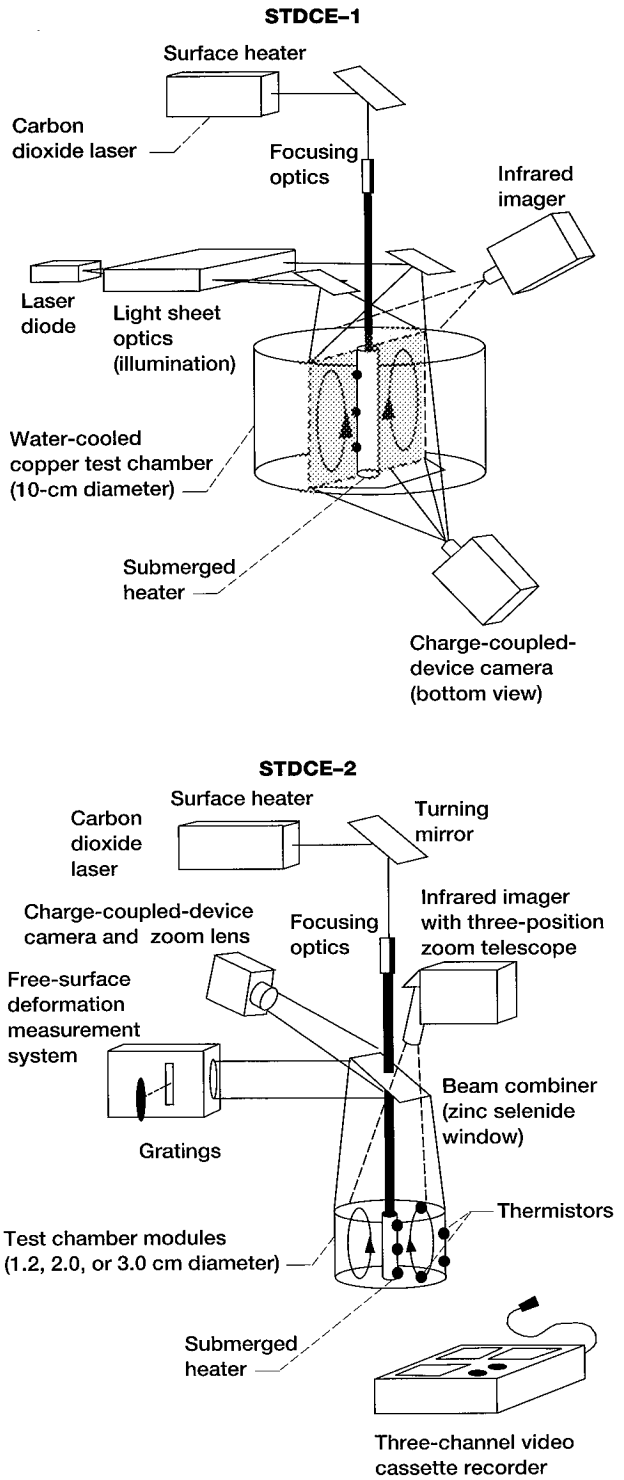

Comparison of STDCE–1 and STDCE–2.

- Changes to the carbon dioxide laser focus to produce smaller heating zones (0.5 to 6 mm)

Modifications were also made to the design of the experiment's front panel so that the crew can change out test modules and make grating changes during tests to optimize the free-surface deformation measurements. Also, electrical and software systems were modified to accommodate the new crew interactions (about 70 hr on-orbit), the new three-deck video cassette recorder, and lessons learned from USML–1.

Bibliography

Kamotani, Y.; and Ostrach, S.: Design of a Thermocapillary Flow Experiment in Reduced Gravity, J. Thermophys. Heat Transfer, vol. 1, no. 1, Jan. 1987, pp. 83–89.

Ostrach, S.: Surface-Tension Gradient Induced Flows at Reduced Gravity. NASA CR–159799, 1980.

Pline, A.D.; and Butcher, R.L.: Spacelab Qualified Infrared Imager for Microgravity Science Applications. Thermosense XII: Proceedings of the International Conference on Thermal Sensing and Imaging Diagnostic Applications, S.A. Semanovich, ed., SPIE Proceedings, Vol. 1313, SPIE, Bellingham, WA, 1990, pp. 250–258.

Pline, A.D.; et al.: Surface Tension Driven Convection Experiment. AIAA Paper 93–4312, 1993.

Pline, A.D.; et al.: Hardware Development for the Surface Tension Driven Convection Experiment. J. Spacecraft Rockets, vol. 27, no. 3, May-June 1989, pp. 312–317.

Wernet, M.P.; and Pline, A.D.: Particle Image Velocimetry for the Surface Tension Driven Convection Experiment Using a Particle Displacement Tracking Technique. NASA TM–104482, 1991.

Lewis contacts: Alexander D. Pline, (216) 433–6614; Thomas P. Jacobson, (216) 433–2872; Robert L. Zurawski, (216) 433–3932
Headquarters program office: OLSMA

Space Acceleration Measurement System To Fly on *Mir*

Everyone on Earth is familiar with the effects of gravity by the simple fact that if gravity were to suddenly disappear, everything on Earth would start to float. Gravity is the force that holds everything on the Earth. The effects of gravity are greatly reduced aboard a spacecraft that is orbiting the Earth, and for this reason astronauts and other objects float inside the spacecraft. The purpose of the Space Acceleration Measurement System (SAMS) is to measure and record the very low levels of gravity and other forces that can exist aboard the spacecraft. Scientists need to know the levels of these forces during the time that their experiments are being performed. If unexpected results occur, the scientists can determine if these results were caused by a disturbance or if they were the product of the experiment. The data can also help scientists to plan the location of an experiment if the experiment is sensitive to certain types of disturbances.

The SAMS instrumentation has flown seven times aboard shuttles. The units have flown once in the middeck, four times in the Spacelab module, once in the cargo bay, and once in the Spacehab module. On six of the missions the SAMS units only recorded data. On the mission where SAMS flew in the cargo bay, the two units not only recorded data but also downlinked data during the mission. The downlinked data proved to be a very valuable asset to the scientists because their entire science objectives were completed when it was determined that disturbances were much lower than anticipated, and the experiment was operated continuously rather than intermittently.

The SAMS units were designed, fabricated, assembled, and tested by a team that consisted of NASA Lewis employees and a support service contractor. SAMS units flew on two missions in 1991, four missions in 1992, and one mission in 1993, and four units have been delivered for flights in 1994. The SAMS team is also preparing one unit to be delivered to Russia early in 1994 to be flown aboard the *Mir* space station. By measuring and recording the microgravity and disturbance levels, it is anticipated that the SAMS unit will assist in locating experiments aboard *Mir*.

Bibliography

Baugher, C.R.; Martin, G.L.; and Delombard, R.: Review of Shuttle Vibration Environment. AIAA Paper 93–0832, 1993.

Baugher, C.R.; Martin, G.L. and DeLombard, R.: Low-Frequency Vibration Environment for Five Shuttle Missions. NASA TM–106059, 1993. (Also AIAA Paper 93–0832, 1993.)

DeLombard, R.: Proposed Ground-Based Control of Accelerometer on Space Station *Freedom*. NASA TM–105960, 1993.

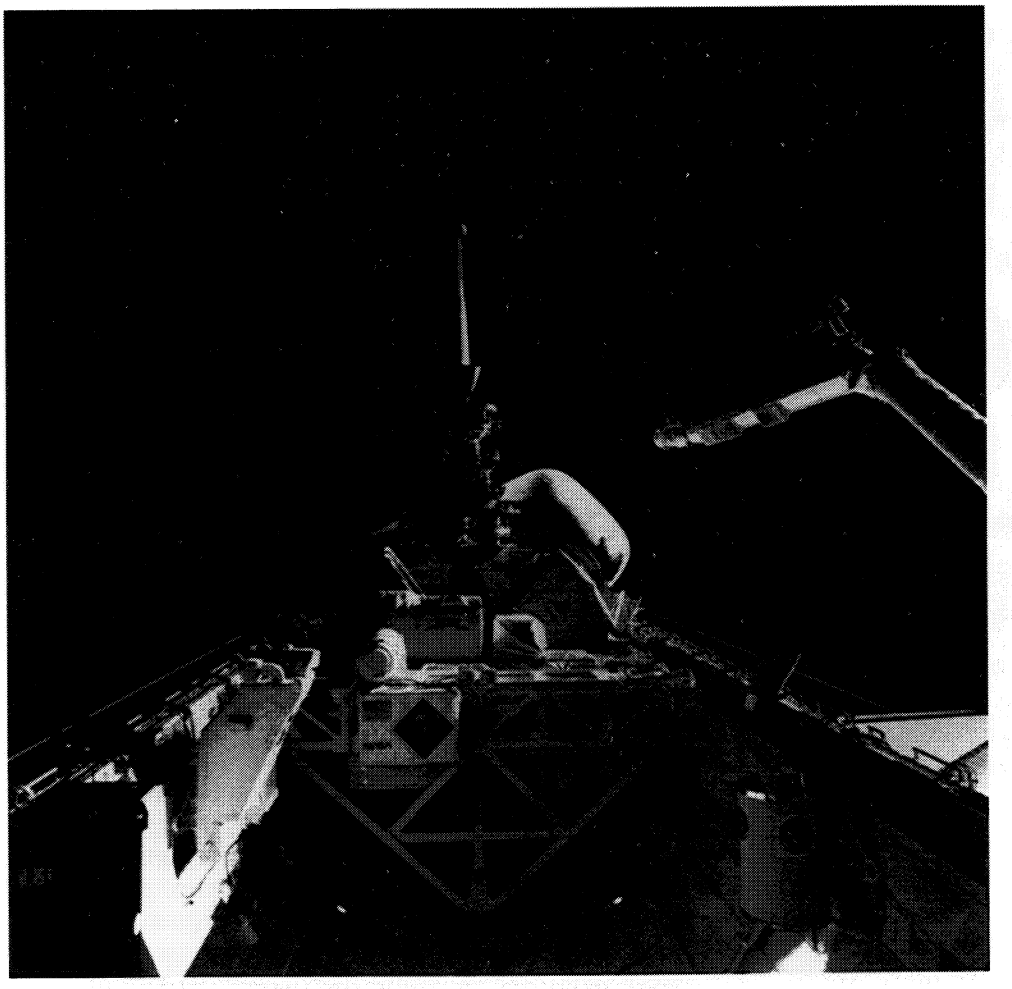

SAMS unit in cargo bay of shuttle. The unit has the American flag and the USMP–1 logo.

Rogers, M.J.B.; et al.: Low Gravity Environment On-Board Columbia During STS–40. AIAA Paper 93–0833, 1993.

Lewis contact: Richard DeLombard, (216) 433–5285
Headquarters program office: OLMSA

Advanced Diagnostic Instrumentation Enhances Combustion Science in Microgravity

The success of combustion experiments in microgravity, whether performed in space or in drop towers and aircraft, is critically dependent on the availability of diagnostic systems for collecting the required scientific data. Until recently, instrumentation was severely limited, consisting primarily of motion pictures and intrusive temperature and velocity probes, such as thermocouples and hot-wire anemometers. Flames in microgravity can be much less vigorous than on Earth and therefore highly susceptible to effects from intrusive probes.

Recently, several nonintrusive or less perturbing probes have been identified, built, and tested in-house at NASA Lewis. Most are based on optical methods, which are also well suited to the acquisition of multidimensional data. Such "full field" measurements are important in microgravity combustion science because fundamental length and time scales and dominating physical mechanisms have not yet been verified.

Because flames in microgravity are often only weakly luminous, there is a strong need for qualitative flame and flow visualization. High-photon-gain, solid-state imaging devices, identified by Dr. Karen Weiland of NASA Lewis, were successfully used aboard the NASA KC–135 aircraft to observe in microgravity the near-infrared

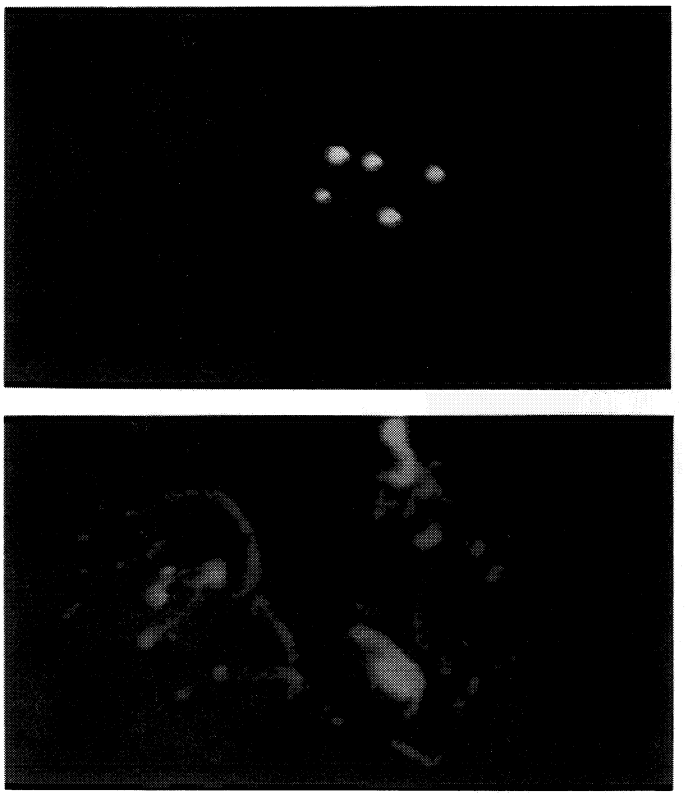

Flame balls (above) and cylinders (below) in reduced gravity aboard KC–135 aircraft.

emission of water produced from premixed hydrogen flames. The emission was heretofore unobservable without chemical dopants. In this testing new flame structures, now known as flame balls and flame strings or cylinders, were discovered by Professor Paul Ronney of the University of Southern California. These imaging devices are now part of his developing space experiment on the structure of flame balls. A similar device, imaging OH emissions in the ultraviolet spectrum, is also now being planned for a space experiment in droplet combustion.

A rainbow schlieren deflectometer (RSD), developed in-house at NASA Lewis, demonstrated a sensitivity exceeding that of conventional interferometric techniques while allowing for far greater mechanical simplicity and durability. An RSD to determine liquid temperatures was tested successfully in the laboratory and is now part of a rocket-based, microgravity experiment in flame spread over liquid fuel pools. Kurt Sacksteder of NASA Lewis flew a similar RSD on the KC–135 aircraft and successfully visualized gas-phase flow structures, heretofore unsuspected and unobserved, ahead of a partial-gravity flame spreading across a solid fuel.

Perhaps most importantly, progress was made in characterizing soot size distributions and soot concentrations (particle number density) in microgravity gas-jet diffusion flames. Soot is a primary contributor to radiant heating in commercial furnaces but also is a known fouling agent in other devices. It is also implicated as a major pollutant on Earth. The processes in which soot forms, grows, aggregates, and oxidizes are not well known, in part because of intrusions of buoyancy on Earth. In microgravity much longer soot "residence times" are available, and it is expected that these studies will yield valuable information about soot processes.

Two soot-measuring devices were successfully demonstrated in the NASA Lewis drop towers by Paul Greenberg of NASA Lewis, Dr. DeVon Griffin of Sverdrup Technology, Inc. (Lewis Research Center Group), and Professor Jerry Ku of Wayne State University. Thermophoretic sampling in a gas-jet diffusion flame collected small soot samples that were then analyzed through transmission electron microscopy. Primary sizes and aggregates of soot in microgravity were shown to be significantly larger than in Earth gravity. Similarly, laser light extinction field measurements were used to determine the two-dimensional particle number densities. Both techniques are now in active development for several spaceflight experiments in microgravity.

Bibliography

Griffin, D.W.; and Greenberg, P.S.: Selected Microgravity Combustion Diagnostic Techniques. NASA CP–10113, 1993.

Ku, J.C.; et al.: Soot Formation and Radiation in Turbulent Jet Diffusion Flames Under Normal and Reduced Gravity Conditions. NASA CP–10113, 1993.

Ross, H.D.; et al.: Flame Spread Across Liquid Pools. NASA CP–10113, 1993.

T'ien, J.S.; et al.: Combustion of Solid Fuel in Low Speed Oxygen Streams. NASA CP–10113, 1993.

Weiland, K.J.: Visualization and Imaging Methods for Flames in Microgravity. NASA CP–10113, 1993.

Lewis contact: Dr. Howard D. Ross, (216) 433–2562
Headquarters program office:

Experiments Simulate Low-Gravity Flame in Normal Gravity

An innovative approach to simulating a low-gravity (spacecraft) diffusion flame in normal gravity applies scaling laws and the similarity between buoyant and forced flow. The knowledge gained can be applied to new, more appropriate methods of evaluating the flammability of spacecraft materials in normal gravity. The diffusion flame structure and extinction characteristics are studied at an extremely low stretch rate, which is representative of a reduced-gravity environment. Both experimental and theoretical investigations are in their second year.

A low-gravity experiment would use a low forced flow to obtain the low stretch rate, but a normal-gravity experiment must use large radii of curvature to obtain low stretch, as the buoyant flow dominates for low forced flow velocities.

The code incorporates gas-phase as well as solid-phase radiation. Parametric studies determined the importance of radiant heat transfer from both the solid and gas phases. Theoretical modeling has focused on the effects of gas-phase and surface radiation on the energy balance of the flame at low stretch rates. Decreasing the stretch rate amplifies the radiation effects with respect to the other energy transfer mechanisms. Numerical simulation has shown that including radiation effects leads to lower temperature flames and extinction at higher stretch rates than would otherwise be the case. The interaction between gas-phase radiation and surface absorption and emission was found to have a strong effect on flame stability at low stretch.

In the experiment a normal-gravity simulation of a low-stretch-rate diffusion flame is generated by using a cylindrical fuel sample of large radii. The normal-gravity setup enables detailed measurements to be made, which are needed for flame structure studies (temperature, flow, species fields, radiative heat loss, and mass burning rate). The laboratory and burner/cage assembly were first developed and certified as safe. Experiments were then conducted that yielded the lowest burning rates obtained on Earth to date for large-radii-of-curvature solid fuel samples. Problems with solid-phase response times and dripping material hindered progress in the experiments. Flame structure probing is continuing.

Qualitative comparisons between experiment and theory show promise in that appropriate trends were predicted in both burning rate and temperature profiles. By detailed comparison between theory and experiment, the goal is to delineate the unique features of diffusion flames at low stretch rates, including the extinction mechanisms. This study, begun in 1992, is funded by the NASA Lewis Director's Discretionary Fund. A third-year funding request has been approved to continue the work. Ultimately, a space experiment will be proposed to verify the simulation. The space experiment will benefit from the normal-gravity work in that it can verify the simulation with fewer, simpler diagnostic measurements.

Bibliography

Rhatigan, J.; and T'ien, J.S.: Gas Phase Radiative Effects on the Burning of a Solid Fuel. Presented at Eastern States Section of the Combustion Institute Fall Technical Meeting, Oct. 1993.

Lewis contacts: Sandra L. Olson, (216) 433–2859; Jennifer Rhatigan, (216) 433–8330
Lewis Director's Discretionary Fund

Pool Boiling Experiment Has Successful Flights

The Pool Boiling Experiment is designed to improve understanding of the fundamental mechanisms that constitute nucleate pool boiling. Nucleate pool boiling is a process wherein a stagnant pool of liquid is in contact with a surface that can supply heat to the liquid. If the liquid absorbs enough heat, a vapor bubble can be formed. The same process occurs when a pot of water boils. The experiment will provide insight into the nucleate boiling process, which has many Earth-bound applications, such as steam-generation powerplants and petroleum and other chemical plants. Also, by studying the test fluid, R–113, some basic understanding of the boiling behavior of cryogenic fluids could be obtained without the large cost of an experiment using an actual cryogen.

The experiment was conceived by Dr. Herman Merte of the University of Michigan and developed by NASA Lewis. The project is supported by the

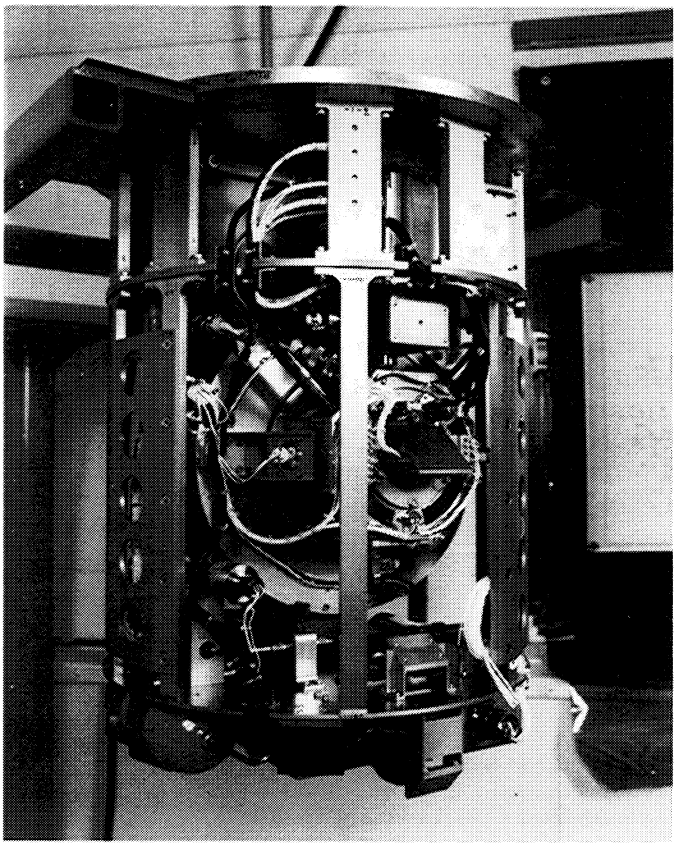

Pool Boiling Experiment.

NASA Headquarters Microgravity Science and Applications Division.

The pool boiling prototype system was initially flown on STS–47 in September 1992, where a considerable amount of scientific data was acquired. The expected boiling pattern was observed in all high-heat-flux cases, but a different pattern was observed in the low-heat-flux cases. These differences appear to be caused by the rewetting of the heater surface. The film data indicate that the saturated cases experienced a more activated boiling process (more vapor than expected was generated).

Some minor modifications were made in the timing sequences in the test matrix for the STS–57 flight. They increased the probability of observing the initial dynamic vapor bubble growth while the camera was running at the higher speed. They also allowed the influence of the stirrer on the active boiling process to be observed more extensively, including its effect on the dryout area, the mean heat transfer coefficient, and the nucleate boiling heat transfer coefficient.

Currently, results appear to indicate the potential for quasi-steady nucleate pool boiling taking place in long-term microgravity with certain combinations of heat flux levels and bulk liquid subcooling. These were the first experiments of nucleate boiling obtained for long periods of microgravity, and the matrix test conditions were selected in part to cover the reasonably broad range of parameters. It is anticipated that these results will provide guidance and direction for further experiments whose objectives would include determining the range of heat flux and subcooling that would ensure the prevention of heater surface dryout.

Lewis contact: Angel M. Otero, (216) 433–3878
Headquarters program office: OLMSA

Solid Surface Combustion Experiment Performs Well

The purpose of the Solid Surface Combustion Experiment (SSCE) is to study the physical and chemical mechanisms of flame spread over solid fuels in the absence of gravity-driven buoyant or externally imposed airflows. Because the controlling mechanisms of flame spread are different in low gravity than in normal gravity, the SSCE results have a practical application in evaluating spacecraft fire hazards. SSCE is the first combustion experiment to fly in the space shuttle and the first such experiment in the NASA spaceflight program since Skylab. It was conceived by Professor Robert A. Altenkirch, Dean of Engineering at Mississippi State University. NASA Lewis designed and built the SSCE payload and also performed engineering, testing, scientific, and flight operations support. The SSCE project was supported in some way by nearly every major element of the Lewis organizational structure.

The SSCE project has been scheduled for a total of eight flights. In the first five flights the fuel sample (ashless filter paper instrumented with three thermocouples) was mounted in a sealed chamber filled with a 50 percent or 35 percent mixture of oxygen in nitrogen at pressures of 1.0, 1.5, and 2.0 atm. The polymethylmethacrylate (PMMA) fuel samples instrumented with three thermocouples were tested at 70 percent or 50 percent mixture of oxygen in nitrogen at

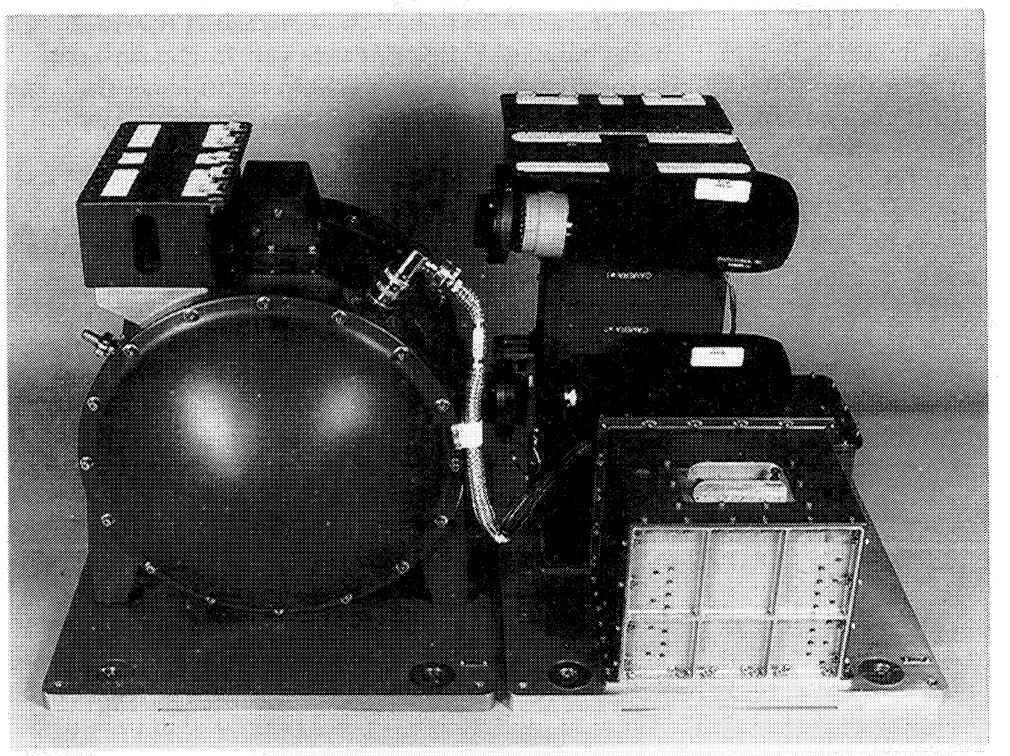

SSCE hardware for polymethylmethacrylate fuel—middeck configuration.

pressures of 1.0 and 2.0 atm. The sample was ignited with an incandescent wire. Two 16-mm motion picture cameras photographed the combustion process from perpendicular perspectives. Temperature (chamber and fuel sample) and pressure measurements were recorded with a digital data acquisition and control system.

The SSCE completed its sixth flight this year, and the final two are planned for 1994. The ashless filter paper portion of the flight test matrix was completed on flights STS–41, STS–40, STS–43, STS–50, and STS–47. This year, aboard the orbiter *Endeavor* (STS–54), the first flight of the PMMA fuel was completed. This test was conducted in a 70 percent mixture of oxygen in nitrogen at 1.0 atm.

The principal investigator, Professor Altenkirch, has developed a numerical simulation of the flame-spreading process from first principles (of fluid mechanics, heat transfer, and reaction kinetics). The spread rates, flame shape, and thermodynamic data from the SSCE flights are being compared directly with the results of the computational model. The flight temperature data indicate that the solid-phase kinetics parameters commonly used to model normal-gravity fuel pyrolysis do not reproduce the fuel regression rates observed. The results from the five flights of ashless filter paper will be used to formulate an improved solid-phase pyrolysis model.

Bibliography

Altenkirch, R.A.; Bhattacharjee, S.; and Sacksteder, K.R.: Implications of Spread Rate and Temperature Measurements in Flame Spread Over a Thin Fuel in a Quiescent, Microgravity Space-Based Environment. Combust. Sci. and Technol., vol. 91, 1993, pp. 225–242.

Vento, D.M.; et al.: The Solid Surface Combustion Space Shuttle Experiment Hardware Description and Ground-Based Test Results. AIAA Paper 89–0503, Jan. 1989.

Lewis contact: John M. Koudelka, (216) 433–2852
Headquarters program office: OLSMA

Thermal Energy Storage Experiments Readied for Shuttle Launch

Advanced technology work is helping to establish the solar dynamic power system for use in Earth-orbiting spacecraft. This system continuously provides electric power by collecting and storing

solar thermal energy that is later converted to electric power while the spacecraft is in the Earth's shadow. The collected solar thermal energy is stored in a heat receiver that consists of many containers holding a fluoride salt which is melted by absorbing the solar thermal energy. Extracting the stored thermal energy causes the fluoride salt to freeze or solidify. When the salt is then melted, it expands approximately 30 percent in volume. The repeated melting and freezing of the salt produces voids in the solidified salt, impacting the heat transfer rate to the salt and the design of the salt containers in the heat receiver. Consequently, understanding and predicting the melt/freeze behavior of the contained thermal energy storage (TES) fluoride salt in the on-orbit microgravity environment help to improve the design and performance of solar dynamic system heat receivers.

Analytical computer codes are now being developed for predicting the void behavior in TES salts for the repeated melt/freeze cycles that occur in an on-orbit heat receiver. Experimental verification of the analytical predictions is needed before applications can be designed. The experimental performance data needed for the TES salts in a long-duration microgravity environment will be

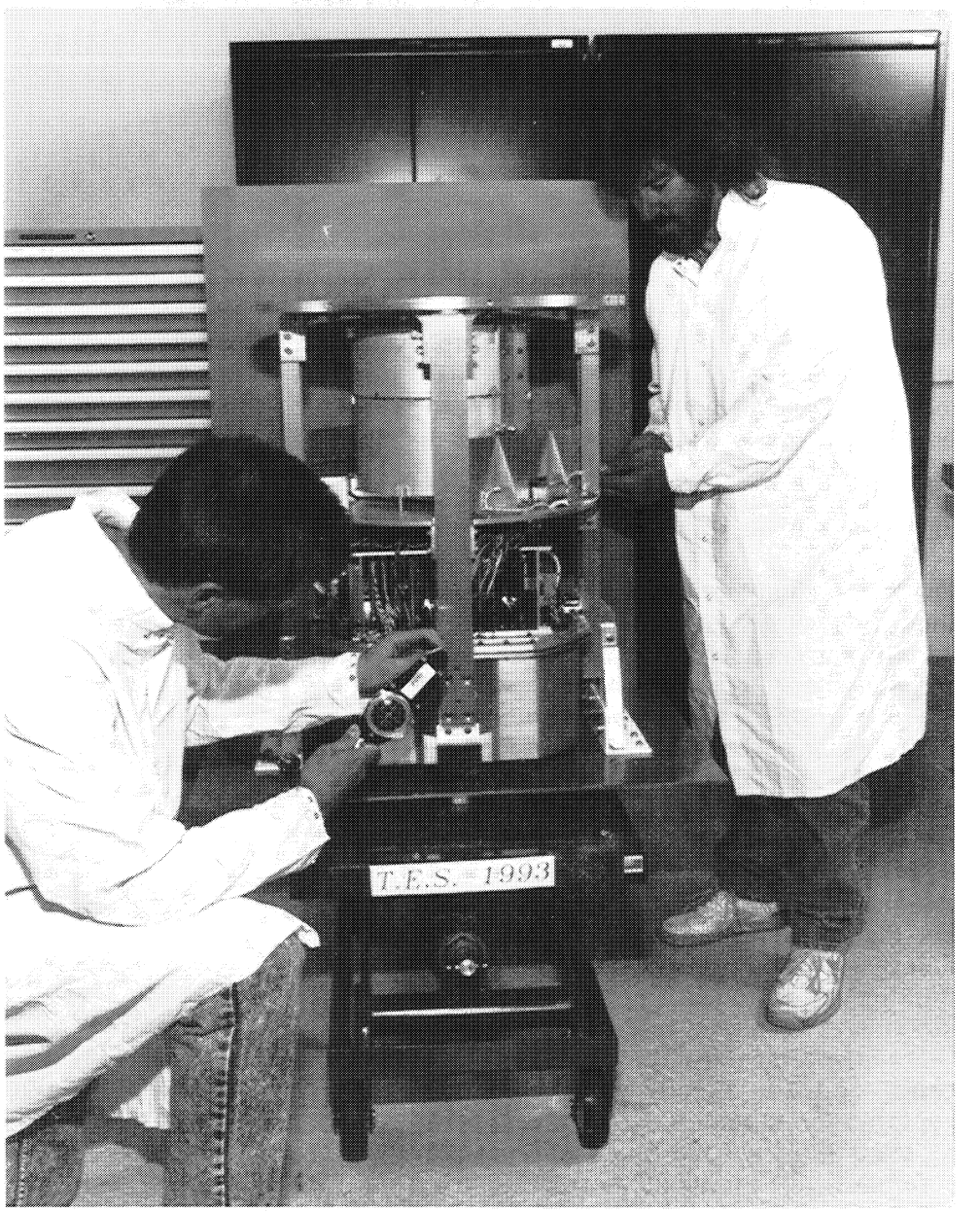

TES payload checkout.

ORIGINAL PAGE
BLACK AND WHITE PHOTOGRAPH

obtained through flight experiments on the space shuttle proposed by the principal investigator, David Namkoong of NASA Lewis. Two separate flight experiments have been developed that will be part of the Hitchhiker payload to be flown on STS–62 in February 1994. Flight data will consist of the time variation of temperature and heater power during the heatup, melt/freeze, and cooldown phases of the experiment. A postflight computer-assisted tomography (CAT) scan of each TES salt container will provide data on void sizes and distribution.

A significant milestone was achieved by the delivery of the two experiment payloads, TES–1 and TES–2, to the Goddard Space Flight Center for random vibration qualification testing. Each experiment payload has been separately tested and has passed the Goddard structural criteria.

NASA Lewis provided the funding, project management, and scientific oversight for the design and development of the two TES flight experiments as well as safety and quality assurance support, specialized hardware development, and the unique skills required for experiment assembly. Work was accomplished by an in-house dedicated project team consisting of engineers and technicians from NASA and Sverdrup Technology, Inc. Commercial vendors were used for fabricating specific hardware components. Subsystem design reviews, random vibration, and electromagnetic interference test work was also provided in-house.

Bibliography

Namkoong, D.: Thermal Energy Storage Flight Experiment in Microgravity. Proceedings of NASA/DOD Flight Experiments Technical Interchange Meeting. NASA TM–108721, 1992.

Skarda, J.R.; Namkoong, D.; and Darling, D: Scaling Analysis Applied to the NORVEX Code Development and Thermal Energy Flight Experiment. AIAA Paper 91–1420, 1991.

Szaniszlo, A.J.: Thermal Energy Storage Flight Project. Presented at the 1992 Space Power Workshop, El Segundo, CA., Apr. 7–10, 1992.

Lewis contact: Andrew J. Szaniszlo, (216) 433–6332
Headquarters program office: OACT

Advanced Space Analysis

Combined Lander and Instrumented Rover Concept Defined

In 1992, NASA's Office of Exploration renewed its efforts to identify small robotic precursor missions to the Moon and Mars as a more affordable way to prepare for human exploration of the solar system. Carnegie Mellon University in Pittsburgh, Pennsylvania, and NASA Lewis teamed up to develop a concept for a lunar lander that would increase the scientific payload landed on the lunar surface by using many of the same subsystems for both the landing spacecraft and the roving system. This concept, the combined lander and instrumented rover (CLIR), has been defined and promises increased return on investment when we again explore planetary surfaces.

CLIR proposes the dual use of as many as possible of the spacecraft systems for both space transportation to the lunar surface and roving on the lunar surface. The spacecraft structure is the most prominent among these. By using the same legs to walk that were used for landing, CLIR saves both structural weight and the complexity of a separate rover deployment system. The roving system is required to handle the shock of lunar landing; modern materials, structural analysis techniques, and robotic mechanism designs have eased this penalty. Dual use of spacecraft control system avionics for both space transportation and roving is enabled by the continuing accelerated progress of space electronics computing and data-handling capabilities. Photovoltaic arrays, supplemented for short periods with spacecraft batteries, can easily be used for both Earth-to-Moon transit and lunar surface operations—as long as the spacecraft is to operate only in lunar daylight and is not expected to survive the roughly 335-hr lunar night. Because of the extreme cold, power system (indeed, overall spacecraft) design for lunar night survival (if required) is a challenge that will be addressed in future studies.

The conceptual design for CLIR has the following features:

Mass at launch (Taurus launch vehicle class)	1314 kg
Mass at landing	134 kg
Science payload	14 kg
Roving range	>100 km
Roving speed	1 km/hr

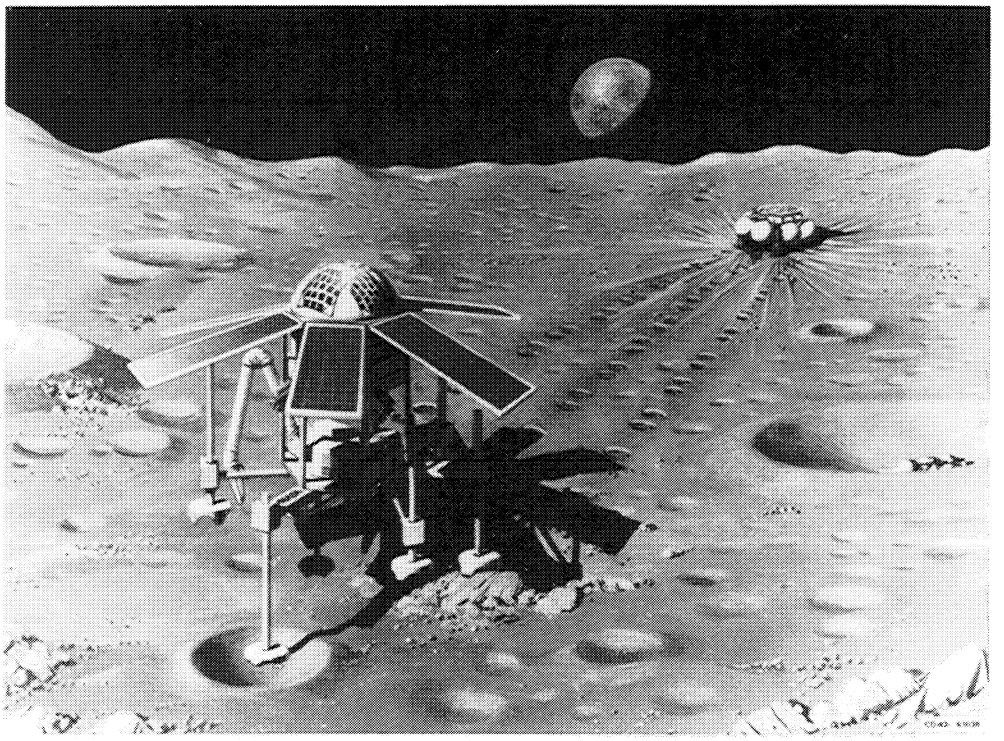

Artist's concept of combined lander and instrumented rover.

Instruments ..... cameras; soil analysis spectrometers
Power system ..... 250-W gallium arsenide photovoltaic arrays; silver-zinc batteries
Propulsion ..... monomethyl hydrazine/nitrogen tetroxide storable bipropellant engines
Communications ..... phased-array patch antennas on hemispherical dome
Mobility system ..... dual translating tripods; lower tripod rotates to turn

In addition to concept development, which is being completed, hardware demonstration and testing for proof of feasibility is ongoing. Carnegie Mellon will build a mobility system demonstrator and demonstrate it over a variety of terrains. NASA Lewis will conduct in-house testing of power systems to expected lunar mission thermal and duty cycle requirements and will test robotic leg translation mechanisms in a simulated lunar environment facility, which includes dust and vacuum.

Lewis contact: Lee S. Mason, (216) 433–7106
Headquarters program office: OACT

Transfer-Orbit Plasma Interaction Experiment Developed

Although several past missions have explored the Earth's magnetosphere and radiation belts, the data returned have given us information on the magnetosphere that is neither complete nor consistent. Mapping of a large portion of the Earth's magnetosphere, as well as understanding the interactions of spacecraft with the plasma in the near-Earth environment, would require large propellant loads if attempted with traditional chemical propellants. Solar electric propulsion offers the capability to travel slowly through a large portion of the magnetosphere while using a relatively small amount of propellant. The match of requirements with capabilities has resulted in the development of the Transfer-Orbit Plasma Interaction Experiment (TROPIX), a magnetosphere mapping mission using an integral solar electric upper stage on a Pegasus-class launch vehicle.

The TROPIX concept proposes the use of solar electric propulsion to carry a 30-kg suite of instruments from a roughly 350-km circular, 60° inclined delivery orbit to near geosynchronous orbit, a mission lasting approximately 1 year. TROPIX would build on the results of the NASA/

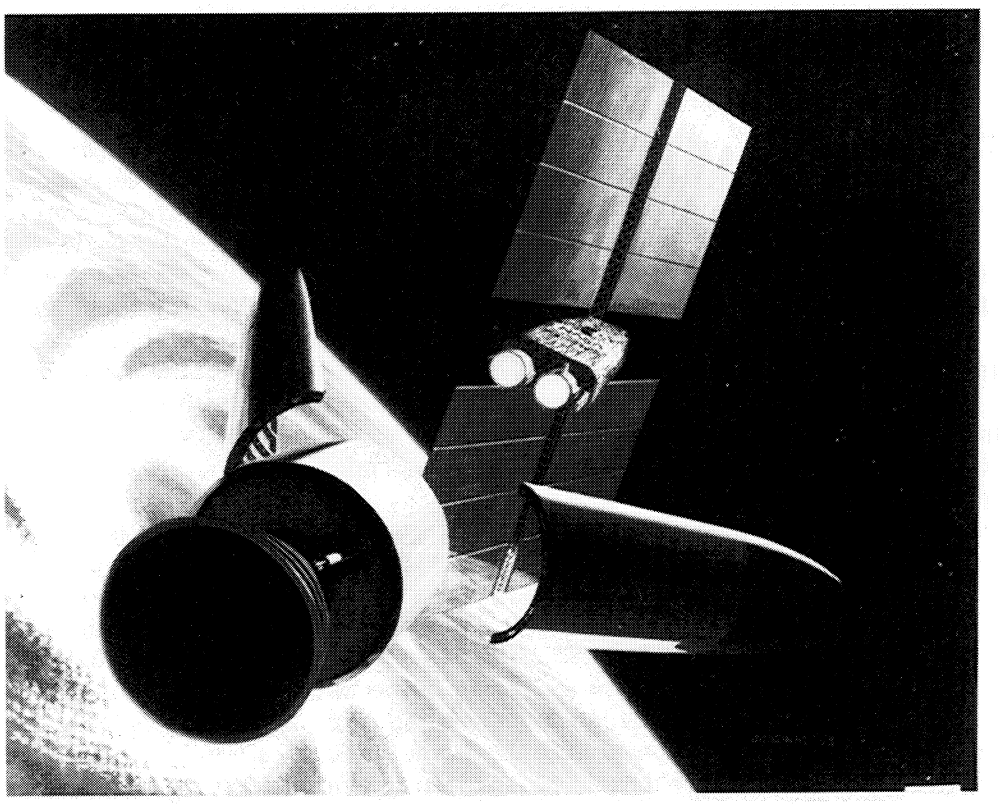

TROPIX spacecraft.

Department of Defense NSTAR ion propulsion experiment to employ the first operational use of primary ion propulsion. Using two 20- or 30-cm thrusters, the solar electric upper stage would operate continuously during the sunlit portions of the orbit. The ion thrusters, in addition to providing thrust for orbit change, would contact the ambient plasma to discharge any spacecraft charge buildup or to vary spacecraft charge as part of the plasma interactions data collection.

The TROPIX concept includes approximately 2.5 kW of beginning-of-life power from gallium arsenide solar arrays with nickel cadmium batteries for spacecraft housekeeping during eclipse, two 20- or 30-cm xenon ion thrusters, a small hydrazine attitude control system, and a science payload consisting of a variety of electromagnetic probes and plasma interaction experiments. The spacecraft has been sized to fit inside a Pegasus fairing, with a launch weight of approximately 350 kg.

The initial concept described here was submitted to the Small Explorer Program announcement of opportunity in the spring of 1993 by a Lewis in-house team, with the participation of space physics scientist Dr. Christopher Russell of UCLA. However, it has also served as a starting point for the discussion and study of a family of missions that could use a small integral solar electric upper stage to achieve objectives otherwise impossible to achieve with small packages. One example is an equatorial magnetospheric mapping mission that would loiter at the magnetopause. Another example is a data relay spacecraft that would use a 5-kW integral solar electric upper stage to deliver a high-power, high-data-rate communications system from Mars (or other planetary bodies depending on launch vehicle size and spacecraft power level). In this way small lander missions, such as the Mars environmental survey discovery missions, could have a much higher data return. Work continues on these ideas, as well as on potential commercial applications of small solar electric propulsion systems.

Lewis contact: J. Mark Hickman, (216) 433–7105
Headquarters program office: OACT

Space Station

Systems Engineering and Integration

Orbiting Vehicle Shadowing and Power Analysis Computer Programs Integrated

For orbiting vehicles, such as the U.S. space station, the Russian *Mir* space station, and most other spacecraft, solar arrays provide the necessary power to operate onboard equipment. Designing an optimum vehicle often results in complex hardware configurations, flight orientations, and flight operations that may cause shadowing of the solar arrays at some times of the year. Therefore, determining the impact of shadowing on power capability is vital. To accomplish this for the space station, a general-purpose orbiting vehicle shadowing program was developed and integrated into the NASA Lewis-developed SPACE (for station power analysis for capability evaluation) program.

Initial versions of the shadowing analysis program only considered solar-array-to-solar-array shadowing. As the space station was reduced in size owing to budgetary considerations, it became apparent that other parts of the space station would also shadow the arrays. The program was revised to assess the shadowing of the entire vehicle after orienting the arrays and the vehicle by using simplified algorithms. The program was integrated into SPACE both to utilize its detailed orbital mechanics and array-pointing algorithms and also to permit power calculations by using its extensive, detailed component models (e.g., solar arrays, batteries, and electronics).

The shadowing code uses a polygon model to describe the spacecraft surfaces, to identify the solar arrays, and to indicate which on-orbit hardware to rotate about specified axes in order to point arrays toward the Sun. The model is then transformed by performing the necessary vehicle and array rotations. For each predefined point on each solar array blanket the program determines if the point is shadowed by finding one polygon that is in front of it. This part of the code utilizes specially designed algorithms derived from graphical ray-tracing methods to greatly speed up the calculations. The resulting information is provided to the solar array model, which determines, based on the solar array operational and design characteristics, how much power the array can produce. This is done for each time step in the Sun part of the orbit. Additionally, graphical files are generated that allow the user to visualize the complex flight orientations and shadow patterns. An Earth-vehicle-shadow plot that shows how the vehicle appears and is shadowed as viewed from the Sun is also produced.

Results from the shadowing model were used in a program-wide assessment of space station operations to determine the effects of shadowing on the station due to space shuttle approach, docking, berthing, and departure; station assembly; and normal station operations. Also, during the redesign process shadowing assessments were provided to the team for each option being considered. Most recently, the shadowing effects on power of the *World Station* (a combination of the U.S. space station and the Russian *Mir* 2) were evaluated.

Work on shadowing analysis has been done as part of the general development of power system evaluation capabilities at NASA Lewis. Use of the orbiting vehicle shadowing program and the integrated SPACE program as part of a generic space vehicle power assessment capability is anticipated to assist in sustaining NASA Lewis' role as a center of excellence in space power and to help meet this Center's mission to satisfy national needs through space power systems development.

Presently, the program is being enhanced to allow an assessment of shadowing on radiator efficiency, to permit fast and easy model creation and modification with a user-friendly model generator, and to enable animated display of shadow patterns and vehicle orientations.

Lewis contact: James Fincannon, (216) 433–5405
Headquarters program office: OSSD

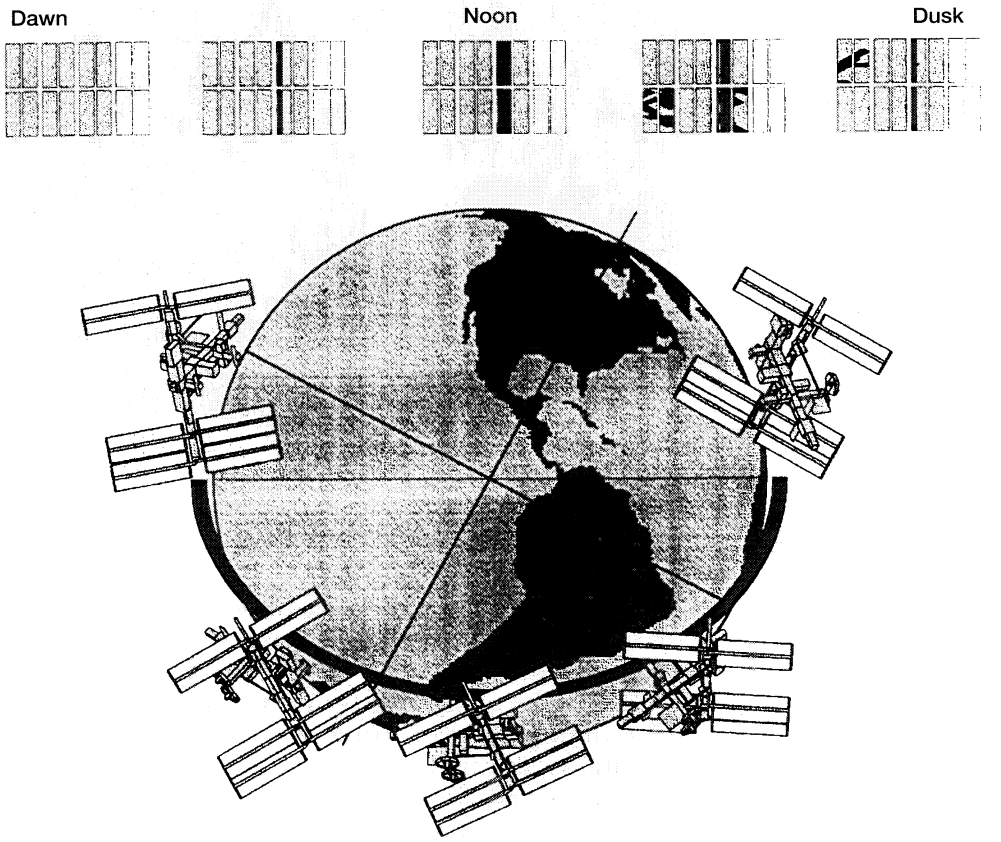

Vehicle orientation and shadowing patterns at various positions around Earth for World Station.

Photovoltaic Power Modules

Space Station Plasma Contactor Developed

A plasma contactor system was selected to control the voltage potential between the space station and the local plasma environment by establishing a mechanism for "grounding" the station to that environment. The space station will operate in a low Earth orbit, where it will encounter the space plasma. Because the large solar arrays will collect more electrons than ions from the plasma and because the station structure will be electrically connected to the negative side of the high-voltage arrays, the main station structure would float at voltages as great as 120 V negative with respect to the plasma. Test data suggest that at these voltages the anodized surfaces on the station structure and the habitation and laboratory modules will incur arcing and deteriorating thermal properties. To obviate these effects, the station potential will be maintained within 40 V of the ambient plasma by using a plasma contactor.

The plasma contactor is a continuously operating, self-modulating device that emits electrons to offset the varying collection of electrons by the arrays. The plasma contactor system consists of orbital replacement units and integration hardware. Each orbital replacement unit has several major components: the plasma contactor unit, the power electronics unit (power supply and controls), the expellant management unit (the xenon gas, tankage, and plumbing), and the orbital replacement unit enclosure (housing structure and external interfaces). Basically, the plasma contactor system will establish a low-

impedance electrical path from the station structure to the local plasma environment by creating a plume of ionized xenon gas constituents. This plume establishes an electrically conducting "plasma bridge" between the station structure and ambient plasma.

Although plasma contactor systems have been flown on spacecraft, the variable emission currents and lifetime performance requirements of the system needed for the space station are pushing the existing technology. To this end, NASA Lewis has begun a plasma contactor development program as part of the station's electric power system. Progress has been made in several important areas. The plasma contactor's hollow cathode assembly design has been completed and validated in performance tests and long-duration wear tests of hollow cathodes and heaters. Additionally, test procedures and materials and process specifications for critical cathode components have been developed. Prototype plasma contactor units have been built and tested over the required emission current ranges. Several have met key performance requirements for the station plasma contactor under operating conditions expected. Testing continues to verify that the plasma contactor unit design will meet the 17,500-hr operating lifetime design requirement. Additionally, several new cryopumped vacuum test facilities have been developed to support characterizations and life testing of components and systems.

From the results of these prototype tests an enclosed-keeper-design plasma contactor unit was baselined as the critical element of the plasma contactor orbital replacement unit for the space station. Typically, this plasma contactor unit has electron emission currents to 10 A and a maximum steady-state input power of 30 to 36 W. Electromagnetic emissions in the 14-kHz to 18-GHz frequency range, and optical emissions in the 3000- to 9000-Å wavelength range radiated by the plasma contactor were measured and appear to pose no major compatibility issues with other space station systems.

A design for an engineering model version of the enclosed-keeper plasma contactor unit was completed and is under fabrication. The first units are scheduled for completion in fall 1993. The plasma contactor unit mass, without power cable and connector, is estimated to be less than 150 g, with a length of approximately 11.5 cm and a diameter of approximately 2.8 cm.

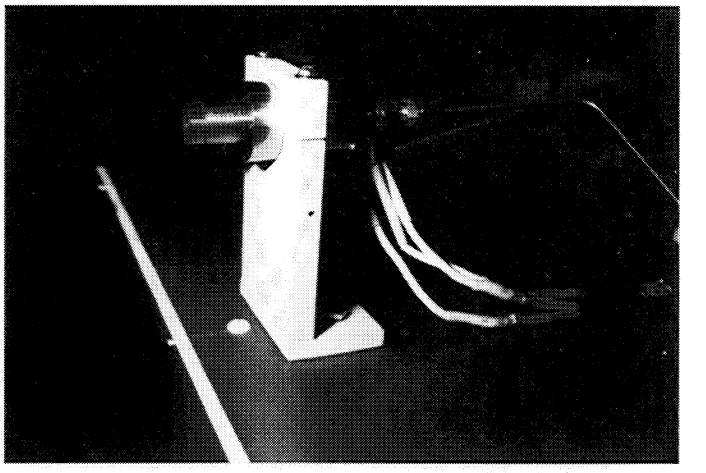

Plasma contactor unit.

The next phase is to initiate functional (performance and lifetime) testing of the engineering-model plasma contactor unit and system. Life testing of the components and the system will be done under emission current and environmental conditions simulating on-orbit space station operations and will continue through the flight hardware development program.

Lewis contacts: Robert D. Corrigan, (216) 433–5379; Michael J. Patterson, (216) 433–7481
Headquarters program office: OSSD

Photovoltaic Power Module Neutral Buoyancy Tested

In December 1992 a neutral buoyancy test of the photovoltaic power module was conducted to evaluate the extravehicular activity (EVA) compatibility of its design and assembly and maintenance procedures. The test was conducted in the Neutral Buoyancy Simulator at NASA Marshall Space Flight Center.

Assembly tests were conducted to evaluate EVA crew and tool accessibility to launch restraint release locations, to the keel trunnion fastener, to the mast motor drive assembly override and clutch release, to radiator cinch, winch, quick disconnect, and deployment motor manual override as well as to evaluate EVA translation on the

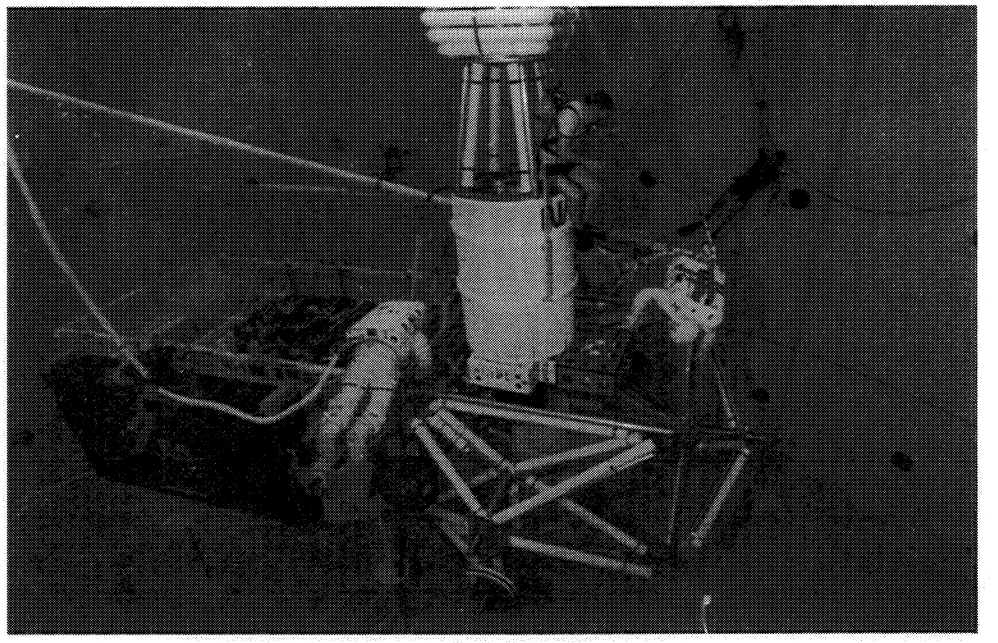

Photovoltaic power module undergoing neutral buoyancy testing.

integrated equipment assembly and solar array wing. Additional assembly tests were conducted to evaluate operational concepts for installation of the short spacer and mobile transporter/crew equipment translation aid rail.

Maintenance tasks under evaluation included removing and replacing orbital replacement units for the integrated equipment assembly battery, the mast canister, the beta gimbal motor's roll ring module, the photovoltaic radiator electronics control unit, the sequential shunt unit, and the remote power controller module. The tests also assessed an EVA connector tool and concepts for EVA jettison of a failed photovoltaic wing.

To minimize the effects of drag, the mockups were primarily of aluminum-frame construction, using polyvinyl chloride tubing to provide buoyancy and nylon mesh to represent solid surfaces. High-fidelity mechanisms realistically represented interfaces critical to performing the EVA evaluation. Mockups for the test were provided by NASA Lewis, Rocketdyne, Loral/Vought Systems, Loral Space Systems, NASA Johnson, and McDonnell Douglas Space Systems Company.

Key findings from the many test results include the following:

- Radiator changeout using two crewmembers, each in a portable foot restraint, and handoff to and from the remote manipulator system were successfully accomplished.
- Binding of the radiator accumulator shrouds can occur when high forces are applied but is easily corrected and prevented with proper communication and coordination between crewmembers and with the application of low forces and slow movements during installation and removal.
- Mast canister changeout using two crewmembers, oriented orthogonally from each other, each in a portable foot restraint, was performed successfully. Control of the mast canister in all degrees of freedom was maintained during the changeout operation.
- The two crew positions tested were optimal for jettison of the solar array wing.
- Two methods for installing the short spacer were successfully completed.
- An adjustment feature should be incorporated into the short spacer design to help alignment and to accommodate any thermal distortion.

Test results have been factored into numerous critical design reviews. Both design changes and assembly and maintenance procedure changes have been implemented on the basis of the test results. As hardware design continues, future tests are planned to verify the design and the EVA operations required to assemble and maintain the photovoltaic power module.

Lewis contact: Monica I. Hoffmann, (216) 433–6765
Headquarters program office: OSSD

FASTMast Fiberglass Flexible Battens Hypervelocity Particle Impact Tested

Each solar array wing on the space station will be supported by a large deployable structure known as a folding articulated square truss mast (FASTMast). This structure includes fiberglass-epoxy composite flexible battens that provide the tension within each mast bay when fully deployed as well as the elasticity during the transition from stowed and deployed conditions. Once in orbit these battens will be exposed to the threat of damage by micrometeoroids and orbital debris. Significant damage to or failure of the battens could preclude the stowage and subsequent replacement of the damaged unit.

NASA Lewis is engaged in a test program to determine the vulnerability of the FASTMast flexible battens to damage by hypervelocity impacts. Because these battens have the highest probability of damage, test results will be used to refine the micrometeoroid and orbital debris analysis performed for the space station FASTMast. Testing is being conducted at the NASA Johnson Space Center's Hypervelocity Impact Research Facility. The fiberglass batten samples have been supplied by the AEC-Able Engineering Company. A 4.3-mm (0.17 caliber), two-stage, light gas hypervelocity gun is being used for the tests.

Testing has been completed on 16.5-in.-long samples. These samples were fabricated by using the same material and manufacturing processes that are presently the baseline for the space station. The batten samples were mounted in individual fixtures designed to support the battens in a strained condition equivalent to a fully deployed FASTMast configuration. They were then subjected to a test matrix of increasing particle sizes to verify the survivability to impacts by the predicted lethal particle size (0.129 cm).

The matrix of particle sizes chosen for the test program ranged from 0.20 to 0.24 cm in diameter. Each test sample was subjected to a single impact. To date, six batten samples have been impacted. Of the six shots, three were direct hits and three were off center, causing partial impacts. The velocities recorded ranged from 6 to 7 km/sec. Tests showed a varying degree of damaged fibers. Those battens impacted by the 0.20-cm particle remained intact with roughly 30 percent of the fibers severed and also remained in the respective deployed configuration within their fixtures. Impacts from the 0.24-cm-diameter particles caused extensive damage, distorting the fibers and contracting the sample. The battens were jolted from their fixtures, losing all predetermined strain.

These tests have shown that particles 0.20 cm in diameter or smaller do not create significant damage to FASTMast fiberglass flexible battens. Although the lethal particle size is continuing to be investigated, it is evident that the current

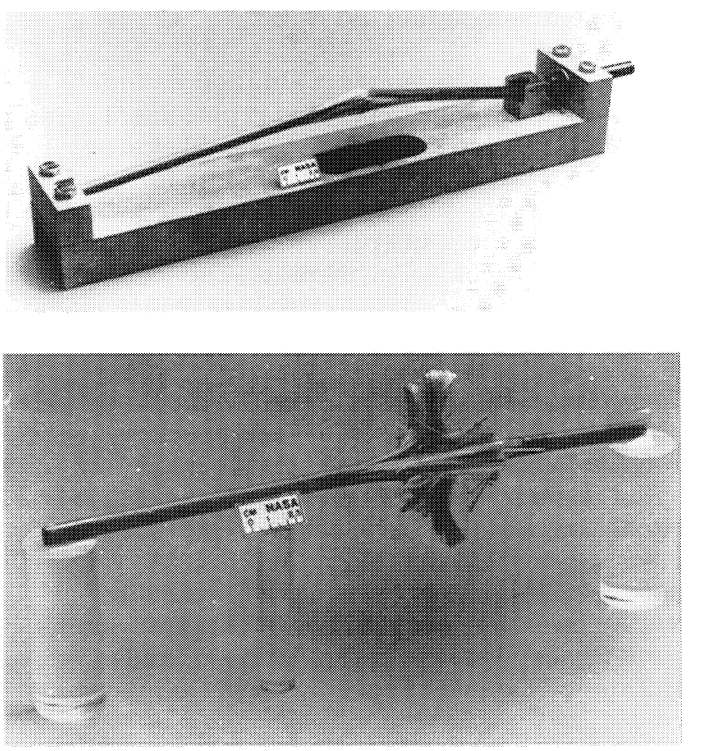

FASTmast fiberglass batten sample for space station solar array after particle impact testing: projectile diameter, 0.20 cm (top); projectile diameter, 0.24 cm (bottom).

FASTMast micrometeroid and orbital debris model for space station is very conservative.

Follow-on to these tests will include additional testing using full-length, 31.75-in., flexible battens having flight type end fittings. Testing is scheduled for the fall of 1993.

Lewis contact: Craig A. Myhre, (216) 433–8741
Headquarters program office: OSSD

Hypervelocity Impact Fails to Induce Arcing and Kapton Pyrolization in a Plasma Environment

NASA Lewis and its contractor successfully completed a test program to determine if hypervelocity impacts could induce Kapton pyrolization and/or cross-conductor arcing on the flat conductor circuit for the space station solar array. The flat conductor circuit extends the length of the 110-ft solar array blanket and is used to carry electric power from the solar cells to the electric power system. Four 110-ft flat conductor circuit sections are used on the solar array. The circuit is exposed to the natural and induced environments of low Earth orbit and is susceptible to the effects of micrometeoroid and orbital debris impacts and ionospheric plasma interactions. These impacts generate a locally high plasma density that might induce arcing between exposed conductor surfaces or the ambient ionospheric plasma. Such effects could prevent the arrays from providing the minimum power required for safe operation.

A series of tests were developed using a flat conductor circuit sample. The test coupon was placed in a plasma environment with several pairs of its adjacent copper conductors biased to +200 V and +40 V relative to the plasma potential, providing a cross-conductor potential difference of 160 V. The coupon was then impacted by particles in the 10- to 100-μm size range by using an electrothermal hypervelocity accelerator. The accelerator generates an extremely hot plasma by discharging a large capacitor bank. As the capacitor bank is energized, the current pulse vaporizes an aluminum foil, exploding the resulting gas and accelerating the projectile load to the target. The projectile load consists of single-size particles that fragment into numerous smaller particles, producing an effect similar to a shotgun blast. Velocities from 5 to 12 km/sec were obtained. The projectile firings were conducted in the HYPER facility at Auburn University.

Two sample sections of flat conductor circuit were tested. The first section had been previously damaged by hypervelocity particle impacts under static conditions. The sample was then placed in a vacuum chamber and exposed to the plasma environment while powered to investigate whether arcing could occur at previously damaged sites.

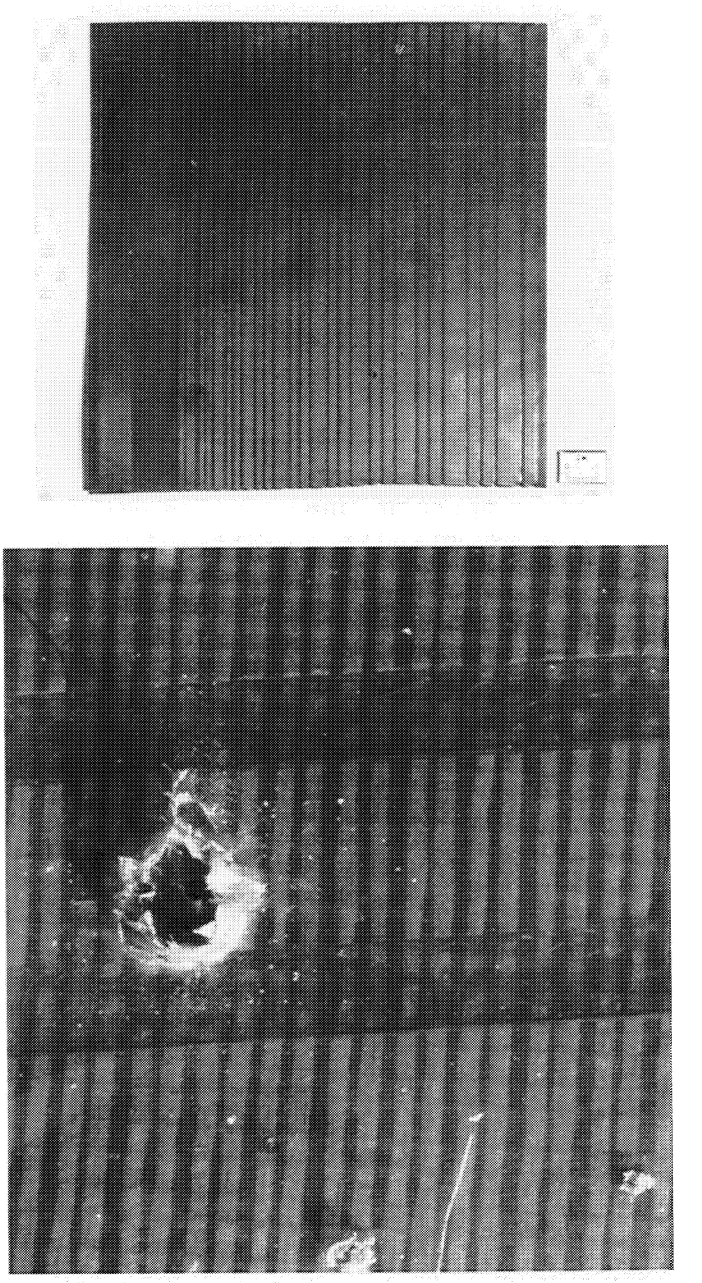

Space station solar array flat conductor circuit coupon before (top) and after (bottom) particle impact testing.

The sample was further damaged by impacts while powered in the plasma environment chamber to investigate whether arcing could occur at or between new and existing sites. The second section was subjected to the plasma environment to observe the location and size of any bubbles or delamination that might occur. Characteristics of the plasma environment were roughly an electron temperature of 0.7 eV and a plasma density of $3\times10^6/cm^3$.

As expected, these tests did not produce any pyrolization, cross-conductor arcing, or other events at a bias potential of +200 V. The plasma interactions generated by the hypervelocity impacts were not sufficient to trigger these events. These tests indicate that hypervelocity-impact-induced pyrolization and cross-conductor arcing are unlikely to occur on the space station flat conductor circuit.

Lewis contact: Craig A. Myhre, (216) 433–8741
Headquarters program office: OSSD

Nickel/Hydrogen Battery Cells Selected for Space Station

NASA Lewis and its contractors are responsible for designing and fabricating the electric power system for the space station, which will circle the Earth every 90 min in a low Earth orbit (LEO). Approximately 55 min of this orbit will be in sunlight and 35 min will be in the Earth's shadow (eclipse). To supply continuous power over the orbit, the electric power system must not only provide power during the sunlight portion by means of solar arrays, but must also store energy for use during eclipse. Nickel/hydrogen (Ni/H_2) cells were chosen as the energy storage system for space station. Because of the limited Ni/H_2 data base on life and performance characteristics in a LEO regime, NASA Lewis began two test programs: one in-house and one at the Naval Weapons Support Center (NWSC) in Crane, Indiana.

For the in-house test program Lewis has built a computer-controlled Ni/H_2 cell laboratory with a data acquisition system to screen a large number of cell designs. Cells were purchased from three vendors through existing Lewis contracts with Yardney Technical Products, Eagle-Picher Industries, and Hughes Aircraft Company. The resulting 39-cell test matrix consists of 13 different cell designs, including both 50- and 65-Ahr capacity cells. All cells have successfully completed acceptance, vibration, and characterization testing and are currently undergoing LEO life testing at a 35-percent depth of discharge (DOD) at either –5 or 10 °C. As of September 1993, 22 cells have successfully completed over 4 years of life testing (23,360 cycles) and the rest have completed over 3 years. The number of completed life cycles ranges from 26,500 to 22,000 cycles. Five cells have reached the end of life. One Eagle-Picher cell failed on cycle 17,175. Four Yardney cells failed on cycles 19,567, 23,541, 25,506, and 25,323.

The Naval Weapons Support Center was contracted by Lewis through an interagency order to characterize and life test a statistically significant number of Ni/H_2 cells to verify the space station requirement of 5-year life at 35-percent DOD. The test matrix consists of Ni/H_2 cells from three vendors: Yardney Technical Products, Eagle-Picher Industries, and Gates Aerospace Batteries. Each vendor supplied 50 "standard" 65-Ahr cells that represent a low-risk, state-of-the-art LEO design. They also supplied 20 "advanced" 65-Ahr cells and 60 "advanced" 81-Ahr cells. For the advanced design the vendors were directed to include at least two recent technology developments that improve cycle life and electrical performance. The 20 advanced 65-Ahr cells from Gates were canceled and 30 additional standard 65-Ahr cells were purchased. All cells were procured through separate Lewis contracts. All life testing is performed in either 10-, 8-, or 5-cell series-connected test packs, at 35- or 60-percent DOD, and at 10 or –5 °C. Effects of various charge methods are also being studied.

As of September 1993, all cells have been delivered to NWSC, have completed acceptance, vibration, and characterization testing, and are currently on life test. Eighty Yardney cells (40 standard 65 Ahr, 20 advanced 65 Ahr, and 40 advanced 81 Ahr) have started life test and have accumulated between 6600 and 18,300 cycles. Six test packs (50 cells) at 60-percent DOD have failed, with the longest one lasting 4700 cycles. One hundred and eight Eagle-Picher cells (48 standard 65 Ahr, 20 advanced 65 Ahr, and 40 advanced 81 Ahr) have started life test and have

accumulated between 6000 and 12,800 cycles. One five-cell pack of 65-Ahr advanced cells at 60-percent DOD and –5 °C has failed after 6904 cycles. The 48 standard 65-Ahr cells are undergoing a special charge control study. Some of the cells are being charged by using a space station baseline charge profile that incorporates a constant current charge followed by a taper charge to 100-percent state of charge. The others are being charged at a constant current terminating at 90- or 94-percent state of charge. The results of these tests were instrumental in the selection of this cell design from Eagle-Picher for use on space station. One hundred Gates cells (60 standard 65 Ahr and 40 advanced 81 Ahr) have started life testing and have accumulated 3700 to 8100 cycles. Thirty of the standard 65-Ahr Gates cells are being used to assess the effect of electrolyte concentration with various charge management techniques. The NSWC will also perform storage tests on cells from each vendor.
The results to date have provided confidence in achieving a 5-year life for Ni/H_2 cells at 35-percent DOD, which is where the space station will operate. Performance at 60-percent DOD, however, has not met the anticipated life predictions.

Lewis contact: David T. Frate, (216) 433–8329
Headquarters program office: OSSD

Space station nickel/hydogen cells undergoing life test.

Nickel/Hydrogen Battery Orbital Replacement Unit Tested

The space station electric power system will use nickel/hydrogen (Ni/H_2) battery cells for power during eclipse portions of the station orbit. Thirty-eight of these cells have been series connected and packaged in an orbital replacement unit (ORU). Two ORU's are connected in series to form one battery, for a total of 76 cells in series. Each photovoltaic power module contains six batteries, or 456 cells. The battery ORU design life is 6.5 years, which translates to 38,000 charge/discharge cycles.

The space station will be the first application for low Earth orbit (LEO) cycling of 76 Ni/H_2 cells in series. Currently, there is no cell life and performance data base for LEO cycling of more than 22 Ni/H_2 cells in series. Thus, NASA Lewis began a unique test program to determine proper charge management and life and performance characteristics of batteries designed for the space station.

The test is being performed at the Power Systems Facility (PSF) at NASA Lewis. The PSF battery test area is designed specifically for this test. The current test is performed in a dual-ORU environmental chamber with nitrogen purge. Additional planned testing will take place in thermal vacuum chambers containing two or three ORU's. Active thermal control is provided through a radiant finned heat exchanger connected to recirculating fluid chillers. All tests are performed by using a custom-designed automatic control and data acquisition system.

The testing is in two phases. Phase 1, conducted on two engineering-model ORU's, is ongoing. It consists of initial ORU characterization and conditioning, followed by individual ORU LEO cycling at 35-percent depth of discharge, using constant-current charges and discharges. Upon completion of the individual cycling the ORU's are placed in series for additional LEO cycling representing the space station on-orbit duty cycle. This additional LEO cycling is performed at 35-percent depth of discharge using a constant-power "peaking" orbit. Upon completion of 3000 series cycles the ORU's will undergo several performance capacity tests to determine any degradation. Long-duration series LEO nonpeaking cycling, at 35-percent depth of discharge, will begin after the performance capacity tests.

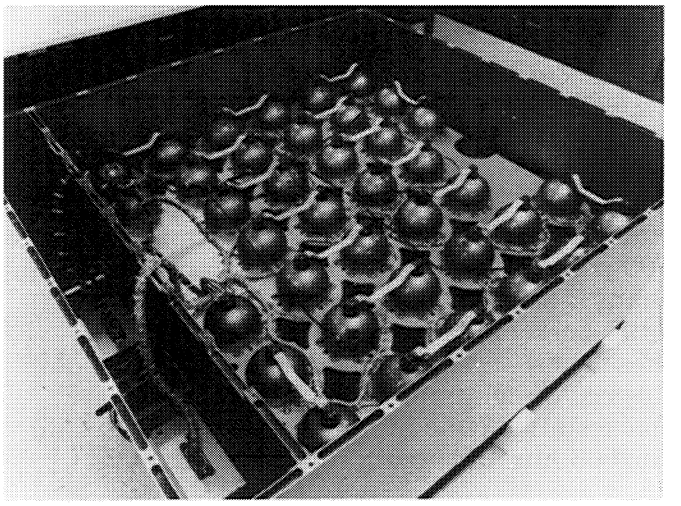

38-Cell nickel/hydrogen battery orbital repalcement unit (without cover).

Phase 2, or "Fleet Leader," testing will be performed on four ORU's (two batteries) and is scheduled to begin in December 1995. It also consists of initial ORU characterization and conditioning. Mission simulation cycling will follow the initial tests. The two engineering-model battery ORU's presently on test at PSF were procured through the space station prime contractor, Rocketdyne. The ORU's were built by Space Systems Loral using engineering-model 89-Ahr-capacity cells from Gates Aerospace Batteries. The four ORU's for the Fleet Leader test will be built using qualification-model 89-Ahr-capacity cells: two with cells from Gates and two with cells from Eagle-Picher Industries.

The two engineering-model ORU's have completed over 2500 series LEO cycles with excellent performance. Individual cell voltage data for all 76 cells are closely matched. Cell pressures have stabilized. No performance anomalies have been observed during the series testing.

Lewis contact: Penni J. Dalton, (216) 433–5223
Headquarters program office: OSSD

Battery Charge/Discharge Unit Bilateral Converter Developed

The battery charge/discharge unit will be used on the space station to regulate battery charge current during the sunlight period and to regulate primary bus voltage during both eclipse and high-power loading demands during sunlight. A 9.6-kW bilateral (bi-directional) converter can supply current in both directions, reducing bus voltage down to the battery voltage or, in the reverse during discharge, boosting battery voltage. This matching of lower and varying battery voltages to a higher primary bus voltage allows the solar arrays to operate at a higher power point, yielding more available power. The use of a bi-directional converter reduces weight because there is only one converter instead of separate charge and discharge converters.

The 9.6-kW bilateral converter consists of four 2.4-kW stages, each of which is 90° phase shifted, interleaved together. Each stage is basically a boost converter with the flyback diode replaced by a field-effect transistor switch and can be used to operate the same converter in a buck mode. Interleaving the four stages also allows paralleling battery charge/discharge units and thus paralleling batteries, increasing the primary bus power capability. The converter also uses super field-effect transistors, which are high-power field-effect transistors packaged into a hybrid for use on the space station.

The battery charge/discharge unit contains a fault isolator, which senses high current during a fault and limits it to allow the fault protection system time to isolate the fault. The isolator interrupts the fault current if it persists for 450 msec. It can detect fault currents and begin current limiting in less than 10 μsec before the battery fault currents reach damaging levels. After the fault has been isolated, it can be reset through computer commands without replacement, reducing on-orbit maintenance time.

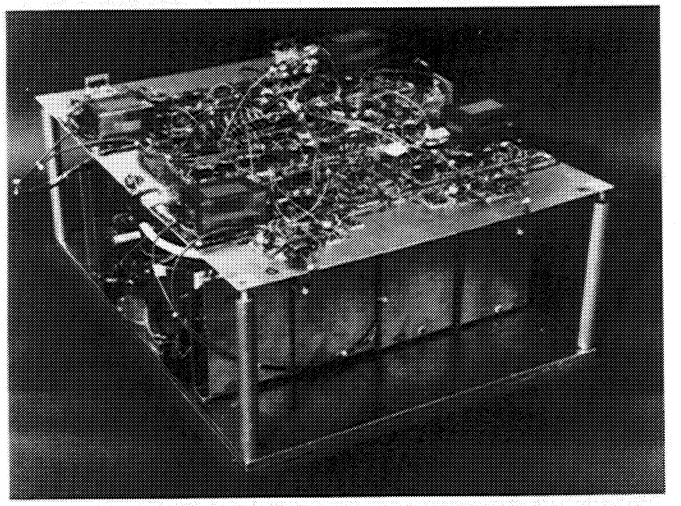

Battery charge/discharge unit's 9.6-kW bilateral converter breadboard.

Battery charge/discharge unit breadboards have been designed, built, acceptance tested, delivered, and integrated into the Space Power Electronics Laboratory at Rocketdyne and are undergoing system tests.

The bilateral converter was developed for NASA Lewis by Space Systems Loral through Rocketdyne, the space station prime contractor.

Lewis contact: Gary W. Wroten, (216) 433–8314
Headquarters program office: OSSD

Electrical Systems

Electric Power System Operations Automated

NASA Lewis has been charged with developing a highly automated system for generating, storing, and distributing electric energy aboard the space station. The paramount objective for this system's operation is to generate and dispatch electric power to the loads while maximizing productivity and without violating any constraints. The initial station operation will use dispatchers aided by human-interactive computational facilities to perform the necessary command and control tasks. These tasks constitute planning and decision-making activities that strive to eliminate unplanned outages. With such an extensive operational phase, products that can increase an operator's efficiency will significantly reduce the space station operating cost. NASA Lewis has been developing prototype computer systems that increase operating efficiency by providing human operators with expert-level advice.

To provide counsel for both normal and abnormal operation, monitoring and diagnostic systems featuring intelligent interfaces between the human operator and the advisory software are being developed. For normal operation the

monitoring system synopsizes the power system's operating characteristics by using a status-at-a-glance design philosophy. For malfunctions, system misbehavior is detected and diagnosed by using four techniques: rules, models, set covering, and trend analysis.

A rule-based system encodes its knowledge in if-then rule structures resembling the pattern recognition and response behaviors of humans. Complex rule patterns tie many different related pieces of information to complex response behaviors. These systems quickly become difficult to build and to maintain when the number of rules describing the knowledge increases. The rule-based technique is used to detect failures in most of the power system's components.

Model-based systems work differently. In them the system is broken into pieces described by simple behavioral models. The individual models are connected to describe the overall system. To detect failures, the performance of the model is compared with measurements from the real system. Discrepancies indicate failures. The particular cause of the failure can be deduced by modifying the simple models until they match the real system's behavior. The model-based technique is used to detect and diagnose failures in the power system's nickel/hydrogen batteries.

The set-covering technique stores all knowledge of component malfunctions as a set of related facts. For failure-cause diagnosis the related facts are failures, their symptoms, and their possible causes. The symptoms are qualitative descriptions of operating tolerance violations. Each failure has causes, and the causes may have causes, and so forth. The relations among component failures, their symptoms, and their causes are indexed much like information in a dictionary. A symptom detected by a rule-based pattern classifier is passed to the set-covering system, which looks up the possible failure causes in the dictionary. The dictionary is easy to build by using information from fault-tree analyses or failure-modes-and-effects analyses (two common reliability engineering practices) and is easy to verify and maintain. The diagnosis is faster than with the model-based technique.

In the particular case of the batteries the operating history is essential for detecting and diagnosing malfunctions. We have used a model-based technique to analyze trends in the operating history. Three trends are maintained: short, medium, and long term. Short-term trends are compared with the results from an analytic model of the battery. Medium- and long-term trends are compared with the battery's expected aging characteristics. The system displays these health

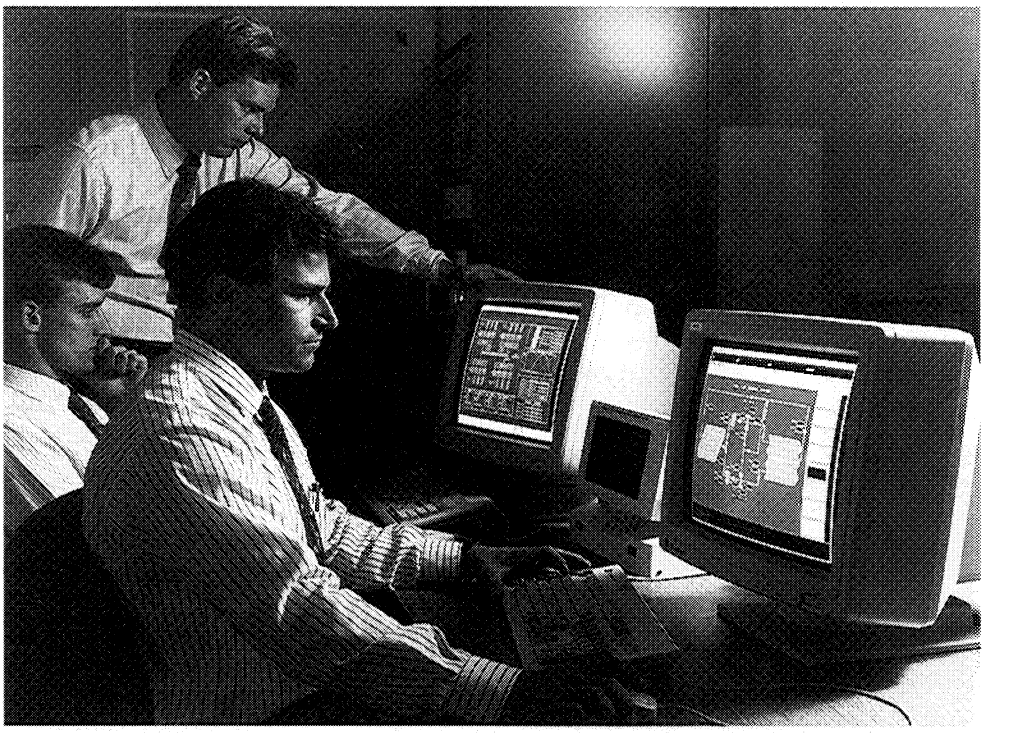

Testing advisory systems in Lewis Engineering Support Center.

trends and alerts the operator if there are any deviations from the expected.

Detecting and diagnosing malfunctions is only part of the operations problem. The conclusions reached by these advisory systems must not mislead, confuse, or inadvertently distract the human operators. Special video displays have been developed to ensure that the advisory systems effectively focus an operator's attention on germane issues. These displays provide the operator with the system's status at a glance. Ground operations tasks can be broken down into three categories: monitoring the system, detecting and fixing problems, and preventing problems. The monitoring screens display the operational status of the power system, highlighting the most critical functions and any functions that are nearing critical limits. The operator can easily see where trouble is brewing and take action accordingly. When a problem does occur, the status screens highlight the portion of the system that indicates the problem. Additional screens are brought up to see what the computer advisory systems have to say about the cause of the problem and what remedial steps to take. Navigating through the various advice screens should be simple and obvious; otherwise the operator may get lost. This is a difficult problem, one which the Lewis team continues to address with the assistance of all the operations personnel, particularly those at the NASA Johnson Space Flight Center who have experience in ground operations. The Lewis team is delivering versions of the advisory systems to Johnson this year to be included in the space station's control center testbed. This testbed is a forum in which operations personnel evaluate potential mission control products.

The amalgamation of diagnostic systems with status-at-a-glance human interfaces reduces the human operator's cognitive workload when she is controlling the electric power system. This system of video displays and diagnostic systems that conveys complex concepts in terms that are clear to its user will facilitate quick and consistent decisions under all operating circumstances.

Lewis contact: James L. Dolce, (216) 433–8052
Headquarters program office: OSSD

Operations

Power Systems Facility Modified for Photovoltaic Power Module Assembly and Testing

NASA Lewis' Power Systems Facility (PSF) will be used for the manufacturing and final assembly and testing of the photovoltaic power module. In preparation the PSF underwent major modifications. A 63-ft-high by 74-ft-long partition wall, a three-floor stock and control area, and a 40-ft expansion of a high-bay area were constructed. The heating, ventilation, and air-conditioning system was upgraded. Computer and communication systems and an ammonia detection and suppression system were installed. The PSF will provide Lewis with superior assembly and test areas for large and small, flight and nonflight hardware.

These modifications to the PSF provided two 63-ft-high bay areas that can operate as class 100,000 clean rooms. One of these areas will be used for the final assembly and testing of the photovoltaic power module. This area has been equipped with a 10-ton crane with true vertical lift to precisely align mating hardware, with a gaseous nitrogen system, and with a shop air system. This high-bay area is equipped with an ammonia detection system because liquid ammonia is used in the thermal control system for the power module and will be used in testing at the PSF. In case of an ammonia leak the detection system will be capable of activating an emergency exhaust system and an ammonia suppression system in the ammonia loading room contained in this high-bay area. The ammonia suppression system, when activated, releases a water mist that will absorb and remove any gaseous ammonia. The exhaust and suppression systems have been installed.

After the photovoltaic power module is assembled and tested, it will be shipped either for additional testing (nonflight hardware) or for launch. The module will leave through the second high-bay area, which is being modified so that the space cargo transporter system can be used. The area has been expanded 40 ft and has two 15-ton cranes and a 2-ton crane. The 15-ton cranes can operate in tandem and allow for easy handling of large packages.

Lewis contact: Frank G. Gati, (216) 433–2655
Headquarters program office: OSSD

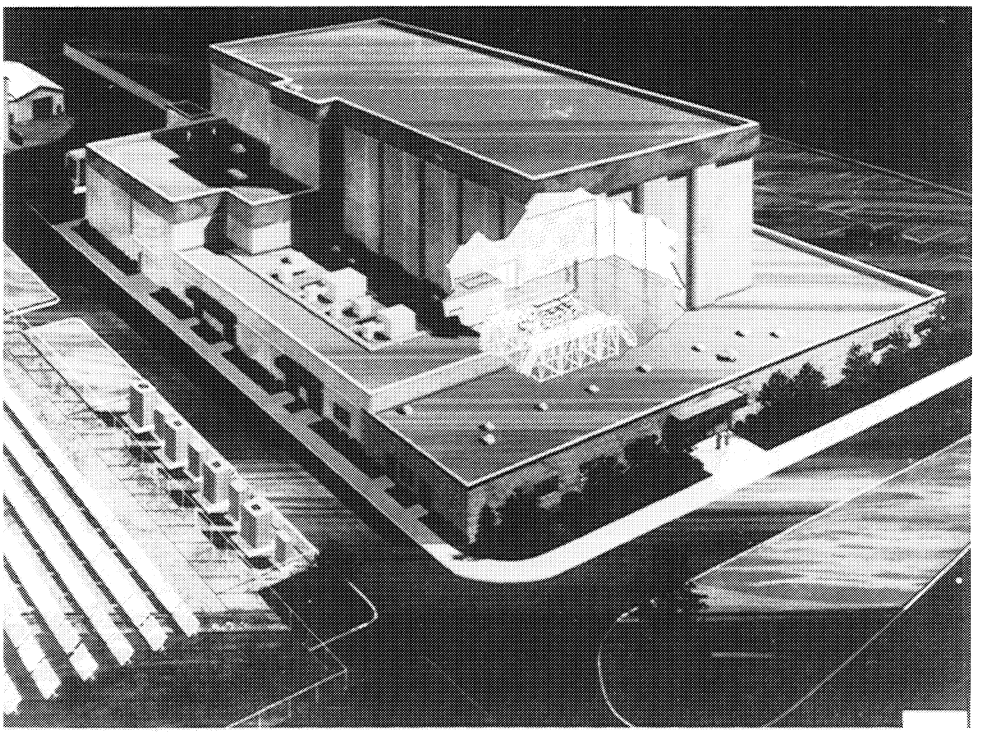

Cutaway PSF depicting the photovoltaic power module under assembly and test.

Solar Array Electrical Simulator Developed

A solar array electrical simulator has been developed at NASA Lewis. The simulator allows the space station electric power system to be tested without the expense and complexity of using an actual photovoltaic array in actual or artificial sunlight.

The one-of-a-kind simulator is designed to simulate the 82-string space station array, nominally rated at 2.65 A, 208 V per string. It provides a dynamic simulation of the nonlinear current-voltage (I–V) characteristics of the actual array and can be programmed to simulate orbital characteristics, including sunrise and sunset transitions, as well as the effects of shadowing and cell failures.

Eighty-two individual current regulators represent the 82 strings of 400 cells in series in the actual array. The regulators are linear regulators using power field-effect transistors. The linear stage provides fast, accurate transient response at the 20-kHz switching frequency of the sequential shunt unit. The I–V characteristic is controlled by a diode function generator circuit. The parameters are based on actual array test data but can be easily altered to simulate different array characteristics.

A dedicated control computer controls the simulator's parameters, monitors operating conditions, and detects faults within the simulator to assure safe, reliable operation. Additionally, an overcurrent fault-protection circuit detects failures in the simulator regulators and prevents the failure from exceeding the safe operating area limits of the hardware. The simulator can be controlled manually by a local touch-screen monitor or an identical remotely located touch-screen monitor or automatically over an IEEE–488 interface.

The equipment is located in three units, plus the remote monitor. A direct-current power supply is the power source for the regulators. A rack contains the string regulators and associated support circuitry and data-monitoring circuits. A console houses the control computer and its interface circuitry. The string regulators use liquid cooling

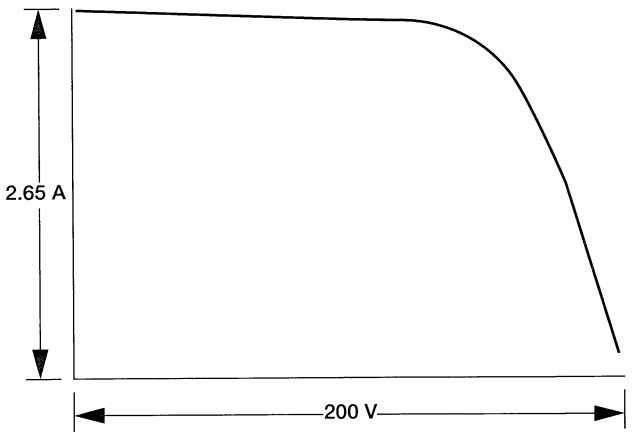

Nominal current-voltage curve for solar array electrical simulator.

to reduce size, audible noise, and air-conditioning load.

The simulator's design and fabrication is being done completely in-house at NASA Lewis. This project is a critical in-line task for the space station that will greatly enhance testing capabilities. Its design was based on solar array simulators built earlier at Lewis to support in-house testing. Test results from breadboard and prototype units have compared closely with flight solar array data, especially with respect to dynamic response and the I–V characteristic. Currently available equipment does not produce a realistic I–V characteristic and has some severe operating range restrictions and a history of frequent failures.

The first unit is undergoing acceptance testing and will be shipped to Loral Space Systems Division to support sequential shunt unit development and engineering-model testing. Two additional units are to be built, tested, and delivered to Rocketdyne, the space station prime contractor, in early 1994.

Lewis contact: Arthur G. Birchenough, (216) 433–6331
Headquarters program office: OSSD

Cryosystem Becomes Operational at Space Power Facility

The Space Power Facility is part of NASA Lewis' Plum Brook Station located near Sandusky, Ohio. Its vacuum chamber is 100 ft in diameter and 122 ft high at the peak of its hemispherical dome. The largest vacuum chamber in the world, the Space Power Facility (SPF), is used to simulate the vacuum of space. It is equipped with a cryosystem to create the cold temperatures of space. This cryosystem furnishes cold nitrogen gas to the surfaces of the cryoshroud. The system was restored to operational status in June 1993 after undergoing rehabilitation and modification. Testing can now be done on the ground to check out large systems that must operate in the space environment.

One of the conditions needed for space simulation, a cold temperature, can be produced in the SPF vacuum chamber by surrounding the test article with cold surfaces called a cryoshroud. A cryoshroud is being built that will be 80 ft long, 40 ft wide, and 23 ft high. The surfaces are made of finned tubes painted black to absorb the heat from the test article. Cold nitrogen gas is pumped through the tubes to cool the surfaces of the cryoshroud.

The scissors-like radiator deployment mechanisms of space station will be tested in the cryoshroud. The folded, stowed radiator will be "soaked" in vacuum at the expected temperature. Then it will be opened up (deployed) within the cold cryoshroud, with lamps on one side to simulate the Sun.

The photovoltaic module of the space station electric power system will also be tested in this cryoshroud. This module consists of the storage batteries, the electric power-conditioning equipment, and the cooling system for this equipment. The cooling system includes the radiator and the pumps that circulate the cooling fluid, which is liquid ammonia. After the module is placed in the cryoshroud, the vacuum and cold of space will be produced and again lamps will simulate the heat of the Sun. The system will be soaked, started, and stopped while its performance is monitored and recorded.

The cryosystem provides the cold nitrogen gas for the cryoshroud zones. The cryosystem was operated successfully in June 1993. During this

operation the system provided nitrogen gas at a temperature of –250 °F to piping loops simulating the cryoshroud zones. The major components of the recirculating gaseous nitrogen portion of the system are two 3000-hp gaseous nitrogen compressors, the gaseous nitrogen heat exchanger, piping, controls, valves, and the cryoshroud zones. The liquid nitrogen portion of the system consists of the loading station, two storage tanks, three pumps, piping, valves, controls, the diffusion pump baffles, and the injector where the liquid nitrogen is sprayed into the gaseous nitrogen stream to make it cold.

Lewis contact: Roger L. Smith, (216) 433–5440
Headquarters program office: OSSD

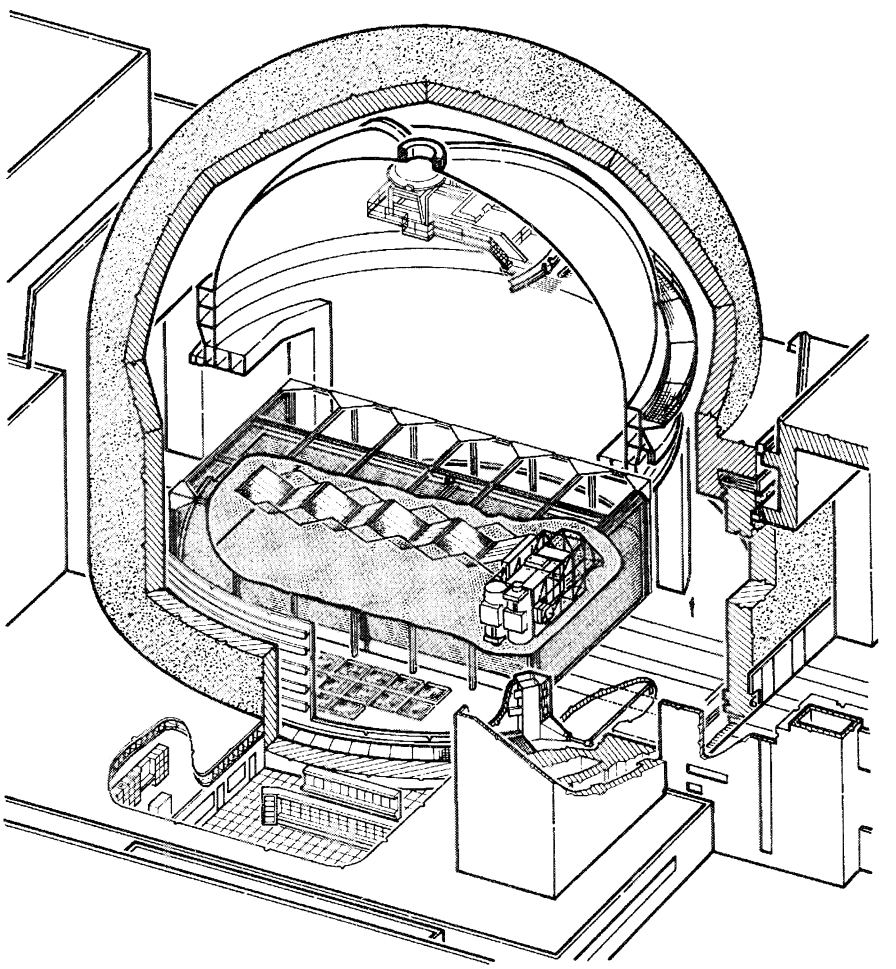

Photovoltaic module with its radiator in Space Power Facility.

Engineering and Computational Support

Electronic and Control Systems

Electromagnetic Interference Test Facility Operated Successfully

The Engineering Directorate has completed the first year of successful operation of its Electromagnetic Interference (EMI) Test Facility. EMI Test Facility staff have issued 12 reports on tests of hardware from major projects, ranging from the Space Acceleration Measurement System (SAMS), used to measure the microgravity environment on SpaceLab missions, to a Russian-manufactured ion thruster brought to NASA Lewis through an interagency agreement.

A portable set of equipment has also been developed for performing most EMI tests (exclusive of radiated susceptibility) at a remote location, when required. This enhanced capability was successfully used in characterizing a prototype plasma contactor, of the type envisioned for use on space station, when operated in a large vacuum chamber. Future tests are planned during which this portable system will be used for testing a laser ignition system, in a research effort to reduce electromagnetic emissions significantly below the levels of conventional high-energy spark ignition sources.

Lewis contact: Noel B. Sargent, (216) 433–2398
Headquarters program office: OACT

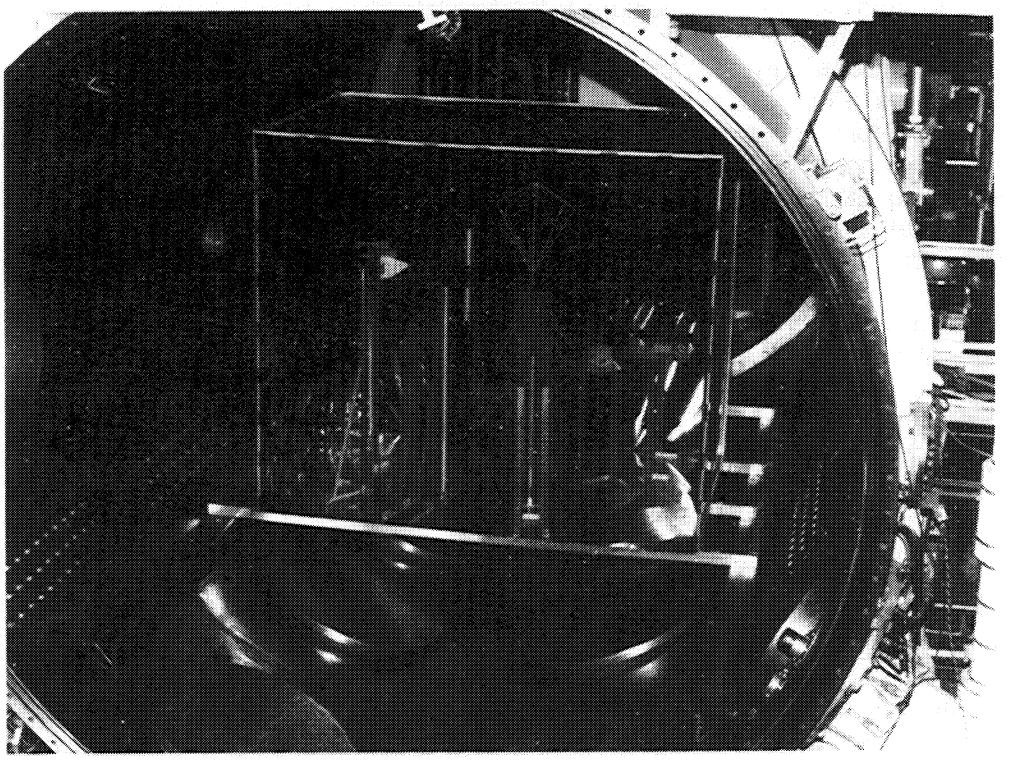

Electromagnetic Interference Test Facility.

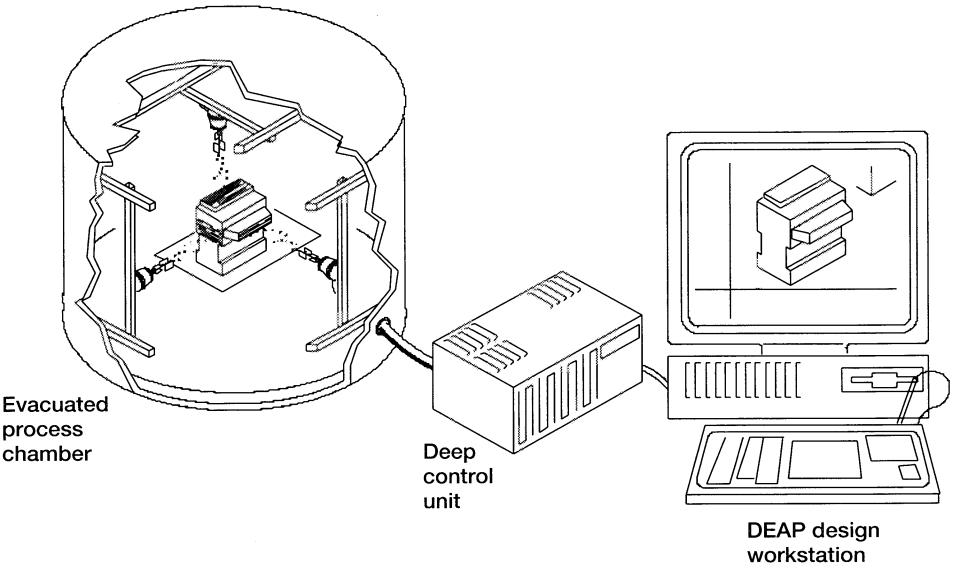

DEAP manufacturing system.

Directional Electrostatic Accretion Process Developed

The directional electrostatic accretion process (DEAP) is a manufacturing technology specifically intended to manufacture metal products for space-based applications from metal resources available in space. The technology is intended to permit future lunar and Martian bases to manufacture their own metal products from raw materials found in space. DEAP technology will be capable of creating free-standing metal forms without the use of molds, dies, or other conventional metalworking tools. It would help eliminate the need to transport large manufacturing facilities into space, thus reducing long-term costs.

The near-term objective of the current project has been to develop key technologies and to create a rudimentary DEAP system that can evolve into an operational manufacturing system. The long-term goal is to develop accretion technology for both space- and Earth-based manufacturing in the 21st century.

Products are formed by depositing tiny droplets of molten metal on a target in a predefined pattern. The layer-upon-layer buildup or "accretion" of these solidified droplets results in a solid product. By precisely controlling the placement of each individual drop, a single system may produce a variety of metal products. The metal droplets are formed by using high-frequency acoustic tone bursts emitted by a highly focused acoustic transducer. This approach eliminates the need for spray nozzles, which are subject to frequent clogging. The placement of the droplets employs electrostatic trajectory control, a technique used by certain ink jet printers.

The first nozzleless acoustic droplet generator was designed and produced for NASA Lewis by Dr. Khuri-Yakub at Stanford University. Since then, an in-house effort has been under way to increase the power output of the design so as to make it more suitable for liquid metal ejection. Current laboratory work involves testing with liquid gallium and indium. A high-temperature device suitable for structural metals such as aluminum is being developed.

The current droplet electrostatic trajectory control uses a computer with an interactive control software package. The droplet impact point may be set by mouse or keyboard input. The computer adjusts the droplet trajectory parameters and ejects the droplet on command. This approach permits experimentation with various accretion patterns.

A space experiment is being considered to validate the use of DEAP in the space environment

and to demonstrate its capability. The space experiment would investigate the behavior of liquid metal accretion in microgravity, where subtle differences in the droplet ejection and impact dynamics have an accumulative effect on the final product.

DEAP is a dual-use technology where ground-based development may lead to commercial uses, as well as space-based applications. DEAP may find applications in microcircuit and micromachine manufacturing, rapid solidification of materials, and a variety of special coating applications. DEAP is inherently modular and can be scaled from simple to large operations in an incremental fashion. Eventually, the process will be able to produce large cast-like products by using large multiaxis arrays. The process can be coupled with laser- or electron-beam technologies and may be suitable for microscopic welding or soldering operations. The process can operate in conjunction with computer-assisted design systems or can employ advanced interactive technologies such as virtual reality.

Lewis contact: Richard C. Oeftering, (216) 433–2285
Headquarters program office: OACT

Structural Systems

TROPIX Spacecraft Needs Dynamic Analysis

TROPIX (Transfer Orbit Plasma Interaction Experiment), a spacecraft to be designed at NASA Lewis, is to serve as a scientific and technical flight experiment. Its mission goals are to significantly increase our knowledge of Earth's magnetosphere and its associated plasma environment in addition to demonstrating solar electric propulsion.

TROPIX is to be launched on an Orbital Sciences Corporation Pegasus XL expendable launch vehicle. This launch vehicle is taken to altitude on an L–1011 aircraft and released and then under its own power places a payload into orbit. These events will impose several different dynamic environments for which the TROPIX spacecraft needs to be structurally certified. Structural certification requires the prediction of structural loads during all phases of launch and on-orbit operations. Accurate loads prediction requires a variety of analytical tools. These tools include SDRC I–DEAS software for creating and postprocessing finite element models, MSC/NASTRAN for finite element analysis, and VAPEPS for assessing the vibroacoustic environment. In addition, these tools will define the environments for structural dynamic and vibroacoustic testing of the spacecraft and scientific packages.

Lewis contacts: Damian R. Ludwiczak, (216) 433–2383;
Mark E. McNelis, (216) 433–8395;
J. Mark Hickman, (216) 433–7105
Headquarters program office: OACT

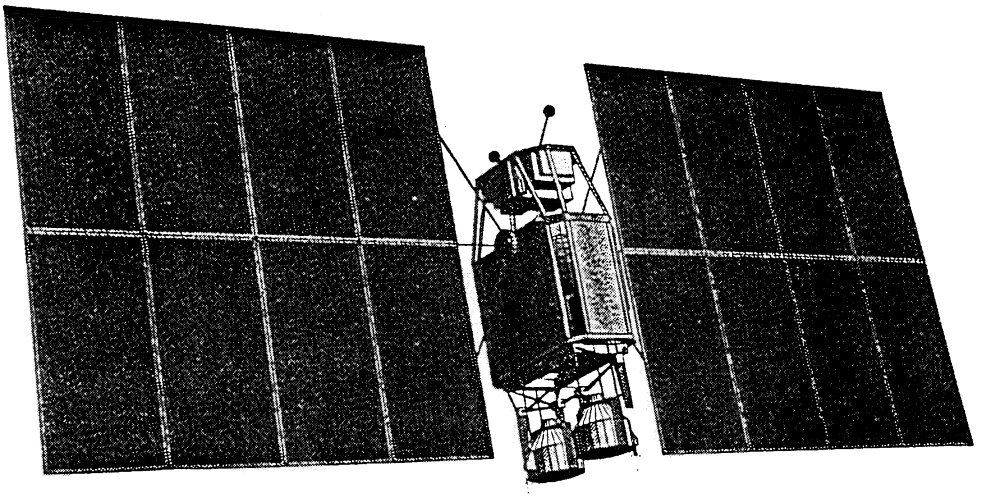

TROPIX spacecraft.

Deployable Solar Array Mast for Space Station Strength Tested

The space station photovoltaic arrays are supported by a deployable mast called FASTMast. The structure, made up of hinged longerons, fiberglass battens, and steel cable diagonal members, enables stowage into a compact canister for launch into space. As the FASTMast is deployed on-orbit from the canister, each bay opens and is stabilized by the fiberglass battens, which are flexed to preload the hinge joints. The cable diagonals, which are unloaded while in the canister, become tension members due to batten preload at each joint. These design features allow the FASTMast to go from a compact stowage configuration to a fully deployed mast, but they also introduce nonlinearities that are difficult to analyze. To assess the strength capabilities and failure modes, a series of tests was devised for a three-bay segment of the 32-bay flight development hardware. The fully instrumented hardware was hydraulically loaded under three types of loading conditions to verify strength and stiffness characteristics of the structure.

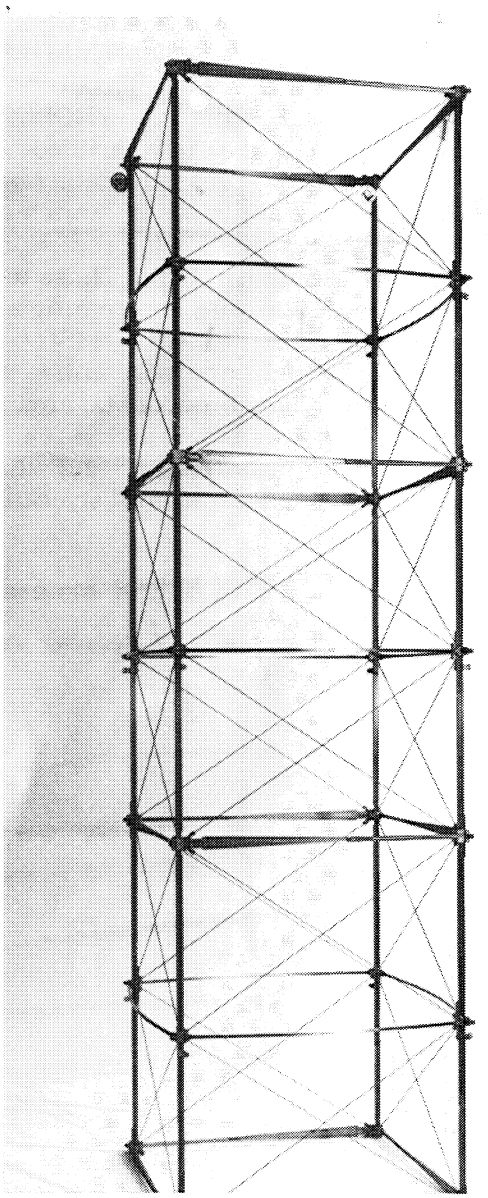

Three-bay segment of deployable solar array mast.

A test tower was built to support the three-bay FASTMast test article and reconfigured to act as a catch-frame in the event of collapse. This fixture also served to mount instrumentation devices for measuring deflections. A rigid top-plate fixture was attached to the test article for the purpose of attaching load devices.

An axial load test was devised to simulate the longeron compression induced by on-orbit bending loads. The goal of this test was to show that the longerons could withstand the full ultimate compressive load without local instability at a hinge joint. The ultimate load tested was below the Euler buckling load of an individual longeron member. No local instability was observed at the target load.

A torsion and axial load test was then performed to further demonstrate that the combined loads would not cause local instability. Torsion loads are reacted by the cable diagonal members connected at the longeron elbow joints. A limit torsion load was applied while the axial compression load through the longerons was ramped to an ultimate load level. This test successfully demonstrated that no interaction occurs for torsion load levels in the linear region of behavior.

Applying a shear load was considered very critical for determining strength capability. Recent on-orbit coupled loads analyses indicate that shear loads may be greater than previously anticipated. Because shear load is reacted through the diagonal members, alternating diagonals will eventually go slack when compression in these members overcomes the initial tension preload. The test demonstrated this characteristic. A nonlinear load-versus-displacement curve showed a dramatic reduction in stiffness beyond the point of inflection. The load was incremented to 2.5 times the design limit load. The mast sustained the load without structural failure.

Supporting analysis was performed for all the test cases by using a detailed finite element model for nonlinear NASTRAN solutions. The trends seen in the testing were also evident in the analysis results. On the basis of these results the model has been correlated for further studies. The ongoing effort for the first quarter of fiscal 1994 is to define the interaction between bending moment and transverse shear loads. This includes testing and analysis.

Lewis contacts: Joseph M. Roche, (216) 433–2575; James E. Hunter, (216) 433–2418
Headquarters program office: OSSD

Computational Support

LIBRA Is Software Architecture for an Electronic Library

The many imaging technologies available today for the capture and display of scientific data are creating new kinds of information that place major demands on infrastructure support. High-speed photography, high-resolution scanning and display devices, digital image-processing techniques for enhancing and restoring images, sophisticated graphics, and results of scientific visualizations are just a few of these technologies. Images and video are as valuable as text and numeric data in day-to-day research.

NASA employs many of these technologies in research areas such as materials science, space experiments, computational fluid dynamics, and thermodynamics. A significant amount of time is invested in capturing and processing data and from it creating visual information ("informedia") that is vital to the research community. But because of its very nature, informedia is not widely distributed to other research organizations, industry, or universities. It is hard to say how much duplicate research is done because of this inaccessibility.

At NASA Lewis, the Lewis Image Browsing and Retrieval Archive (LIBRA) Project is an effort to create an informedia library. The goal is to provide direct access to geographically disperse informedia through an intuitive graphical user interface to support scientific and interdisciplinary research. Meeting this goal requires easy and intuitive access to heterogeneous distributed information repositories, specialized search and retrieval techniques, mass storage, and high-speed, high-capacity networks.

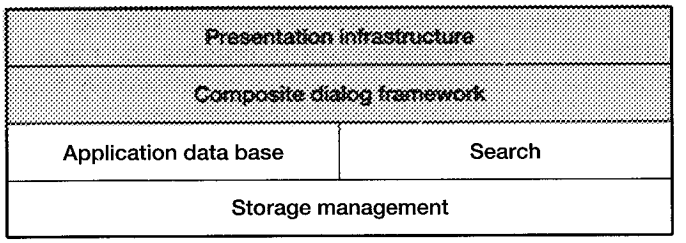

Library architecture.

The current phase of the LIBRA Project is focused on storing and retrieving images. However, once implemented, the informedia library can easily be extended to store and retrieve media of any type, largely owing to the object-oriented design of the library. The library is composed of five modules. The goal of the design was to isolate the presentation of the library contents from the application as much as possible so that changes in the presentation impact the application minimally and vice versa. Object-oriented analysis and design techniques were used to design each module. The graphical user interface is divided into two modules, the presentation infrastructure and the composite dialog framework. The presentation infrastructure models the static portion of the screen designs only. TeleUse, a user interface management system, was used to design these static screens and to create the presentation classes. The composite dialog module is a reusable framework for implementing the functionality behind the presentation screens. This framework increases the maintainability of the user interface by encapsulating the callback mechanisms required into higher level abstractions and reduces the impact of presentation changes on the application.

The full-text search module provides the interface between Personal Library Software (PLS) and the application data base and storage management software. PLS, an off-the-shelf software package, supports indexing and full-text searching of textual information. Images will be stored with abstracts describing the image. The ability to search text rather than key field information (i.e., there is no imposed vocabulary) provides a more flexible and accurate mechanism for identifying and retrieving the images. An electronic library is

only as useful as the information that can be found. It is vitally important to employ the most sophisticated search techniques to effectively find any and all relevant information available.

The application data base was implemented by using ObjectStore from Object Design. ObjectStore is an object-oriented data base management system that provides the facilities of a conventional system, such as persistence, concurrency control, transaction management, recovery, query language, and performance, as well as additional capabilities to support the object-oriented paradigm. The key concepts for the object-oriented environment are data abstraction, inheritance, encapsulation, and polymorphism. These concepts provide a model well suited to developing applications involving complex data structures, complex data relationships, and distributed environments, such as required by an electronic library. A library metaphor was used to design the application data base. That is, the data base is the repository of books, chapters, sections, etc. The granularity of the metaphor can be defined to suit the application. The library metaphor was also used for presenting the informedia as well because it is a universal concept that is intuitive and easily used.

Lewis contact: Maureen F. Cain, (216) 433–8928
Headquarters program office: OA

Compact Experimental Data Analysis and Reduction System Developed

CEDARS is a system developed for the workstation to support the postprocessing of data recorded on the real-time Escort systems in the test facilities at NASA Lewis. The CEDARS system imports or collects data from these systems, stores the data in a data base, has a general processing capability, and includes a graphics interface that integrates processed data with plot specifications in interactive and batch mode.

The CEDARS concept was originally developed for the postprocessing of data from classified Escort tests and was intended to be a stand-alone system dedicated to the reduction, analysis, and publication of experimental data. The system has recently been configured to provide a postprocessing environment for general-purpose analysis of test facility data.

Although CEDARS provides full-service data reduction, its primary element is the graphical interface. CEDARS provides a point-and-click style of interactive plotting programs with two- and three-dimensional plots, black-and-white display, color plots, color display, image capabilities, and hard copy. CEDARS also utilizes PV–WAVE visualization software from Visual Numerics. In addition to providing workstation and device portability, PV–WAVE has a wide range of graphics capabilities as well as interactive and programmed operating modes.

A data base utilizing the bdx subroutine library developed at NASA Lewis is the machine-independent mechanism for storing CEDARS data. This interim storage method will eventually be replaced by the recently purchased commercial relational data base package INTERBASE marketed by Borland.

Consultation, programming support, and training is provided for CEDARS applications. CEDARS is currently supported on Sun, SGI, and DEC workstations, either stand-alone or networked, and can be operated locally or from any X-terminal. The minimum version of the operating systems required is as follows: Sun Os 4.0.3 for Sun3; Sun Os 4.1.1 for Sun4/IPC; IRIX 3.3 for SGI; and Ultrix 4.1 for DECstation. The recommended memory requirement is 32 megabytes.

Version 3.1 or higher of PV–WAVE is required. This version is available for the above workstations on a central file server. The CEDARS software is also available on a file server. These programs may be downloaded when secure processing is required.

Lewis contact: June E. Thompson, (216) 433–5233
Headquarters program office: OA

Lewis Advanced Cluster Environment Installed

Approximately one year ago, a cluster of high-end workstations was installed to form the Lewis Advanced Cluster Environment (LACE). LACE, which is located in Lewis' Advanced Computational Concepts Laboratory, consists of 32 interconnected IBM RS/6000 Model 560 compute servers and a Model 970 file server. All of the machines can be used to run parallelized code specifically written to run across multiple processors. The combined processing power of the cluster equals about one gigaflop, or one billion floating-point operations per second.

The LACE support team is working with the High-Performance Computing and Communications Program (HPCCP) to provide testbed systems for the exploration of massively parallel architectures. Thus, the cluster will serve as a testbed for the design, modification, and testing of code to be used in a parallel as well as a distributed computing environment. The LACE project will help in determining which computing platforms are suited to different types of code at Lewis. Today's emerging massively parallel architectures differ in processor types and memory; therefore, one platform may outperform another for some codes but not for others. The cluster is a stepping stone to IBM's next generation of massively parallel systems.

Lewis will use the new computing environment for jet propulsion modeling, computational chemistry, structural and turbine blade analysis, and fluid dynamics. LACE will allow researchers to explore new ways of performing computational research more efficiently and economically. Calculations can be performed on individual processors and then combined for a single, final result. The cluster can also be combined with different platform architectures to solve problems requiring various levels of power or diverse capabilities.

Another use of the cluster will be to create a batch/interactive environment in which to test some of the applications and codes currently running on Lewis' supercomputers and midrange computing platforms. If some codes can be offloaded to workstations, it will be more cost effective to purchase additional clusters for production use, reserving Lewis' supercomputers for the jobs that they perform best.

Lewis contact: Karen A. Pischel, (216) 433–5198
Headquarters program office: OA

Telecommuting With ISDN Studied

It is widely accepted that personal communications services represent a family of applications featuring remote access to network-based services. Under this broad description, "telecommuting" with the Integrated Services Digital Network (ISDN) is now an accepted concept. Telecommuting can provide a person who works at home or in a satellite office the ability to access, use, and send back files to a corporate computing environment at speeds up to 64 kb/sec by using public data networks. With data exchanged at rates of 64 kbs, performance is much improved over modems that are limited to 14.4 kbs.

NASA Lewis is actively investigating the work-at-home concept using ISDN. This perspective means that the computer workstation will become the new communications center, combining many existing communications media with new ones while creating new paradigms for the expression and sharing of ideas. People will gain new freedom in where they work and how they access information. ISDN represents both the logical evolution of communications technology and the convergence of interactive user computing with work environments spanning large geographies. Telecommuting reduces the need for expensive and environmentally polluting travel. It is currently a law in some parts of the country to alleviate problems created by traffic and pollution.

Pilot users have been identified on a variety of platforms from personal computers to high-end workstations to implement this concept on a laboratory-wide scale. Equipment has been procured for conducting a controlled study. A survey on the sociological impact of this new work atmosphere is planned. The ISDN lines, provided by Ameritech, will terminate in a terminal server on the laboratory and will interface to the campus backbone, thereby providing complete network access to the employee working at home. The employee will also have access to the Lewis telephone system through a digital phone that is provided as an integral part of the ISDN system. Feasibility of providing desktop videoconferencing will be investigated in these trials by using state-of-the-art data compression techniques. Results of the study will be available by December 1993.

Lewis contact: Fredric N. Goldberg, (216) 433–5074
Headquarters program office: OA

Lewis Advanced Communications Testbed Built

An asynchronous transfer mode (ATM) communications testbed has been built at NASA Lewis to assist in the analysis and development of a highly reliable data communications backbone and associated services in support of multimedia and other high-performance computing architectures. This technology is aimed at providing data throughput superior to any available today. Any deficiencies perceived today in media utilization are expected to be overcome. As with any new technology the primary objective in this testbed will be to investigate any shortfalls in this new endeavor.

The testbed has two Fore Systems' ASX–100 switches with each having four interfaces on a 100-Mbs port and four DS3 (45 Mbs) interfaces. The four DS3 ports on each of the switches are connected to each other to elicit an aggregate 180-Mbs path between the switches. Ten Sbus adapter cards have been procured for Sun-stations and connected to the SBus backplane of the workstations to implement the SBus slave interface protocol. The SBus adapters support Berkeley Socket interfaces, which give application access to transmission control protocol/internet protocol (TCP/IP) over the ATM testbed and Fore's proprietary application programming interface through which applications can access various asynchronous adaptation layers. Users have been identified and a fiber path to the individual users has been established and tested. The switches support standard simple network management protocol (SNMP) agents for network management.

A project has begun to establish metrics and conduct performance measurements in order to generate empirical data on quality of service requirements. The metrics range from throughput to cell loss, cell delay jitter, and traffic distribution. The second aspect of this study is designed to investigate the ease of distributed file systems using network and Andrews file systems on the ATM platform. Preliminary review of the Fore-supplied proprietary application programming interface indicates that the implementation of network and distributed file systems over ATM is straightforward. Further study is planned on the specifics of the Fore-supplied SNMP and its associated management procedures to understand and address issues of internetworking of SNMP with Open Systems Interconnects' connection management internet protocol. Lastly, considering the testbed as a backbone provider, the project team is looking into traffic studies to analyze performance with heterogenous sources and a multiprotocol environment. The team is also studying desktop video conferencing systems using INSOFT's Communique! product over RasterOps hardware. The testbed also supports the Grand Challenge initiatives in providing a high-bandwidth path to effect distributed and remote computing.

Lewis contact: Jennifer L. Lazbin, (216) 433–8252
Headquarters program office: OA

NASA Lewis Starts High-Performance Computing K–12 Project

NASA Lewis has started a K–12 project as part of the High-Performance Computing and Communications Program (HPCCP). The goal as well as the challenge of the project is to introduce HPCCP technology into the K–12 school system for the benefit of mathematics, science, and engineering studies.

The Lewis pilot K–12 project comprises high schools of varying computer literacy and diverse settings—Barberton, Fairview Park, Cleveland East Tech, and Garrett Morgan School of Science. All pilot schools received a MacIntosh Quadra 800, a Hewlett Packard printer, and a starter suite of software packages for the MacIntosh. The NASA Lewis Teacher Resource Center also received a MacIntosh and an Iris Indigo for Internet access. NASA Lewis has provided a 56-kb dedicated link to Fairview High School to support access to the Internet. A router is in place at the remote end to effect OARnet access to the school as a Lewis subnet. NASA Lewis has also provided an Iris Indigo to Fairview High School to complement an existing Novell IPX local area network at the school.

Teacher training was a focal point of the Lewis K–12 project. To create the proper training environment and to make the training germane to the teachers, Lewis hired two area high school teachers for the summer of 1993. One of the teachers was sent to Ames, Iowa, to attend John Ziebarth's three-week training class. The Iowa program is an established high-performance computing class for high school teachers. By combining this

knowledge and the efforts of NASA and RMS Technologies, Inc., personnel, a two-week training course was created. Twelve teachers from the area schools were trained. The classes highlighted instruction in Fortran, MacIntosh basics, Internet, Unix, Visualization, MAPLE, and the National Education Supercomputer at Lawrence Livermore National Laboratory.

To bring an aeronautics focus to the Lewis K–12 program, an adopt-a-class project was started during the training. Thirteen Lewis researchers came to a training session. The researchers discussed with the teachers various ways to begin formal plans for the Lewis people to adopt a class and to begin the process of defining a project for the 1993–94 school year.

The fiscal 1994 Lewis K–12 plan will build upon the preceding year's efforts. The plan calls for adding a MacIntosh at each of the pilot schools where appropriate and bringing four or five new schools into the program.

Lewis contact: Gregory J. Follen, (216) 433–5193
Headquarters program office: OA

Lewis Research Academy

Turbomachinery Flows Modeled

A mathematical analysis has yielded a set of equations governing the conceptual flow model currently used to design turbomachinery blading. These equations govern the time-averaged flow state existing within a typical passage of a blade row embedded in a multistage machine. These equations have formed the basis of a series of computer codes, some of which have been written to operate on parallel computing platforms. To date, these codes have been used to examine radial, mixed, and axial flow turbines and axial and centrifugal compressors. These simulations addressed subsonic, transonic, and supersonic machines.

Recently, these three-dimensional viscous flow codes have been coupled to an unsteady flow code. The combination of codes will allow examination of the performance of a blade row as well as the unsteady air loads caused by flow distortions introduced by neighboring blade rows. The calibration of this unsteady code is currently under way, and a report outlining the mathematical development of the unsteady code is in progress.

Lewis contact: Dr. John J. Adamczyk, (216) 433–5829
Headquarters program office: OA

Adverse-Pressure-Gradient Boundary Layer Transition Analysis Incorporates Viscous Effects

Predicting boundary layer transition is one of the major unresolved issues in aircraft design. This phenomenon is commonly studied experimentally by artificially introducing relatively two-dimensional, small-amplitude, single-frequency disturbances in the flow with an excitation device. These disturbances are initially well described by linear stability theory, and their two-dimensional linear behavior can persist over long streamwise distances when the excitation levels are sufficiently small. But the disturbances usually become three-dimensional and nonlinear at sufficiently large downstream distances. The initial nonlinear stage is reasonably well understood and is associated with a resonant-triad interaction between a fundamental two-dimensional mode and a pair of oblique subharmonic modes. This stage is effectively a parametric resonance regime because the oblique modes do not affect the plane wave. However, a nonlinear stage ultimately will develop where the waves in the resonant triad are fully interacting.

Most experiments are carried out on a thin, flat plate carefully aligned with the upstream flow. Transition in technological devices, however, often occurs in regions with adverse-pressure gradients, and the onset of transition usually occurs about four or five wavelengths upstream of the resulting transition point. In an adverse-pressure-gradient situation the linear instability waves are essentially inviscid instabilities of the Rayleigh type. A previously worked out (ref. 1) asymptotic analysis of the fully interactive nonlinear stage for this flow situation has now been extended (ref. 2) to incorporate viscous effects and to allow the fundamental disturbance to have a larger initial amplitude so that it becomes strongly nonlinear before or just as the parametric resonance stage occurs.

The unsteady flow evolves through a number of different stages. The wave interaction is initially of the parametric resonance type, which enhances the spatial growth rate of the subharmonic but leaves that of the fundamental unaffected, with both components essentially being linear. As the fundamental undergoes nonlinear saturation due to self-interaction effects, the subharmonic evolution becomes controlled by the parametric resonance effects and occurs on a shorter streamwise scale than that of the fundamental. The subharmonic amplitude continues to increase during this nonlinear-fundamental stage, even when the fundamental amplitude saturates, and it eventually becomes large enough to influence the fundamental. This leads to a new, fully coupled stage of development in which all waves evolve on the same shorter streamwise length scale and in which viscous effects are unimportant.

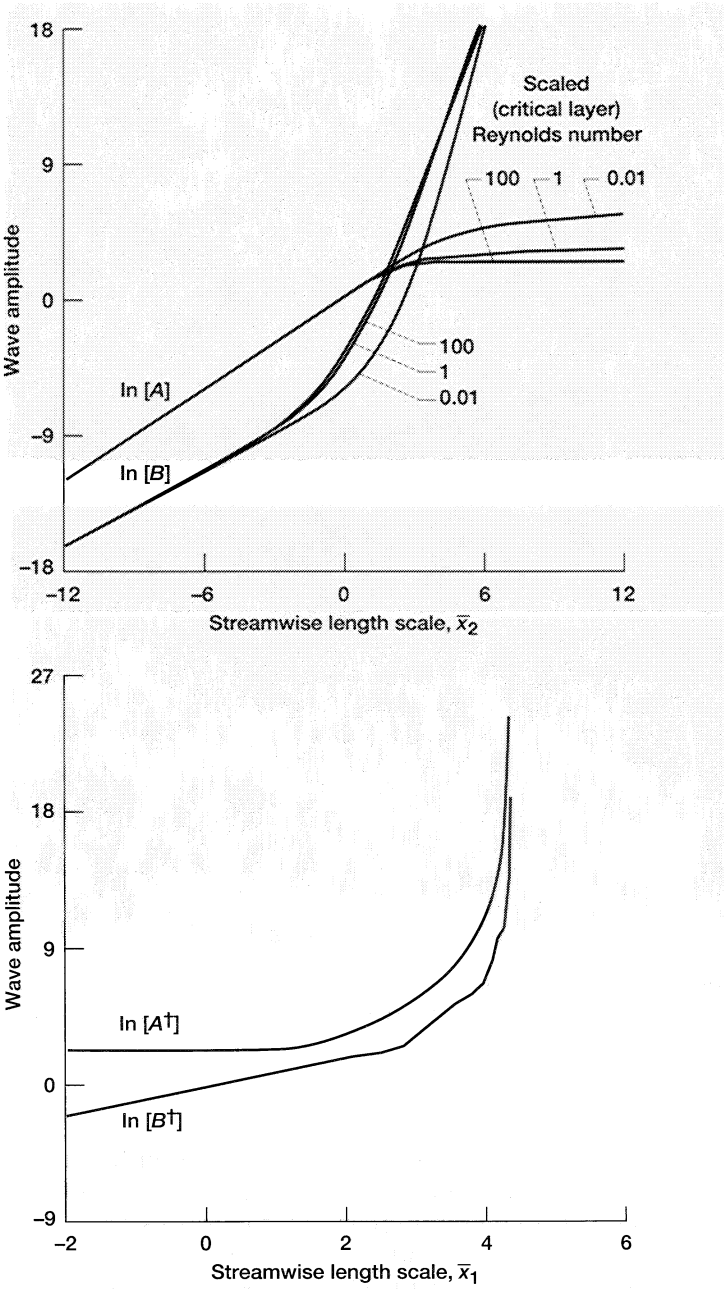

Streamwise evolution of scaled fundamental and subharmonic amplitudes, A and B, in parametric resonance stage (top) and of rescaled fundamental and subharmonic amplitudes in fully coupled stage (bottom).

References

1. Goldstein, M.E.; and Lee, S.S.: Fully Coupled Resonant-Triad Interaction in an Adverse-Pressure-Gradient Boundary Layer. J. Fluid Mech., vol. 245, 1992, pp. 523–551.

2. Wundrow, D.W.; Hultgren, L.S.; and Goldstein, M.E.: Interaction of Oblique Instability Waves With a Nonlinear Plane Wave. To appear in J. Fluid. Mech. (1993).

Lewis contact: Dr. Lennart S. Hultgren, (216) 433–6070
Headquarters program office: OA

Computational Aeroacoustics Studied

Computational aeroacoustics is concerned with predicting the aerodynamically generated sound from first principles, starting from the time-dependent differential equations. At NASA Lewis jet noise is emphasized because it is a barrier to the development of high-speed civil transport. The sound source is given by the fluctuations in the flow field. Large-eddy simulations are used to obtain the acoustically efficient large scales while modeling the unresolved smaller scales. Because the objective here is to obtain the correct physical fluctuations in the flow field, special attention must be paid to the algorithm used and to the boundary condition.

A snapshot of the vorticity field for a Mach 1.5 jet with random inflow disturbances demonstrates the "wave like" nature of large-scale structure in a supersonic jet. A snapshot showing how the Reynolds stress ρ_{uu}, which is the dominant sound source, fluctuates at a Strouhal number of 0.5 demonstrates the ability to capture the sound source directly by computation. Several approaches are adopted to predict the far-field sound resulting from the calculated source. These approaches include acoustic analogy, Kirchhoff's method, and finite differencing.

Lewis contact: Dr. Reda R. Mankbadi, (216) 433–8569
Headquarters program office: OA

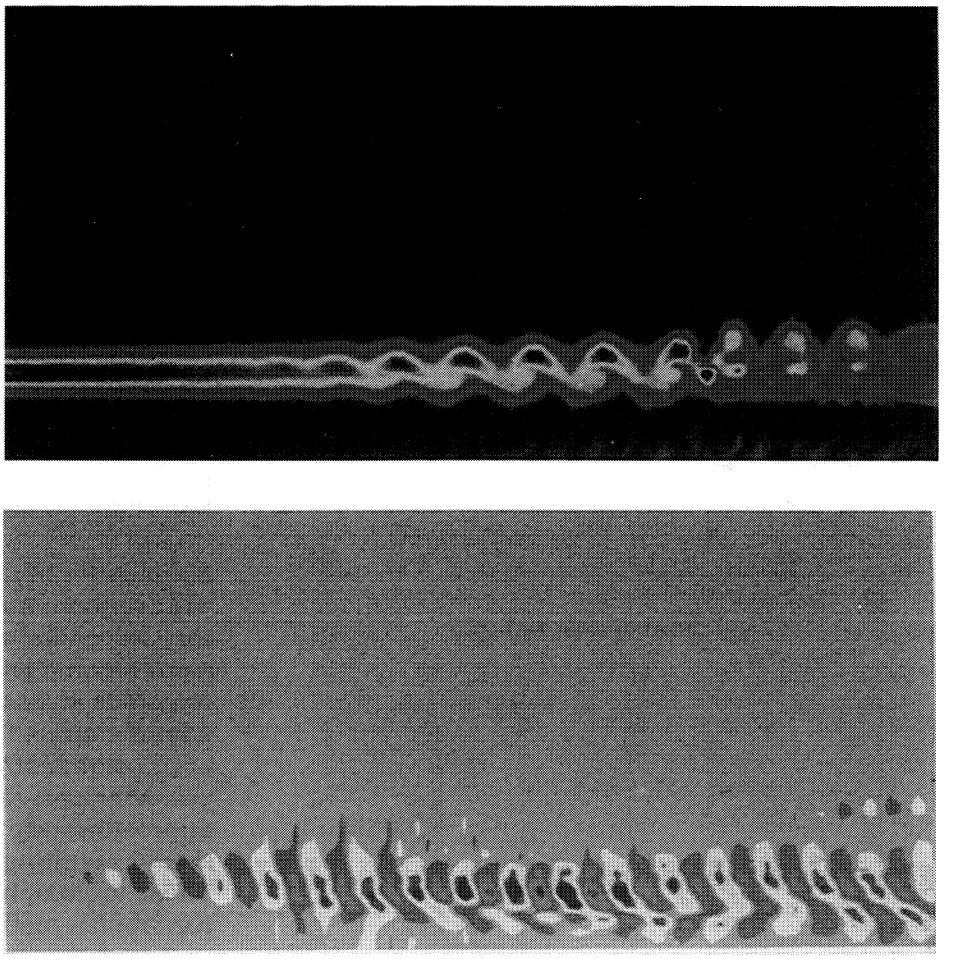

Vorticity magnitude for Mach 1.5 jet with random inflow disturbances. Reynolds stress ρ_{uu} at Strouhal number of 0.5.

Analysis Predicts Refractive Index Effects on Radiation Heat Transfer in Semitransparent Materials

Some ceramic materials being developed and evaluated for high-temperature applications are partially transparent to radiant energy. Infrared and visible radiation from high-temperature surroundings, such as in a combustion chamber, penetrates into the material, heating it internally. Because temperatures in the material are elevated, internal energy emission becomes significant. This is especially true for materials with high refractive indices, since internal emission depends on the square of the refractive index. In addition, the energy transfer within the material depends on internal radiant absorption and scattering and on heat conduction. As a result, radiant energy can affect internal temperatures of some ceramic engine parts and coatings that partially transmit radiation in portions of the wavelength spectrum. This property also applies to other types of materials, such as lithium fluoride used for high-temperature thermal storage.

Internal temperature distributions and heat flows in partially transmitting materials are being predicted by radiative heat transfer analysis. This is a continuing in-house research effort. In our most recent work radiation combined with heat conduction is analyzed in composite plane layers with refractive indices typical of ceramic materials. Each outside boundary is heated by differing amounts of radiation and convection, and the

effect of interface reflections is included. Because the refractive index is larger than 1, there are total internal reflections at the boundaries for some energy directed outward from within the layer. The reflections distribute energy within the layer and considerably influence the temperature distribution.

Results have been obtained for composites with as many as three layers that are either gray or have two- or three-band spectral variations of the absorption coefficient. A ceramic layer reinforced by another material was simulated, and the behavior of a ceramic coating used to protect another ceramic was examined. Various amounts of isotropic scattering were included to simulate internal reflections within the ceramic due to a granular or reinforcing structure. The solutions provided temperature distributions that show thermal performance and can be used to estimate thermal stresses.

The surfaces and interfaces are assumed to be diffuse. Some ceramics may have a smooth surface that reflects in a mirror-like fashion, so that a directionality is associated with reflected and transmitted rays. This effect was examined for the basic case of a layer at uniform temperature. The spectral absorptance of the layer differed from the diffuse results only when the layer was rather optically thin.

Some recent work has further developed the two-flux and diffusion methods to provide a simplified analysis including refractive index effects. Spectral models have been developed for both methods, and calculations for both the temperature distribution and radiative transfer compare well with exact numerical solutions. The two-flux model was found easier to evaluate if the layer is somewhat optically thin. The diffusion model applies accurately only in an optically thick region. A hybrid model is being developed where the two-flux model is used in optically thin spectral regions, and diffusion is applied in the optically thick regions. Preliminary calculations show good comparisons with exact numerical solutions.

Bibliography

Siegel, R.; and Spuckler, C.M.: Refractive Index Effect When Specifying Diffuse or Specular Surfaces for a Radiating Layer. To be published in J. Heat Transfer, 1994.

Siegel, R.; and Spuckler, C. M.: Approximate Solution Methods for Spectral Radiative Transfer in High Refractive Index Layers. Int. J. Heat Mass Transfer, vol. 37, Mar. 1994.

Spuckler, C.M.; and Siegel, R: Refractive Index Effects on Radiative Behavior of a Heated Absorbing-Emitting Layer. J. Thermophys. Heat Transfer, vol. 6, no. 4, Oct-Dec. 1992, pp. 596–604.

Spuckler, C.M.; and Siegel, R: Refractive Index and Scattering Effects on Radiative Behavior of a Semitransparent Layer. J. Thermophys. Heat Transfer, vol. 7, no. 2, Apr.-June, 1993, pp. 302–310.

Spuckler, C.M.; and Siegel, R.: Refractive Index and Scattering Effects on Radiation in a Semitransparent Laminated Layer. To be published in J. Thermophys. Heat Transfer, 1994.

Lewis contact: Dr. Robert Siegel, (216) 433–5831
Headquarters program office: OA

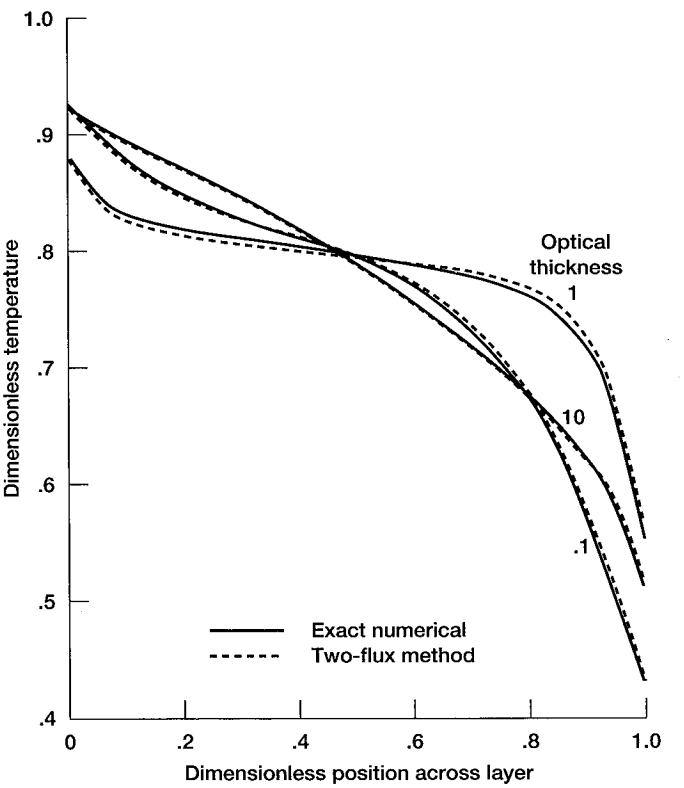

Temperatures predicted by two-flux model compared with exact numerical solution in a gray layer with refractive index of 2.

New Computational Techniques Predict Energy of Defects

A great deal of progress has been made in developing quantum mechanical techniques for calculating the mechanical properties of real materials for static geometries. However, these techniques have not reached the point where calculation of configurational energy minimization, dynamic effects, and thermal effects can be accomplished in reasonable computing time. Consequently, NASA Lewis has been developing new semi-empirical methods that accurately predict the energy of defects and can be used efficiently to accomplish the latter goals.

Different classes of materials, such as metals, semiconductors, and ceramics, require different approaches because of bonding differences. Lewis is developing techniques that build on our previous discoveries of the universal binding energy equation and on the similarities between these different classes. At this point many properties of metals and semiconductors have been successfully predicted, and the approaches have been used to calculate alloy properties. Current research in extending the techniques has concentrated on methods for including thermal effects, which will also enable the prediction of phase diagrams in alloys and the development of configurational energy minimization techniques.

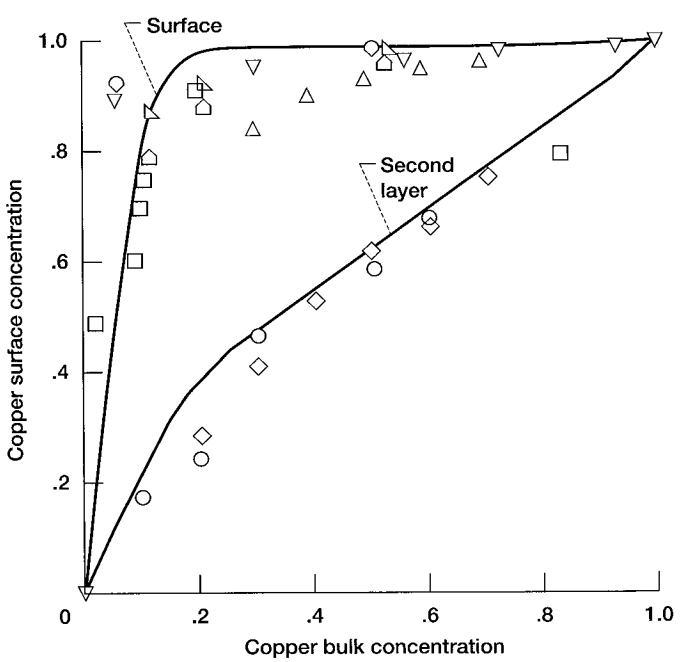

Surface segregation in binary alloys: Copper surface and second-layer concentrations as function of bulk concentration for copper-nickel alloy above phase separation temperature—predicted by NASA Lewis method (curves) and measured in various experiments (data points).

Bibliography

Good, B.; Bozzolo, G.; and Ferrante, J.: Surface Segregation in Cu-Ni Alloys. Phys. Review B, vol. 48, no. 24, Dec. 15, 1993, pp. 18 284–18 287.

Kobistek, R.J., et al.; Multilayer Relaxation and Structure of Ordered Alloys. To be published in Surface Science, 1994.

Lewis contact: Dr. John Ferrante, (216) 433–6069

Headquarters program office: OA

Technology Transfer and Utilization

Technology Transfer

Carbide Site Competition Epitaxy Disclosed to Three Companies

Members of the NASA Lewis High-Temperature Integrated Electronics and Sensors (HTIES) team have recently transferred a major technological advancement in a rapidly emerging semiconductor field to three U.S. companies. The advancement, called carbide site competition epitaxy, was disclosed to Westinghouse, General Electric, and Cree Research, Inc., for use in their silicon carbide (SiC) semiconductor electronics efforts.

All three companies are developing SiC electronics for use in harsh conditions where silicon, the semiconductor used in nearly all of today's electronics, cannot function. Silicon carbide's demonstrated ability to function under extreme high-temperature (as high as 600 °C (1200 °F)), high-power, and/or high-radiation conditions will enable significant improvements to a far-ranging variety of commercial applications and systems. These range from improved high-voltage switching for more efficient electric vehicles and energy savings in public electric power distribution to more powerful microwave electronics for radar and cellular communications to cleaner burning more fuel-efficient jet aircraft and automobile engines. According to GE, "SiC electronics for high-temperature controls should reduce cooling system weight and associated power loss for distributed controls that will increase [jet] engine maintainability and survivability." Silicon carbide electronics will also figure into a variety of NASA and Department of Defense space and aeronautics missions, from planetary probes needing to withstand high-radiation space environments and Venus' scorching atmosphere to advanced supersonic and hypersonic aerospace vehicles.

Although Cree Research is already marketing a family of limited-capability silicon carbide devices (most notably the only blue-light-emitting diodes on the market today), SiC semiconductor electronics technology is relatively immature compared with well-developed silicon-based electronics. A number of technical issues remain to be solved before SiC devices are ready for widespread incorporation into the above-mentioned systems. One such limiting issue involves the purity and quality of the semiconductor crystal, which naturally affects the performance and capabilities of SiC semiconductor devices. The site competition epitaxy technology developed by NASA Lewis offers much greater control of SiC crystal purity, to the point where vastly improved SiC devices are now possible. In a NASA Lewis demonstration of the technology, the new growth process was used to fabricate SiC diodes that operate at 2000 V, the highest voltage ever recorded for silicon carbide devices. (See page 6 for current-voltage rectifying characteristics.)

This superior crystal growth technology was transferred to Westinghouse, General Electric, and Cree Research, Inc., in early 1993. Since that time Westinghouse has been using the technique on a regular basis to produce most of its prototype SiC electronic devices, including record-breaking SiC microwave devices. Cree Research has also expressed interest in using the technology, which is in the process of being patented through the Ohio Aerospace Institute.

Lewis contacts: Dr. Philip G. Neudeck, (216) 433–8902; Dr. David J. Larkin, (216) 433–8718
Headquarters program office: OACT

Turbomachinery Design and Analysis Codes Transferred to Smaller Engineering Companies and Consultants

Spinoff of NASA aeronautics and space research has traditionally been a great benefit to small enterprises. Many existing products of small companies have been historically developed through the time-honored, cut-and-try approach to solving engineering problems. With the advent of modern computers and the development of sophisticated computer codes for analysis and design of many engineering components, small companies are seeking to upgrade their product performance by applying these more sophisticated

methods. Because developing computer codes is expensive, these companies have looked to NASA to provide the necessary analysis and design tools. It is not always within these companies' means to utilize the most advanced computational tools, which may require expensive computational resources. Thus, they must rely on less sophisticated tools.

Analysis and design tools developed by NASA that do not require advanced computers are sufficiently sophisticated to guide a designer in improving the performance of a turbomachinery component. These codes may consist of correlations for losses based on an existing understanding of the flow physics or may model most but not all of the relevant physics of the component. In either case their use has allowed designers at smaller companies and the consultants who serve some of those companies to significantly improve their product offering.

These types of codes have been used to improve the performance of a fan in a small respirator unit, to analyze the flow in a rotating heart pump, to analyze the jib and mainsail flow for a racing yacht, and to analyze the airflow in jet engine compressors.

Lewis contact: Jerry R. Wood, (216) 433-5880
Headquarters program office: OA

Icing Computer Codes Support Industry's Stated Needs

The Icing & Cryogenic Technology Branch has pioneered the development of a series of computer codes that support industry's stated needs to reduce the time and cost for developing ice protection systems and for certifying aircraft for flight into forecasted icing. Included are codes that predict ice accretion shapes, water droplet trajectories, electrothermal deicer operation, and helicopter main rotor performance in icing.

These codes are considered research codes because we are still improving their analytical models by incorporating new results from a parallel experimental icing research program. But current debugged versions are always available to U.S. organizations, and the icing branch provides the codes, users manuals, and technical support to requestors. Several companies integrate the NASA icing codes into their own code methodologies. And several aircraft companies run the codes not only for their own immediate design needs, but also for cross-checking on their subcontractors' ice protection system designs.

Ice accretion codes.—The ice accretion prediction code LEWICE is an excellent example of R&T transfer. LEWICE is regarded as the *industry standard* in the United States and has been requested by over 80 U.S. organizations. One university plans to include LEWICE in an interdisciplinary course in aircraft design. Several graduate students have trained on LEWICE and have gone into industry to work in aircraft icing. LEWICE is recognized internationally as well, and we receive many requests for it from foreign organizations, even though we are unable to give it to them.

LEWICE is used to predict the shape of in-flight ice that accretes on wings, tails, engine inlet lips, aircraft instruments, and other aircraft components. The LEWICE code consists of three main modules: (1) a flow field code that calculates the flow field around the component and passes velocities, pressures, and temperatures to the other two modules; (2) a droplet trajectory code that predicts where and how much water impinges on the aircraft component; and (3) a thermodynamic module that performs mass and energy balances to determine how much water freezes at each point on the component.

In a typical application of LEWICE the dimensions of an ice shape would be calculated for an airplane wing. From the dimensions a simulated ice shape would be fabricated and attached to the leading edge of a scale-model's wing. The model would be tested in a wind tunnel to measure the effects of the simulated ice on airplane performance and stability and control. The next step would be to fabricate and attach simulated ice shapes to the actual aircraft and fly it to determine its changes in performance, stability, and control. Sometimes, the wind tunnel testing is bypassed to go directly to flight testing with the simulated ice shapes. The U.S. Navy required one of their contractors to use LEWICE to predict ice growth on the inlet of a fighter aircraft.

We provide both two- and three-dimensional versions of LEWICE. The flowfield codes available with LEWICE include a nonviscous panel code, an Euler code, or a Navier-Stokes code.

Droplet trajectory codes.—NASA, Lewis two- and three-dimensional droplet trajectory codes are also extensively used by industry and other government agencies. These codes predict where the droplets impinge, and this information determines the extent of coverage the ice protection system must provide. The droplet trajectory code is also used to predict the water flux distribution, and this information is used to determine the surface heat flux distribution required to evaporate the water or simply to keep it running wet.

The trajectory code is ordinarily run in conjunction with an external inviscid panel code or with the Euler or Navier-Stokes codes. We are planning to develop a version that can be used in conjunction with an engine inlet internal flow code such as PARC3D. This will allow us to calculate the impingement of water on the walls throughout the entire inlet duct to determine if ice protection is required inside the duct. This version will also be coupled with the LEWICE code to predict where the ice will build up on the duct's inside walls.

Electrothermal deicer codes.—NASA Lewis, through a grant to the University of Toledo, has developed several versions of an electrothermal deicer design and analysis code. The University of Toledo coordinated with a helicopter manufacturer and an ice protection systems manufacturer to ensure that the resulting code would meet their needs. This transient heat conduction code can analyze an electrical heater blanket composed of several layers, such as heaters, insulation, adhesives, and aircraft structure. It also predicts the melting and freezing of an ice layer on top of the heater blanket and includes an ice shedding model. Fixed-wing and rotary-wing aircraft manufacturers and ice protection systems manufacturers use the code to determine the deicer heat flux requirements, the maximum internal operating temperatures, and the heater cycle on-off times. Some companies have funded the University of Toledo to tailor the NASA codes to their own specific needs.

Rotor-rerformance-in-icing code.—NASA Lewis has contracted with the U.S. helicopter industry to develop a computer code that predicts the change in main rotor performance during an icing encounter. This code utilizes experimental data obtained from two key test programs funded by NASA. The first test was of several currently used main rotor airfoils in a high-speed icing tunnel. These tests resulted in a lookup table of lift and drag losses as a function of flight and atmospheric conditions. This table was incorporated into the rotorcraft companies' rotor performance codes. The second test was of a subscale model rotor operating in the NASA Lewis Icing Research Tunnel. This highly successful joint NASA/industry test program provided flight-type data to validate, calibrate, and improve the rotor-performance-in-icing code. The rotor performance code has been used by U.S. rotorcraft manufacturers to determine the required extent of ice protection coverage and to predict the degradation of rotor performance during an icing encounter. Helicopter manufacturers plan to submit such calculations to the Federal Aviation Administration in support of the icing certification process. The goal is to reduce the amount of expensive, high-risk flight testing by replacing some of the flight tests by code prediction results.

Lewis contact: John J. Reinmann, (216) 433–3900
Headquarters program office: OA

Fiber Optic Probe Detects Cataracts

A fiber optic probe originally developed for materials processing aboard the space shuttle shows promise as a diagnostic tool for detecting cataracts in the human eye at very early formative stages.

Developed by Dr. Rafat Ansari, a Case Western Reserve University research scientist working under a cooperative research agreement with the Materials Division, and Dr. Harbans Dhadwal at the State University of New York at Stoneybrook, the small fiber optic probe can detect protein crystals suspended in the fluid inside the eye. It is suspected that these crystals, over time, form into a cloudy mass on the lens—causing cataracts. The device is small enough to fit in a shirt pocket. An optical fiber transmits a laser beam into the eye, at very low power levels to avoid eye damage; light scattered from within the eye back to the instrument is picked up by a second optical fiber. After processing on a laptop computer, the pattern of light scattering can be recorded to become a permanent record for the patient; changes in protein particle size could indicate the early onset of cataracts.

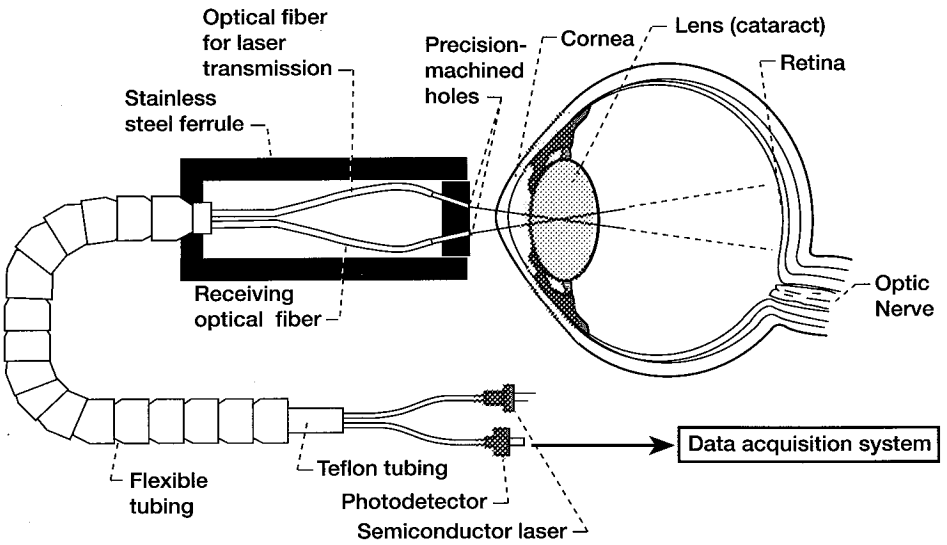

Fiber optic system for early detection of cataracts.

Once a series of voluntary patient studies is completed using a prototype tool, pharmaceutical companies may be able to develop drugs that dissolve the protein crystals and neutralize a developing cataract at its earliest stage—possibly eliminating the need for cataract surgery.

The fiber optic probe can also measure the sizes of extremely small particles that are suspended in solutions; this capability may have use in industrial applications as well as in the field of opthamology.

Lewis contact: Dr. Rafat Ansari, (216) 433-5008
Headquarters program office: LMSA

Ion Exchange Membrane Purifies Water

A new material for removing toxic metals from water may benefit industries that produce large amounts of contaminated waste water. NASA Lewis researchers have developed an ion exchange membrane that in laboratory tests can effectively remove contaminants, such as mercury, lead, cadmium, silver, copper, zinc, nickel, yttrium, and chromium, from water. Tests demonstrate that the new material is easy to use and inexpensive to produce. The material is also strong, flexible, and chemically stable in storage. The material is a joint invention of Dr. Warren Philipp of the Materials Division and Dr. Kenneth Street of the Chemical Sampling and Analysis Office of the Office of Environmental Programs.

The ion exchange membrane was originally developed as a separator in batteries for use in spaceflight. The separator can be made in a variety of forms and sizes, including thin films, coatings, pellets, and fibers for use in larger systems. This variability means that the material is suitable for use in a number of applications and environments: as woven fiber filters for home water filters, packed columns of pellets for industrial use, and coatings on screens that can be drawn through ponds and lakes which are contaminated. An additional important feature of the material is that absorbed or collected metals can be reclaimed through destructive or nondestructive processes. In the destructive process, used ion exchange material is ashed and produces carbon dioxide and water vapor. Oxides of the absorbed metals remain as ash and can be recycled. In the nondestructive process, heavy metals are removed from the ion exchange material and reclaimed by acid stripping. The ion exchange material is then reusable, and the metal concentrates removed can be recycled.

Laboratory tests confirmed that this ion exchange material successfully removes heavy metals from waste water. In setting up the final stage of the testing process, NASA awarded a grant to the Advanced Manufacturing Center (AMC), a division of the Cleveland Advanced Manufacturing Program—an organization closely affiliated with Cleveland State University (CSU), to work with Aetna Plating Company of Cleveland to demonstrate the ion exchange material's performance in an industrial setting. In 1993, Aetna and NASA

Lewis signed a Space Act Agreement further defining this effort. In 1994, AMC/CSU will test the ion exchange material in Aetna's electroplating operation and evaluate its ultimate effectiveness in removing heavy metals from waste water.

Lewis contacts: Dr. Warren H. Philipp, (216) 433–5501; Dr. Kenneth Street, (216) 433–5032
Lewis Research Center Director's Discretionary Fund

Tribometer (Pin-on-Disk Wear Testing System) Marketed Commercially

Originally designed and developed by materials researchers at NASA Lewis, the ISC–200PC Tribometer System is now a commercial product offered by the Implant Sciences Corporation of Wakefield, Massachusetts. The system, designed for unattended operation in testing or laboratory settings, performs automated testing and records data on the surface characteristics—wear behavior, coefficient of friction, and integrity of films and coatings—of a wide range of material types, including metals, composites, ceramics, plastics, and glass.

System users place material to be tested in the system's turntable fixture and specify test variables, such as speed and pressure, to be applied to a pin in contact with the sample surface. When the system's turntable rotates, sliding wear and friction force are applied to the sample. Pins can be fabricated from a wide range of materials, so that nearly any combination of metal, glass, composite, ceramic, or plastic substrates can be used in creating a sample/pin pairing for test purposes. Data can be displayed in real time on a color monitor, by using Implant Sciences PC Stripchart, and can be viewed as recorded or compiled over time for later retrieval and analysis.

Lewis contact: Dr. Mary Zeller, (216) 433–2061
Headquarters program Office: OA

CARES Software Boosts Industrial Competitiveness

The CARES series of integrated design programs were developed by NASA Lewis' Structural Integrity Branch. The branch combines the three disciplines of analytical modeling, mechanical testing, and nondestructive evaluation to understand and predict the behavior of advanced high-temperature materials, particularly brittle ceramic and intermetallic matrix composites. The CARES computer program is used worldwide for fracture and life prediction of structural ceramic components for automotive, aerospace, electronic, and nuclear applications. CARES is an enabling technology primarily created to foster the introduction of ceramic materials in demanding engine environments to achieve breakthrough gains in energy efficiency and emissions reduction. The specific purpose of the project is to transfer and upgrade technology for understanding and predicting the behavior of brittle ceramic materials. Customers receive a series of integrated computer programs accompanied by appropriate user manuals, documentation, and consulting services. The underlying technology consists of expertise in statistics, fracture mechanics, and probabilistic design techniques for advanced structural ceramics and brittle materials in general. Use of CARES is primarily intended to ensure that ceramic components survive high temperatures and stresses in a variety of applications. To accomplish this, CARES incorporates the capability to design for any component shape and service environment. The resulting software is a comprehensive general-purpose design tool for government, industry, and academia that predicts the probability of a ceramic component failing as a function of its time in service.

During the past three years over 100 companies have obtained the CARES software. The latest version of the software, CARES/LIFE, is restricted to U.S. dissemination for a period of at least two years. The overriding interactions are with domestic users. The CARES and CARES/LIFE programs are comprehensive design tools developed for industry, academia, and government. Current customers represent a wide range of interests (from commercial to military) and comprise a variety of industries including aerospace, automotive, electronics, glass, and nuclear. Within these organizations the ultimate recipients of this software are engineers and material

Ceramic valves and engine components.

scientists, who design parts and evaluate materials, respectively.

As the only general-purpose public domain integrated design program for predicting the reliability of brittle materials in the United States, CARES has tremendous impact on helping U.S. industrial competitiveness. The CARES probabilistic design methodology is necessary for accurate failure prediction and efficient structural utilization of brittle materials subjected to arbitrary stress states. This technology applies to materials such as glass, graphite, and advanced ceramics including silicon nitride and silicon carbide. Many commercial products, such as turbocharger rotors, rocker arm and cam followers, poppet valves, radiant heater tubes, heat exchangers, and prototype ceramic turbines, are widely designed by using the CARES series of software. In addition, these programs are used to design large infrared transmission windows, glass panels for skyscrapers, ceramic packaging for microprocessors, cathode ray tubes, and even ceramic tooth crowns and knee caps. The software is also used by educators to teach probabalistic methods to engineering students.

The CARES series of programs are actively maintained and new capabilities are being developed. Users are surveyed regarding the technology and software. They are encouraged to publish and share their results with NASA. Information collected is being used to prepare a booklet of products designed with this technology.

Bibliography

Nemeth, N.N.; Manderscheid, J.M.; and Gyekenyesi, J.P.: Designing Ceramic Components With the CARES Computer Program. Am. Ceram. Soc. Bull., vol. 68, 1989, pp. 2064–2072.

Nemeth, N.N.; Manderscheid, J.M.; and Gyekenyesi, J.P.: Ceramic Analysis and Reliability Evaluation of Structures (CARES) Users and Programmers Manual. NASA TP–2916, 1990.

Salem, J.A.; et al.: Reliability Analysis of a Structural Ceramic Combustion Chamber. ASME Paper 91–GT–155, 1991.

Nemeth, N.N.; et al.: Time-Dependent Reliability Analysis of Monolithic Ceramic Components Using the CARES/LIFE Integrated Design Program. Life Prediction Methodologies and Data for Ceramic Materials, ASTM STP–1201, C.R. Brinkman, and S.F. Duffy, eds., American Society for Testing and Materials, Philadelphia, 1993.

Nemeth, N.N.; et al.: Designing Ceramic Components for Durability. Am. Ceram. Soc. Bull., vol. 72, no. 12, Dec. 1993.

Lewis contact: Noel N. Nemeth, (216) 433–3215
Headquarters program office: OA
Funding also from Department of Energy

Company Uses Reliability/Cost Analysis Methods Developed at NASA and Saves $1.1 Million

NASA Lewis has developed an analysis method called CARRAC (for combined analysis of reliability, redundancy, and cost). Its first use in industry has saved $1.1 million in capital outlay.

CARRAC, developed in the Power Technology Division at NASA Lewis, can be used universally. Given a number of alternative choices involving reliability and cost, the CARRAC user can make an optimal choice that will minimize total cost. For example, a designer may have a number of choices concerning which power supply may be used in a communications satellite. The first power supply may cost $10 million and have a mission reliability of 0.93. The second power supply may cost $30 million with a reliability of 0.99. Which one should be used? That depends upon what costs will be incurred if the power supply fails. CARRAC makes an objective choice to minimize the total cost.

One function of CARRAC is to examine the expected cost of failure. This cost is the cost that would be incurred if the subsystem under study fails multiplied by the probability of failure of the subsystem. For the example just cited, if the cost of failure was $250 million (because the failure of the power supply took down the whole satellite), then the first (lower cost and less reliable) power supply should be chosen. If the cost of failure was $450 million, then the second (higher cost and more reliable but more expensive) supply should be used.

The first industry user of CARRAC techniques was the Southwestern Power Administration (Tulsa Office). They were in the process of making a decision regarding the purchase and installation of an additional (fourth) transformer at one of their power substations. The new transformer would help handle the predicted increased load. Like the prior three, the new transformer would be rated at 37.5 MVA. The analysis methods that they had used in the past had indicated that they should purchase the new transformer, but they decided to also try a different analysis approach using CARRAC techniques. They had some experience and equations that related reduction in transformer life (less reliability) under mild overload conditions. They also had numbers indicating the value of lost loads (if transformers started failing). The new analysis using CARRAC techniques (looking at the alternatives and adding in the expected cost of failure) indicated that they should not purchase and install the new transformer. Southwestern Power accepted the results of the new analysis, they did not put in the new transformer, and they decided to wait another 10 years before looking at the question again. The cost of a 37.5-MVA transformer is about $600,000, and the cost of associated switches, relays, and installation is about $500,000. The total savings in capital outlay resulting from this user's application of CARRAC was $1.1 million.

A computer program has been written to execute the CARRAC techniques. Beta test versions of the program have been distributed to about 20 groups inside NASA and in industry. The computer program has both tabular and graphic (what if) outputs, and it can cover cases from the very simple to the much more complex. The computer program covers methods of redundancy (with three associated ways of looking at redundancy of overhead), partial to catastrophic failures, and the time domain (where failure rates and mission times are used instead of reliability numbers). Also included are cases with and without salvage value. The CARRAC computer program operates on IBM personal computers and clones with VGA graphics.

Lewis contact: Richard L. Patterson, (216) 433–8166
Headquarters Program Office: OACT

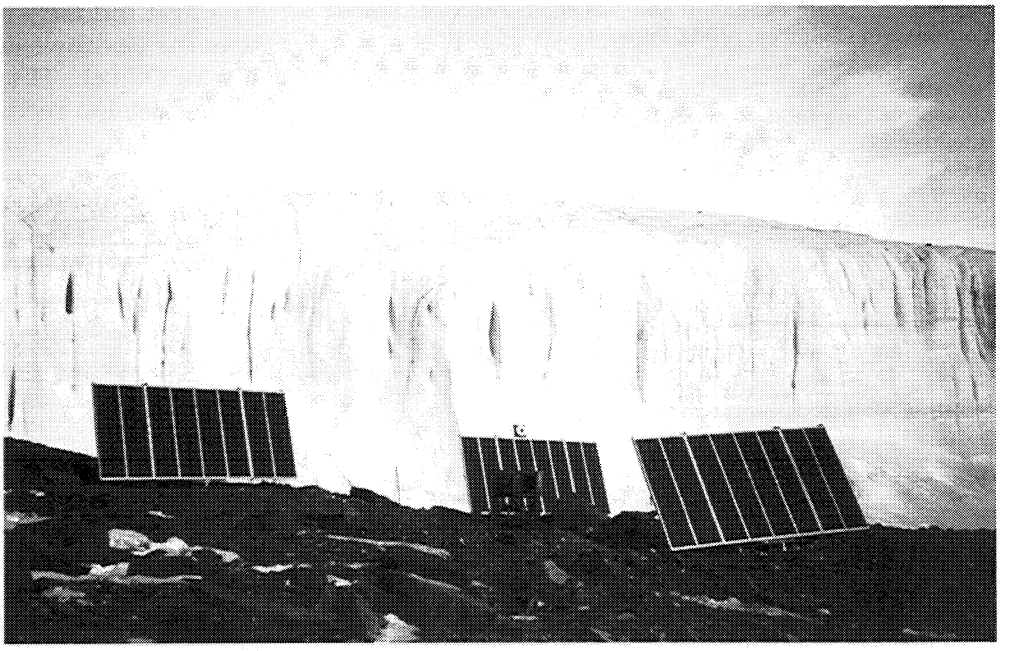

Field testing of photovoltaic power system in Antarctica.

Photovoltaic Power System Tested for Use in Antarctica

A field-deployable solar power system built by NASA Lewis has been transferred to the National Science Foundation (NSF) Office of Polar Programs for use in Antarctic field camps operated by the NSF as part of the U.S. Antarctic Program. The power system was field tested in Antarctica during the 1992–93 austral summer as part of the joint NASA/NSF Antarctic Space Analog Program, an activity that uses Antarctica to test systems that may one day be used in the exploration of other planetary surfaces, such as the Moon and Mars.

Conceived and built within 15 months by a team of NASA Lewis researchers, the 1.5-kW power system supplied an Antarctic research team with power to support both their living quarters and a small laboratory. Consisting of three silicon photovoltaic subarrays, lead-acid battery modules, and an electrical distribution system to supply both 120 V ac and 12 V dc, the power system provided electricity for personal computers and printers, laboratory equipment, lights, fans, and a microwave oven. Prior to installation of the system at the Lake Hoare field camp, power had been supplied by diesel generators, which require fuel and produce objectionable exhaust gases and noise.

The success of this solar power system in Antarctica prompted the NSF to request transfer of the system from NASA so that similar systems can be built and installed in other field camps around the Antarctic continent. Use of solar power for large base power augmentation in the future would reduce NSF's dependence on diesel fuel supplies and lessen the environmental impact associated with the use of such fuels.

Lewis contact: Lisa L. Kohout, (216) 433–8004
Headquarters program office: OACT

Diamondlike Carbon Coatings Protect Sunglass Lenses

Diamondlike carbon (DLC) coatings are currently begin placed on Bausch and Lomb Ray-Ban sunglass lenses. The DLC coated lenses are at least 10 times more resistant to scratches than ordinary glass lenses. The process being used by Diamonex, Inc., is based on ion beam technology originally developed in-house at NASA Lewis.

In 1980 NASA Lewis began research on diamond and diamondlike film deposition by low-pressure vacuum deposition processes. The resulting research led to the innovation of a direct dual-ion-

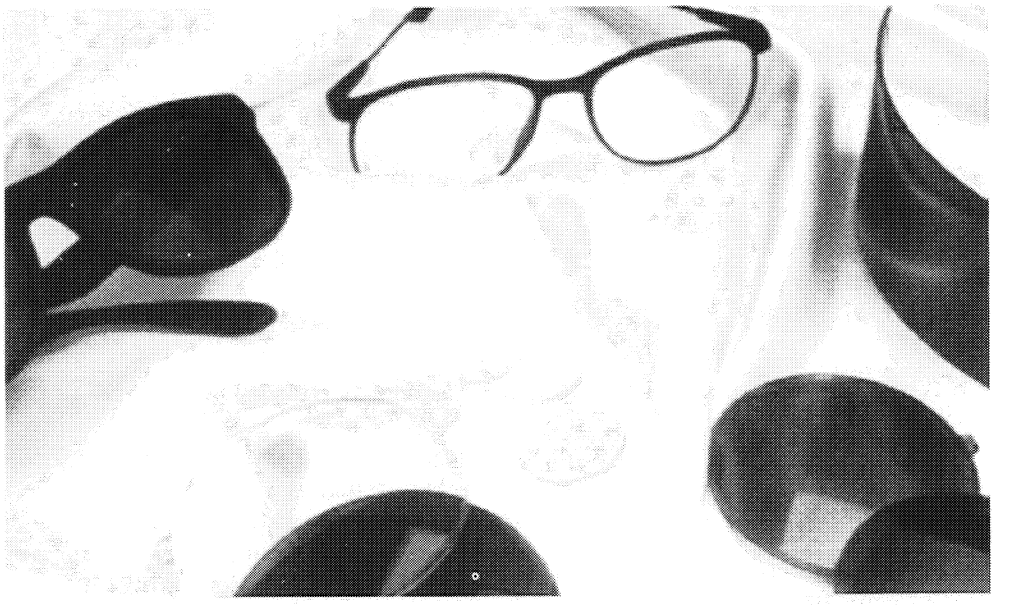

Lewis and Diamonex, Inc., have teamed up to develop a scratch-resistant protective diamond coating for sunglass lenses.

beam deposition process that enabled abrasion-resistant, transparent, diamondlike carbon films to be deposited at room temperature on a wide variety of substrates. This innovation was patented (Patent No. 4,490,229 on December 25, 1984) and licensed by NASA to Air Products and Chemicals, Inc., in July 1988.

The United States Government's first Technology Assistance Agreement was established with Air Products in August 1988 to assist in transferring the dual-ion-beam diamondlike film deposition technology to Air Products. A Space Act Agreement was established with Air Products in April 1990 to assist in the collaborative technology development needed by Air Products in order to apply this technology for optical lenses. The license was later assigned to Diamonex, Inc., who through a joint venture company including Diamonex, Inc., and Gentex Optics, Inc.—called Optical Diamond Products, L.P., is producing diamondlike coated sunglass lenses. Optical Diamond Products is currently providing Bausch & Lomb with diamondlike-carbon-coated, scratch-resistant lenses for their new Ray-Ban DiamondHard line of Survivors sunglasses.

Current Lewis efforts have focused on developing improved transparency DLC films by using the dual-beam deposition processes. If extremely clear hard coatings can be deposited, Diamonex, Inc., will use the process to produce protective and antireflective coatings for prescription eyeglass lenses.

Lewis contacts: Michael J. Mirtich, (216) 433–5616; Bruce A. Banks, (216) 433–2308; James S. Sovey, (216) 433–7454
Headquarters program office: OACT

SCORE Integrated Circuit Marketed Commercially

The use of fiber optic links for distributing control information to monolithic microwave integrated circuit (MMIC) phase shifters and amplifiers is seen as a key integration technology for large high-frequency MMIC arrays. The broad fiber bandwidth allows multiple control lines to be multiplexed on a single fiber, reducing the number of interconnections. The mechanical flexibility of the optical fiber supports simple, space-conservative array configurations. Fiber links eliminate much of the weight and volume associated with conventional signal distribution media, such as coaxial cable or other metal conductors. Optical fiber has very low crosstalk and electromagnetic interference.

The key component in a fiber optic link is the optical receiver. This type of optoelectronic interface circuit (OEIC) converts the incoming optical signal (light) to an electronic signal (radio-frequency). Typically, the optical receiver consists of a photodetector, a low-noise amplifier, and a demultiplexer circuit. Ideally, these circuits are monolithically integrated on a single gallium arsenide substrate, creating a monolithic optical receiver on a chip.

Development efforts by NASA Lewis' Space Electronics Division and Honeywell have resulted in a system-ready monolithic chip with a demultiplexer and added advanced digital capabilities, including built-in clock recoverability and addressability. Bandwidth is very broad, with the data rate variable from 10 to 400 megabits per second.

The self-contained optical receiver (SCORE) chip redefines the state of the art for optical data link applications. Honeywell now offers the fully monolithic, foundry-compatible circuit as a commercial product (Part Number OEIC Rx-400) and is marketing it for a variety of applications requiring optical fiber data links. In addition to optical control for MMIC arrays in commercial communications systems and NASA missions, the OEIC will support spacecraft and aircraft optical signal distribution systems including robotics. Honeywell commercial/military products enabled by SCORE include high-speed fiber data buses (TRW and Honeywell Satellite Systems), fiber-linked helmet displays, and high-speed fiber links for offices and supercomputers (Honeywell MICRO SWITCH Fiber Link Products). Honeywell is also pursuing spacecraft up/down and cross-link applications for international SONET/ATM telecommunications.

Lewis contact: Richard R. Kunath, (216) 433–3490
Headquarters program office: OACT

Technology Utilization

Over the past year the NASA Lewis Technology Utilization Office served as a liaison for numerous short- and long-term technology transfer projects and networking arrangements. Examples of such ongoing and completed projects and arrangements, begun in 1993, are described here.

EMI Shielding Materials Being Developed

After reading about a NASA Lewis-developed composite technology featured in NASA Tech Briefs magazine, the president of Sigma Electromagnetic Shielding Technologies (Sigma Tech) contacted the NASA Lewis TU Office hoping to develop a material capable of shielding electromagnetic interference (EMI) by applying Lewis technology and expertise. Working together, Sigma Tech and Lewis experts hope to develop a magnetic shielding material by combining carbon fibers with an iron halide through an intercalation process and reducing the iron electrochemically to the metal state within the fibers.

Preliminary production and testing forecasts for 1993 have identified these selected types of composites as inexpensive and highly effective against electromagnetic interference. This collaborative effort between NASA Lewis and Sigma Tech, formalized under a reimbursable Space Act Agreement signed earlier this year, is expected to carry this research effort up to commercialization.

Lewis contact: Dr. James R. Gaier, (216) 433–6687
Headquarters program office: OACT

Automobile Antennas Characterized and Improved

Engineers employed at Tenatronics, Ltd., an automobile antenna manufacturer, visited the NASA Lewis TU Office to discuss the company's need for up-to-date antenna research data. The TU staff arranged a tour of Lewis' Antenna and Radiofrequency System Laboratory for the visiting engineers to familiarize them with Lewis' pertinent facilities and capabilities. After an initial review of the company's product capabilities, Lewis experts from the Space Electronics Division

electrically characterized the antennas currently built by Tenatronics; this involved measuring antenna impedance, reflection coefficients, and optimum operating frequencies. Tenatronics now hopes to conduct further research in Lewis' unique far-field anechoic chamber as soon as appropriate instrumentation for these tests becomes available. Once this remote testing is complete, Tenatronics feels that the company will be in a leading position in the antenna industry.

Lewis contact: Richard R. Kunath, (216) 433–3490
Headquarters program office: OACT

U.S. Competitiveness in Die Casting Industry Improved

In early 1993, a NASA Lewis TU Office staff member visited the Rex Buckeye Company to discuss the company's current manufacturing dilemma involving a two-piece shot sleeve they developed for companies in the die casting industry. One of Buckeye's customers reported that the shot sleeve's silicon nitride (Si_3N_4) liner failed by cracking after a run of only 400 shots, less than 1 percent of the liner's expected life.

The TU staff analysis revealed that the failure was due to uneven heating of the metal sleeve, which surrounds the Si_3N_4 liner. The unevenness in temperature caused compressive loading levels above failure limits. TU staff recommended two solutions: Either preheat the shot sleeve assembly to 100 °F to reduce the uneven stress, or redesign the shot sleeve liner to include a key for positive control to eliminate the need for a tight fit between liner and sleeve. It was later proven that both approaches successfully eliminate premature failure.

Lewis contact: Anthony F. Ratajczak, (216) 433–2225
Headquarters program office: OACT

Microwave Radiation of Bone Tumors Investigated

Dr. Steven Reger of the Cleveland Clinic contacted the NASA Lewis TU Office to discuss the possibilities of using various technologies, including microwaves, as a method of eradicating bone tumors.

Bone tissue, like all other types of living tissue, is vulnerable to the invasion of cancerous cells, which can lead to the formation of malignant tumors. These tumors establish themselves at sites inside the inner bone cavities and may continue to grow into the calcified layers of the bone. One way to combat the spread of this growth is to raise the temperature of the tumorous cells to a level that would destroy the cancer cells. Lewis researchers spearheading this project agreed that the inner cavity could be heated through microwave radiation. Previous medical research using microwave radiation has been confined to frequencies below 1 GHz.

It is the objective of this project to investigate the effects of using high-frequency microwave radiation for heating inner bone cavities. Currently, pig bone marrow has been used because its properties closely resemble those of human bone marrow. Planned activities for this project ultimately involve the characterization of human marrow.

Lewis contact: Richard R. Kunath, (216) 433–3490
Headquarters program office: OACT

Sensor-Driven Rehabilitation Equipment Used in Hospitals

Impulse Technology, Inc., has developed a new physical rehabilitation system with the help of NASA engineers.

Impulse Technology, Inc., planned their physical rehabilitation system, VIDEO TRAQ, to enable physical therapists and medical personnel to detect neuromuscular and musculoskeletal deficits by using patented force/time sensor technology. The chief executive officer of Impulse contacted the NASA Lewis TU Office with questions centered around the company's use of sensors. Two NASA engineers worked with Impulse: A Lewis sensor expert consulted the company's technical staff and addressed their questions regarding state-of-the-art sensor technology. A Lewis metallurgist provided additional data relating to superior material choices. Impulse adopted Lewis' recommendations and completed prototype production in 1992. Medical patients use VIDEO

TRAQ to measure the improvement of their rehabilitating muscles. Athletes use the system to measure muscular development and reaction time.

Over the past year, Impulse enjoyed growing commercial success. Virtually every hospital within a 40-mile radius of Impulse Technology's Cleveland office has committed to purchase, including the Cleveland Clinic and Lutheran Hospital.

Lewis contact: Anthony F. Ratajczak, (216) 433–2225
Headquarters program office: OACT

Innovative Technology Transfer Initiatives Begun

In 1993 the NASA Lewis Office of Interagency and Industry Programs implemented the first annual Strategic Technology Evaluation Program (STEP), an 8-week summer program in which 12 competitively selected, interdisciplinary graduate students from Case Western Reserve University's Weatherhead School of Business evaluated the commercial potential of 120 Lewis patents. The students completed a market opportunity analysis on 45 patents and/or disclosures identified as having substantial commercial potential. As a result, nine companies are interested in pursuing either license agreements or a further evaluation of individual patents. Twenty-eight companies collectively expressed interest in participating in a NASA Lewis/Great Lakes Industrial Technology Center (GLITeC) coatings and surface modification consortium. Eleven additional companies stated a strong desire for an ongoing relationship with Lewis.

Lewis contact: Kim A. Veris, (216) 433–6355
Headquarters program office: OACT

Space Act Agreement Signed With GLITeC

In August 1993, NASA Lewis entered into a reimbursable space act agreement with the Great Lakes Industrial Technology Center (GLITeC) to improve Federal technology transfer support to companies located primarily within the country's Midwest region. Through this agreement GLITeC—NASA's regional technology transfer center—works hand-in-hand with Lewis researchers and TU Office staff to provide easy access to Lewis technology by private sector organizations. Also, as a result of this agreement the administrative processing time of short- and long-term reimbursable applications projects significantly decreased because GLITeC also serves as a financial liaison. We anticipate this agreement to be an increasingly successful mechanism for transferring technology from NASA Lewis.

Lewis contact: Stephen M. Riddlebaugh, (216) 433–5565
Headquarters program office: OACT

Author Index

A

Adamczyk, Dr. John J. 144
Addy, Harold E. 63
Alterovitz, Dr. Samuel A. 95
Ansari, Dr. Rafat 152
Arnold, Dr. Steven M. 61, 62
Arpasi, Dale J. 11

B

Banks, Bruce A. 92, 157
Barranger, Dr. John P. 5
Behrendt, Dr. Donald R. 36, 38
Bencic, Timothy J. 25
Benson, Thomas J. 15
Bhasin, Dr. Kul B. 97
Birchenough, Arthur G. 133
Bond, Thomas H. 18
Bowman, Dr. Randy R. 45
Budinger, James M. 103

C

Cain, Maureen F. 140
Castner, Raymond S. 21
Cauley, Michael A. 94, 99
Chamis, Dr. Christos C. 49, 58, 59
Civinskas, Kestutis C. 28
Cooper, Beth A. 29
Corrigan, Robert D. 122
Curran, Dr. Frank M. 73
Curren, Arthur N. 100

D

Dalton, Penni J. 128
De Groh, Kim K. 85, 92
DellaCorte, Dr. Christopher 40
DeLombard, Richard 111
Dever, Joyce A. 85
Dimofte, Dr. Florin 63
Doherty, Michael P. 108
Dolce, James L. 131
Dudenhoefer, James E. 88, 89, 90, 91

E

Eldridge, Dr. Jeffrey I. 41

F

Ferrante, Dr. John 148
Fincannon, James 120
Follen, Gregory J. 143
Fralick, Gustave C. 8
Frate, David T. 127

G

Gaier, Dr. James R. 158
Garg, Dr. Sanjay 8
Gati, Frank G. 131
George, Jeffrey A. 108
Ginty, Carol A. 33
Goldberg, Fredric N. 141
Gray, Dr. Hugh R. 33

H

Halford, Dr. Gary R. 60
Harding, Dr. David R. 46
Hardy, Terry L. 69
Harrington, Douglas E. 23, 24
Hasan, Dr. Mohammad M. 79
Hickman, J. Mark 119, 137
Hoffmann, Monica I. 124
Holcomb, Joesph M. 2
Hollansworth, James E. 93
Huff, Dennis L. 30
Hultgren, Dr. Lennart S. 145
Hung, Dr. Ching-cheh 86
Hunter, James E. 139
Hwang, Dr. Danny P. 32

I

Ivancic, William D. 101, 102

J

Jacobson, Thomas P. 110
Jankovsky, Amy L. 64
Jayne, Douglas T. 42
Johns, Albert L. 25
Jurns, John M. 80

K

Kalinowski, Joseph M. 35
Kascak, Albert F. 55
Kerczewski, Robert J. 98
Kerwin, Paul T. 15
Kohout, Lisa L. 156
Koudelka, John M. 115
Krainsky, Dr. Isay L. 106
Kunath, Richard R. 158, 159

L

Lam, David W. 22
Lant, Christian T. 5
Larkin, Dr. David J. 6, 149
Lavelle, Thomas M. 2
Lazbin, Jennifer L. 142
Lee, Dr. Richard Q. 96
Lei, Dr. Jih-Fen 4, 5
Leonhardt, Todd A. 47
Lerch, Bradley A. 60
Lewicki, David G. 20
Linne, Diane L. 65
Long-Davis, Mary Jo 21
Ludwiczak, Damian R. 137

M

Mankbadi, Dr. Reda R. 145
Mason, Lee S. 118
Matus, Dr. Lawrence G. 6
Maul, William A. 66
McArdle, Jack G. 22
McNelis, Mark E. 137
Melis, Matthew E. 49
Mirtich, Michael J. 157
Misra, Dr. Ajay K. 45
Moore, Thomas J. 35
Moran, Matthew E. 82
Morscher, Gregory N. 39
Mularz, Dr. Edward J. 13

Murthy, Dr. Durbha V. 56
Myhre, Craig A. 125, 126

N

Neiner, George H. 25
Nemeth, Noel N. 155
Neudeck, Dr. Philip G. 6, 149
Niedzwiecki, Richard W. 17
Noebe, Ronald D. 35, 48

O

Oeftering, Richard C. 137
Olson, Sandra L. 113
Opila, Dr. Elizabeth J. 44
Otero, Angel M. 114

P

Palaszewski, Bryan A. 67
Palko, Joseph L. 52
Patterson, Michael J. 75, 122
Patterson, Richard L. 155
Paxson, Daniel E. 5
Pereira, Dr. J. Michael 49
Petrik, Edward J. 104
Philipp, Dr. Warren H. 153
Pischel, Karen A. 141
Pline, Alexander D. 110
Powell, J. Anthony 6
Power, John L. 76
Proctor, Margaret P. 70

R

Ratajczak, Anthony F. 159, 160
Reinmann, John J. 151
Rhatigan, Jennifer 113
Richard, Jacques C. 8
Riddlebaugh, Stephen M. 160
Robinson, Raymond C. 43
Roche, Joseph M. 139
Ross, Dr. Howard D. 112
Roth, Dr. Don J. 50

S

Sankovic, John M. 74
Saravanos, Dr. Dimitrios A. 49
Sargent, Noel B. 135
Saunders, John D. 30
Sayir, Dr. Ali 37
Schneider, Dr. Steven J. 78
Shalkhauser, Kurt A. 105
Shaltens, Richard K. 83, 86
Siegel, Dr. Robert 147
Singh, Dr. Mrityunjay 36, 38
Smialek, Dr. James L. 42
Smith, Roger L. 134
Smithrick, James E. 89
Sovey, James S. 75, 157
Stearns, Carl A. 43
Stefko, George L. 56
Steinetz, Dr. Bruce M. 54
Stephens, Joseph R. 34
Stochl, Robert J. 81
Street, Dr. Kenneth 153
Strom, Thomas N. 15
Suder, Kenneth L. 12
Szaniszlo, Andrew J. 117

T

Tabata, William K. 70
Thompson, June E. 140

V

Van Fossen, Dr. G. James 9
Veris, Kim A. 160
Verrilli, Michael J. 60

W

Wendt, Dr. Bruce J. 13
Westfall, Leonard J. 37
Williams, Dr. W. Dan 4
Williamson, Gary S. 71
Wilson, Jack 26
Wood, Jerry R. 150
Wroten, Gary W. 129

Z

Zeller, Dr. Mary 153
Zurawski, Robert L. 110
Zuzek, John E. 94

REPORT DOCUMENTATION PAGE

Form Approved
OMB No. 0704-0188

Public reporting burden for this collection of information is estimated to average 1 hour per response, including the time for reviewing instructions, searching existing data sources, gathering and maintaining the data needed, and completing and reviewing the collection of information. Send comments regarding this burden estimate or any other aspect of this collection of information, including suggestions for reducing this burden, to Washington Headquarters Services, Directorate for Information Operations and Reports, 1215 Jefferson Davis Highway, Suite 1204, Arlington, VA 22202-4302, and to the Office of Management and Budget, Paperwork Reduction Project (0704-0188), Washington, DC 20503.

1. AGENCY USE ONLY (*Leave blank*)

2. REPORT DATE

3. REPORT TYPE AND DATES COVERED
Technical Memorandum

4. TITLE AND SUBTITLE
Research & Technology 1993

5. FUNDING NUMBERS
None

6. AUTHOR(S)

7. PERFORMING ORGANIZATION NAME(S) AND ADDRESS(ES)
National Aeronautics and Space Administration
Lewis Research Center
Cleveland, Ohio 44135–3191

8. PERFORMING ORGANIZATION REPORT NUMBER
E–8187

9. SPONSORING/MONITORING AGENCY NAME(S) AND ADDRESS(ES)
National Aeronautics and Space Administration
Washington, D.C. 20546–0001

10. SPONSORING/MONITORING AGENCY REPORT NUMBER
NASA TM–106376

11. SUPPLEMENTARY NOTES
Responsible person, Walter S. Kim, Organization 9400, (216) 433–3742

12a. DISTRIBUTION/AVAILABILITY STATEMENT
Unclassified - Unlimited
Subject Category 01 and 31

12b. DISTRIBUTION CODE

13. ABSTRACT ***(Maximum 200 words)***

This report selectively summarizes the NASA Lewis Research Center's research and technology accomplishments for the fiscal year 1993. It comprises approximately 200 short articles submitted by the staff members of the technical directorates. The report is organized into seven major sections: Aeronautics, Aerospace Technology, Space Flight Systems, Space Station, Engineering and Computational Support, Lewis Research Academy, and Technology Transfer and Utilization. A table of contents by subject has been developed to assist the reader in finding articles of special interest. This report is not intended to be a comprehensive summary of all research and technology work done over the past fiscal year. Most of the work is reported in Lewis-published technical reports, journal articles, and presentations prepared by Lewis staff members or by contractors. In addition, university grants have enabled faculty members and graduate students to engage in sponsored research that is reported at technical meetings or in journal articles. For each article in this report a Lewis contact person has been identified, and where possible, reference documents are listed so that additional information can be easily obtained. The diversity of topics attests to the breadth of research and technology being pursued and to the skill mix of the staff that makes it possible.

14. SUBJECT TERMS
Aeronautics; Aerospace engineering; Space flight; Space station power supplies; Materials; Structural analysis; Computational fluid dynamics; Computer programming

15. NUMBER OF PAGES
164

16. PRICE CODE
A08

17. SECURITY CLASSIFICATION OF REPORT
Unclassified

18. SECURITY CLASSIFICATION OF THIS PAGE
Unclassified

19. SECURITY CLASSIFICATION OF ABSTRACT
Unclassified

20. LIMITATION OF ABSTRACT